Copyright is owned by the Author of the thesis. Permission is given for a copy to be downloaded by an individual for the purpose of research and private study only. The thesis may not be reproduced elsewhere without the permission of the Author.

MODELLING THE GREENHOUSE ENVIRONMENT

AND THE

GROWTH OF CUCUMBERS

(*Cucumis sativus* L.)

A thesis
submitted in partial fulfilment
of the requirements for the degree
of

Doctor of Philosophy

in

Agricultural Engineering

at

Massey University

Colin Mark Wells

1992

Massey University Library
Thesis Copyright Form

Title: MODELLING THE GREENHOUSE ENVIRONMENT AND THE GROWTH OF CUCUMBERS (*Cucumis sativus* L.)

(1) I give permission for my thesis to be made available to readers in the Massey University Library under conditions determined by the Librarian.

(2) I do not wish my thesis, or a copy, to be sent to another institution without my written consent for 12 months.

(3) I agree that my thesis may be copied for Library use.

Signed: Colin Mobbs

Date: 20 FEBRUARY 1992

The copyright of this thesis belongs to the author. Readers must sign their name in the space below to show that they recognise this. They are asked to add their permanent address.

NAME AND ADDRESS DATE

ABSTRACT

Mathematical models which describe the greenhouse environment, and the growth of a crop of cucumbers, in that environment, have been developed and tested. The models have been used to predict: the response of the greenhouse to varying weather conditions, the growth of the crop leaf canopy, and the weight and number of fruit harvested.

The greenhouse environment has been modelled using a system of non-linear differential equations, derived from a consideration of the energy and mass balances of the glazing, internal structure, crop canopy, root media, floor, deep soil layers, and the greenhouse air space. The equations have been solved for five minute time steps, using measured values of outside weather conditions and control inputs as boundary values.

Entry of solar radiation into the greenhouse, and absorption by various surfaces, has been determined using transmission tables generated using a "ray-tracing" light transmission model. The light transmission model has been calibrated in a separate experiment. The incoming solar radiation has been partitioned between diffuse, direct, photosynthetically active and near infra-red radiation, for use in the crop model.

Validation experiments have been performed to test the greenhouse environment simulation model. The results of the validation exercise showed that the model was capable of predicting the temperatures in the greenhouse, within a few degrees. The mean errors were smaller for the crop canopy, root medium, and floor, than for the glazing or air temperature. Prediction errors for relative humidity and carbon dioxide concentration were more variable.

An existing model of cucumber development rate, and leaf expansion, has been modified and validated. This gave good results when adequate account was taken of leaf senescense, and initiation of lateral growths.

Sub-models for photosynthesis, respiration, and assimilate partitioning have been developed, and combined with the greenhouse environment and leaf expansion models. The combined model has been used to predict the course of growth of a cucumber crop over one growing season, and the number and weight of fruit harvested. The predictions have been compared to results from a test crop. This revealed that while the total number of fruit harvested was accurately predicted, the total weight of harvested fruit was not.

The models are intended to be used in the study of optimal control of the greenhouse environment.

ACKNOWLEDGEMENTS

I would like to thank my chief supervisor, Dr. Cliff Studman (Agricultural Engineering Department) and my co-supervisors, Drs. Paul Austin, Bob Chaplin, and Tim Hesketh (Department of Production Technology), for their assistance during the course of this project.

I would also like to express my appreciation to all the technical staff (Agricultural Engineering Department), especially Mr. Leo Bolter, and his family, who assisted with much of the data collection.

Many thanks to all those who helped in some way, particularly staff at the Plant Growth Unit, and at Fruit and Tree Division, DSIR.

Funding for the purchase of the data collection system was provided by grants from the C. Alma Baker Trust, University Grants Committee, and the Massey University Research Fund.

And finally I would like to express my gratitude to David, Denise, Daniel, Jeremy, Joshua, and James, for their love and support in times of desperation!

This thesis is dedicated to Karen, Amy-Lee, and Adam, who will at last have their husband and father to themselves again!

The Grand Academy of Lagado

The first man I saw was of meagre aspect, with sooty hands and face, his hair and beard long, ragged and singed in several places. His clothes, shirt and skin were all of the same colour. He had been eight years upon a project for extracting sunbeams out of cucumbers, which were to be put into vials hermetically sealed, and let out to warm the air in raw inclement summers. He told me he did not doubt that in eight years more he should be able to supply the Governor's gardens with sunshine at a reasonable rate.

..... from Guilliver's Travels
by Jonathon Swift

TABLE OF CONTENTS

LIST OF TABLES

LIST OF FIGURES

LIST OF PLATES

LIST OF SYMBOLS

SYMBOL IN TEXT	SYMBOL IN MODEL	DESCRIPTION	UNITS
A	ARM(I) or ARL(I)	area of a leaf	cm^2
A_{bot}	Abot	open area of bottom ventilators and doors	m^2
A_c	Ac	surface area of the crop canopy (one side only)	m^2
A_f	Af	area of the greenhouse floor	m^2
A_g	Ag	surface area of the greenhouse glazing	m^2
A_h	Ah	surface area of the greenhouse heating system	m^2
A_m	Am	exposed surface area of the root medium bags	m^2
A_s	As	surface area of the greenhouse structure	m^2
A_{top}	Atop	open area of top ventilator windows	m^2
$Age(i)$	AgeFruM(I) or AgeFruL(I)	age of the i-th fruit	day
Assim	Assim	assimilation rate of the crop	$mgCO_2.plant^{-1}.s^{-1}$
α	A	slope of the leaf pattern curve during the primordial phase of leaf development	$cm.cm^{-1}.day^{-1}$
α_d	Ad	delay value of parameter α	$cm.cm_{-1}.day_{-1}$
α_s	As	stationary (normal) value of parameter α	$cm.cm^{-1}.day^{-1}$
B_c	Bc	solar radiation absorbed by the crop per unit floor area	$W.m^{-2}$
$\overline{B}_c$	Bcave	average daily solar radiation intensity at the top of the crop	$W.m^{-2}$
B_f	Bf	solar radiation absorbed by the floor per unit floor area	$W.m^{-2}$
B_g	Bg	solar radiation absorbed by the glazing per unit floor area	$W.m^{-2}$
B_m	Bm	solar radiation absorbed by the root medium per unit floor area	$W.m^{-2}$
$\overline{B}_p$	Bpar	average daily photosynthetically active radiation at top of crop	$MJ.m^{-2}$
B_s	Bs	solar radiation absorbed by the greenhouse structure per unit floor area	$W.m^{-2}$
b	B	slope of the leaf pattern curve during the expanding phase of leaf development	$cm.cm^{-1}.day^{-1}$
b_d	Bd	delay value of parameter b	$cm.cm^{-1}.day^{-1}$

b_s	Bs	stationary (normal) value of parameter b	$cm.cm^{-1}.day^{-1}$
Cloud	Cloud	cloud cover fraction	-
C_{ao}	Cao	rate of sensible heat loss from greenhouse due to ventilation	$W.m^2$
C_{ca}	Cca	rate of convection from the crop to the inside air per unit floor area	$W.m^{-2}$
C_{fa}	Cfa	rate of convection from the floor to the inside air per unit floor area	$W.m^{-2}$
C_{ga}	Cga	rate of convection from the glazing to the inside air per unit floor area	$W.m^{-2}$
C_{go}	Cgo	rate of convection from the glazing to the outside air per unit floor area	$W.m^{-2}$
C_{ha}	Cha	rate of convection from the heating system to the inside air per unit floor area	$W.m^{-2}$
C_{ma}	Cma	rate of convection from the root medium to the inside air per unit floor area	$W.m^{-2}$
C_{pa}	Cpa	specific heat capacity of inside dry air	$J.g^{-1}.^{\circ}C^{-1}$
C_{pc}		specific heat capacity of the crop	$J.g^{-1}.^{\circ}C^{-1}$
C_{pcl}	Cpcl	specific heat capacity of clay minerals	$J.g^{-1}.^{\circ}C^{-1}$
C_{pf}		specific heat capacity of the dry fraction of the floor layer	$J.g^{-1}.^{\circ}C^{-1}$
C_{pgb}	Cpgb	specific heat capacity of the glazing bars	$J.g^{-1}.^{\circ}C^{-1}$
C_{pgl}	Cpgl	specific heat capacity of the greenhouse glazing material	$J.g^{-1}.^{\circ}C^{-1}$
C_{pm}		specific heat capacity of the dry fraction of the root medium	$J.g^{-1}.^{\circ}C^{-1}$
C_{po}	Cpa	specific heat capacity of outside dry air	$J.g^{-1}.^{\circ}C^{-1}$
C_{pom}	Cpom	specific heat capacity of organic matter	$J.g^{-1}.^{\circ}C^{-1}$
C_{ps}	Cps	specific heat capacity of the greenhouse structure	$J.g^{-1}.^{\circ}C^{-1}$
C_{pq}	Cpq	specific heat capacity of quartz minerals	$J.g^{-1}.^{\circ}C^{-1}$
C_{pv}	Cpv	specific heat capacity of water vapour	$J.g^{-1}.^{\circ}C^{-1}$
C_{pw}	Cpw	specific heat capacity of liquid water	$J.g^{-1}.^{\circ}C^{-1}$
C_{pl}	Cpl	specific heat capacity of the dry fraction of the 1st soil layer	$J.g^{-1}.^{\circ}C^{-1}$

C_{p2}	Cp2	specific heat capacity of the dry fraction of the 2nd soil layer	$J.g^{-1}.^{\circ}C^{-1}$
C_{p3}	Cp3	specific heat capacity of the dry fraction of the 3rd soil layer	$J.g^{-1}.^{\circ}C^{-1}$
C_{p4}	Cp4	specific heat capacity of the dry fraction of the 4th soil layer	$J.g^{-1}.^{\circ}C^{-1}$
C_{p5}	Cp5	specific heat capacity of the dry fraction of the 5th soil layer	$J.g^{-1}.^{\circ}C^{-1}$
C_{sa}	Csa	rate of convection from the greenhouse structure to the inside air per unit floor area	$W.m^{-2}$
CO_{2a}	CO2a	carbon dioxide concentration of the inside air	$\mu l.l^{-1}$
CO_{2o}	CO2o	carbon dioxide concentration of the outside air	$\mu l.l^{-1}$
c	C	logarithm of the relative length of the unfolding leaf	-
c_d	Cd	delay value of parameter c	-
c_s	Cs	stationary (normal) value of parameter c	-
D_m	BagD	diameter of the root medium bags	m
DM_c	DMc	total dry matter of the crop	gDM
d	D	characteristic dimension	m
E_{ao}	Eao	latent heat loss from the inside air due to ventilation per unit floor area	$W.m^{-2}$
E_{drain}	Edrn	advective energy loss from the root medium due to drainage per unit floor area	$W.m^{-2}$
E_{drip}	Edrip	advective energy loss from the glazing due to dripping per unit floor area	$W.m^{-2}$
E_{irr}	Eirr	advective energy addition to the root medium due to irrigation per unit floor area	$W.m^{-2}$
E_{up}	Eup	advective energy exchange between the root medium and the crop due to water uptake per unit floor area	$W.m^{-2}$
EOT	EOT	equation of time	minute
e_a	ea	vapour pressure of inside air	Pa
e_a'	esat	saturated vapour pressure of inside air	Pa
e_o	eo	vapour pressure of outside air	Pa
F	FDC	fraction of dividing cells in a leaf	-
F_{cc}	Fcc	self view factor of the crop	-

F_{cf}	Fcf	view factor of the crop to the floor	-
F_{cg}	Fcg	view factor of the crop to the glazing	-
F_{ch}	Fch	view factor of the crop to the heating system	-
F_{cm}	Fcm	view factor of the crop to the root medium	-
F_{cs}	Fcs	view factor of the crop to the structure	-
F_{fc}	Ffc	view factor of the floor to the crop	-
F_{fg}	Ffg	view factor of the floor to the glazing	-
F_{fh}	Ffh	view factor of the floor to the heating system	-
F_{fm}	Ffm	view factor of the floor to the root medium	-
F_{fs}	Ffs	view factor of the floor to the structure	-
F_{gsky}	Fgsky	view factor of the glazing to the sky	-
F_{hc}	Fhc	view factor of the heating system to the crop	-
F_{hf}	Fhf	view factor of the heating system to the floor	-
F_{hg}	Fhg	view factor of the heating system to the glazing	-
F_{hh}	Fhh	self view factor of the heating system	-
F_{hm}	Fhm	view factor of the heating system to the root medium	-
F_{hs}	Fhs	view factor of the heating system to the structure	-
F_{mc}	Fmc	view factor root medium to crop	-
F_{mf}	Fmf	view factor root medium to floor	-
F_{mg}	Fmg	view factor root medium to glazing	-
F_{mh}	Fmh	view factor root medium to heating system	-
F_{mm}	Fmm	self view factor of the root medium	-
F_{ms}	Fms	view factor root medium to structure	-
F_{sc}	Fsc	view factor of the structure to the crop	-
F_{sf}	Fsf	view factor of the structure to the floor	-
F_{sg}	Fsg	view factor of the structure to the glazing	-

F_{sh}	Fsh	view factor of the structure to the heating system	-
F_{sm}	Fsm	view factor of the structure to the root medium	-
F_{ss}	Fss	self view factor of the structure	-
F_{sun}	FracSun	fraction sunlit leaf area	-
FAI	FAI	exposed floor area index	-
$\mathcal{F}_{cg}$	SFcg	combined emissivity view factor from the crop to the glazing	-
$\mathcal{F}_{ch}$	SFch	combined emissivity view factor from the crop to the heating system	-
$\mathcal{F}_{cs}$	SFcs	combined emissivity view factor from the crop to the structure	-
$\mathcal{F}_{fc}$	SFfc	combined emissivity view factor from the floor to the crop	-
$\mathcal{F}_{fg}$	SFfg	combined emissivity view factor from the floor to the glazing	-
$\mathcal{F}_{fh}$	SFfh	combined emissivity view factor from the floor to the heating system	-
$\mathcal{F}_{fm}$	SFfm	combined emissivity view factor from the floor to the root medium	-
$\mathcal{F}_{fs}$	SFfs	combined emissivity view factor from the floor to the structure	-
$\mathcal{F}_{gsky}$	SFgsky	combined emissivity view factor from the glazing to the sky	-
$\mathcal{F}_{hg}$	SFhg	combined emissivity view factor from the heating system to the glazing	-
$\mathcal{F}_{hs}$	SFhg	combined emissivity view factor from the heating system to the structure	-
$\mathcal{F}_{mc}$	SFmc	combined emissivity view factor from the root medium to the crop	-
$\mathcal{F}_{mg}$	SFmg	combined emissivity view factor from the root medium to the glazing	-
$\mathcal{F}_{mh}$	SFmh	combined emissivity view factor from the root medium to the heating system	-
$\mathcal{F}_{ms}$	SFms	combined emissivity view factor from the root medium to the structure	-
$\mathcal{F}_{sg}$	SFsg	combined emissivity view factor from the structure to the glazing	-
f_{ao}	fao	rate of water vapour exchange between the inside and outside air per unit floor area	$g.m^{-2}.s^{-1}$

f_{ca}	fca	rate of water vapour exchange between the crop and the inside air per unit floor area	$g.m^{-2}.s^{-1}$
f_{drain}	fdrn	rate of water loss from the root medium by drainage per unit floor area	$g.m^{-2}.s^{-1}$
f_{drip}	fdrip	rate of water loss from the underside of the glazing by dripping per unit floor area	$g.m^{-2}.s^{-1}$
f_{fruit}	ffruit	rate of water loss from the crop by removal of fruit	$g.m^{-2}.s^{-1}$
f_{ga}	fga	rate of water vapour exchange between the glazing and the inside air per unit floor area	$g.m^{-2}.s^{-1}$
f_{irr}	firr	rate of water addition to the root medium by irrigation per unit floor area	$g.m^{-2}.s^{-1}$
f_{ma}	fma	rate of water vapour exchange between the root medium and the inside air per unit floor area	$g.m^{-2}.s^{-1}$
f_{up}	fup	rate of water uptake by the crop from the root medium per unit floor area	$g.m^{-2}.s^{-1}$
f_{gross}	FGross	rate of carbon dioxide removal from inside air by photosynthesis per unit floor area	$mgCO_2.m^{-2}.s^{-1}$
f_{growth}	FGrowth	rate of carbon dioxide addition to inside air by growth respiration per unit floor area	$mgCO_2.m^{-2}.s^{-1}$
f_{resp}	FResp	rate of carbon dioxide addition to inside air by maintenance respiration per unit floor area	$mgCO_2.m^{-2}.s^{-1}$
f_{vent}	Fvent	rate of carbon dioxide removal from inside air by ventilation per unit floor area	$mgCO_2.m^{-2}.s^{-1}$
$Field$	Field	field capacity of the root medium	$m^3H_2O.m^{-3}$
Gr	Gr	Grashof number	-
G_{fl}	Gfl	rate of conduction between the floor and the first soil layer per unit floor area	$W.m^{-2}$
G_{fm}	Gfm	rate of conduction between the floor and the root medium per unit floor area	$W.m^{-2}$
G_{12}	G12	rate of conduction between the 1st and 2nd soil layers per unit floor area	$W.m^{-2}$
G_{23}	G23	rate of conduction between the 2nd and 3rd soil layers per unit floor area	$W.m^{-2}$
G_{34}	G34	rate of conduction between the 3rd and 4th soil layers per unit floor area	$W.m^{-2}$

G_{45}	G45	rate of conduction between the 4th and 5th soil layer per unit floor area	$W.m^{-2}$
G_{5d}	G5d	rate of conduction between the 5th soil layer and the deep ground per unit floor area	$W.m^{-2}$
G_{sg}	Gsg	rate of conduction between the greenhouse structure and the glazing per unit floor area	$W.m^{-2}$
GAI	GAI	glazing area index	-
g	g	gravitational constant	$m.s^{-2}$
HAI	HAI	surface area of the heating system relative to the floor area	-
$\hat{H}_a$	Ha	enthalpy of the inside air per unit floor area	$J.m^{-2}$
$\hat{H}_c$	Hc	enthalpy of the crop canopy per unit floor area	$J.m^{-2}$
$\hat{H}_f$	Hf	enthalpy of the greenhouse floor layer per unit floor area	$J.m^{-2}$
$\hat{H}_g$	Hg	enthalpy of the greenhouse glazing per unit floor area	$J.m^{-2}$
$\hat{H}_m$	Hm	enthalpy of the root medium bags per unit floor area	$J.m^{-2}$
$\hat{H}_s$	Hs	enthalpy of the greenhouse structure per unit floor area	$J.m^{-2}$
$\hat{H}_1$	H1	enthalpy of the 1st soil layer per unit floor area	$J.m^{-2}$
$\hat{H}_2$	H2	enthalpy of the 2nd soil layer per unit floor area	$J.m^{-2}$
$\hat{H}_3$	H3	enthalpy of the 3rd soil layer per unit floor area	$J.m^{-2}$
$\hat{H}_4$	H4	enthalpy of the 4th soil layer per unit floor area	$J.m^{-2}$
$\hat{H}_5$	H5	enthalpy of the 5th soil layer per unit floor area	$J.m^{-2}$
h_{ao}	hao	advective heat transfer coefficient for ventilation heat loss	$W.m^{-2}.^{\circ}C^{-1}$
h_{Cca}	hCca	convective heat transfer coefficient of the crop	$W.m^{-2}.^{\circ}C^{-1}$
h_{Cfa}	hCfa	convective heat transfer coefficient of the floor	$W.m^{-2}.^{\circ}C^{-1}$
h_{Cga}	hCga	convective heat transfer coefficient of the inside of the glazing	$W.m^{-2}.^{\circ}C^{-1}$
h_{Cgo}	hCgo	convective heat transfer coefficient of the outside of the glazing	$W.m^{-2}.^{\circ}C^{-1}$
h_{Cha}	hCha	convective heat transfer coefficient of the heating system	$W.m^{-2}.^{\circ}C^{-1}$

h_{Cma}	hCma	convective heat transfer coefficient of the root medium	$W.m^{-2}.^{\circ}C^{-1}$
h_{Csa}	hCsa	convective heat transfer coefficient of the greenhouse structure	$W.m^{-2}.^{\circ}C^{-1}$
h_{Cfm}	hGfm	conductance between the floor and the root medium	$W.m^{-2}.^{\circ}C^{-1}$
h_{Cf1}	hGf1	conductance between the floor and the 1st soil layer	$W.m^{-2}.^{\circ}C^{-1}$
h_{C12}	hG12	conductance between the 1st and 2nd soil layers	$W.m^{-2}.^{\circ}C^{-1}$
h_{C23}	hG23	conductance between the 2nd and 3rd soil layers	$W.m^{-2}.^{\circ}C^{-1}$
h_{C34}	hG34	conductance between the 3rd and 4th soil layers	$W.m^{-2}.^{\circ}C^{-1}$
h_{C45}	hG45	conductance between the 4th and 5th soil layers	$W.m^{-2}.^{\circ}C^{-1}$
h_{C5d}	hG5d	conductance between the 5th soil layer and the deep ground	$W.m^{-2}.^{\circ}C^{-1}$
h_{Csg}	hGsg	conductance between the greenhouse structure and the glazing	$W.m^{-2}.^{\circ}C^{-1}$
h_{Rcg}	hRcg	radiative heat transfer coefficient from the crop to the glazing	$W.m^{-2}.^{\circ}C^{-1}$
h_{Rch}	hRch	radiative heat transfer coefficient from the crop to the heating system	$W.m^{-2}.^{\circ}C^{-1}$
h_{Rcs}	hRcs	radiative heat transfer coefficient from the crop to the structure	$W.m^{-2}.^{\circ}C^{-1}$
h_{Rfc}	hRfc	radiative heat transfer coefficient from the floor to the crop	$W.m^{-2}.^{\circ}C^{-1}$
h_{Rfg}	hRfg	radiative heat transfer coefficient from the floor to the glazing	$W.m^{-2}.^{\circ}C^{-1}$
h_{Rfh}	hRfh	radiative heat transfer coefficient from the floor to the heating system	$W.m^{-2}.^{\circ}C^{-1}$
h_{Rfm}	hRfm	radiative heat transfer coefficient from the floor to the root medium	$W.m^{-2}.^{\circ}C^{-1}$
h_{Rfs}	hRfs	radiative heat transfer coefficient from the floor to the structure	$W.m^{-2}.^{\circ}C^{-1}$
h_{Rgsky}	hRgsky	radiative heat transfer coefficient from the glazing to the sky	$W.m^{-2}.^{\circ}C^{-1}$
h_{Rhg}	hRhg	radiative heat transfer coefficient from the heating system to the glazing	$W.m^{-2}.^{\circ}C^{-1}$
h_{Rhs}	hRhg	radiative heat transfer coefficient from the heating system to the structure	$W.m^{-2}.^{\circ}C^{-1}$

h_{Rmc}	hRmc	radiative heat transfer coefficient from the root medium to the crop	$W.m^{-2}.^{\circ}C^{-1}$
h_{Rmg}	hRmg	radiative heat transfer coefficient from the root medium to the glazing	$W.m^{-2}.^{\circ}C^{-1}$
h_{Rmh}	hRmh	radiative heat transfer coefficient from the root medium to the heating system	$W.m^{-2}.^{\circ}C^{-1}$
h_{Rms}	hRms	radiative heat transfer coefficient from the root medium to the structure	$W.m^{-2}.^{\circ}C^{-1}$
h_{Rsg}	hRsg	radiative heat transfer coefficient from the structure to the glazing	$W.m^{-2}.^{\circ}C^{-1}$
I_{opdr}		intensity of direct PAR radiation above the crop	$W.m^{-2}$
I_{pbeam}	Ibeam	intensity of the direct PAR radiation beam absorbed in a layer of the crop	$W.m^{-2}$
I_{pdf}	Idf	intensity of diffuse PAR radiation absorbed in a layer of the crop	$W.m^{-2}$
I_{pdr}	Idr	intensity of direct PAR radiation absorbed in a layer of the crop	$W.m^{-2}$
I_{psc}		intensity of scattered PAR radiation absorbed in a layer of the crop	$W.m^{-2}$
I_{shd}	Ishd	intensity of PAR radiation absorbed by shaded leaves in a layer of the crop	$W.m^{-2}$
I_{sun}	Isun	intensity of PAR radiation absorbed by sunlit leaves in a layer of the crop	$W.m^{-2}$
i	I	leaf number	-
J		Julian day number	day
K_{bdf}	Kbdf	extinction coefficient for diffuse radiation in a stand of "black" leaves	-
K_{bdr}	Kbdf	extinction coefficient for direct radiation in a stand of "black" leaves	-
K_{d}	Kd	diffuse fraction index	-
K_{df}		extinction coefficient for diffuse radiation in real leaves	-
K_{dr}		extinction coefficient for direct radiation in real leaves	-
K_{ndf}	Kndf	extinction coefficient for NIR diffuse radiation in real leaves	-
K_{ndr}	Kndr	extinction coefficient for NIR direct radiation in real leaves	-
K_{pdf}	Kpdf	extinction coefficient for PAR diffuse radiation in real leaves	-

K_{pdr}	Kpdr	extinction coefficient for PAR direct radiation in real leaves	-
K_t	Kt	sky clearness index	-
k_f	kf	thermal conductivity of the floor	$W.m^{-1}.^{\circ}C^{-1}$
k_m	km	thermal conductivity of the root medium	$W.m^{-1}.^{\circ}C^{-1}$
k_1	k1	thermal conductivity of the 1st soil layer	$W.m^{-1}.^{\circ}C^{-1}$
k_2	k2	thermal conductivity of the 2nd soil layer	$W.m^{-1}.^{\circ}C^{-1}$
k_3	k3	thermal conductivity of the 3rd soil layer	$W.m^{-1}.^{\circ}C^{-1}$
k_4	k4	thermal conductivity of the 4th soil layer	$W.m^{-1}.^{\circ}C^{-1}$
k_5	k5	thermal conductivity of the 5th soil layer	$W.m^{-1}.^{\circ}C^{-1}$
Le	Le	Lewis number	-
L	LM or LL	length of a leaf	cm
L_i	LM(I) or LL(I)	length of the i-th leaf	cm
L_{i+1}		length of the i+1-th leaf	cm
L_R		reference length for a primordial leaf	cm
L_U		length of the unfolding leaf	cm
LAI	LAI	leaf area index	-
LCT		local civil time	hrs
LE_{ca}	LEca	rate of evaporative heat loss from the crop per unit floor area	$W.m^{-2}$
LE_{ga}	LEga	rate of evaporative heat loss from the glazing per unit floor area	$W.m^{-2}$
LE_{ma}	LEma	rate of evaporative heat loss from the root medium per unit floor area	$W.m^{-2}$
LST		local solar time	hrs
M_a	Ma	molecular mass of dry air	$gDA.mol^{-1}$
M_c		molecular mass of carbon dioxide	$gCO_2.mol^{-1}$
M_w	Mw	molecular mass of water	$gH_2O.mol^{-1}$
MAI	MAI	root medium surface area index	-
Nu	Nu	Nusselt number	-
Nu_{forced}	Nufor	Nusselt number for forced convection	-
Nu_{free}	Nufre	Nusselt number for free convection	-
N_{plant}	Nplant	number of plants in the greenhouse	plant
N_v	Nv	airchange rate	hr^{-1}

NC_i	NCM(I) or NCL(I)	relative number of cells along the mid-rib of the i-th leaf	cell.cell^{-1}
n	N	number of leaves below the unfolding leaf in which cell division is occurring	-
P_o	Po	barometric pressure	Pa
P		plastochron index of plant	-
P_{CO_2}	PCO2	carbon dioxide limited rate of photosynthesis for a single leaf	mgCO$_2$.m^{-2}.s^{-1}
P_{en}	Pend	endogenous rate of photosynthesis for a single leaf	mgCO$_2$.m^{-2}.s^{-1}
P_g		rate of gross photosynthesis for a single leaf	mgCO$_2$.m^{-2}.s^{-1}
P_{gmax}	PGmax	maximum rate of gross photosynthesis for a single leaf	mgCO$_2$.m^{-2}.s^{-1}
P_{nmax}	PNmax	maximum rate of net photosynthesis for a single leaf	mgCO$_2$.m^{-2}.s^{-1}
P_{shd}	PGshd	rate of gross photosynthesis for a single shaded leaf	mgCO$_2$.m^{-2}.s^{-1}
P_{sun}	PGsun	rate of gross photosynthesis for a single sunlit leaf	mgCO$_2$.m^{-2}.s^{-1}
P_t	Pt	rate of gross photosynthesis for a layer of sunlit and shaded leaves	mgCO$_2$.m^{-2}.s^{-1}
PGR_f'	PGRFmax	maximum potential growth rate of a fruit	mgDM.s^{-1}
$PGR(i)_f$	PGRFruM(I) or PGRFruL(I)	potential growth rate of the i-th fruit	mgDM.s^{-1}
q	Q	rate of leaf initiation in the apex of a stem	leaves.d^{-1}
q_s	Qs	stationary rate of leaf initiation in the apex of a stem	leaves.d^{-1}
Re	Re	Reynolds number	-
R	R	universal gas constant	J.mol^{-1}.K^{-4}
R_{cg}	Rcg	rate of net radiation exchange between the crop and the glazing per unit floor area	W.m^{-2}
R_{ch}	Rch	rate of net radiation exchange between the crop and the heating system per unit floor area	W.m^{-2}
R_{cs}	Rcs	rate of net radiation exchange between the crop and the greenhouse structure per unit floor area	W.m^{-2}
R_d	Rd	dark respiration rate for a single leaf	mgCO$_2$.m^{-2}.s^{-1}
R_{d20}	Rd20	dark respiration rate for a single leaf at 20°C	mgCO$_2$.m^{-2}.s^{-1}
R_{gsky}	Rgsky	rate of net radiation exchange between the glazing and the sky per unit floor area	W.m^{-2}

R_{fc}	Rfc	rate of net radiation exchange between the floor and the crop per unit floor area	$W.m^{-2}$
R_{fg}	Rfg	rate of net radiation exchange between the floor and the glazing per unit floor area	$W.m^{-2}$
R_{fm}	Rfm	rate of net radiation exchange between the floor and the root medium per unit floor area	$W.m^{-2}$
R_{fs}	Rfs	rate of net radiation exchange between the floor and the greenhouse structure per unit floor area	$W.m^{-2}$
R_{hf}	Rhf	rate of net radiation exchange between the heating system and the floor per unit floor area	$W.m^{-2}$
R_{hg}	Rhg	rate of net radiation exchange between the heating system and the glazing per unit floor area	$W.m^{-2}$
R_{hs}	Rhs	rate of net radiation exchange between the heating system and the structure per unit floor area	$W.m^{-2}$
R_{mc}	Rmc	rate of net radiation exchange between the root medium and the crop per unit floor area	$W.m^{-2}$
R_{mg}	Rmg	rate of net radiation exchange between the root medium and the glazing per unit floor area	$W.m^{-2}$
R_{mh}	Rmh	rate of net radiation exchange between the root medium and the heating system per unit floor area	$W.m^{-2}$
R_{ms}	Rms	rate of net radiation exchange between the root medium and the structure per unit floor area	$W.m^{-2}$
R_{sg}	Rsg	rate of net radiation exchange between the greenhouse structure and the glazing per unit floor area	$W.m^{-2}$
RGR_{ci}		relative growth rate of cells along the mid-rib of the i-th leaf	$cell.cell^{-1}.day^{-1}$
RGR_{p}		relative growth rate of the plant per plastochron	$cm.cm^{-2}.plast^{-1}$
RGR_{pi}		relative growth rate of the i-th leaf per plastochron	$cm.cm^{-2}.plast^{-1}$
RGR_{t}		relative growth rate of the plant per unit time	$cm.cm^{-2}.day^{-1}$
RGR_{ti}	RGR	relative growth rate of the i-th leaf per unit time	$cm.cm^{-2}.day^{-1}$
RH	RH	relative humidity of inside air	%
RWC_{c}		relative water content of the crop	-
RWC_{m}		relative water content of the root medium	-

r_{ao}	rao	advective mass transfer resistance between inside and outside of the greenhouse	$s.m^{-1}$
r_m	rm	mesophyll resistance	$s.m^{-1}$
r_{Vca}	rVca	boundary layer resistance of the crop for water vapour transfer	$s.m^{-1}$
r_{Vci}	rVci	internal leaf resistance for water vapour transfer	$s.m^{-1}$
r_{Vga}	rVga	boundary layer resistance of the glazing for water vapour transfer	$s.m^{-1}$
r_{Vma}	rVma	boundary layer resistance of the root medium for water vapour transfer	$s.m^{-1}$
S_c	Sc	circumsolar component of global solar radiation	$W.m^{-2}$
S_{df}	Sdf	diffuse component of global solar radiation	$W.m^{-2}$
S_{dr}	Sdr	direct component of global solar radiation	$W.m^{-2}$
S_{df}'	Sdf	diffuse component of global solar radiation corrected for circumsolar radiation	$W.m^{-2}$
S_{dr}'	Sdr	direct component of global solar radiation corrected for circumsolar radiation	$W.m^{-2}$
S_g	Sg	global solar radiation on the horizontal at the ground	$W.m^{-2}$
S_n	Sn	near infra-red solar radiation	$W.m^{-2}$
S_{ndf}	Sndf	diffuse component of near infra-red solar radiation	$W.m^{-2}$
S_{ndr}	Sndr	direct component of near infra-red solar radiation	$W.m^{-2}$
S_o	So	extra-terrestrial radiation on a horizontal surface	$W.m^{-2}$
S_p	Sp	photosynthetically active solar radiation	$W.m^{-2}$
$\overline{S}_p$	Light	average daily photosynthetically active radiation at the top of the crop	$J.m^{-2}.d^{-1}$
S_{pdf}	Spdf	diffuse component of photosynthetically active solar radiation	$W.m^{-2}$
S_{pdr}	Spdr	direct component of photosynthetically active solar radiation	$W.m^{-2}$
S_{sc}	Ssc	solar constant	$W.m^{-2}$
SAI	SAI	greenhouse structure area index	-
SLA	SLA	specific leaf area of the crop	$m^2.kgDM^{-1}$
s		slope of the saturation vapour pressure curve	$Pa.^{\circ}C^{-1}$
T_a	Ta	temperature of the inside air	$^{\circ}C$

$\overline{T}_c$	Temp	average daily crop temperature	°C
T_{ad}	Tad	dew-point temperature of the inside air	°C
T_{aw}	Taw	wet-bulb temperature of the inside air	°C
T_c	Tc	temperature of the crop canopy	°C
T_{cloud}		temperature of the cloud base	°C
T_d	Td	temperature of the deep ground	°C
T_f	Tf	temperature of the floor layer	°C
T_g	Tg	temperature of the greenhouse glazing	°C
T_h	Th	logarithmic mean temperature of the heating system	°C
T_m	Tm	temperature of the root medium	°C
T_o	To	temperature of the outside air	°C
T_{od}	Tod	dew point temperature of the outside air	°C
T_{ow}	Tow	wet bulb temperature of the outside air	°C
T_s	Ts	temperature of the greenhouse structure	°C
T_{sky}	Tsky	apparent radiant temperature of the sky	°C
T_1	T1	temperature of the 1st soil layer	°C
T_2	T2	temperature of the 2nd soil layer	°C
T_3	T3	temperature of the 3rd soil layer	°C
T_4	T4	temperature of the 4th soil layer	°C
T_5	T5	temperature of the 5th soil layer	°C
t	T	time	s
u_a	Ua	inside air velocity	$m.s^{-1}$
$\overline{u}_o$	Uo	outside wind speed at 10m above ground	$m.s^{-1}$
V_{gb}	Vgb	volume of glazing bars	m^3
V_m		volume of root medium	m^3
V_s	Vs	volume of structure	m^3
W		width of a leaf	cm
WHC_c	WHCc	water holding capacity of the crop	$gH_2O.gDM^{-1}$
WHC_m	WHCm	water holding capacity of the root medium	$gH_2O.gDM^{-1}$
w		humidity ratio	$gH_2O.gDA^{-1}$

X	X	eccentricity of the leaf angle distribution	-
X_{circ}		circumsolar radiation correction factor	-
x_b	Fbark	fraction of bark in the root medium	$m^2.mDM^{-3}$
x_{omm}	xomm	fraction of organic matter in the root medium	$m^2.mDM^{-3}$
x_{qm}	xqm	fraction of quartz minerals in the root medium	$m^2.mDM^{-3}$
Y	Y	parameter of the leaf angle distribution function	-
α	SAzi	azimuth of the solar beam	°
α_{cndf}	Acndf	absorptivity of the crop for diffuse near infra-red radiation	-
α_{cndr}	Acndr	absorptivity of the crop for direct hear infra-red radiation	-
α_{cpdf}	Acpdf	absorptivity of the crop for diffuse photosynthetically active radiation	-
α_{cpdr}	Acpdr	absorptivity of the crop for direct photosynthetically active radiation	-
α_{fn}	Afn	absorptivity of the floor for near infra-red radiation	-
α_{fp}	Afp	absorptivity of the floor for photosynthetically active radiation	-
α_{gdf}	Agdf	absorptivity of the glazing for diffuse radiation	-
α_{gdr}	Agdr	absorptivity of the glazing for direct radiation	-
α_{mn}	Afn	absorptivity of the root medium for near infra-red radiation	-
α_{mp}	Afp	absorptivity of the root medium for photosynthetically active radiation	-
α_{sdf}	Asdf	absorptivity of the structure for diffuse radiation	-
α_{sdr}	Asdr	absorptivity of the structure for direct radiation	-
α_{struc}	StrucAF	light absorption factor of structure	-
β	SAlt	solar altitude	°
Γ	Compoint	compensation point carbon dioxide concentration	$\mu l.l^{-1}$
Γ_{25}	Comp25	compensation point carbon dioxide concentration at 25°C	$\mu l.l^{-1}$
γ	Gamma	the psychrometric constant	$Pa.°C^{-1}$
Δ_a	da	average depth (height) of the greenhouse inside airspace	m

Δ_f	df	thickness of the floor layer	m
Δ_{gl}	dgl	thickness of the glazing	m
Δ_m	BagH	depth of the root medium bags	m
ΔT_h	delT	temperature difference between inlet and outlet of heater	°C
Δ_1	dl	thickness of the 1st soil layer	m
Δ_2	d2	thickness of the 2nd soil layer	m
Δ_3	d3	thickness of the 3rd soil layer	m
Δ_4	d4	thickness of the 4th soil layer	m
Δ_5	d5	thickness of the 5th soil layer	m
δ		solar declination angle	°
ϵ_c	ec	emissivity of the crop	-
ϵ_f	ef	emissivity of the floor	-
ϵ_g	eg	emissivity of the glazing	-
ϵ_h	eh	emissivity of the heating system	-
ϵ_m	em	emissivity of the root medium	-
ϵ_s	es	emissivity of the structure	-
$\epsilon_{sky}(0)$		emissivity of a clear sky	-
$\epsilon_{sky}(C)$	esky	emissivity of a cloudy sky	-
ζ_h	HBlock	radiation interception coefficient of the heating system	-
ζ_s	SBlock	radiation interception coefficient of the greenhouse structure	-
η	Eff	actual light use efficiency factor	$mgCO_2.J^{-1}$
η_{pot}	Eff0	potential light use efficiency factor	$mgCO_2.J^{-1}$
θ_a	La	exponential decay constant for the parameter a during primordial phase of leaf development	plast
θ_b	Lb	exponential decay constant for the parameter b during expanding phase of leaf development	plast
θ_c	Lc	exponential decay constant for the parameter c used to determine the unfolding leaf	-
θ_p	Lp	plastochron constant of adaptation	plast
ι		angle of incidence between a leaf and the solar beam	°
K_c	Kmc	hydraulic conductivity of the crop	$gH_2O.m^{-1}.s^{-1}.bar^{-1}$
κ_a	K	thermal diffusivity of air	$m^2.s^{-1}$
Λ		latitude of the greenhouse	°

λ_o	Lamb	latent heat of vapourization of water at reference temperature of 0°C	$J.g^{-1}$
ν_a	v	kinematic viscosity of air	$m^2.s^{-1}$
Ξ_a	XCO2a	carbon dioxide content of inside air per unit floor area	$mgCO_2.m^{-2}$
ξ_a	XiCO2a	carbon dioxide concentration of inside air	$mgCO_2.m^{-3}$
ξ_o	XiCO2o	carbon dioxide concentration of outside air	$mgCO_2.m^{-3}$
ρ_a	rhoa	density of dry air inside the greenhouse	$gDA.m^{-3}$
ρ_c		density of carbon dioxide in the greenhouse	$gCO_2.m^{-3}$
ρ_{cndf}	Rhocndf	reflectivity of a canopy of non-horizontal leaves and underlying floor for diffuse NIR radiation	-
ρ_{cndr}	Rhocndr	reflectivity of a canopy of non-horizontal leaves and underlying floor for direct NIR radiation	-
ρ_{cpdf}	Rhocpdf	reflectivity of a canopy of non-horizontal leaves and underlying floor for diffuse PAR radiation	-
ρ_{cpdr}	Rhocpdr	reflectivity of a canopy of non-horizontal leaves and underlying floor for direct PAR radiation	-
ρ_{dr}		reflectivity of a canopy of non-horizontal leaves for direct radiation	-
ρ_f		reflectivity of the floor	-
ρ_{hor}		reflectivity of a canopy of horizontal leaves for direct radiation	-
ρ_{ndr}	Rhondr	reflectivity of a canopy of non-horizontal leaves for direct NIR radiation	-
ρ_{nhor}	Rhonhor	reflectivity of a canopy of horizontal leaves for direct NIR radiation	-
ρ_{pdr}	Rhopdr	reflectivity of a canopy of non-horizontal leaves for direct PAR radiation	-
ρ_{phor}	Rhophor	reflectivity of a canopy of horizontal leaves for direct PAR radiation	-
σ	Sigma	the Stephan-Boltzmann constant	$W.m^{-2}.K^{-4}$
σ_n	Sign	scattering coefficient for NIR radiation	-
σ_p	Sigp	scattering coefficient for PAR radiation	-

τ_{cb}	Taucb	transmissivity of a canopy of "black" leaves for far infra-red radiation	-
τ_{cndf}	Taucndf	transmissivity of the crop for diffuse near infra-red radiation	-
τ_{cndr}	Taucndr	transmissivity of the crop for direct near infra-red radiation	-
τ_{cpdf}	Taucpdf	transmissivity of the crop for diffuse photosynthetically active radiation	-
τ_{cpdr}	Taucpdr	transmissivity of the crop for direct photosynthetically active radiation	-
τ_{gdf}	Taugdf	transmissivity of the glazing for diffuse radiation	-
τ_{gdr}	Taugdr	transmissivity of the glazing for direct radiation	-
τ_{R}	TauRF	greenhouse light transmission correction factor	-
Φ_{a}	Phia	thermal capacity of the dry air fraction of the inside air per unit floor area	$J.m^{-2}$
Φ_{c}	Phic	thermal capacity of the dry fraction of the crop per unit floor area	$J.m^{-2}$
Φ_{f}	Phif	thermal capacity of the dry fraction of the floor layer per unit floor area	$J.m^{-2}$
Φ_{g}	Phig	thermal capacity of the glazing per unit floor area	$J.m^{-2}$
Φ_{m}	Phim	thermal capacity of the dry fraction of the root medium per unit floor area	$J.m^{-2}$
Φ_{s}	Phis	thermal capacity of the dry fraction of the greenhouse structure per unit floor area	$J.m^{-2}$
Φ_{1}	Phi1	thermal capacity of the dry fraction of the 1st soil layer per unit floor area	$J.m^{-2}$
Φ_{2}	Phi2	thermal capacity of the dry fraction of the 2nd soil layer per unit floor area	$J.m^{-2}$
Φ_{3}	Phi3	thermal capacity of the dry fraction of the 3rd soil layer per unit floor area	$J.m^{-2}$
Φ_{4}	Phi4	thermal capacity of the dry fraction of the 4th soil layer per unit floor area	$J.m^{-2}$
Φ_{5}	Phi5	thermal capacity of the dry fraction of the 5th soil layer per unit floor area	$J.m^{-2}$
X_{a}	Xa	moisture concentration of the inside air per unit floor area	$g.m^{-2}$
X_{c}	Xc	moisture concentration of the crop per unit floor area	$g.m^{-2}$

X_c'	Xc	maximum moisture concentration of the crop per unit floor area	$g.m^{-2}$
X_f	Xf	moisture concentration of the floor layer per unit floor area	$g.m^{-2}$
X_g	Xg	concentration of moisture on the underside of the glazing per unit floor area	$g.m^{-2}$
X_m	Xm	moisture concentration of the root medium per unit floor area	$g.m^{-2}$
X_m'	Xm	maximum moisture concentration of the root medium per unit floor area	$g.m^{-2}$
X_1	Chil	moisture concentration of the 1st soil layer per unit floor area	$g.m^{-2}$
X_2	Chi2	moisture concentration of the 2nd soil layer per unit floor area	$g.m^{-2}$
X_3	Chi3	moisture concentration of the 3rd soil layer per unit floor area	$g.m^{-2}$
X_4	Chi4	moisture concentration of the 4th soil layer per unit floor area	$g.m^{-2}$
X_5	Chi5	moisture concentration of the 5th soil layer per unit floor area	$g.m^{-2}$
χ_a	Chia	absolute humidity of the inside air	$g.m^{-3}$
χ_o	Chio	absolute humidity of the outside air	$g.m^{-3}$
ψ_c	Psic	water potential of the crop	bar
ψ_m	Psim	water potential of the root medium	bars
Ω_c	Capc	hydraulic capacitance of the crop	$bars^{-1}$
Ω_m	Capm	hydraulic capacitance of the root medium	$bars^{-1}$
ω		hour angle of the sun	°

1 INTRODUCTION

1.1 HISTORICAL DEVELOPMENT OF THE GREENHOUSE

For nearly two thousand years mankind has known something of the benefits of placing plants under transparent shelters and providing supplementary heating to grow horticultural products in locations that have naturally unsuitable environments. Stanghellini (1987) in the entertaining and enlightening introduction to her thesis reports on the use of such techniques by the Romans to appease the tastes of the rich and powerful. Indeed it would appear that the Emperor Tiberius developed a taste for cucumbers which had to be satisfied daily. Plinius (77 A.D.) reports that these were 'grown in baskets fitted with wheels, so that they could easily be brought into the sun and on wintery days could be withdrawn into transparent shelters', which were most likely fashioned from mica. However, even at this early date there were critics of such 'high-technology', as Seneca (63 A.D.) who complained that: 'Are not living against Nature, they who covet a rose in winter, and by means of the vapours of hot water and by the apt modification of the environment, breed in wintertime that spring flower?' and Plinius (77 A.D.) wrote: 'Men are never satisfied with the things as Nature likes. Even [some] vegetables have to be grown only for the rich!'.

As glass became a common material, and techniques for producing it in flat sheets improved the 'orangeries' of the Baroque and Renaissance periods were developed (Van den Muijzenberg, 1980). These forerunners of the modern glasshouse were typically constructed as a 'lean-to' with an equatorial facing glass wall, and later roof, supported against a solid wall. Bot (1983) points out that during this period the greatest efforts were made to improve the light transmission, by including more glass in the wall and then the roof as better materials and construction techniques developed. Production in these enclosures was far from profitable, and aimed mainly, as in Roman times, at satisfying the tastes and curiosities, of the nobility and their friends. Later, this form of glasshouse was used commercially, particularly for the production of grapes at higher latitudes, in Europe.

By the turn of the century, construction techniques had advanced to the stage where the single span glasshouse, with glass in all the walls and the roof, was common. It was not until early in the century, however, that the first multi-span glasshouses were constructed. It is perhaps at this time that glasshouse growing 'came-of-age', as a commercially viable horticultural industry, albeit on a relatively small scale, supplying niche markets with expensive tastes. Since that time the industry has grown steadily, to become an important part of the agricultural economies of

several European nations, particularly The Netherlands, and the practice of growing under cover has been exported to North America, Japan, The Mediterranean, The Middle-East, and Australia and New Zealand, very often by growers of Dutch origin.

Perhaps the single greatest change in the greenhouse industry, since the Second World War, has been the introduction of plastics, both film and rigid sheets, as alternative glazings to glass. Due to the relatively lower cost of film plastic clad greenhouses, compared to traditional glasshouses, the 'plastics revolution' has done much to boost the greenhouse industries of Second and Third World countries. What was once solely a technique associated with increasing temperature for horticultural production in colder northern latitudes, is now a globally used technique of environmental modification, under a wide variety of climatic types. Associated with this has been a proliferation of greenhouse coverings, shapes, sizes, structures, and control techniques.

The next most important change in the nature of the greenhouse industry was to occur in the 1970's, when the price of energy escalated rapidly. This has galvanised growers, engineers, economists, horticulturalists, and biologists from every country with more than a few hectares of greenhouses, to embark on a somewhat frenzied search for optimal solutions to the management and control of protected cultivation systems. This is evident from the number of International Symposia related to the subject since that time: four specifically on energy in protected cultivation ([Sweden] Larsen, 1979; [Ireland] O'Flaherty & van der Borg, 1981, [U.S.A.] Short, 1984; and [U.K.] Bailey & Ferrero, 1989), plus biological aspects of energy saving ([Italy] Tongoni & Serra, 1988), potential productivity ([Japan] Takakura, 1978), high-technology ([Japan] Kozai, 1988b), control ([The Netherlands], van der Borg, 1978, Germing, 1985, [East Germany], Vogel, 1989), and modelling ([West Germany] Krug & Liebig, 1988).

Even a brief study of the material published from these symposia in the various volumes of Acta Horticulturae reveals a trend toward a closer dialogue between engineers, economists, biologists, plant physiologists and horticulturalists on the subject of optimal control and management strategies for greenhouse production. Today, in several nations with major greenhouse industries, interdisciplinary teams have been formed to tackle the problems of the industry on a broad front. The Netherlands, (Challa et al, 1988), West Germany, (Krug, 1989a), East Germany (Vogel et al, 1989), and Japan (Kozai, 1988a), can be cited as prime examples.

Closely parallel to the development of plastics, and the need for energy conservation, came several revolutions in the field of electronics and control. The invention of the transistor, and solid-state electronics that followed, considerably reduced the bulk and price of electronic equipment.

By the 1960's the more advanced greenhouse industries had adopted electronic control systems using solid-state electronic and analogue control techniques (Udink ten Cate, 1980). Feed-back control systems were used to control the greenhouse air temperature by way of automatic ventilators and heating systems, while solid-state timers were used to control irrigation.

The second major innovation came with digital electronics and the wide availability of micro-processors and analogue to digital conversion technology. Early digital control systems for greenhouses were developed around commercially available minicomputers (van Meurs, 1980), but by the late 1970's purpose built digital control systems appeared, primarily from Dutch companies such as Brinkman and Priva. The reason for the rapid adoption of these systems, in The Netherlands, was their competitive price when applied to the large scale enterprises of the Dutch greenhouse industry. On a large greenhouse complex, a single microprocessor based system could perform the tasks of many analogue controllers and timers. Furthermore the digital systems could record important environmental states, gathered from the greenhouse, and manipulate, store, retrieve, and display the results, giving the growers a great deal more information to work with in order to make crop management decisions.

Stimulated by the prospect of more powerful control solutions, using digital technology, several researchers began to look at the question of optimization of the greenhouse environment (Enoch, 1978a, 1978b, Udink ten Cate and van de Vooren, 1978, Seginer, 1980, Challa et al, 1981). The rationale for this can be found by considering that it is largely the greenhouse environment, in conjunction with crop management practises, such as planting density, pruning, and pest control, which determine both the productivity of the crop and the energy consumed to produce the crop. In this last decade, optimization of the greenhouse environment has been a major focus of international research, but little of this work has filtered down to the design of commercial control systems to become operative in real greenhouses. As pointed out by Seginer (1980) the main impediment to optimization is a lack of quantitative knowledge of the response of the crop to its environment, from which suitable models can be constructed.

1.2 JUSTIFICATION AND OUTLINE OF RESEARCH

In 1984, when this study began, the view from New Zealand as to where the greenhouse industry was heading in terms of energy conservation, environmental control and optimization was far from clear. From our comparative isolation, it appeared that while significant work had been done in both the engineering and biological aspects of greenhouse production, combined work was less obvious. Furthermore, much of the work

from Northern Europe needed to be assessed as to its applicability to protected cultivation in New Zealand, with its generally higher solar radiation levels and more temperate climate.

At this time a workshop on 'Energy in New Zealand Greenhouses' was organized under the auspices of the now defunct New Zealand Energy Research and Development Committee, as part of Contract 3298, and related to Contract 3255 (Breuer, 1985). Other documents arising from these contracts were: a survey of grower attitudes to energy in greenhouses (Phillips, 1984), and a survey of energy consumption and economics of greenhouses in the Auckland and Christchurch regions (MacKenzie, 1984). A further contract funded from this source looked at energy research in horticulture in Scandinavia and The Netherlands (Studman, 1984). These studies concluded that on the whole the New Zealand greenhouse industry was inefficient in its use of energy. The studies also recommended a wide range of techniques for, energy conservation, utilization of alternative fuels (solar and geothermal in particular), and improved control and management, as well as a programme of technology transfer and demonstration projects (Breuer, 1985). Withdrawal of government funding for energy research, massive reorganization within the government sectors responsible for agricultural research, and lack of organized grower involvement, have meant that these reports has gone largely unheeded.

Several speakers at the workshop highlighted the need for a better understanding of the relationship between the plant and its environment before significant progress on questions of control and management could be made, thus echoing the sentiments expressed by leading overseas researchers (Seginer, 1980, Udink ten Cate, 1980), and our own view point (Wells & Studman, 1984).

With this in mind a research programme was proposed with the aim of developing and testing mathematical models of the dynamic response of the greenhouse environment and of a crop growing within that environment. These models would not only add to the quantitative understanding of the dynamics of the greenhouse system but could then be used to study the efficacy of new controller designs, variations in environmental management practises, and new technologies, such as thermal screens, solar storage and closed cycle cooling systems.

In 1986 funding was secured in order to set up an environmental data logging system in a greenhouse. A data-logging system was duly purchased, and set up in a 100m^2 glasshouse at Massey University, Palmerston North. This included a variety of sensors to monitor the inside and outside environments, the response of the plants, and the actions of the control system. Information was collected from the greenhouse in the absence of

plants and during the full growing seasons of two crops of cucumbers. The first season was used as a trial to test the data logging system and the non-destructive plant measuring systems.

Based on fundamental physical principles and previous work by other researchers, models of the energy and mass balance of the greenhouse environment and the crop were developed and validated against the measured data. A model describing the development of cucumber plants and expansion of the leaf surface area, as a function of average environmental conditions, was also modified and tested against data collected from the cucumber crops. Research was also carried out on suitable models to predict short term photosynthetic production, maintenance and growth respiration, and dynamic partitioning of assimilated carbon amongst the various organs of the cucumber plants. Crop productivity was then determined by combining the environmental simulation model, the crop developmental model, and the photosynthesis, respiration, and partitioning models, and simulating the whole growth season. The results of this process were compared to the measured yield figures for the crops, to test the validity of the combined model.

1.3 ORGANIZATION OF THE THESIS

Chapter 2 contains general background information on modelling techniques and the nature of the greenhouse industry both internationally and in New Zealand.

Detailed information on the test greenhouse, the environmental data-logging system, and measurements of the cucumber crop have been included in Chapter 3.

Solar radiation entry in the greenhouse is discussed in Chapter 4. Models to predict light transmission and absorption by the greenhouse are evaluated and a modified model is validated. This is used to generate input to a combined greenhouse environment and cucumber crop model.

The greenhouse environment model is developed in Chapter 5, starting with a review of existing greenhouse environment simulation models. The model is dynamic in nature, being based on the differential equations governing the energy and mass balances of the greenhouse system. The model is validated against data collected from the test greenhouse.

Crop models are reviewed in Chapter 6 and models for photosynthesis (including radiation absorption in the crop canopy), respiration, partitioning, and development are derived. The leaf expansion model is validated separately against non-destructive measurements of a cucumber crop grown in the test greenhouse. The overall predictions of the combined

greenhouse environment and cucumber growth models, in terms of number and weight of fruit harvested, are then compared with the actual harvest records for the crop.

Conclusions and recommendations for further research are contained in Chapter 7, together with a discussion of the implications of this study to the greenhouse industry.

In Appendix 1 natural ventilation of a test greenhouse is considered. A non-linear parameter estimation technique is used to fit an empirical model for ventilation rate as a function of environmental and control variables.

In Appendix 2 an empirical model of stomatal response to environmental conditions is presented.

Listings of the greenhouse environment and crop simulation program, modified sections of the light transmission program, and data files are contained in Appendix 3.

2 OPTIMIZATION OF GREENHOUSE PRODUCTION

2.1 THE NATURE OF THE GREENHOUSE ENVIRONMENT

The greenhouse environment is the totality of the variables which determine the state of the air surrounding the aerial parts of the plants (the aerial environment), and the state of the soil, or media, surrounding the roots of the plants (the root environment).

The state variables of the aerial environment are:

- solar radiation intensity (including ultraviolet (UV), visible or photosynthetically active (PAR), and near infra-red (NIR) radiation)
- long wave radiation intensity (emitted from surrounding surfaces)
- temperature
- moisture content (humidity)
- gas composition (carbon dioxide and oxygen)
- air velocity within the plant canopy

The state variables of the root environment are:

- temperature
- moisture content
- physical condition of the media
- nutrient availability
- pH
- gas composition (carbon dioxide and oxygen)

Since these environmental state variables are important to all plants, whether grown outside or under cover, it is important to consider what effect the presence of the greenhouse has on the environment within it. Businger (1963) states that the earliest theory on the influence of the greenhouse, developed in the late 19th century, was the mousetrap theory (so called "greenhouse effect") which ascribed the high temperatures obtainable in a glasshouse to the ability of glass to transmit solar

radiation into the structure, while preventing long-wave radiation from the plants and soil from leaving. In 1909, Wood carried out an experiment which showed that the mousetrap theory was invalid and ascribed the temperature rise to the lack of air exchange between the inside and outside. He compared the temperature in a glass shelter to that in a shelter made of rocksalt, which is transparent to long wave radiation, and found no significant difference, when the two shelters were placed in the sun. A similar experiment (Van Gulik, 1910) showed that the rate of temperature decrease under the rocksalt was only slightly greater than under glass, but can largely be discounted due to the fact that the experiment was carried out inside a room where net long wave radiation was insignificant.

Little research was conducted on the greenhouse environment until after World War II. Businger (1963) developed an energy budget model for a glasshouse and concluded that the greenhouse effect contributed about 20% of the temperature rise inside compared with outside, the remainder being the result of reduced air exchange. He also concluded that the natural greenhouse environment of an uncontrolled closed greenhouse would be like that of a desert, with no precipitation, and wide temperature fluctuations rising to 40 or 50°C above ambient during daylight hours and falling to close to ambient during the night.

Other pertinent observations can be drawn about the greenhouse environment compared to the ambient environment. Solar radiation levels will be lower, and the spectral characteristics modified as a result of variable transmission and reflection characteristics of the glazing. Net long wave exchanges will be reduced due to isolation from the sky, which acts as a major sink for long wave heat fluxes, and thus there will be significant changes in the energy balances of the surfaces within the greenhouse. The humidity will be increased and the gas composition modified due to reduced exchange rates with the ambient. Air velocities will be reduced and thus potentially reduce heat and mass transfer rates from the plants and the soil surface. The lack of natural precipitation will affect the soil moisture content, and thus soil temperature, gas composition, and the chemical and biochemical processes taking place there. The alteration to the energy and mass balance of the plants, both in the aerial and root environments may cause significant shifts in the rates of the biological processes affecting the rates of development and growth.

2.2 THE NATURE OF GREENHOUSE CROP PRODUCTION

The state of the environment affects both the state of the plant and the rate of biochemical processes within the plant.

Many alternative state variables for a plant could be proposed, depending on the level and detail of the study. On a macroscopic level plant architecture (size, shape and arrangement of organs) is important since this affects light capture. Also for an ornamental plant, the appearance will effect the marketability of the crop. On a microscopic level, the concentration and location of each chemical within the plant could be considered, since these affect the rate of the fundamental life processes of photosynthesis, respiration, protein formation and breakdown, translocation, and nutrient uptake. In the middle ground lie states such as temperature, moisture content, dry matter content and distribution, and the relative concentration of the major chemical groups (carbohydrates, proteins, lipids, lignins, organic acids, and minerals). The states used to describe a plant or crop will thus depend on the level at which information is desired.

The common crops grown under protected cultivation can be divided into four broad categories: vegetable crops (usually annual salad vegetables such as tomatoes, cucumbers, melons, lettuce, and peppers), cut-flower crops (perennial or semi-perennial plants grown for bloom production such as roses, chrysanthemums, and carnations), ornamental crops (pot plants such as poinsettia, African violets, ferns, and many others typically of tropical or sub-tropical origin), and nursery crops (propagation of seeds, cuttings, and clonal material for use in other sectors of the horticultural industry). Often the last two categories are combined since their requirements are similar and they are often found within the same enterprise. Due to the very different nature of the requirements of vegetable and cut-flower crops it is most unusual to find commercial enterprises which combine these two types of production. However, the combinations of vegetable and [vegetable] nursery, cut-flower and ornamental plus nursery, or cut-flower and nursery are more common. Usually the nature of a greenhouse enterprise is dictated by the preferences and experience of the owner or grower, possibly tempered by the nature of the local climate and market, or access to a transport distribution network if the crop is to be marketed further afield.

2.2.1 Greenhouse Vegetable Production

Greenhouse vegetable production is typically arranged around the production of one or more salad crops on a rotational basis within a calendar year.

2.2.1.1 Once-A-Year Mono-Cultures

The simplest system is a mono-culture. This has the advantage of reducing the amount of specialized ancillary equipment required to handle the crop, (planting, spraying, pruning, harvesting, grading, and packaging), and the specialist crop knowledge that the grower must accumulate. For crops with a

relatively long season such as tomatoes or cucumbers one or two crops may be grown. Usually the main crop will be grown during the winter when prices are high due to lack of competition from outdoor grown varieties. This means that the crop initially requires supplementary heating but will grow into increasing light levels in spring which results in higher overall yields. The exact planting date should be managed to ensure that the crop is producing when the market prices are best, tempered by the production and heating costs, in order to maximise the profitability of the crop. This is not easy to do since the heating cost will vary depending on the weather, and market prices may vary considerably due to the supply and demand situation during the harvest period. In reality most growers will base their decisions on what happens in an average year and accept that fortunes may change from year to year.

While soil growing is still common, perhaps the most significant recent trend in greenhouse vegetable production has been the adoption of hydroponic (soil-less) growing systems, particularly the Nutrient Film Technique (NFT), rockwool, sand, and bag culture systems.

The principal environmental management concerns of a vegetable grower generally relate to the management of temperature, and the supply of water and nutrients. A grower may also be interested in humidity and its effect on plant diseases, but generally speaking no effort is made to control humidity precisely, but simply to limit the occurrence of very high humidities, usually by ventilation. Water and nutrients are usually supplied at fixed rates based on recommendations for the crop, which slightly over supply the real need. Many modern greenhouses combine irrigation and nutrient application in a technique called fertigation. This is the norm for hydroponic growing systems. Recently there has been a trend toward adjusting the amount and frequency of irrigation based on the integral of solar radiation received inside the greenhouse, to more closely match the crop's needs and conserve water, and nutrients.

Control of the air temperature emerges as the only system which is normally controlled using conventional closed loop feed-back control techniques. Temperature management is critical in greenhouse vegetable production, and the mono-culture system offers the greatest flexibility for temperature manipulation. It has been shown that the long term response of many vegetable crops is related to daily average temperature rather than instantaneous temperature (Slack & Hand, 1983). Thus it is now the norm in vegetable production to programme variable day and night temperatures to reduce heating costs at night and ventilation requirements during the day.

The mean and amplitude of diurnal temperature variation may also vary throughout the life of the crop depending on developmental stage (for example propagation, vegetative phases, fruit initiation, harvest). For all

the important vegetable crops, recommended temperature programmes, or "blue-prints", have been developed. While these are often used widely between different locations and even different nations they should be treated with some caution, as not only do they take into account the response of the plant, but also the fuel prices prevailing at the time and in the location that they were developed. Blue-prints therefore provide valuable guide lines but should not be treated as the final word in temperature management.

2.2.1.2 Rotational Multi-cultures.

The decision to crop twice in one year, must be made on a combination of economic and practical grounds. If a second crop is planted in summer, at the end of the productive life of the main crop, then there may be practical problems associated with cooling the greenhouse, and the crop may not be competitive with outdoor varieties. Decisions related to environmental modification will be similar to those decided above.

Bi-cultural systems usually revolve around a main crop of tomatoes, cucumbers, or melons, supplemented by a secondary crop of shorter duration such as beans, peppers or lettuce, depending on the local economics.

2.2.1.3 Rotational Mono-cultures

Short turn around crops such as lettuce, and the new mono-stem tomato production system, are often grown year round in blocks within a greenhouse, on a rotational basis. Crop yield is very dependant on light levels and thus the grower may consider the use of supplementary lighting during winter to maintain a more even production rate from month to month. In this single environment system, temperature regulation will be based on average crop requirements, with the possibility of some seasonal variations based on light levels and the economics of heating versus current market prices.

2.2.2 Greenhouse Cut-Flower Production

Cut-flower production under protected cultivation is typically associated with the production of at least one of the common cut-flowers used by florists (roses, carnations, orchids, chrysanthemums, gypsophila, alstermeria, and statice). Since these are mostly perennial plants decisions about crop planting dates are irrelevant. The main aim of the grower is to control flowering of the plants to produce high quality blooms at a rate to meet market demands. This generally means a steady base level of production with peaks to meet important dates such as Valentine's Day and Mother's Day, when prices are higher. Control of bloom production in this way poses several problems. Where production is related to light

intensity, as is the case for most cut-flower crops, the natural annual cycle of production, can be modified using shade, and supplementary assimilation lighting. The former is relatively cheap, while the latter is expensive. Temperature may also be used to control plant production but only within the extent allowed by the effect of temperature on quality.

With many cut-flower varieties day-length is an important determinant of floral initiation, and therefore day-length control is essential. Techniques for day-length modification include photo-period lighting (at low intensities) and blackout screens. Temperature and humidity are important determinants of bloom quality and thus accurate control is required. Adequate heating and ventilation capacity is essential, and often some form of evaporative cooling is used.

2.2.3 Greenhouse Ornamental and Nursery Production

Ornamental plant production under cover probably presents the greatest management problems to a grower. To be economically viable most enterprises of this sort must grow a range of different crops. The environmental requirements for optimum production will be different for each species and cultivar, and will vary throughout the life of a crop. Therefore some compromises must be made. Generally an enterprise of this nature will have different environments devoted to broad categories of crop requirement. Typically separate growing environments would be provided for propagation, and growing-on of temperate plants, tropical plants, and desert plants. The grower must then decide how to manage the plant material flow through each of these environments to ensure that the area that is available is used with the maximum efficiency. Environmental regulation is thus more straight forward since a standard set of conditions can be maintained in each environment all year round.

Only on very large enterprises, where each environment is dedicated to the production of a specific plant, can environmental programming be considered. In this case however, it is more usual to move the plants through a progression of different environments, rather than leaving the plants in a single environment and change the environment as the plants develop. To reduce the amount of labour involved with moving plants various forms of portable benches have been developed.

2.2.4 Summary

In summary it is possible to identify a decision making process through which greenhouse growers must go, in order to effectively manage their greenhouse facilities. While the importance of each step to profitability may vary between enterprises, at some stage these steps are common to all greenhouse production systems.

- The greenhouse facility is planned and constructed. Decisions on size, form and glazing type affect initial cost (and hence debt servicing), maintenance costs, light levels available, and energy requirements to run the facility.

- The crop or crops to be grown are selected. This affects initial cost (for seeds or plants), expected return, utilisation level of the facility, and the broad range of acceptable environmental conditions that must be maintained.

- Planting dates are chosen. This will affect the cost of growing the crop in relation to the duration of stay in the greenhouse, expected harvest date (and hence market prices), and prevailing outside weather conditions (hence heating/cooling costs).

- Environmental control trajectory is selected. This affects costs in conjunction with the chosen planting date, and largely determines the final yield and quality.

- Crop management decisions are made during the life of the crop. Spraying, pruning and harvesting require inputs of materials and labour, and affect final yield and quality.

The role of engineering research in the above scheme of management decisions has traditionally been in the first stage, in designing the facility. More recently, however, engineers have contributed research to the selection of appropriate environmental control strategies, by applying the theory of optimal control to the greenhouse production system (Seginer, 1980, Udink ten Cate, 1983). The aim of the research described in this thesis was to contribute to the understanding of the dynamic nature of the greenhouse environment, and the resulting response of a crop. The method chosen to accomplish this aim was to use mathematical models and numerical simulation techniques to predict the state of the greenhouse environment, and the crop, in response to changing outside weather disturbances, and control inputs. In order to validate these models, environmental and crop data was collected from a real greenhouse, over a two year period.

2.3 MODELS AS TOOLS FOR OPTIMIZATION AND CONTROL

Before considering the various published models of the greenhouse environment, it is worth considering the basic types of model which are available.

2.3.1 Of Axioms, Empiricism and Analytical Models

The Concise Oxford Dictionary defines an axiom as an 'established principle, or self-evident truth'. In model building, as in most endeavours, axioms are used without a great deal of thought. For instance, the Law of Conservation of Mass, and the First Law of Thermodynamics, which form the underlying basis of an energy and mass balance model, are often considered to be established principles, yet without the assumption of their validity, any model based on these axioms is also invalid.

The terms Black-box and empirical are used to describe models which predict the relationship between outputs and inputs to a system at a particular organisational level without trying to explain the internal nature of these relationships. More recently, the term 'time series' model has come into general use by control engineers. Time series models relate the values of outputs, at a discrete moment in time to the values of the inputs and outputs at past discrete moments in time. A time series model therefore is a discrete representation of a system that may be either continuous or discrete (see section 2.3.4).

Analytical models describe the relationship between outputs and inputs of a system with reference to processes occurring at subordinate levels, and therefore increase the understanding of the nature of the internal relationships within a system. It must be pointed out that, at some level within an analytical model, recourse to empiricism is necessary. Analytical or explanatory models take their name from the process by which they are derived. A system is first analysed, by breaking it down into smaller parts, and then the model of the system is synthesized from representations of these constituent parts. Ideally, the constituent parts of the model should be general and axiomatic. However, to achieve this the degree of abstraction required may be far greater than warranted by the desired aims of the modelling exercise. In this case the modeller must resort to using empirical models to describe the response of some parts of the system.

2.3.2 Dynamic and Steady State Models

Models which predict the rate of change of the states of a system with time, are said to be dynamic. An analytical model which is dynamic will be defined by a set of differential equations describing the motion of the system states. Integration of these equations, in time, reveals the position of the states of the system.

Steady state models form a subset of dynamic models in which the time varying parameters are set to zero. Thus, it is assumed that such a system

attains steady state instantaneously in response to a step input change. A steady state analytical model is defined by a set of algebraic equations, which when solved reveal the steady state values of the system variables.

When the rate of change of the surroundings is similar to, or smaller than, the time constant of the system, then a steady state model will be a poor approximation and a dynamic model should be used.

2.3.3 Deterministic and Stochastic models

A deterministic model makes definite predictions about the magnitude of an output variable without any associated prediction of the likely variability of that variable. A stochastic model considers the probability distribution of the output variable and will predict the expected value, or mean output, and the associated variance. Due to the increased complexity of stochastic models their use is usually limited.

2.3.4 Continuous and Discrete Models

A continuous model is one in which the output of the model changes continuously with time, whereas a discrete model is one in which the output changes only at certain times and is constant between those times. Discrete models have arisen from the use of computers, and numerical solution techniques, which cannot use continuously varying analogue signals directly, but must convert these to discrete digital representations.

2.4 IDENTIFICATION OF THE GREENHOUSE SYSTEM

Several authors have developed systems models of greenhouse production (Copet & Videau, 1981, Udink ten Cate, 1983, Bögemann, 1984). A feature of these representations is their similarity. All these authors have identified greenhouse production as hierarchical systems containing three levels (Figure 2.1).

The lowest level is the greenhouse environment and it associated control. The next level above this is the short term response of the crop, which is determined by the instantaneous levels of the environmental states and the state of the plants itself. From the point of view of optimal control, it has been suggested that it is at this level that the set-point trajectories for the lower level should be determined (Udink ten Cate & Challa, 1984). The third level includes the long term response of the crop, in terms of development and yield, to the greenhouse environment and other management practises. It is at this level where the grower makes decisions as outlined in section 2.2.4.

Various authors have begun to investigate the possibilities of optimizing the operation of greenhouse systems using predictive models as tools (Seginer, 1980, Challa et al, 1981, Shina & Seginer, 1989, Jones et al, 1989c). It is on this basis that this thesis will proceed, building on the foundation of existing models of the greenhouse environment, and crop growth, to produce and validate a model for the production of greenhouse cucumbers.

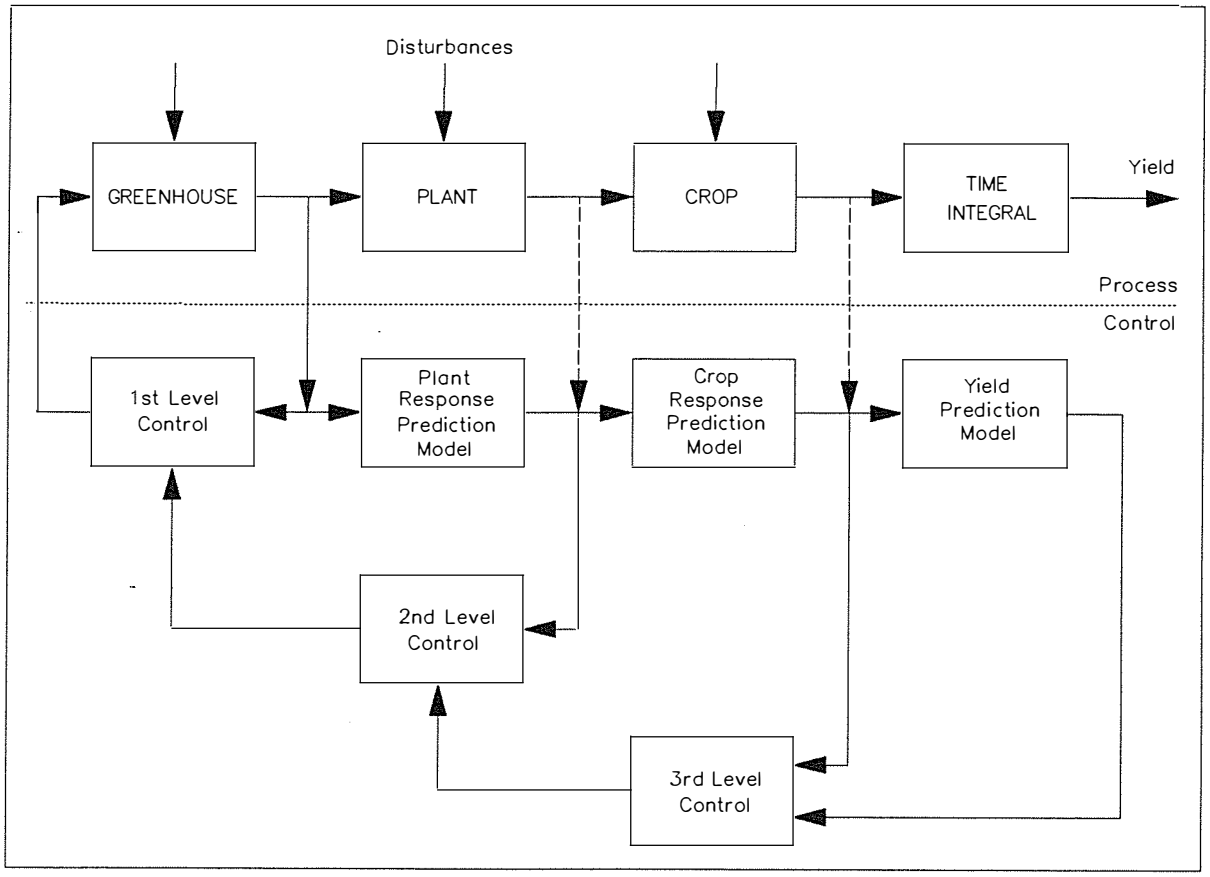

Figure 2.1. Three Level Representation of the Greenhouse System

3 EXPERIMENTAL PROCEDURES

In this chapter the various experiments performed in order to validate the simulation models will be described. The first section describes the collection of data describing the greenhouse environment. The second section deals with data describing the growth and development of the cucumber crop.

3.1 MEASUREMENT OF THE GREENHOUSE ENVIRONMENT

In order that the greenhouse energy and mass balance model described in Chapter 5 could be validated, the environment in a single-span glass-clad greenhouse, (Glasshouse No. 23) sited in the Plant Growth Unit (PGU) at Massey University, Palmerston North, was monitored during parts of four successive years. The data-logging system was initially installed during the early months of 1987. The system was first tested between July 8th, 1987 and October 27th, 1987, during which time a crop of cucumbers was present in the house. Based on this first monitoring period certain refinements were made to the data-logging system and additional sensors were added. Two further experiments were conducted with a crop of cucumbers present between July 5th, 1988 and November 21st, 1988, and again between August 30th, 1989 and December 20th 1989. In addition, three periods of monitoring were conducted with no plant material present in the house, June 21st to August 1st, 1989, August 16th to August 29th, 1989, and January 16th, to January 30th 1990. This information is summarised, with other details of the experiment in Table 3.1.

Table 3.1. Schedule of Experiments

Date	Activity
18/05/87	Commenced installation of data-logging equipment in No. 23 greenhouse at Plant Growth Unit.
19/05/87	Seeds sown in 75 mm peat pots in nursery greenhouse.
09/06/87	Tests on greenhouse ventilation system commenced.
15/06/87	Tests on greenhouse ventilation system concluded.
16/06/87	Seedlings transplanted to PB18 bags in greenhouse. Full calibration of all temperature and moisture sensors.
08/07/87	Trial data-logging on greenhouse environment commenced.
30/07/87	Measurements of leaf area performed for leaf area correlations.
11/08/87	First harvest of fruit.
27/10/87	Last harvest of fruit.

Table 3.1. Schedule of Experiments (continued)

Date	Activity
08/06/88	Seeds sown in 75 mm peat pots in nursery greenhouse.
28/10/87	All plants removed from greenhouse. Data-logging concluded for season.
25/06/88	Tests on greenhouse ventilation system commenced.
28/06/88	Tests on greenhouse ventilation system concluded.
29/06/88	Seedlings transplanted to PB18 bags in greenhouse.
05/07/88	Data-logging of greenhouse environment commenced.
18/08/88	First non-destructive measurements of leaf areas and node numbers.
30/08/88	First harvest of fruit.
18/10/88	Experiment to determine potential growth rate of fruit commenced.
20/10/88	Fruit collected for determination of dimensional correlations and moisture content.
08/11/88	Last harvest of fruit for media trials.
21/11/88	Last non-destructive measurements of leaf areas and node numbers.
22/11/88	Experiment to determine potential growth rate of fruit concluded.
25/11/88	Last actual harvest of fruit.
26/11/88	All plants removed from greenhouse. Data-logging concluded for season. Destructive measurement of 8 trial plants.
21/06/89	Data-logging of environment commenced in empty greenhouse.
01/08/89	Data-logging suspended.
02/08/89	Seeds sown in 75 mm peat pots in nursery greenhouse.
03/08/89	Further tests on greenhouse ventilation system.
16/08/89	Data-logging of greenhouse environment recommenced.
30/08/89	Seedlings transplanted to PB18 bags in greenhouse.
02/09/89	First non-destructive measurements of leaf areas and node numbers.
10/10/89	First harvest of fruit.
13/12/89	Last non-destructive measurement of leaf areas and node numbers.

Table 3.1. Schedule of Experiments (continued)	
Date	Activity
15/12/89	Last harvest of fruit.
20/12/89	All plants removed from greenhouse. Data-logging concluded for season. Destructive measurements of 8 trial plants.
16/01/90	Data-logging in empty greenhouse commenced.
30/01/90	Data-logging in empty greenhouse concluded.

3.1.1 Description of the Greenhouse and Site

The greenhouse used in the experiments was typical of glasshouses erected in New Zealand in the 1960's and 70's (Plate I), consisting of lapped glass panes held between aluminium glazing bars running in the vertical plane of the house supported by a steel frame. The overall dimensions of the house were 15.5 m long by 6.6 m wide. The height from the ground to the gutter was 2.1 m, and to the ridge 4.0 m, giving a roof slope of 30° (Figure 3.1). The glass panes measured 605 mm high by 750 mm wide in the side walls and roof, and 605 mm high by 580 mm wide in the end walls. The overlaps were approximately 10 mm and tight, but not sealed. The glazing bars were supported by a steel frame consisting of 75 x 75 angle purlins running in the horizontal plane over portal frames at 3 m centres constructed from 125 x 65 mm RSJ's (rolled steel joists). Two aluminium sliding doors at each end of the house opened to a maximum of 2.5 m and were 2.4 m high. Framing for the doors in each end wall were 75 x 75 RHS's (rectangular hollow sections). The portal frames were bolted to a concrete nib wall foundation which formed a continuous perimeter around the edge of the floor. All steel members had been painted with a grey coloured, zinc based paint.

The major axis of the house was 60° east of north, giving the greenhouse a predominantly east-west alignment. A similar greenhouse was situated to the south-east with a gap of 4 m. Another row of similar greenhouses was situated 6 m away to the north-east. A row of smaller greenhouses was situated 6 m away to the north-west, and a utility building was 3 m away to the south-west. These buildings cast significant shadows during low sun elevations. A hill to the east of the site meant that sunrise time for the site was delayed by approximately 30 minutes on average. The northern and western sides of the site were flat, and thus the site is relatively exposed to the prevailing west to north-west wind. The southern aspect of the site is flat, but covered by other buildings of the PGU, and the local DSIR station. An orchard with newly established shelter belts was sited approximately 400 m to the south-west. These shelter belts grew significantly during the four years of the experiments.

Plate I. No 23 Greenhouse, Plant Growth Unit, Massey University. View of Greenhouse looking West.

Ventilation was achieved via continuous side vents, and a continuous gull-wing ridge vent. The side vent openings were 630 mm deep and the operating mechanism allowed a maximum opening angle of 40°, giving a maximum opening of 440 mm. The ridge vent openings were 600 mm deep, with a maximum opening angle of 33°, giving a maximum opening of 340 mm. Each of the four ventilator windows was driven by a 240 VAC electric motor and a worm gear driving a threaded push rod operating a bell crank mechanism.

Heat was supplied by four horizontal discharge unit heaters supplied with hot water at approximately 80°C from the central gas-fired calorifier. This calorifier supplied heat to approximately 50 separate environments within the PGU via a two pipe (supply/return) system, with four separate underground circuits. Pressure in the supply line at the boiler house was maintained at a head of approximately 15 m by a centrifugal pump. At the greenhouse, hot water flowed from the underground supply main through 1¼" steel pipe to the unit heaters via an isolating gate valve and a solenoid control valve positioned in the south-east corner of the house. Water returned to the return main via a similar pipe and another isolating gate valve. The solenoid valve did not seal properly which meant that a minimum flow of approximately 1.2 $l.min^{-1}$ was always present, giving rise to a

background heat input of approximately 2 kW. During the later half of November 1989 the central heating system was completely shut down when repairs to a leaking main circuit were carried out.

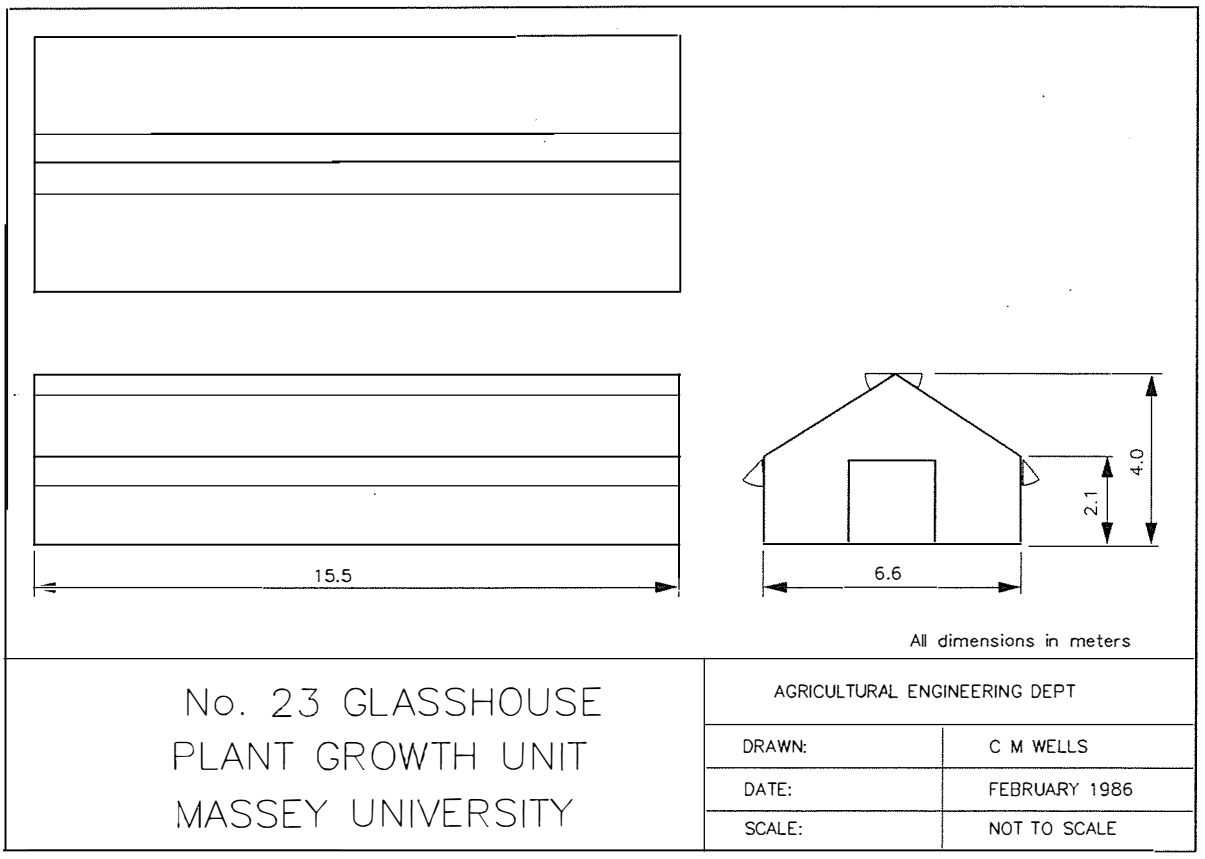

Figure 3.1. Plan of No. 23 Greenhouse, Plant Growth Unit

The air temperature in the greenhouse was controlled by an electronic control system manufactured by PYE Ltd, circa 1970. A resistance temperature sensor was mounted in an aspirated screen hung in the centre of the greenhouse approximately 1.5 m above the ground. The controller had separate heating and ventilation set-points which were selected via potentiometers on the front panel. The heating control was on/off with an internal specified dead-band, which appeared to be approximately 2°C. The ventilator control was time-proportional[1], with on and off cycle times which could be specified by the user via front panel potentiometers. These were usually set to give a 40 second on cycle and 60 second off cycle, as experience had shown this to give reasonable control, while avoiding hunting of the system. However, due to frequent changes of personnel

1 When the measured air temperature was above the set-point the ventilators were driven open for the specified on cycle time. The system then waited for the specified off cycle time before again comparing the temperatures. If the air temperature was below the set-point then the ventilators were driven closed for the specified on cycle time. Limit switches on the drive mechanism over-rode these commands to protect the drive motor.

responsible for growing the cucumber crop, these settings were often varied without warning. Over-ride switches were also provided to isolate individual ventilators. Thus it was possible to operate the house with any combination of vents. Additional controls for misting were not used.

The cucumber crops were watered and fed via a trickle irrigation system. Two main lines ran down either side of the greenhouse. Laterals, with micro-tube whiskers, ran into the centre of the greenhouse down each row. The head works (nutrient tanks, injection pumps and filters) were situated in the north-west corner of the house. Irrigation was controlled using a programmable time clock. Overhead watering lines were also fitted but these were not used.

The house was also fitted with an LPG burner (Barta type) for carbon dioxide enrichment, but this was not used during the experiments.

The floor of the house was soil, covered with a layer of black polyethylene. The floor of the house had been formed to give a raised path down the centre of the house, and between each row. The cucumber plants were grown in 6 litre black polyethylene planter bags (PB18's) and placed in the resulting depressions, which sloped toward the outside perimeter of the house to afford drainage.

Crop wires ran from gutter to gutter, at appropriate spacing, and the cucumbers were trained on to these using string (Plate II).

3.1.2 Data-Logging System

The data-logger used in the experiments to measure the greenhouse environment was a Campbell Scientific 21XL (Campbell Scientific, 1984) with two additional AM32 multiplexers. This gave a total input capability of 78 single ended analogue voltage inputs, and four pulse counting channels. In addition 6 digital and 4 controlled analogue outputs were available for controlling measurement equipment (2 of each were used to control the multiplexers). A 12 VDC supply was also available to power transducers. The lead acid battery was kept continually charged by a trickle charger. This was necessary as considerable use was made of the 12 volt supply.

Full use was made of the data-loggers programming features in order to obtain the output data in a nearly usable form, and thus avoid unnecessary post data-logger manipulation of data. The environmental variables were scanned at 30 second intervals and output every 5 minutes. Variables were either averaged, totalized, or sampled, depending on the nature of the variable. After the program was developed it was saved on to a cassette tape. This facilitated rapid re-programming, which was required after the system was shut down between experiments.

Plate II. Cucumbers soon after transplanting. View looking North.

Output data was stored on cassette tapes using a SC93 interface and a data cassette recorder. Using C60 cassettes, one week's data could be stored on one side of a cassette. Occasionally short cassettes caused information to be lost if the cassette reached the end before the tape was due to be changed. In most cases however this information could be retrieved by backing up the data-logger's output ring memory and performing a complete memory dump. For this reason the maximum possible available memory was assigned to output data after the program was developed.

The data-logger, multiplexers, and various other electrical equipment was housed in an old refrigerator, with the refrigeration plant and some insulation removed, which was placed in the south-western corner of the greenhouse underneath the controller (Plate III). This proved most effective at keeping the equipment clean, dry, and free from spray contamination.

3.1.3 Measured Variables

The measured variables can be divided into two categories, boundary variables required to drive the simulation model, and internal variables necessary to validate the predictions of the model. The measured variables are listed in Table 3.2, along with the type of measuring instrument used.

Plate III. The Data-Logging System.

Table 3.2. Data-Logging Instrumentation

Measured Variable	Instrument	Model & Make
Outside Temperature	Encapsulated AD590 Temperature Sensor in aspirated screen	Ag. Eng. Dept.
Outside Wet Bulb Temp	AD590 in aspirated screen	Ag. Eng. Dept.
Outside Solar Radiation	SRI3 Pyranometer	Solar Radiation Inst.

Table 3.2. Data-Logging Instrumentation (continued)		
Measured Variable	Instrument	Model & Make
Outside Wind Speed	Cup anemometer	Weathertronics 2030
Outside Wind Direction	Wind Vane	Weathertronics 2020
Inside Temperature	AD590 in aspirated screen	Ag. Eng. Dept.
Inside Wet Bulb Temp.	AD590 in aspirated screen	Ag. Eng. Dept.
Soil Temperatures	Encapsulated AD590	Ag. Eng. Dept.
Media Temperatures	Encapsulated AD590	Ag. Eng. Dept.
Media Moisture Content	Gypsum Block	Monitor Inc.
Leaf Temperatures	Thermocouple (Type T)	Ag. Eng. Dept.
Glass Temperatures	Thermocouple (Type T)	Ag. Eng. Dept.
Heating System Temps	Thermocouple (Type T)	Ag. Eng. Dept.
Heater Water Flow	Electromagnetic Flowmeter	Kent Veriflux
Inside Solar Radiation	SRI3 Pyranometer	Solar Radiation Inst.
Inside Solar Radiation	Linear pyranometers	Delta T Devices TSL
Inside PAR	Filtered pyranometer	Delta T Devices TSLF
Inside Net Radiation	SRI5 Net Radiometer	Solar Radiation Inst.
Inside Net Radiation	Linear Net Radiometers	Delta T Devices TRL
Ventilator Position	Potentiometer system	Ag. Eng. Dept.
Carbon dioxide Concentration	Infra-Red Gas Analyser	Fuji Instruments
Internal Air Movement	Hot-Bulb Anemometer	Dantec 54N50/54R10
Transpiration Rate	Lysimeter Platform Weighing System Computer Interface Controller	Ag. Eng. Dept. August Sauter Mettler Wormald 1830
Tipping Bucket Rain Gauge	Tipping Bucket Raingauge	Promatic
Stem Sap Flow	Dynagauge Stem Heat Balance system	Dynamax Inc. SGA10-WS

3.1.3.1 Boundary Variables

The boundary variables required to drive the model were as follows: air temperature, humidity, wind-speed, and solar radiation, all measured outside the greenhouse, the soil temperature at a depth below the penetration depth of the daily temperature cycle, the heat input from the heating system, and the degree of opening of the ventilators and doors.

Plate IV. Wind Vane and Anemometer on 10 m Mast. View looking West.

The wind speed was measured at the top of a 10 m mast attached to the utility building at the southern end of the greenhouse (Plate IV). The anemometer produced a frequency output which was read using a pulse counter channel on the data-logger. A wind vane was also set in place at this point. This device proved to be unreliable as the potentiometer within the device was not sufficiently robust to withstand the frequent wind shifts

encountered at the site, for more than 12 months. Early indications showed that the ventilation was not significantly dependent on wind direction. Thus when some difficulty was encountered in purchasing a replacement potentiometer of sufficient durability the instrument was removed for servicing but not replaced.

Outside air temperature and humidity were measured with a wet and dry bulb psychrometer mounted 5 m above ground level on the some mast as the anemometer. The psychrometer design incorporated a small 240 VAC fan drawing air vertically over the sensors, which were housed inside a double concentric screen with a large diameter weather hat, and a wet bulb reservoir. All parts of the screen and weather hat were painted with a gloss white paint to minimise solar radiation gains. The sensors used were integrated circuit, current limiting, temperature sensors (AD590), with a nominal temperature coefficient of 1 $\mu A.K^{-1}$. The circuitry was supplied in a metal can configuration (TO5) and was wired with screened extension leads and encased in acrylic resin to provide a water proof barrier. The encapsulating resin was turned down to leave a sensing bulb of approximately 6 mm diameter and 10 mm length. Each sensor was calibrated against a secondary calibrated mercury-in-glass thermometer and a high precision digital multimeter, using an ice-water slurry (0°C), a steam retort (100°C) and a water bath (various temperatures between 5°C and 50°C). Sensors were selected for greatest linearity over the range 0°C to 35°C. While the slopes were close to the manufacturers specification of 1 $\mu A.K^{-1}$, the 0°C measurement varied between 275 and 280 μA. At the data-logger the current signal was converted to a voltage using a high tolerance 1 kohm shunt resistor. This gave the sensor a resolution of 1 $mV.°C^{-1}$. The time constant of the sensors was determined to be approximately 1 minute in air for the dry sensor.

The solar radiation intensity on the horizontal (global radiation) was measured using a hemispherical pyranometer (solarimeter) type SRI3 from Solar Radiation Instruments. The solarimeter was placed on the northern corner of the flat roof of the utility building to avoid direct shadows and minimise the effect of the mast on the diffuse sky radiation from the southern sky. The solarimeter was calibrated against a Kipp & Zonen, Linke-Feussner type Pyrheliometer, belonging to the Fruit & Tree Division

of DSIR (formally Plant Physiology Division), using a shadow technique.[2] Calibration was performed at the beginning and end of each major experiment. No significant drift was found in any of the instruments.

The deep soil temperature was measured by placing an AD590 temperature sensor, similar to those described above, at a depth of 1 m under the greenhouse floor. The sensor was 1.8 m from the north-west side wall and 4.2 m from the south-west end wall.

The energy input to the heating system was determined from a heat balance on the heating fluid. The hot water flow rate was measured by placing a mass flow meter in the heating pipe. The water temperature at inlet and outlet was recorded by attaching thermocouples to the outside of the pipes and insulating the pipes with expanded polyethylene foam, to minimise the temperature drop in the pipe walls.

The opening of the ventilators was measured by attaching bicycle chains to the ventilators and running them over a sprocket and shaft running in a bearing fixed to the window frame. The sprocket drove a multi-turn 1 kohm linear precision wire-wound potentiometer via a flexible coupling (Plate V). The resistance of the potentiometer was determined using a high tolerance 1 kohm resistor to form a half bridge. The free ends of the chains were weighted to ensure that they remained taut. Similar devices were built for each double door with the chain fixed to one door and the potentiometer to the other. A roller mounted on the door frame and a weight on the free end ensured that the chain did not sag when the door was opened wide.

3.1.3.2 Internal Variables

In order to provide sufficient information to validate the predictions of the model the following internal variables were determined: temperature of the glass, internal air temperature and humidity, leaf temperature, media temperature, media water potential, temperature in the soil at various depths, net infra-red radiation above and below the crop, net solar radiation above and below the crop, photosynthetically active radiation

---

2 Under a clear sky, while the sun was high in the sky, the direct beam radiation was recorded using the normal incidence pyrheliometer, while the total and diffuse radiation were measured by the pyranometer being calibrated by alternately exposing and shading the pyranometer with a circular cardboard shape at the end of a long thin stick. The size and height of the shading device above the detector was arranged to shade the outer glass hemisphere completely, while making the subtended angle as close as possible to that of the collimeter tube of the pyrheliometer. Repeated use of this technique resulted in consistent readings from which a calibration could be derived.

above the crop, presence of condensation on the underside of the glazing, carbon dioxide concentration of the inside air, internal air-movement rate, transpiration rate of the crop, and water uptake rate of the crop.

Plate V. Window opening Measurement System.

The temperature of the glass was determined by glueing fine thermocouples to the inside and outside of two sheets of glass which were placed on opposite sides of the roof. One measuring location was directly above the other sensors, and the other was directly opposite. Condensation on the underside of the glass was measured by glueing a small resistance grid (as used in an artificial leaf used to control misting) to the underside of the same glass panes used for the temperature measurements. The resistance of the grid changed with condensation and was measured in a half bridge with a high tolerance 1 kohm resistor.

Internal air temperature and humidity were determined using a wet and dry bulb psychrometer of the same type as was used outside (see previous section). The psychrometer was suspended below the radiation sensors 1.5 m above the floor between two rows of cucumbers 2.0 m from the north-west side wall and 4.0 m from the south-west end wall.

Leaf temperatures were measured at six sites in the vicinity of the psychrometer using thermocouples in a technique based on that of Stanghellini (1987). Sensors were placed at three levels within the crop canopy, to determine the degree of stratification within the canopy. Each sensor was made up of six fine thermocouples wired in series to form a small thermopile. The hot junctions were held gently against the leaf by fingers of nylon tube mounted in a modified laboratory clamp, three on top of the leaf and three below the leaf directly opposite those above. The cold junctions were encased in acrylic resin with an AD590 temperature sensor which served as the reference (Plate VI).

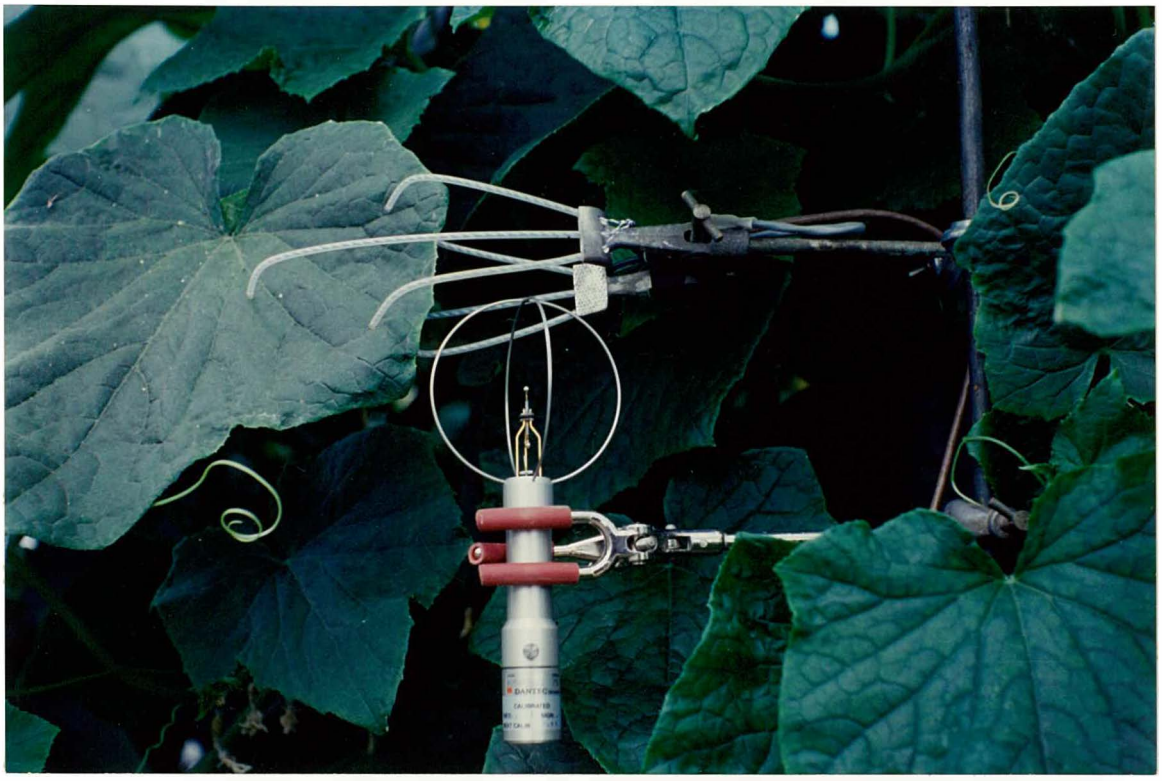

Plate VI. Leaf Temperature Measurement and Hot Bulb Anemometer.

The media temperature was measured using AD590 temperature sensors encased in acrylic resin. The media water potential was measured using gypsum blocks. In each experiment four different media were used, therefore eight measurements were made, two for each media type.

Soil temperature was measured using AD590 temperature sensors encased in acrylic resin. Initially seven sensors were put in place, just below the surface, at 5 cm, 15 cm, 30 cm, 50 cm, 75 cm, and 100 cm. However, during most of the experiments only the surface, 5 cm, 15 cm, 50 cm, and 100 cm (deep ground boundary value) were used. It was discovered that by the 1989 experiment the 5 cm sensor was malfunctioning due to breakdown of the acrylic resin.

Short wave radiation was measured above and below the crop using 1.2 m long linear tube pyranometers. Two devices were mounted above the crop, one facing upwards and one facing downwards, in order to measure crop canopy reflectivity. Another pair was placed below the crop (at the top of root medium bags) to measure canopy transmission and floor reflectivity (Plate VII). The devices were aligned with the major axis of the greenhouse and were thus subject to occasional shadows from the gutter, and purlins. A hemispherical solarimeter of the same type as used outside was also mounted above the crop to act as a reference to the outside radiation level. Also mounted above the crop was a filtered linear tube pyranometer. This device measured the near infra-red component of the solar radiation from which the photosynthetically active radiation was determined. The linear devices were calibrated against the hemispherical devices, at the same time as the calibration against the Kipp & Zonen pyrheliometer, and found to be in excellent agreement with the manufacturer's calibration.

Plate VII. Linear Pyranometers and Linear Net Radiometer.

The total net radiation above and below the crop was measured using 1.2 m long linear tube net radiometers. A hemispherical net-radiometer was also mounted above the crop, close to the linear device to act as a reference. All the net radiometers were inflated and purged with a constant supply of dry air from a small compressor, pressure tank and drying system. The linear devices were calibrated against the hemispherical device, which was calibrated against the Kipp & Zonen pyrheliometer with the filter removed

(measuring total solar radiation). As with the pyranometers the net radiometers were found to be in excellent agreement with the manufacturer's calibration.

The carbon dioxide concentration inside the greenhouse was determined using an infra-red gas analyser. This device was designed for continuous operation as a controller, and while having only limited accuracy ($\pm$ 10 $\mu 1.1^{-1}$) proved to be reliable and robust. The instrument was re-calibrated at regular intervals (fortnightly) against reference gas cylinders at 0 $\mu 1.1^{-1}$ and 2060 $\mu 1.1^{-1}$. Drifts were never more than 20 $\mu 1.1^{-1}$. The voltage output of the device was found to be non-linear and for this reason a calibration curve was developed by calibrating the instrument with a series of known carbon dioxide concentrations obtained from a gas metering system installed in the Photosynthesis/Photo Inhibition Laboratory at the Fruit and Trees Division, of the DSIR.

Internal air-movement within the crop was measured using a low velocity thermo-anemometer. This device had a resolution of 1 $cm.s^{-1}$. The voltage output of the analyser was measured directly with the data-logging system. At the end of the experiments the calibration of the device was independently checked in a wind tunnel, and found not to have changed from the manufacturer's calibration.

The transpiration of the crop was measured using a weighing lysimeter similar to that described by Stanghellini (1987) (Plate VIII). One or two plants were placed on a platform consisting of a galvanized steel tray and a light weight aluminium frame, onto which the plant was trained rather than the crop wires. Drainage was provided for the tray. The whole platform was placed on a set of electronic platform weighing scales. These scales had a maximum tare of 60 kg and a resolution of 0.1 g. The scales were placed on a concrete slab, in an insulated pit. This allowed the media bag to be at the same height as the other surrounding bags, and also to keep the temperature of the scales as constant as possible. The temperature in the pit was monitored with an AD590 temperature sensor. The scale was connected to an evaluator unit which was programmed to register the weight to 0.1 g, by specifying a part count of 0.1 g. The output of the evaluator unit was serial ASCII in current loop configuration. In order to communicate with conventional computing equipment (either TTL or CMOS level voltage loops) a current to voltage interface was used.

In order to synchronise the lysimeter with the other measuring systems a programmable controller was used which could be programmed in BASIC. The controller was programmed to continuously request information from the scale system, which responded with the weight plus a great deal of miscellaneous information. The controller then sorted out the weight and processed this information through a low pass filter, to remove high

frequency noise caused by air-movement disturbing the scale. The total weight was then divided up into a tare weight to the nearest two kilograms, and the remainder to 0.1 g. The tare weight was conveyed to the data-logger via four lines of a parallel port. Each line corresponded to 2, 4, 8 or 16 kg respectively, and thus any multiple of 2 kg between 0 and 30 kg could be signaled by setting the voltage high or low (CMOS levels). A fifth line was used to convey an alarm status to the data-logger, if the scale did not respond to repeated requests from the controller. This would occur if the scale would not settle sufficiently long enough for a reading to be taken, or after a power failure, where the scale had to be zeroed by lifting the platform and plants off the scale for 20 seconds. At the beginning of each data-logger scan cycle, the data-logger was programmed to signal the beginning of a new scan cycle to the controller via a control voltage output. The controller was programmed to stop interrogating the scale and to reply to the data-logger by polling one of its parallel lines the exact number of times corresponding to the current remaining weight. The speed of polling was controlled with a wait loop to give a frequency just below the maximum readable by a pulse counter channel on the data-logger, but sufficiently fast to ensure that all the information was sent before the beginning of the next data-logger scan cycle. Upon completion of this task the controller waited for the data-logger to signal the end of a scan cycle, at which time it returned to interrogating the scale for a new weight. The data-logger was programmed to reconstruct the tare weight and store this separately. The reason for this rather long-winded procedure was that the total weight to 0.1 g exceeded the resolution of the data-loggers output stages (only 5 significant digits) and also the largest integer value in the double precision pulse counter. This system was found to be very reliable with only one or two spurious readings produced in any one day.

Drainage from the lysimeter platform was measured using a small tipping bucket rain-gauge, and a pulse counting channel on the data-logger. This device has a cup size of 5 ml giving a measurement resolution of 5 g. Compared to the resolution of the scale this was large and therefore it was not possible to correct the transpiration figures with the drainage information. Furthermore, considerable delays between the water draining from the scale and the cup tipping resulted at low drainage flows, while at high drainage flows (during watering) it was observed that the cup would sometimes not return to the level position and erroneous measurements resulted. However it was always possible to tell when drainage was occurring and therefore when transpiration results should be ignored, as was also suggested by Yang et al (1989).

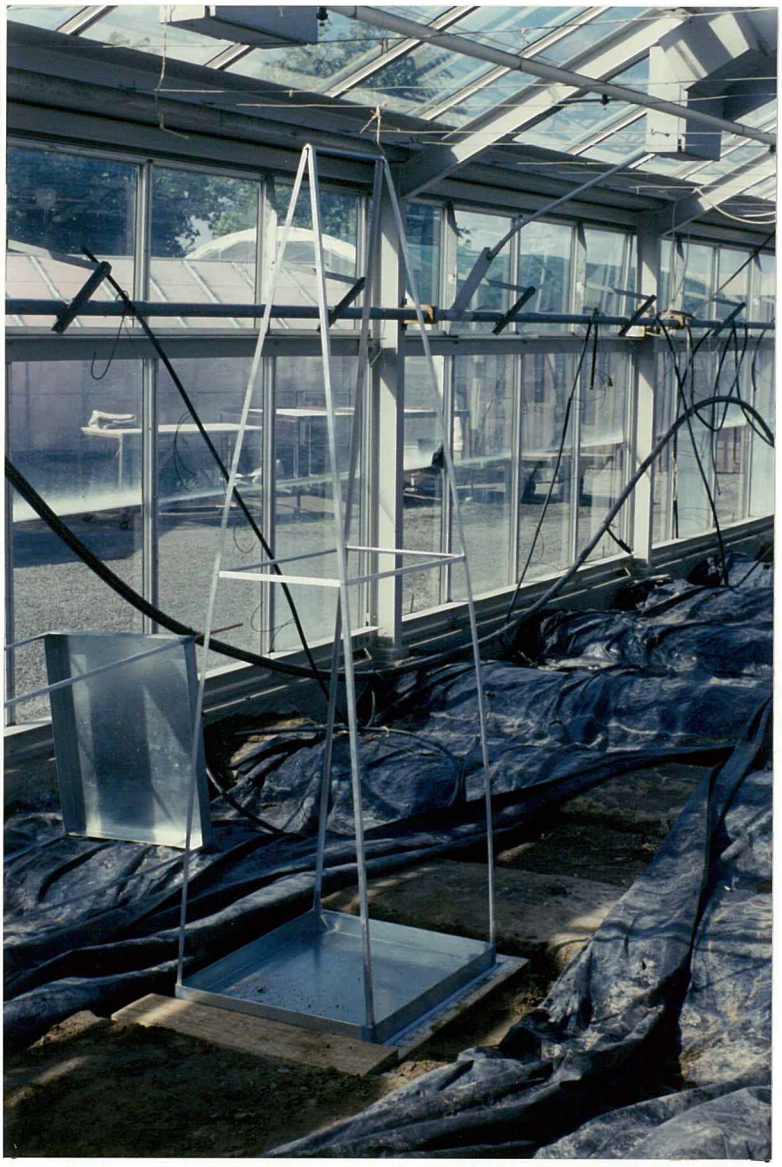

Plate VIII. The Lysimeter Platform during Construction.

In late 1989 a sap-flow gauge was added to the measurement system, in order to determine plant water uptake. The device used the heat balance technique (Baker & Van Bavel, 1987) and is especially easy to use with a Campbell data-logger. The system was installed as per the manufacturer's recommendations, and the data-logger program modified accordingly.

3.2 DETERMINING NATURAL VENTILATION OF THE GREENHOUSE

The air exchange rate of the greenhouse was determined using carbon dioxide as a tracer gas. The concentration decay rate method (Nederhoff et al, 1985) was used. Pure carbon dioxide, from liquid filled cylinders was released into the greenhouse through four nozzles spaced equally along the greenhouse until the concentration rose above 2000 $\mu l.l^{-1}$. An unused compressed air line running the length of the greenhouse under the ridge at

gutter height was modified for this purpose. Due to the high pressures available at the nozzles the concentration could be raised rapidly, in a matter of 50 to 60 seconds, and mixing was very good. The concentration was monitored with the infra-red gas analyser as it fell from 2000 $\mu l.l^{-1}$ to around 1000 $\mu l.l^{-1}$. During this time the outside wind speed and direction, and inside and outside air temperatures were monitored. The process was repeated for various settings of the ventilators and doors. The exponential decay constant was determined using linear regression and the air exchange rate calculated.

Over a three year period a total of 90 such decay rate experiments were performed. From this original data 70 runs with regression coefficients greater than 90% were selected to fit an empirical model of air-exchange rate versus wind speed, temperature differential and ventilator opening.

3.3 DETERMINING LIGHT TRANSMISSION OF THE GREENHOUSE

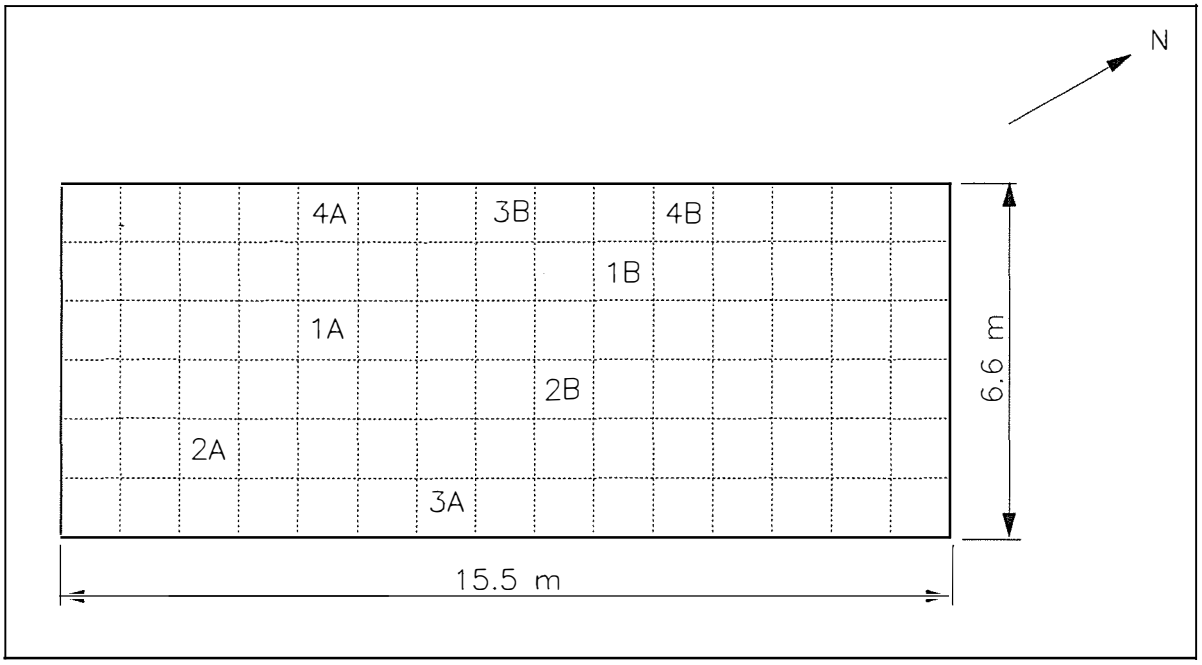

Figure 3.2. Position of Pyranometers for Light Transmission Tests

During the winter of 1989 a series of experiments was conducted to validate the light transmission model described in Chapter 4. Over a four week period from July 3rd to July 29th tube pyranometers were set up in 9 locations approximately 200 mm above floor level. The locations were chosen at random but included 3 sites along the northwest wall and the main measuring site (Site 1A Figure 3.2). Data from the tube pyranometers was collected at the same time as the other variables mentioned in section 3.1.3, with the exception of those referring to the crop and root media,

since no crop was present. From this data 20 days were chosen to analyze, 4 consecutive days for each site. Included in this was data from 7 days of overcast, 7 days of clear skies, and 6 days of partially cloudy skies.

3.4 MEASUREMENT OF THE CUCUMBER CROP

In order to validate the models for development and growth of a cucumber crop various measurements were made of the three crops of cucumbers grown in the greenhouse at the same time as data was being collected to validate the energy and mass balance model of the greenhouse. The cucumbers were grown by the Department of Horticulture as part of cultivar and media trials.

3.4.1 The 1987 Crop and Experiments

The 1987 crop consisted of three cultivars 'Sandra' (normal crop) and two new cultivars, 'Nun Elka 4465', and 'Nun Elka 4467'. The seed was planted on May 19th into peat blocks in a nursery house maintained at a minimum temperature of 18°C. The plants were transplanted, after four weeks, into the growing house on June 16th into 6 litre planter bags containing bark, with a base fertilizer mix. A fourth trial in each block involved 'Sandra' planted into bark with pumice added to improve aeration. Each trial contained 14 plants in a double row. Each block was replicated four time in each of the four corners of the house using a randomized design. At each end of the house a double guard row was planted. Thus in total 280 plants were present in the house. The first harvest was made on August 11th (12 weeks) and the last harvest on October 27th (23 weeks). Fruit numbers and weights from each trial were recorded. On July 30th the leaf area index of the crop was analysed. The length and width of every leaf on 224 plants were measured. From the leaves measured in this way, 105 leaves were removed and measured using a Li-Cor area meter. From this data the correlations in section 6.2.1.1, between length, width and area, were developed.

3.4.2 The 1988 Crop and Experiments

The 1988 crop involved 'Sandra' alone in a media trial. The experiment was set out as in 1987 but the four trials consisted of different ratios of bark and pumice in the root media. These were 100% bark, 75% bark, 50% bark and 25% bark. The seed was sown on June 8th and transplanted on the June 29th (3 weeks). First harvest occurred on August 30th (10 weeks) and last harvest on November 21st (23 weeks). Between the August 18th and the November 21st, at approximately weekly intervals, non-destructive measurements were performed on 8 plants (2 from each trial from 1 block) to

determine the number and area of leaves present, using the correlations previously developed, and the size, weight and positions of the fruit present.

Periodically fruit were removed and measured to develop a correlation between length, diameter, fresh weight and dry weight of the fruit. For each fruit the length and mid section diameter were measured with calipers and then weighed. Selected samples were then taken from a number of fruit and dried in a standard test to determine moisture content and dry weight.

At the end of the trial the 8 plants were measured destructively to determine total leaf area, and fresh weight, stem fresh weight, and root weight. Samples were also dried to determine moisture content and dry weight.

An experiment was also conducted to determine the potential sink strength of fruit using a technique similar to that described by Marcelis et al (1989). On October 18th, on one guard row, all but one fruit was removed from each plant. These fruit were between 10 and 25 mm in length and from the 15 to the 20th axil. The size of each fruit was measured every two to three days, and all other new fruits removed. Excessive lateral growth was also removed. Five fruit were allowed to grow well past normal maturity until November 22nd (approximately 40 days after leaf opening). The others were picked at close to normal maturity (about 20 days), and another single fruit allowed to form. From this data typical maximum growth rate curves were developed.

3.4.3 The 1989 Crop and Experiments

The 1989 crop was also a media trial with 'Sandra' alone. In this trial the media was a mixture of pumice and potting mix, with the four trials being 100% pumice, 75% pumice, 50% pumice, and 25% pumice. For this trial only single rows of plants were used, making the total plant population 140 plants. The seed was sown on August 2nd, and transplanted out on August 30th (4 weeks). First picking occurred on October 10th (10 weeks) and the last picking on December 25th (20 weeks). Between September 2nd and December 20th four plants were measured non-destructively, at approximately weekly intervals. Particular emphasis was placed on tracking the development of these plants in terms of fruit numbers, size, and abortion, as well as leaf growth. At the end of the crop these four plants were measured destructively, for leaf area, and inter-node distance.

4 SOLAR RADIATION ENTRY INTO A GREENHOUSE

In this chapter models for the prediction of solar radiation partitioning and transmission into greenhouses are reviewed, and a combined model is presented for use in subsequent models of the greenhouse environment (Chapter 5), and the production of a cucumber crop (Chapter 6).

4.1 MODELLING INCIDENT SOLAR RADIATION

In the following a model is developed to partition incident global radiation into direct and diffuse components, and into photosynthetically active and near infra-red components, after reviewing the relevant literature.

4.1.1 Review

Solar radiation is one of the primary energy inputs to the greenhouse system. It provides energy for photosynthesis and transpiration of the crop, as well as maintaining the energy balance of the greenhouse cover, air-space, and the underlying soil. Due to the differing response characteristics of the various components of the greenhouse system to different parts of the solar spectrum it is necessary to be able to divide the incoming solar radiation into appropriate wave bands. (Norman, 1980, Weiss & Norman, 1985, Spitters et al, 1986). For a study such as this, which involves estimating photosynthetic response of plants, it is convenient to divide the solar spectrum into four wave bands. These are: ultraviolet radiation (UV), for wavelengths less than 400 nm; photosynthetically active radiation (PAR), for wavelengths between 400 and 700 nm; near infra-red radiation (NIR), for wavelengths between 700 and 3000 nm, and thermal or far infra-red radiation (FIR), for wavelengths greater than 3000 nm (Goudriaan, 1977). Furthermore, the directional nature of solar radiation is also important, particularly in determining the transmission and absorption properties of the greenhouse cover and the crop (Norman, 1980). Thus, it is necessary to distinguish between direct radiation, arriving along the path of the solar beam, and diffuse radiation, arriving from the sky vault as a result of scattering processes in the atmosphere.

Of the four solar radiation wave bands, described above, only the PAR and NIR bands need be considered. This is because, according to the NASA/ASTM standard spectral irradiance curve (Thekaekara, 1976), only 8.7% of the extra-terrestrial radiation, measured outside the earth's atmosphere, is in the ultraviolet region, and only 2.2% is in the far infra-red region. At the earth's surface these are reduced to approximately 3% and zero

respectively, due to scattering and ozone absorption of ultraviolet and water vapour absorption of far infra-red radiation. Therefore, both fractions can be disregarded for studies of this nature (Goudriaan, 1977).

Of the extra-terrestrial radiation, approximately 38% is in the PAR band and 51% is in the NIR band (Thekaekara, 1976). At the earth's surface this ratio is modified due to absorption in the NIR band by water vapour. At mid-latitudes most studies have found that the PAR fraction is relatively constant, under a wide range of sky conditions. Estimates of this fraction vary from 0.45 (Meek et al, 1982) to 0.50 (Szeicz, 1974). Weiss and Norman (1985) reported a value of 0.46. Their data was very consistent, except at solar elevations less than 20°, where the PAR fraction increased to approximately 0.6. Some reports have found that the PAR fraction increases with increasing cloud cover, particularly in tropical latitudes (Britton & Dodd, 1976, Stigter & Musabilha, 1982). This trend was also reported by Goudriaan (1977). These results can partially be explained by considering that the NIR is strongly absorbed by water vapour, and will therefore be reduced by increasing air mass, (low solar elevation), and increasing precipitable water (typical of the tropics). On the other hand, the PAR is not strongly absorbed by water vapour (Duffie & Beckman, 1980).

The shift from clear to overcast skies also greatly affects the ratio of direct and diffuse radiation. Therefore, it is usual to analyse the partitioning of solar radiation in relation to the sky clearness index, K_t, defined as (S_g/S_o), the ratio of global radiation S_g (W.m^{-2}), measured on the horizontal at the ground, to extra-terrestrial radiation, S_o (W.m^{-2}), measured on a plane parallel to the earth's surface.

The extra-terrestrial radiation is related to solar elevation β according to:

$$S_o = S_{sc}[1 + 0.033\cos(360J/365)]\sin\beta \qquad (4.1)$$

where the solar constant, S_{sc}, is approximately equal to 1353 W.m^{-2} (Duffie & Beckman, 1980). The cosine term accounts for the annual variation in the sun-earth distance, and J is the Julian day number.

The solar elevation, β, and solar azimuth, α, can be determined from standard relationships (Duffie & Beckman, 1980).

$$\sin(\beta) = \sin(\Lambda)\sin(\delta) + \cos(\Lambda)\cos(\delta)\cos(\omega) \qquad (4.2)$$

$$\sin(\alpha) = \frac{-\cos(\delta)\sin(\omega)}{\cos(\beta)} \qquad (4.3)$$

and

$$\cos(\alpha) = \frac{\cos(\Lambda)\sin(\delta) - \sin(\Lambda)\cos(\delta)\cos(\omega)}{\cos(\beta)} \tag{4.4}$$

where Λ is the latitude of the site ($^\circ$), δ is the solar declination ($^\circ$), and ω is the hour angle from solar noon ($^\circ$).

The declination, δ, can be found from the equation of Cooper (1969):

$$\delta = 23.45\sin\left(\frac{360(284+J)}{365}\right) \tag{4.5}$$

The hour angle, ω, is the angular displacement of the sun east or west of the local meridian, at 15° per solar hour, and is negative in the morning, and positive in the afternoon.

$$\omega = 15(LST - 12) \tag{4.6}$$

Local Solar Time, LST, is the time at the local meridian relative to the motion of the sun. The highest point in the sun's apparent arc occurs at solar noon, when the sun crosses the meridian, from east to west. Any other solar time is defined relative to solar noon by equal division of the solar path around the zodiac.

Local Solar Time can be calculated from the Local Civil Time, LCT, and the Equation of Time, EOT, with accounts for variation in the rotational speed of the earth.

$$LST = LCT - EOT \tag{4.7}$$

According to Duffie & Beckman (1980) the Equation of Time can be calculated from:

$$EOT = 9.87\sin(2B) - 7.53\cos(B) - 1.5B \tag{4.8}$$

where

$$B = \frac{360(J-81)}{364} \tag{4.9}$$

Local Civil Time is found from the Standard Time by correcting for the longitudinal variation between the local meridian and the reference meridian, at the rate of 4 minutes per degree of longitude. For New Zealand Standard Time, $NZST$, the reference meridian is 180° of longitude.[1] New Zealand Standard Time is equal to Greenwich Mean Time plus 12 hours.[2]

The partitioning of the global radiant flux, S_g ($W.m^{-2}$), between direct, S_{dr}, and diffuse, S_{df}, components has been studied extensively to determine the incident radiation on inclined surfaces of solar collectors. Correlations between the diffuse fraction of global radiation, $K_d = (S_{df}/S_g)$, and the clearness index, $K_t = (S_g/S_o)$, have been developed from hourly, daily or monthly average solar radiation data. Hourly data has been analysed for, Melbourne, Australia (Bugler, 1977), Toronto, Canada (Orgill & Hollands, 1977), Hamburg, West Germany (Bruno, 1978), de Bilt, The Netherlands (de Jong, 1980), 5 USA cities (Erbs et al, 1982), Cabauw, The Netherlands (van den Brink, 1982). The commonly used correlations of Erbs et al (1982), and Orgill & Hollands (1977) are shown in Figure 4.1, along with the correlation of de Jong (1980), for solar elevations of 15°, 30°, and 45°. For solar elevations greater than 45°, de Jong's correlations are all similar to that at 45°.

The results of these studies revealed that the diffuse fraction is strongly correlated to clearness index, and to a lesser extent solar elevation, particularly for low elevations with high clearness index. Most researchers have chosen to ignore the problem of solar elevation, assuming that the effect of solar angle was no greater than other sources of scatter in the data. It can be seen from Figure 4.1 that for clearness indices below 0.3 the global radiation is almost completely diffuse, and that between 0.3 and 0.8 there is an almost linear relationship between the diffuse fraction and clearness index. For clearness indices greater than 0.8 the diffuse fraction is approximately constant at around 20%, except at low solar elevations.

Analyses considering the effect of solar elevation, as well as clearness index, have been carried out by Bugler (1977) and de Jong (1980). Bugler correlated the diffuse fraction against the ratio of global radiation to clear sky total radiation. Since the clear sky radiation is dependent on air mass, the problem of variation with solar elevation is partially dealt with. De Jong correlated the diffuse fraction against clearness index, and

---

1 For Palmerston North (40.4°S, 175.6°E) the longitude correction is 4(175.6-180) or -17.6 minutes.

2 During all the experiments New Zealand Standard Time was used, regardless of season, to avoid the complication of changes between Standard Time and Daylight (Summer) Time.

included the effect of solar elevation for higher clearness indices (Figure 4.1). This model was used by Spitters et al (1986) to separate out diffuse radiation, as part of a crop canopy photosynthesis model.

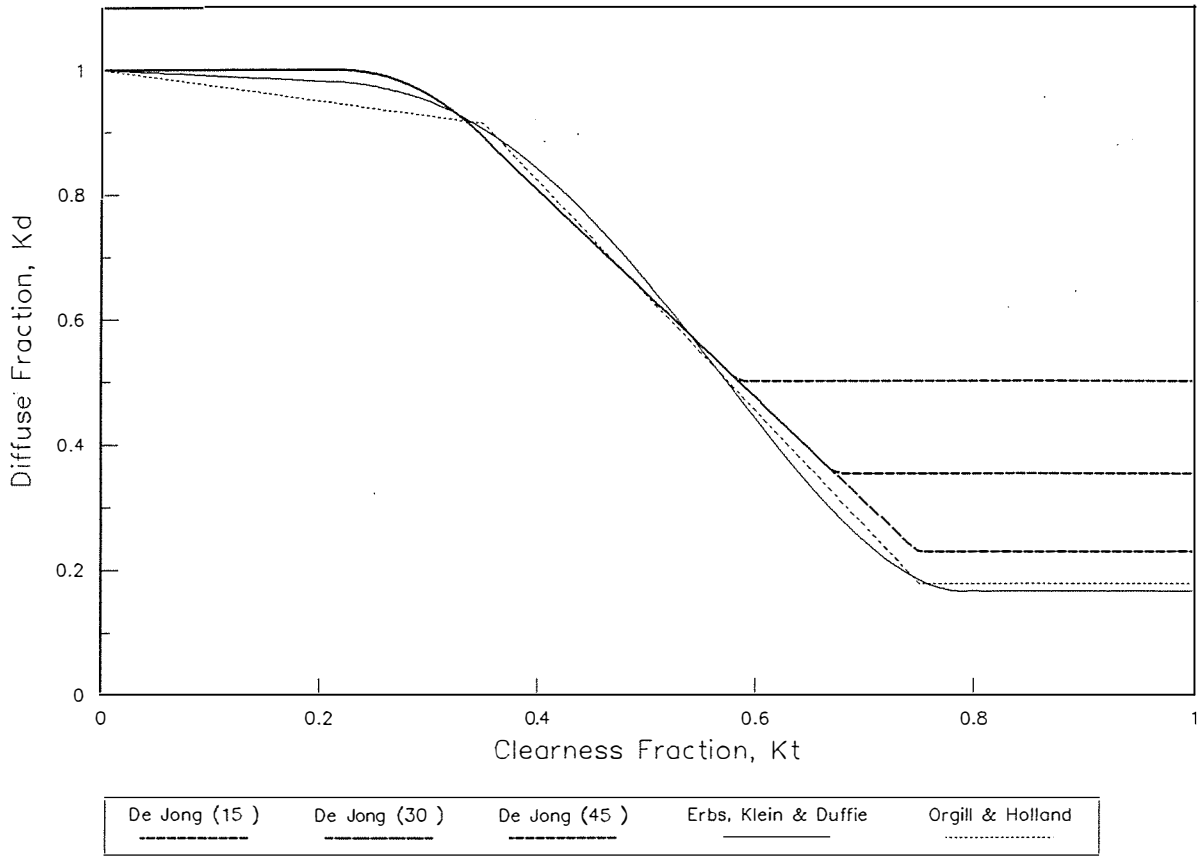

Figure 4.1. Selected Correlations of Diffuse Fraction K_d versus Clearness Index K_t

A more elaborate analysis of solar radiation partitioning has been carried out by Weiss & Norman (1985). Observations of total PAR and diffuse PAR where made simultaneously with measurements of global and diffuse radiation. The PAR fraction was assumed to be constant at 0.46. The direct fraction of the calculated PAR and NIR, was determined as a function of the estimated fraction of direct radiation in each band for a clear sky, and the ratio of measured global radiation to estimated clear sky global radiation.

Although the Weiss & Norman model appears to give satisfactory results, when compared to other models, there are some problems. The authors assumed that the solar constant, excluding the UV band was 1320 $W.m^{-2}$. However, according to the NASA/ASTM standard spectral irradiance data (Thekaekara, 1976) this value should be 1235 $W.m^{-2}$, if the UV is excluded, and 1205 $W.m^{-2}$, if the far infra-red radiation is also excluded. There also appeared to be a discrepancy in the calculation of the diffuse radiation from a clear sky. The direct radiation transmitted on the horizontal was

subtracted from the beam extra-terrestrial radiation, rather than the horizontal extra-terrestrial radiation, to find the scattered fraction potentially available as diffuse radiation. Finally, any model which requires the estimation of clear sky radiation is arbitrary, depending on the choice of atmospheric extinction coefficients. Preliminary experiments showed considerable differences between the direct and diffuse components of clear sky radiation predicted by the model of Weiss & Norman and that of Hottel (1976), and that of Spencer (1972).

4.1.2 Separation of Diffuse Radiation

For this study the correlation of de Jong (1980) was used to calculate the diffuse fraction of the total global radiation. The reason for this was that de Jong's correlation includes the effect of solar elevation at high clearness indices, but is simpler than the correlation of Bugler (1977), since it avoids the necessity to estimate clear sky radiation.

The diffuse fraction, K_d, was calculated from the clearness index, K_t, according to:

$$K_d = 1 \qquad 0 \le K_t \le 0.22 \qquad (4.10a)$$

$$K_d = 1 - 6.4(K_t - 0.22)^2 \qquad 0.22 < K_t \le 0.35 \qquad (4.10b)$$

$$K_d = 1.47 - 1.66K_t \qquad 0.35 < K_t \le K_{crit} \qquad (4.10c)$$

$$K_d = K_\beta \qquad K_{crit} < K_t \le 1 \qquad (4.10d)$$

where

$$K_\beta = 0.847 - 1.61\sin(\beta) + 1.04\sin^2(\beta) \qquad (4.11)$$

and

$$K_{crit} = \frac{(1.47 - K_\beta)}{1.66} \qquad (4.12)$$

The direct radiation flux can be found from the global and diffuse fluxes according to:

$$S_{dr} = S_g - S_{df} \qquad (4.13)$$

Under overcast skies the diffuse radiation is approximately isotropic, i.e. of equal intensity from all angles of the sky vault. This gives rise to the so called uniform overcast sky (UOC). However, Moon & Spencer (1942) proposed a standard overcast sky (SOC), where the radiance rises by a

factor of three from the horizon to the zenith. The radiance is defined to be the amount of radiant energy received per unit time on unit horizontal surface per unit solid angle of the sky hemisphere. This distribution was later confirmed by Grace (1971). The radiance of the standard overcast sky, R ($W.m^{-2}.steradian^{-1}$), is given by:

$$R = R_z(1+2\sin\beta)/3 \tag{4.14}$$

where the radiance at the zenith, R_z ($W.m^{-2}.steradian^{-1}$), is found by integration over the whole sky vault to be:

$$R_z = \frac{9S_{df}}{7\pi} \tag{4.15}$$

Later analysis showed that there was little difference in radiation transmission calculated using the UOC and SOC (see section 4.3). Thus the simpler UOC distribution was used throughout the analysis.

4.1.3 Circumsolar Radiation

Under clear skies the presence of aerosols in the atmosphere generates Mie scattering with a predominantly forward direction. This gives rise to anisotropic diffuse radiation with greatest intensity in the direction of the sun. Initially the clear sky distribution (CSD) of Pokrowski (Walsh, 1961) was used, as suggested by Critten (1983a). This anisotropic distribution can be approximated, however, by a direct beam, the circumsolar component, superimposed on an isotropic background distribution (UOC).

Under a clear sky the circumsolar component is $\cos^2(90°-\beta)\cos^3\beta$ times the remaining diffuse component (Temps & Coulson, 1977). It is therefore assumed that the circumsolar portion behaves like beam radiation, and is added to give a corrected direct radiation, S'_{dr}, and that the remaining diffuse radiation, S'_{df}, is isotropic. To interpolate between a clear sky and a completely overcast sky, Klucher (1978), found that the circumsolar correction factor should be multiplied by $1-(S_{df}/S_g)^2$. Thus the circumsolar correction factor is:

$$X_{circ} = [1-(S_{df}/S_g)^2]\cos^2(90°-\beta)\cos^3\beta \tag{4.16}$$

And the circumsolar component can be found from:

$$S_c = \left(\frac{X_{circ}}{1+X_{circ}}\right)S_{df} \tag{4.17}$$

Now the corrected direct and diffuse components can be calculated from:

$$S'_{dr} = S_{dr} + S_c \tag{4.18}$$

and:

$$S'_{df} = S_{df} - S_c \tag{4.19}$$

4.1.4 Separation of PAR and NIR

Under clear skies the total PAR is 50% of the global radiation, while under overcast skies it is 60% of the global radiation. Thus the PAR component can be estimated from the global radiation as follows:

$$S_p = [0.6 - 0.1(1 - (S_{df}/S_g)^2)]S_g \tag{4.20}$$

It follows then that the NIR component will be:

$$S_n = S_g - S_p \tag{4.21}$$

Observations by Burtin et al (1981) showed that for clear skies the diffuse fraction of PAR was 1.4 times that of the diffuse fraction for the whole spectrum. Spitters et al (1986) have suggested that this factor should be reduced to 1.3 to take account of the weighting of the photosynthetic action spectra across the PAR band. For overcast skies the diffuse ratios are uniform across the whole solar spectrum. Thus the fraction of diffuse PAR can be found from:

$$S_{pdf} = [1 + 0.3(1 - (S_{df}/S_g)^2)](S'_{df}/S_g)S_p \tag{4.22}$$

It follows then that the direct PAR is:

$$S_{pdr} = S_p - S_{pdf} \tag{4.23}$$

that the diffuse NIR is:

$$S_{ndf} = S'_{df} - S_{pdf} \tag{4.24}$$

and that the direct NIR is:

$$S_{ndr} = S_n - S_{ndf} \tag{4.25}$$

Equations 4.1 to 4.25 form a model from which the measured global radiation, S_g, could be partitioned into its constituent parts for any given time of the day, for any location, and any day of the year.

4.2 MODELLING LIGHT TRANSMISSION BY THE GREENHOUSE

In the following section, models of solar radiation transmission into greenhouses are discussed, and the calibration of such a model is described.

It has long been recognized that the intensity of solar radiation inside greenhouse structures has a significant effect on crop productivity. Prof. W. Renard of the Institute of Horticultural Engineering, Hannover (Schulze, 1955) stated that as early as 1720 a Prof. Boerhave of Leiden, reported on the importance of light in the greenhouse. Various early reports concluded that the light penetration into a greenhouse was a complex function of greenhouse construction, glazing type, orientation and slope of the various surfaces, the latitude of the site, and the nature of the incident radiation (Lawrence, 1950, 1963, Seemann, 1952). In fact as early as 1812, MacKenzie had studied the problem and concluded that a hemisphere would give maximum light penetration. While this shape was used in the winter gardens of the 18th and 19th century (van den Muijzenberg, 1980), for commercial greenhouses, the hemispherical shape was impractical.

The most common greenhouse shape to develop, in practice, was the symmetrical single span shed, with a rectangular floor plan. This was relatively simple to construct, and therefore relatively inexpensive. In order to increase the land utilization, Dutch growers developed the first multi-span greenhouse configuration, the Dutchlite or Venlo greenhouse. This type of greenhouse had a very narrow span, typically only two metres, with only one pane of glass in each roof section, supported at the gutter and ridge and on either side by a glazing bar. The glazing bars were originally wooden, but in more modern greenhouses are made of steel or aluminium. Usually every second or third pane of glass, on alternate sides of each roof, was made to open for natural ventilation. Due to the narrow span, the Venlo style greenhouse has a low ridge and smaller volume.

In the British Isles, the 'ridge and furrow' multi-span configuration was developed. Each roof section contained several panes of glass between the ridge and the gutter, which where over-lapped at the joins. Wider spans than the Dutch Venlo, were obtained, but more structure was required to support the larger roof, and greater waste volume was created in the roof apex. Spans of up to 13 m have been built, but these require a considerable amount of support structure. Over the years the size of glass panes has increased, reducing the number of glazing bars, thus reducing the amount of light intercepted by opaque members. Modern multi-spans now usually have

two or three panes of glass, up to 1.2 m in length, in each roof section, with the lower panes fixed, and the upper pane as part of a continuous or staggered ridge vent. This allows spans of 4 to 6 m to be achieved, with an acceptable level of opaque structural componentry.

The introduction of plastic glazings, both rigid and film, has seen a return to more rounded forms, particularly tunnels, and inflated structures. The diffusing nature of most plastics, combined with the more rounded shapes, means that the light environment, under a plastic greenhouse, may be very different to that under a glasshouse of similar shape and size. The problems, however, remain essentially the same, that is, to determine the optimum greenhouse shape and orientation, for a particular location, taking into consideration the glazing material used, the light transmission obtainable, and the cost of the structure.

Over the last four decades various researchers have studied the light penetration or transmission of greenhouses. Several methods have been used, which can be divided into three categories: tests on full size greenhouses, tests on scale models, and mathematical models.

4.2.1 Transmission of Full Size Greenhouses

Schulze (1955) reported that tests on full scale greenhouses began in 1951, at the Institute of Horticultural Engineering, Hannover, in conjunction with the first Federal Horticultural Show, at which a large number of different greenhouses were constructed for display purposes. Radiation sensors were placed inside and outside these greenhouses, in order to directly determine the light transmission, by comparing the two signals. Several difficulties were encountered with this technique. The most important of these was the uneven distribution of light within the greenhouse, making it almost impossible to determine a place were the sensor could be placed inside the greenhouse which would give a representative value for the greenhouse as a whole. To integrate the light transmission both spatially and in time, would have required many simultaneous measuring points.

Despite these limitations several authors have used this technique to study the light transmission of greenhouses. Edwards and Lake (1964, 1965) conducted tests on a large-span east-west aligned glasshouse during various stages of construction. Diffuse light transmission was found to be 69%, while direct light transmission varied from 57%, in summer, to 68%, in winter. From their data it appeared that between 15% and 20% of the light interception could be attributed to structural members, and thus reflection and absorption by the glazing was of the order of 10% to 20% of the incident light.

Giacomelli et al (1988) studied the transmission of a bow-type, air-inflated, double polyethylene greenhouse. They found that the average transmission of total solar radiation (0.285 to 2.8 μm) was 67.4%, and of PAR radiation (0.4 to 0.7 μm) was 67.1%.

Skov (1989) compared the light transmission of identical single span greenhouses clad with a single layer of glass and double acrylic plates. Again, these results highlighted that different values are obtained depending on the position of the sensors.

4.2.2 Transmission of Scale Models of Greenhouses

Schulze (1955) reported on extensive tests on light transmission that were carried out on scale models in a test chamber using artificial illumination. In this study considerable emphasis was placed on the construction of the test chamber, referred to as an isoloscope, the artificial light sources for direct and diffuse light, and the light measurement system, to ensure that the tests would be as representative of reality as possible. Using the isoloscope Schulze investigated the effect of construction parameters such as roof slope, side wall height, and orientation for single span greenhouses. Schulze concluded, as others had (Lawrence, 1950, Seemann, 1952), that in the Northern European winter a steep-roofed greenhouse was superior to one with a flatter roof. The superiority of east-west alignment, compared to north-south alignment, was also shown. Schulze also concluded, that from the point of view of light transmission, adequately spaced single span greenhouses would be superior to multi-span constructions.

4.2.3 Mathematical Models of Greenhouse Light Transmission

Although mathematical modelling of greenhouse light transmission is complex, many models have been developed (Table 4.1).

In relation to mathematical modelling of greenhouse light transmission several general comments can be made. Firstly, it is very difficult to compare the results of modelling studies, since the underlying assumptions and simplifications used, are often very different. Secondly, in general, the newer models tend to make less simplifications and are therefore considerably more complex, requiring considerable computing power to solve, but hopefully are better representations of reality. Thirdly, at some point it becomes necessary to trade off between the complexity of the model, and the increased accuracy that more detail will give. Fourthly, prediction of light transmission by large multi-span greenhouses can be significantly simplified, compared to single span greenhouses, if the effect of the side

walls is ignored. Fifthly, a common feature of all models, reviewed to date, is that they consider the light incident at the floor of the greenhouse, in the absence of a crop.

Table 4.1 Mathematical Models of Greenhouse Light Transmission

Author(s)	Date	Country	Type and Use
Nisen	1962	Belgium	Single span without structure
Manbeck & Aldrich	1967	USA	Analytical for direct light
Stoffers	1967 1971	The Netherlands	Multi-span for direct and diffuse radiation
Bowman	1970	United Kingdom	Analytical for diffuse light
Deltour & Nisen Basiaux et al	1970 1973	Belgium	Effect of diffusing cover materials
Takakura et al	1971	Japan/USA	Single span glasshouse
Smith & Kingham Kingham & Smith	1970 1971	United Kingdom	Single span glasshouse
Kirsten	1973	West Germany	Single and multi-spans
Kozai Kozai & Kimura Kozai et al	1977 1977 1978	Japan	Ray tracing method for single and multi-spans, direct and diffuse light
Thomas	1978	United Kingdom	Specularly reflecting back wall
Critten	1983a	United Kingdom	General ray tracing method
Bot	1983	The Netherlands	Multi-spans
Bellamy & Ward Bellamy	1984 1991	New Zealand	General ray tracing method
Kurata	1989b	Japan	General ray tracing method

The model of Manbeck & Aldrich (1967) calculated the transmission of direct light through the roof panels of a greenhouse. Takakura et al (1971) and Smith & Kingham (1971) modelled single span greenhouse and included the light entering through the walls. Stoffers (1967, 1971) modelled the diffuse and direct light transmission into multi-span greenhouses. Kirsten (1973) modelled light transmission into a large number of different shaped single span greenhouses, as well as some multi-span geometries.

Kozai (1973, 1974, 1975, 1977) and Kozai & Kimura (1977) introduced a mathematical model of greenhouse light transmission which can be considered the forerunner of so called 'ray tracing' methods. In this model the light entering through each glass pane was calculated, and traced to the point of

interception by the floor. Thus the effect of light interception by the glazing bars, at the primary light interception surface, was automatically included. In a later version of the model, a Monte Carlo method was introduced, where a specified number of light rays, incident on each surface, were selected at random (Kozai et al, 1978). Thus a ray could either be intercepted by a glazing bar, or transmitted by a glass pane. Transmitted rays would then either be intercepted by a structural member, arrive at another glazed surface, or arrive at the floor. Accuracy of the simulation depended on the number of rays considered, and hence the computational time. None of these models considered transmitted light that was subsequently reflected, by internal surfaces, down to the floor.

Bot (1983) overcame the problem of internal reflection by considering only large multi-span structures, where the average light transmission is not significantly affected by side wall transmission, or reflection. This model considered internal reflection from the underside of the roof panels, which added significantly to the light transmission at low sun angles. The light interception of the glazing bars, and the ridge and gutter systems, which cast significant shadows in traditional Venlo greenhouses, was also included.

Critten (1983a, 1983b) developed a sophisticated ray-tracing model to simulate light transmission in single and multi-span greenhouses. Internal reflection was considered, along with polarization effects, and distortion of the traced beam through multiple reflections. This latter effect was treated by tracing two points on the side of each grid element, as well as a beam through the centre of each element. This considerably increased the simulation time, but improved the accuracy of the prediction of the light intensity distribution on the floor, when the grid element size was relatively large compared to the division of the floor. However, a significant limitation of this model was that while light interception by the glazing bars was considered at the primary light interface, this effect was ignored at subsequent interfaces. Thus the effect of internal reflection may have been over-estimated, as reported by Kurata (1989b). Furthermore, in the versions of the model supplied by Dr. Critten for evaluation in this project, light blockage by the internal support structure and absorption within the glazing material was ignored.

In subsequent studies, Critten (1987a, 1987b) has evaluated the light interception by structural members independently. The resulting structural transmission factor was then assumed to be superimposed over the transmission factor for the glazing (Critten, 1987c). The calculations were performed on a Mainframe computer and required considerable time to complete (Critten, 1988, Pers. Comm.). In order to reduce the time required to complete the simulation several simplified versions of this model have been developed, which considered the greenhouse to be either infinitely

long, infinitely wide, or both, in order to reduce the three dimensional problem to either a two dimensional or one dimensional problem, similar to that considered by Bot (1983). Critten has used this model in numerous related studies of light transmission of greenhouses (Critten, 1984, 1985a, 1985b, 1986, 1989, Critten & Legg, 1987).

Concurrent with the developments of Critten, and others in Europe and Japan, a similar model was developed in New Zealand (Bellamy & Ward, 1984, Bellamy, 1991). Bellamy's model was similar to that of Critten's, but with some important differences. Polarization was ignored, as was beam distortion on reflection, but interception by the underlying support structure, and glazing bars, was included at all interfaces, as was absorption by the glazing material. Double glazing could be simulated as well as the effect of applying a specular reflector to the inside of any surface.

In Bellamy's model each glazed surface was divided into small elements using a grid system, and a ray was traced through the centre of each grid element. At each interface the transmission, and absorption of the glazing were calculated depending on incident angle. Absorption by the glazing bars and structural members was also included, by assuming that a proportion of every ray was absorbed according to the area of these members, projected in the direction of the ray, relative to the area of glazing. All structural elements were assumed to be black. The model traced the path of the primary transmitted and reflected rays until either the floor was reached, or three subsequent surfaces were encountered. Reflections from these subsequent intersections were also considered. If the distribution of light across the floor was required to any degree of accuracy, then the grid element size had to be relatively small compared to the floor grid size. Bellamy suggested that for ±2% accuracy, grid element sizes of 0.2 m and 0.005 m would be required for diffuse and direct radiation respectively. The accuracy of the average transmission across the whole floor was, however, relatively insensitive to grid element size, and grid sizes of 2 m and 0.2 m were required for diffuse and direct radiation respectively.

A model similar to that of Critten's and Bellamy's has also been developed by Kurata (1989b). Although details of the model are not readily available, Kurata stressed the point, that this model dealt with internal reflection more realistically, by considering that the reflected rays could be intercepted by structural members both prior to, or directly after, the reflection process. Kurata (1988, Pers. Comm.) has suggested that some of the conclusions drawn by Critten, regarding the optimal shape of greenhouses in high latitudes, may be erroneous, due to over-estimation of the importance of internally reflected light. Furthermore, the differences

in the conclusions of Critten and Kozai, regarding the transmission of greenhouses, may be explained by the fact that their models respectively over-estimated and under-estimated the importance of internal reflection.

4.3 DEVELOPMENT AND VALIDATION OF A LIGHT TRANSMISSION MODEL

In this section the development and validation of a greenhouse light transmission model is described. The criteria for the model were as listed below.

1. The model should accurately predict the amount of solar radiation transmitted by the greenhouse, incident at the top of the plant canopy, for each of the diffuse, direct, PAR and NIR components.

2. The model should be applicable to a single span greenhouse.

3. The model should also predict the amount of solar radiation absorbed by the glazing, the glazing bars, and the internal structure, for use in the greenhouse environment simulation model.

3. The predictions should be readily usable by the greenhouse environment and crop models.

4.3.1 Choice of Basic Model

For this section of the study I am indebted to Dr. Don Critten, AFRC, Silsoe, UK, and Dr. Larry Bellamy, Lincoln University, New Zealand, who generously gave me access to source code for their respective models.

The models of Critten and Bellamy were selected as possible starting points on the basis that they were available, and they met at least the first two criteria set out above. It was also clear, from private communications, that the modifications necessary to meet the other criteria could be performed on the models.

Copies of the computer source code of the models of Critten and Bellamy were obtained. Both were coded in FORTRAN77. Only minor changes were needed to compile these models on the Massey University mainframe computers. After some initial experimentation with the two models, the decision was made to modify the model of Bellamy, in order to produce a set of light transmission tables for the test greenhouse, which could be used as input to the environmental and crop simulation models. There were three main reasons for this choice. Firstly, Bellamy's model included the effect of the internal structure within the model, whereas Critten's model required a post simulation correction factor to be applied.

Secondly, Bellamy's source code was structured in such a way that adaptation of the model was significantly simpler. Bellamy's model calculated the direct radiation transmission for each floor element, then calculated the average direct transmission, and then finally calculated the diffuse radiation transmission, as a weighted average of the direct transmission values. Critten's model, on the other hand, calculated the diffuse transmission within the main program, for various assumed sky types, for each floor element. It was not immediately clear, how the intermediate results for each sky vault element, averaged over the whole floor, could be extracted.

Thirdly, the method used by Bellamy to account for absorption of radiation in the glazing material, and light interception by the glazing bars, and internal structural elements, lent itself to an adaptation to calculate the amount of radiation being absorbed within each plane surface, as a fraction of the total incident radiation. This information was required, since the proposed greenhouse model would consider the energy balance of the glazing and internal structure. The version of Critten's model, as supplied, did not account for absorption within the glazing, or interception by the internal structure.

4.3.2 Division of Sky Vault

Some experimentation revealed that dividing the sky vault into 180 elements according to the following scheme, resulted in elements of approximately equal solid angle, and therefore luminous intensity. Firstly, the Great Circle from the horizon to the zenith was divided into nine elements, each of 10°. The rings created were then divided according to the following pattern. The upper most ring, about the zenith, was divided into four sectors each of 90°. The next ring down was divided into eight sectors each of 45°. Twelve sectors were created from the third ring, and sixteen from the fourth. This pattern was continued to finish with 36 sectors, each of 10°, for the ninth ring, just above the horizon. The next obvious choice of division would have been 5° intervals in the Great Circle. This leads, however, to 684 sectors, or nearly 4 times the processing time required, for only a limited increase in accuracy.

4.3.3 Modifications to Existing Transmission Model

Version 1 of Bellamy's program was modified to run in direct transmission mode, assuming that the sun was centred in each of the sky vault sectors in turn. This required the addition of two loops to the program code to calculate the azimuth and elevation of the sun at the centre of each sky vault sector sequentially (Lines 182 to 196 of main program GST2.F). Listings of the new main program GST2.F and modified subroutines RAY.F and

TRANS.F may be found in Appendix 3. Other subroutines where not modified. The new program was compiled using a FORTRAN77 compiler, and linked and run in a UNIX environment.

The direct light transmission for each floor element, as well as the overall transmission, was calculated using the existing code. A minor modification was made to reduce the transmission at each glazing interface by a fixed ratio, to account for additional light losses at each primary cover plane (line 23 of subroutine TRANS.F). To determine the absorption of radiation in each plane of the greenhouse the absorption at each light ray intersection was calculated from the intensity of the incident beam, and the absorptivity (one minus the sum of transmissivity and reflectivity) at lines 21, 33 and 46 of subroutine RAY.F.

A new array was added to the main program ABSORB(50) at line 4 of GST2.F to contain the absorptivity data. ABSORB and DIRT were also added to all common blocks. The factor DIRT was added to the information read from input file SHAPE.DAT at line 21 of GST2.F, and the appropriate format statement modified at line 22. The average absorptivity for each plane of the greenhouse relative to the greenhouse floor area was calculated at lines 260 to 266 of GST2.F. Minor amendments were made to the WRITE statements at lines 267, 268 and 272, along with their respective FORMAT statements.

A new output file GHOUSE.DAT was opened at line 4 of GST2.F. This file contained the transmission and absorption data for a quarter of the sky vault. For a greenhouse with even sloped roofs, symmetrical about both axes, it was only necessary to simulate a quadrant (i.e. 45 sectors) between the major and minor axes of the house, and superimpose this result, after rotation and translation, to calculate the effect of light from the full hemisphere (Lines 298 to 326 of GST2.F). The average transmission and absorption for direct light, emitted from each sector of the sky, was then stored in SKY.DAT for later use in the greenhouse simulation model, and to calculate the diffuse light transmission and absorption.

For an asymmetrical building, light from the sectors in a half hemisphere, or the whole hemisphere must be considered, depending on whether the building is asymmetrical in one axis or both.

A separate program was developed to calculate the diffuse transmission and absorption, from the direct transmission and absorption figures output from the model described above. This program, DIFF2.F, is also listed in Appendix 3. The following sky radiance distributions were used: uniform overcast sky (UOC), standard overcast sky (SOC), and clear sky (CSD) (see section 4.1.2). The clear sky distribution was evaluated with the sun in each sector in turn.

4.3.4 Trial 1. Absorption by the Greenhouse Elements

In order to determine the effect of absorption by the glazing, glazing bars, and internal structure, the program was run several times with each new component added. The initial run was made using the dimensions of the test greenhouse but with no structure or glazing bars, and assuming that there was no internal absorption within the glass. In this case all losses were attributable to reflection. In the second run the internal absorption of the glass was included. The glazing bars and internal structure were then added in the third and fourth runs. Three further simulations were carried out with 5%, 10%, and 15% extra absorption at each glass element, to investigate the effect of possible dust accumulation.

4.3.4.1 Results

Figure 4.2 shows the results of adding the various greenhouse components progressively to the overall predicted light transmission.

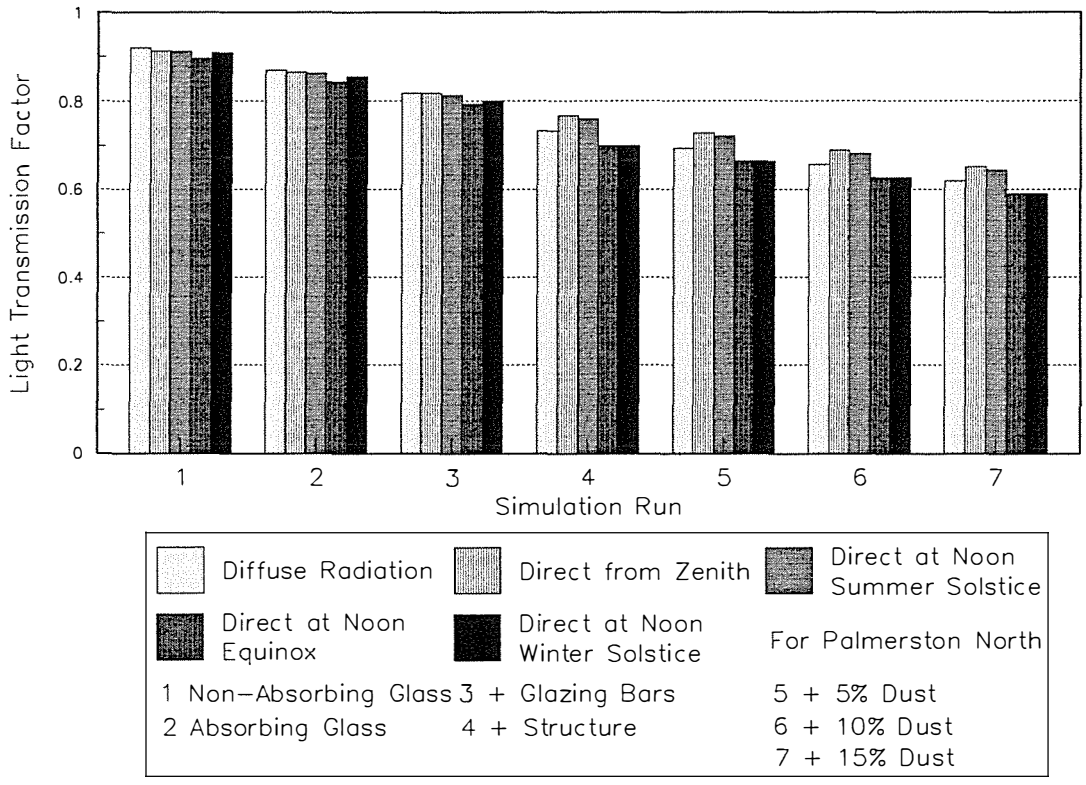

Figure 4.2. Effect of Greenhouse Components and Dust on Light Transmission

The transmission factor was defined as the amount of solar energy arriving at the floor, relative to the amount that would have arrived on the same floor area, in the absence of the greenhouse. Thus, it was theoretically possible to have a transmission factor greater than one, if the structure internally reflected light toward the floor. This is shown in Figure 4.3. The solar radiation arriving in the absence of the greenhouse is $S_g A_f$,

however the total amount of solar radiation being collected by the greenhouse is $S_g A_{shadow}$, and a fraction of this will be reflected down to the floor at the back wall, adding to the overall transmission factor.

As expected the transmission of direct radiation was highest with light arriving from close to the zenith and decreased for lower sun angles. This was particularly marked when the internal structure was included, since the profile of the internal structural members was not great when viewed from the zenith, but was quiet pronounced when viewed from the north, at low sun angles. The major axis of the test greenhouse was aligned 30° north of the east-west line.

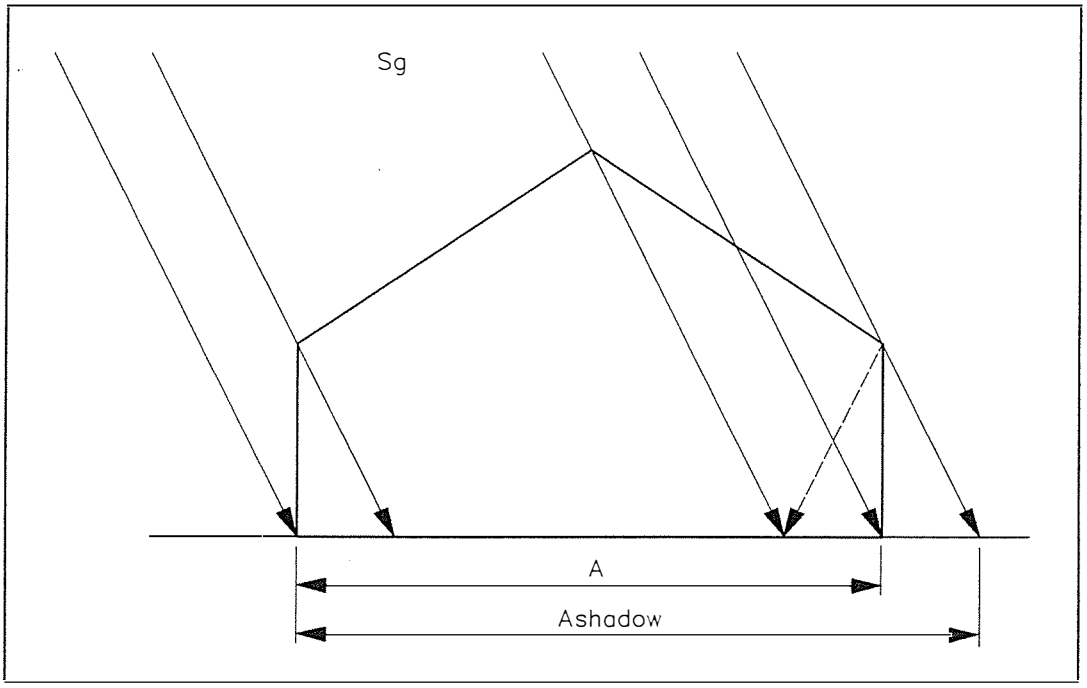

Figure 4.3. Increased Transmission due to Internal Reflection

It can be seen that reflection caused losses of approximately 10%, absorption by the glass reduced the transmission by approximately 5%, and interception by the glazing bars and structure, 5% and 10% respectively. Absorption by dust reduced transmission by about 3%, for every 5% increase in absorption.

Figure 4.4 shows the effect of the greenhouse components on the absorption of solar radiation. It should be noted that the absorption factor was defined as the total amount of solar energy absorbed, relative to the amount of energy that would have arrived at the floor, in the absence of the structure. Since the greenhouse structure collected solar radiation from a wider area than its own floor, except when light came from the zenith, it was possible to have an absorption factor greater than unity (Figure 4.3).

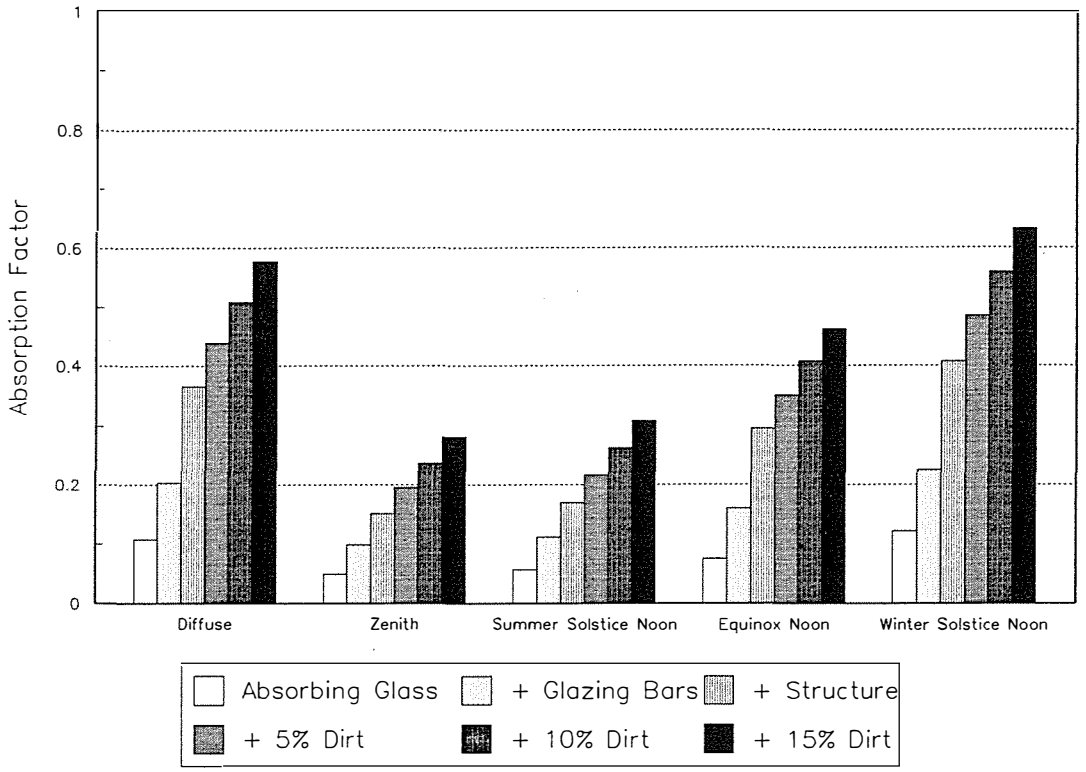

Figure 4.4. Effect of Greenhouse Components and Dust on Absorption

As expected, the absorption increased as more components were added, and as the solar elevation decreased, which caused the shadow area of the greenhouse to increase, and the greenhouse to collect radiation from a wider area (Figure 4.3).

4.3.5 Trial 2. Effect of Reference Plane Height

The preceding process was repeated with no walls to determine the level of radiation transmission at the gutter height, and with shorter walls to determine the transmission factor one metre above ground level. In each of these simulations, it was assumed that no light was reflected off the floor, and therefore, all light passing the horizontal reference plane was travelling downward.

4.3.5.1 Results

The results of these simulations, are shown in Figure 4.5, for diffuse light, and for direct light from the zenith, and at solar noon on the equinox, and the solstices, at Palmerston North.

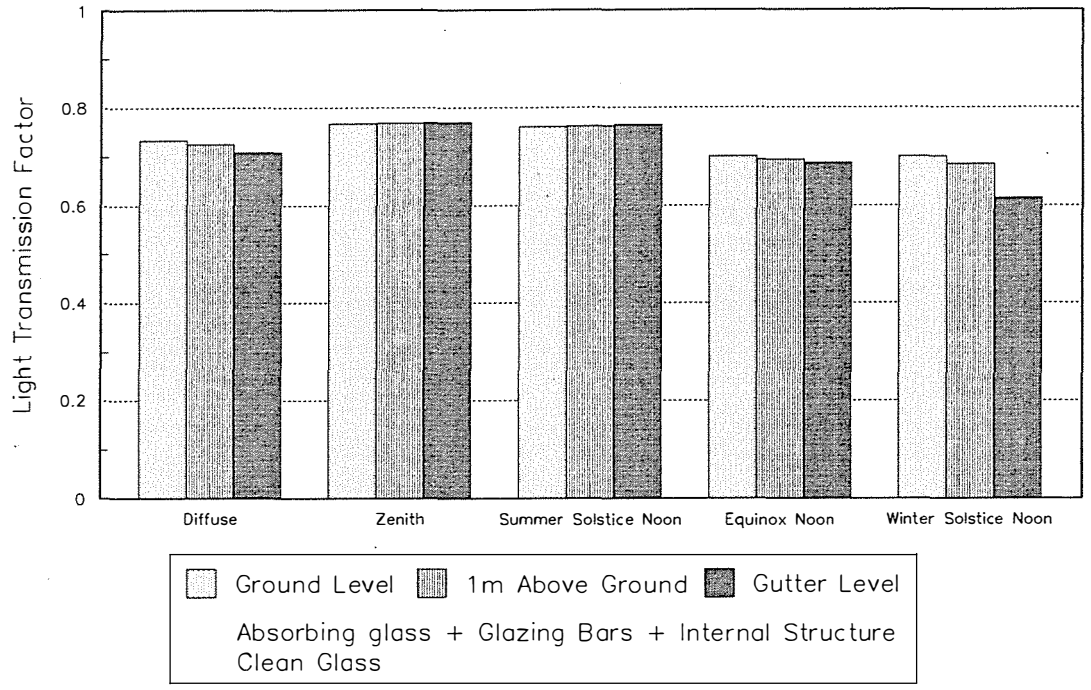

Figure 4.5. Effect of Reference Plane Height on the Light Transmission Factor

Only at the low sun angle (winter solstice) was there a marked variation between the light transmission predicted at the gutter level, or at 1 m height, compared to that at the floor. The transmission, at the floor, was greater than that at the gutter, showing the effect of light entry through the side walls, at low sun angles. It was decided, however, that the predictions of light levels at the floor, of an empty house, could be used to predict the light levels at the top of a crop canopy, regardless of height.

4.3.6 Trial 3. Evaluation of Diffuse Sky Distributions

As stated in section 4.3.3 a separate computer program was developed to calculate the transmission factor for diffuse radiation. Three distributions were tested, the Uniform Overcast Sky (UOC), the Standard Overcast Sky (SOC) and a Clear Sky Distribution (CSD) (see section 4.1.2).

4.3.6.1 Results

For all the simulations there was no more than 0.5% difference between the predicted diffuse transmission from the UOC and the SOC models. Predictions of absorption by the glazing and structure were within 5% of each other. Differences between the overcast and clear sky models, however, were more marked, particularly when the sun was low in the sky. For solar altitudes

below 10°, the clear sky transmission factor was as much as 25% more than that for the overcast sky models. A copy of the output file DIFF.DAT can be found in Appendix 3 (section A3.2.5). However, due to the low intensities occurring while the sun was in this region of the sky, it was decided, to use the uniform overcast sky model, with the circumsolar correction (see section 4.1.3). This simplified the amount of information required to be made available to the greenhouse environment simulation model.

4.3.7 Trail 4. Validation of the Modified Model

A series of experiments were carried out as described in section 3.3, in order to validate the light transmission model. For each measurement point on the floor, the direct and diffuse transmission values were determined from the output of previous simulation runs assuming that there was no additional absorption of radiation by dust on the glass. The measured global radiation for each five minute measurement period was partitioned between direct and diffuse radiation, using the de Jong correlation (equations 4.10 to 4.13, section 4.1.2). The solar azimuth and elevation were determined from equations 4.2 to 4.9 (section 4.1.1). The amount of diffuse and direct radiation was then calculated using equations 4.18 and 4.19 after being corrected for the circumsolar radiation component (equations 4.16 and 4.17, section 4.1.3). The overall radiation transmission was determined by multiplying the corrected direct and diffuse radiant intensities by the appropriate direct and diffuse transmission factors for the particular floor element and sun position in question.

Measured and predicted radiation levels, and transmission factors, were initially compared by eye. Under overcast conditions, with predominantly diffuse radiation, and a central location within the greenhouse (Location 2B on Figure 3.2), the fit was reasonably good. The composition of outside global radiation, determined from the de Jong correlation is shown in Figure 4.6. Figure 4.7 compares the measured and predicted radiation intensities inside the greenhouse to the measured global radiation outside the greenhouse. Figure 4.8 shows the same data plotted as the measured and predicted light transmission factor. Note that the model tended to over-predict the radiation transmission characteristics.

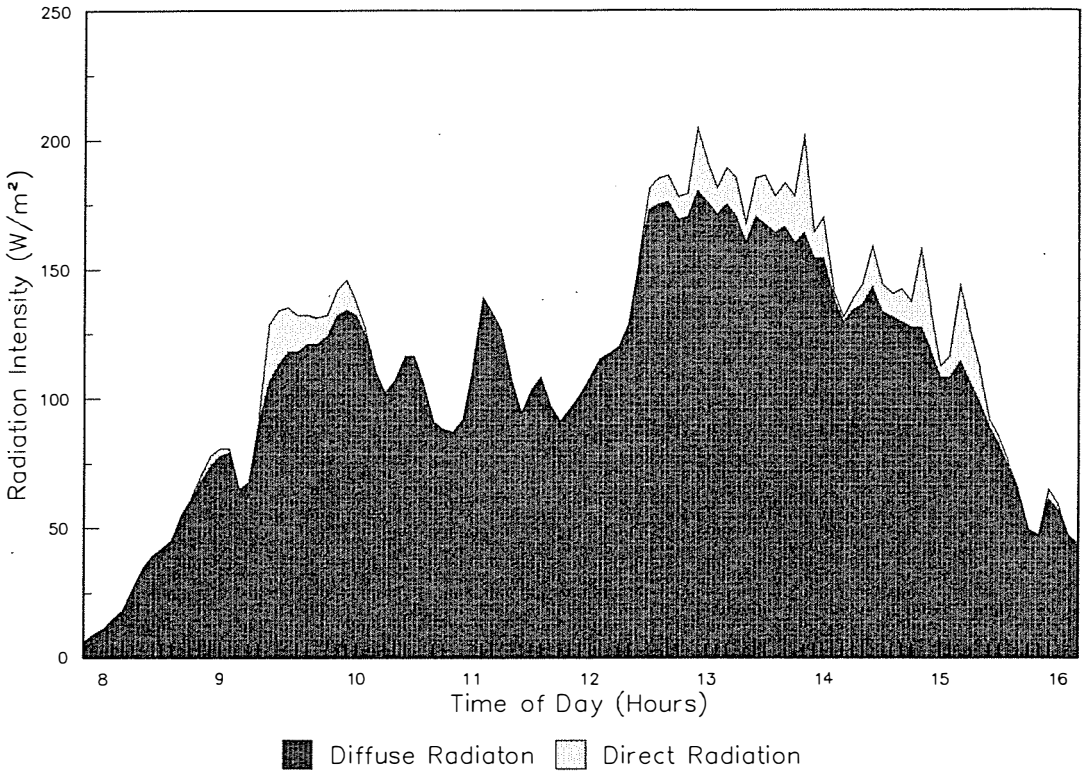

Figure 4.6. Diffuse and Direct Components of Global Radiation on 14/7/89.

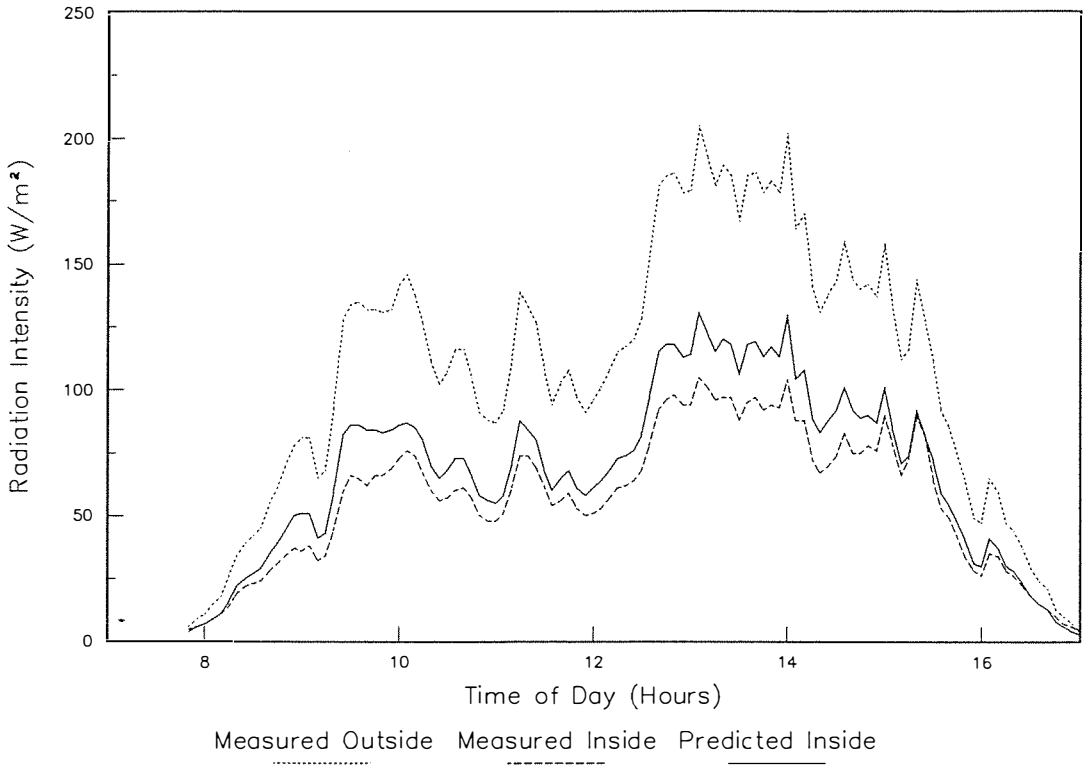

Figure 4.7. Predicted and Measured Light Transmitted into Test Greenhouse under Predominantly Diffuse Radiation Conditions (Point 2B 14/7/89).

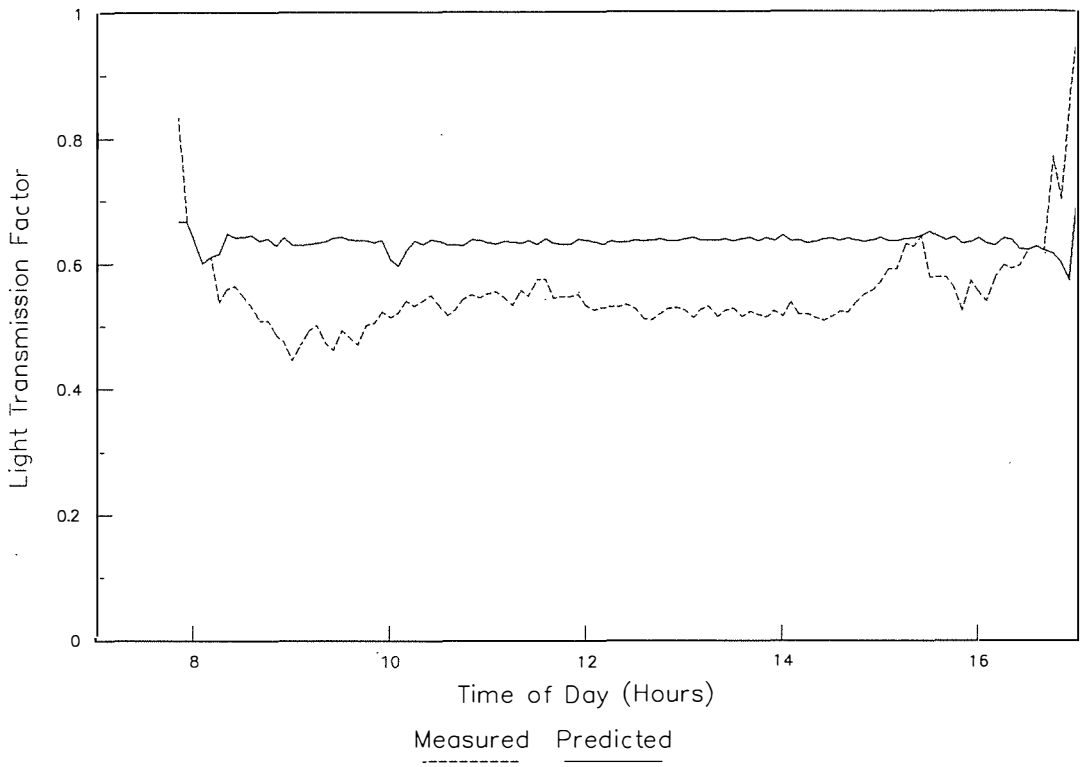

Figure 4.8. Predicted and Measured Light Transmission Factors under Predominantly Diffuse Radiation Conditions (Point 2B 14/7/89).

Under clear skies the presence of shadows cast by structural elements, particularly the gutter, was noticeable, particularly for internal locations. Figure 4.9 shows the direct and diffuse components of solar radiation on a clear day during the test period. The large dip between 11am and noon was due to the passage of a large cloud formation in an otherwise clear sky. Figures 4.10 & 4.11 show the effect of structural members on the measured readings and highlight the difficulty of taking representative measurements. The position of the light sensor for this test (1A) is shown in Figure 3.2. In Figure 4.11 the large dips in the measured light transmission factor can be attributed to shading by the ridge at about 1100 hrs, two roof purlins at 1230 hrs and 1330 hrs, the gutter between 1430 hrs 1500 hrs, and a wall purlin at 1500 hrs. Note that the model over-predicts the radiation transmission factor in the morning, when light enters through the North-East end wall farthest from the measuring site, and underestimates in the afternoon, when the light enters from the North-West side wall adjacent to the sensor.

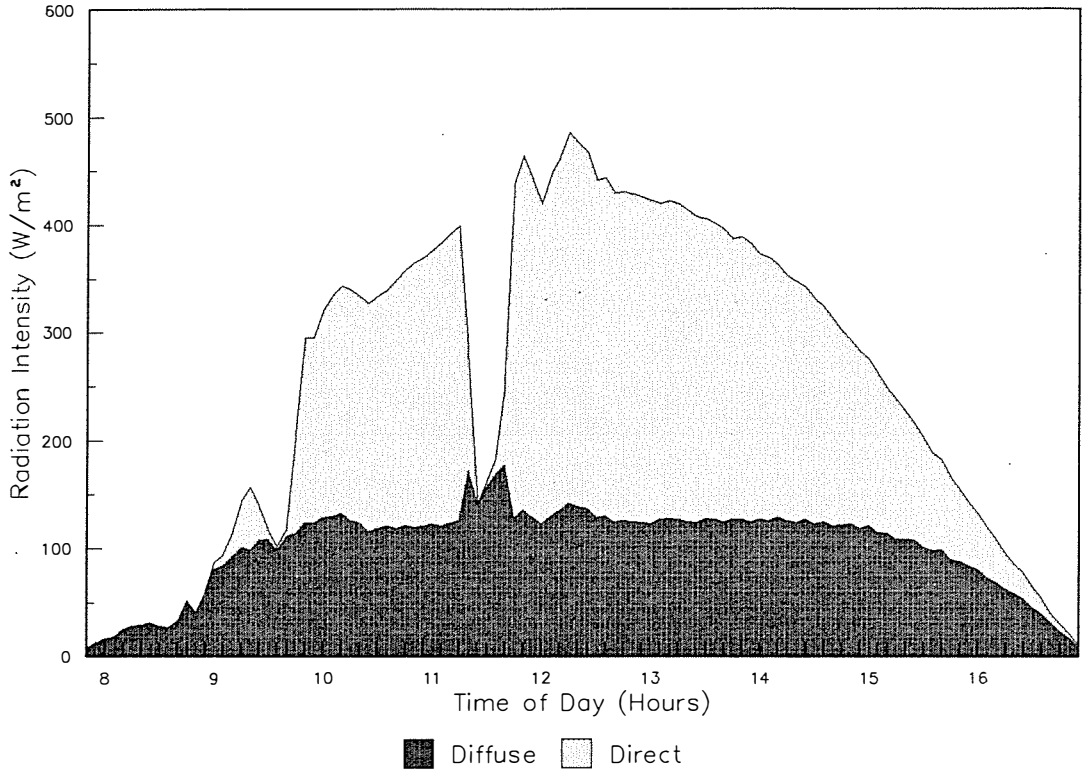

Figure 4.9. Diffuse and Direct Components of Global Radiation on 9/7/89

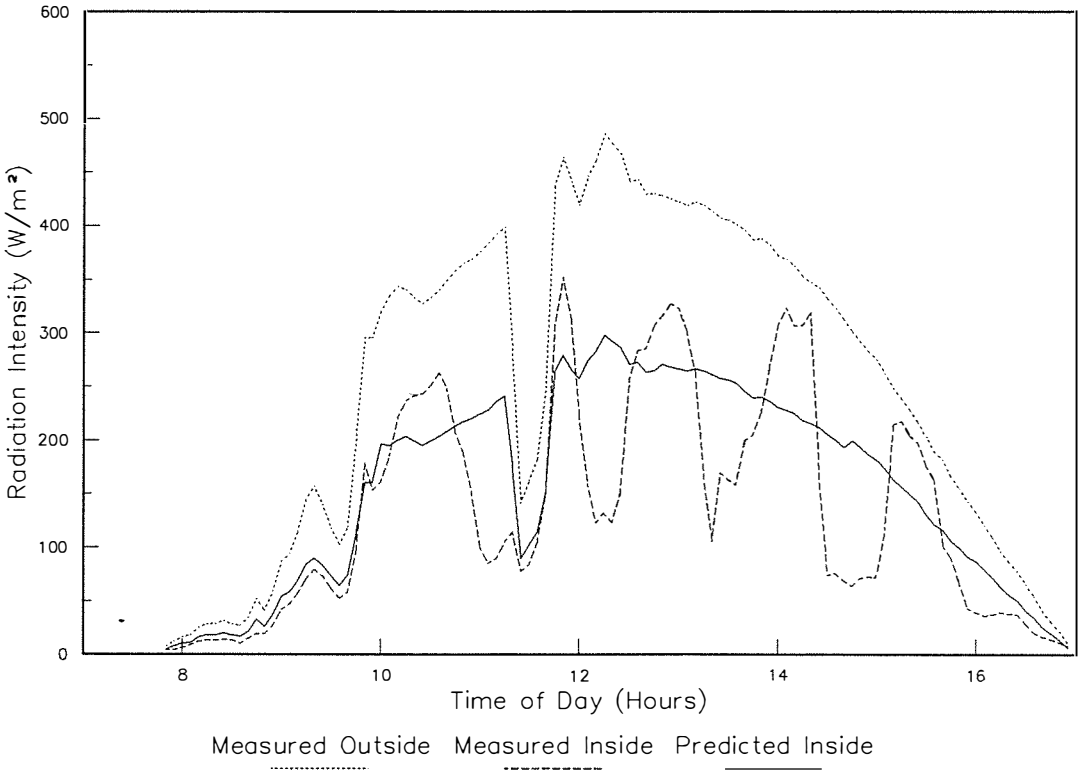

Figure 4.10. Predicted and Measure Light Transmitted into Test Greenhouse under Clear Sky Conditions (Point 1A 9/7/89)

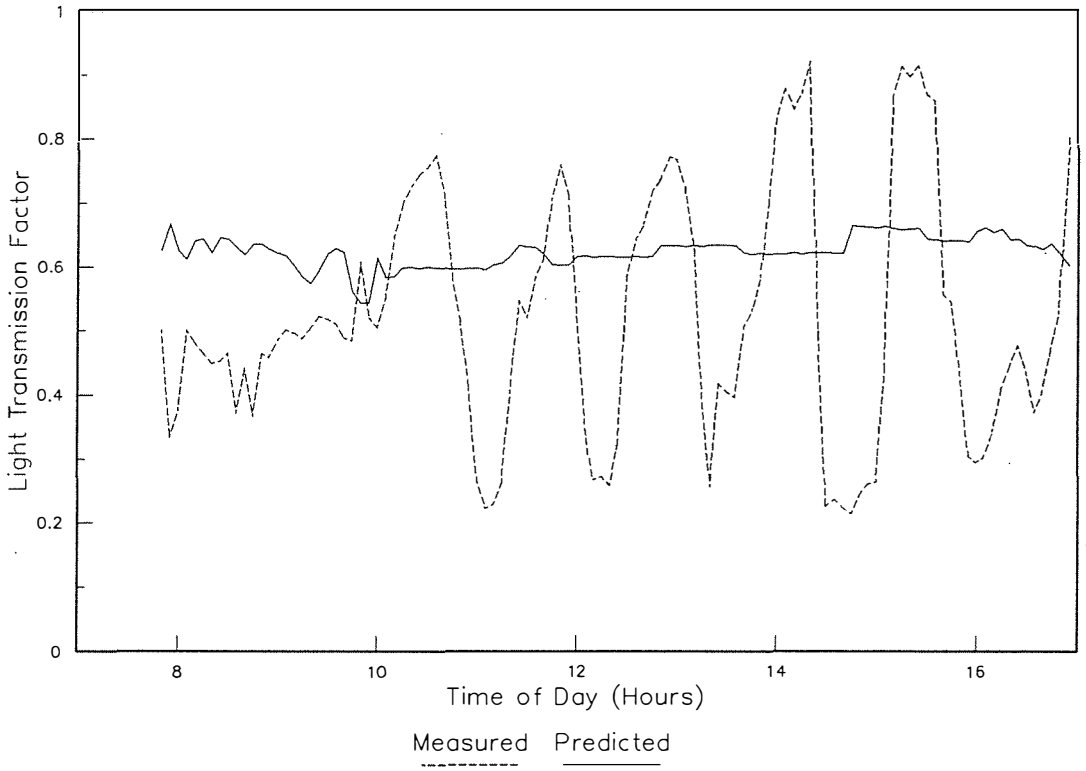

Figure 4.11. Predicted and measured light transmission factors under clear sky conditions (Point 1A 9/7/89).

Figures 4.12 to 4.14 show the outside radiation conditions, measured and predicted light transmission, and measured and predicted light transmission factors for a North-West perimeter location (4B on Figure 3.2), under clear sky conditions. For this situation the model over-predicted light transmission in the morning, when direct light entered from the North-East end wall. This was most likely due to interference by end wall structures and adjacent buildings. In the afternoon the model under-predicted light transmission when the direct light entered through the immediately adjacent North-West side wall. In this case there was in fact less interference by structural members than predicted by the model.

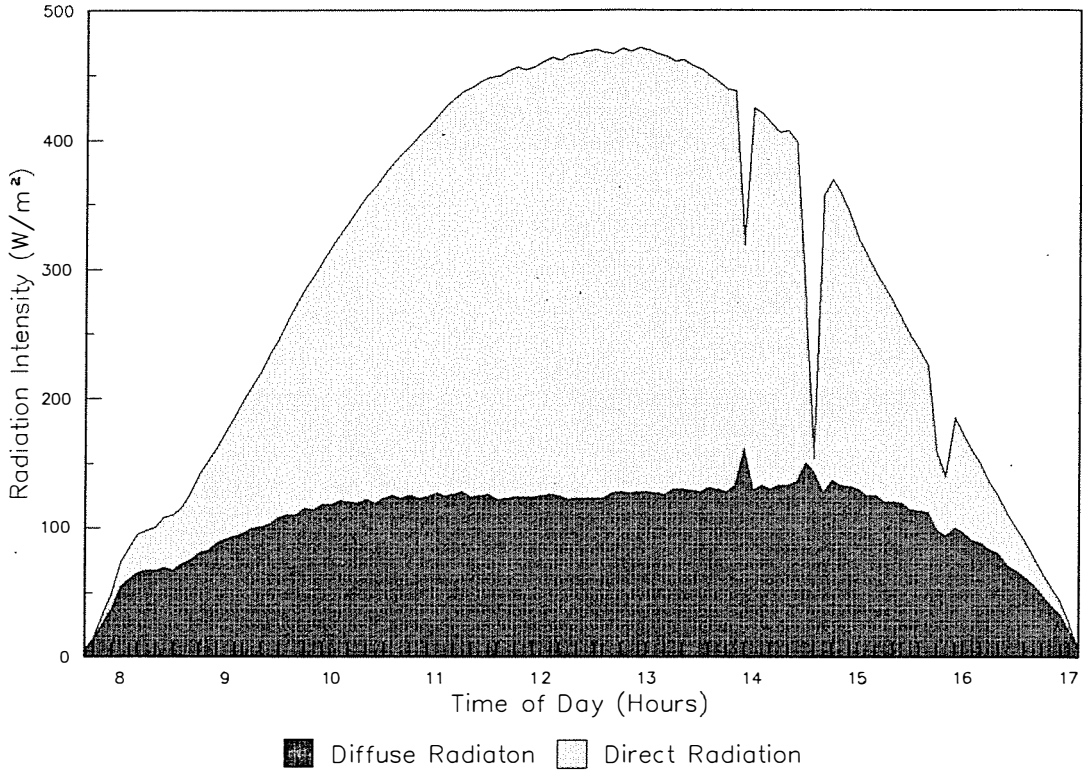

Figure 4.12. Diffuse and Direct Components of Global Radiation on 23/7/89

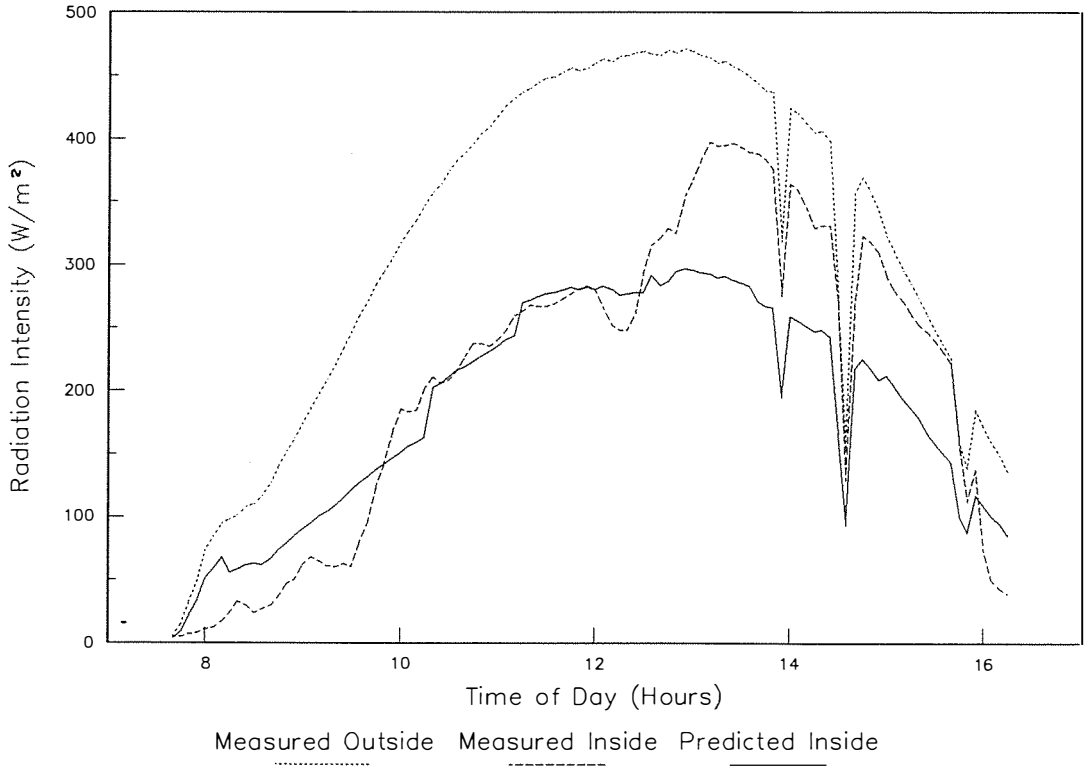

Figure 4.13. Predicted and Measured Light Transmitted into Test Greenhouse under Clear Sky Conditions (Point 4B 23/7/89)

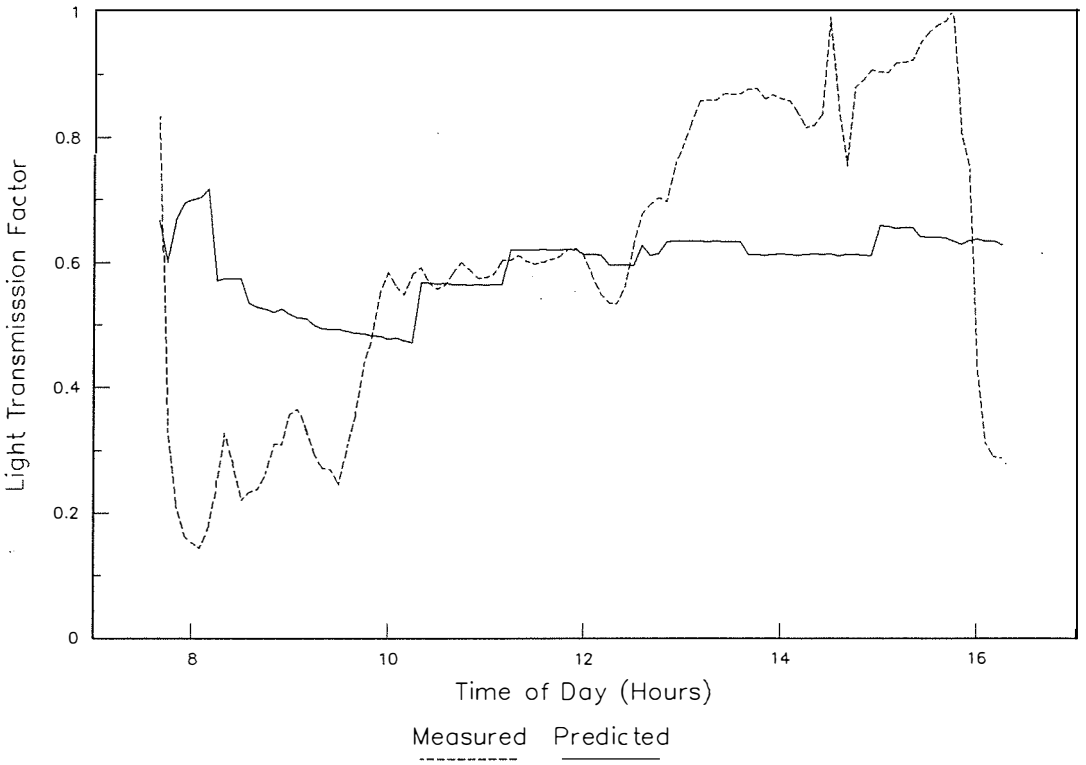

Figure 4.14. Predicted and Measured Light Transmission Factors under Clear Sky Conditions (Point 4B 23/7/89).

The outside radiation conditions, measured and predicted light transmission, and measured and predicted light transmission factors for an internal location, (1A), on a partially cloudy day are shown in Figures 4.15 to 4.17. Note once again that the model tended to over-predict in the morning, and over-predict in the afternoon, except where shadows were caused by structural members.

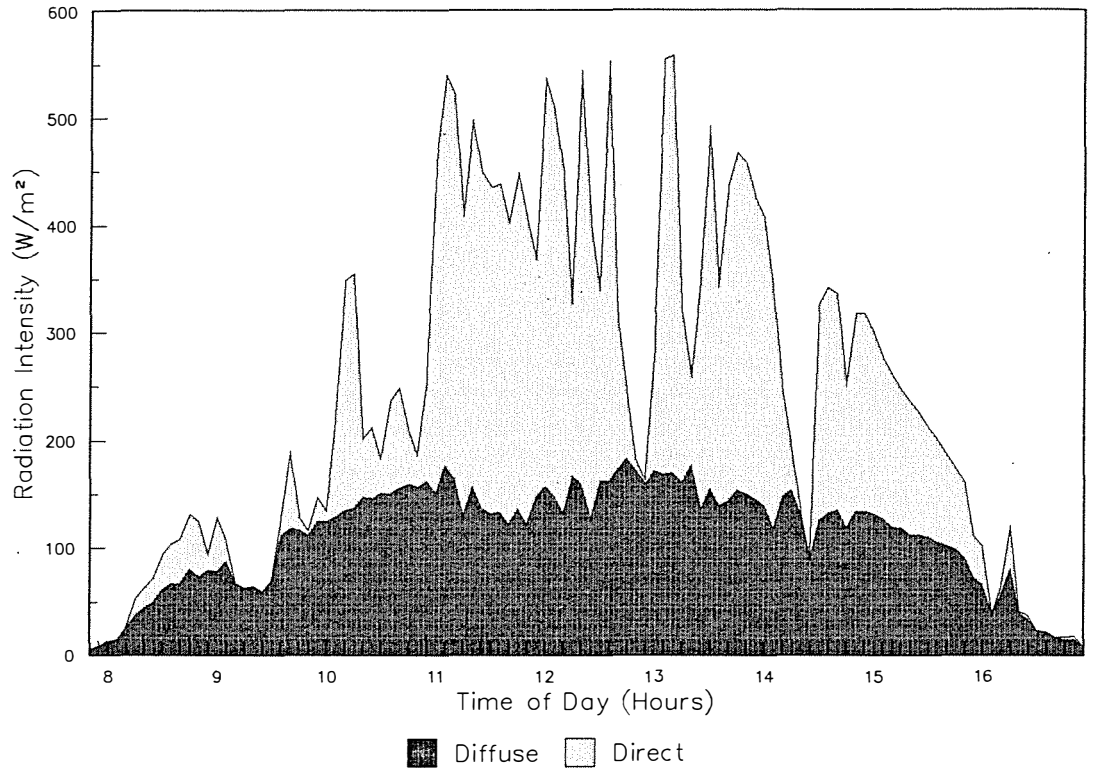

Figure 4.15. Diffuse and Direct Components of Global Radiation on 7/7/89

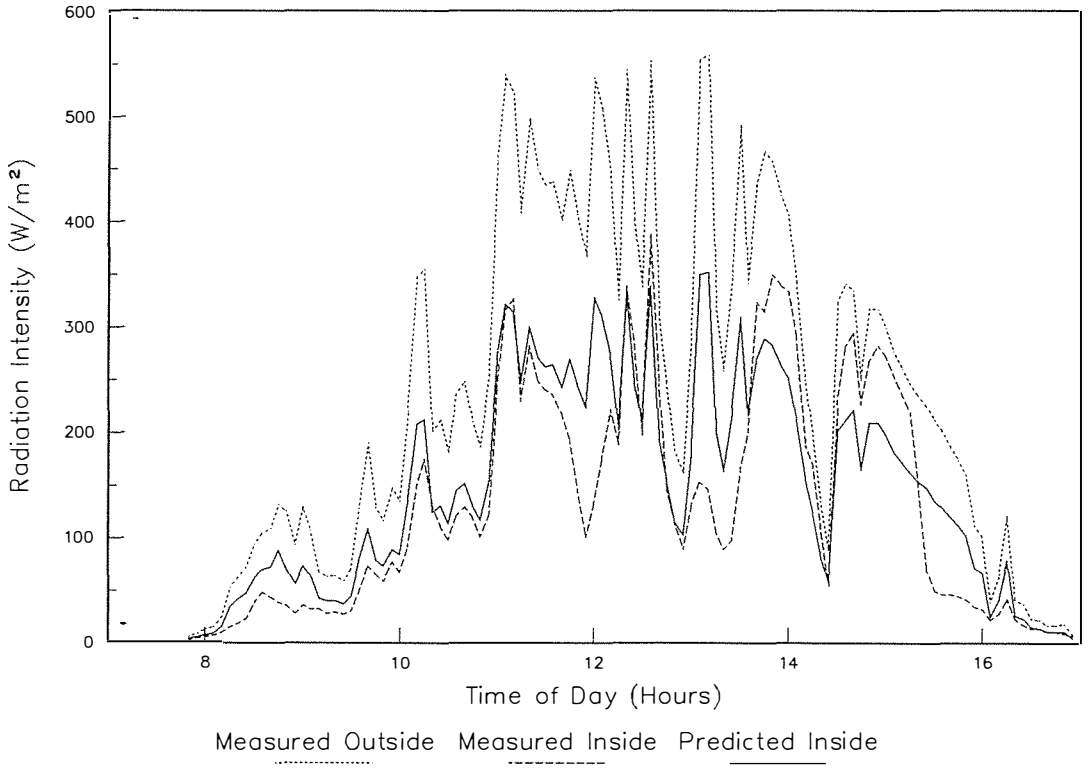

Figure 4.16. Predicted and Measured Light Transmitted into Test Greenhouse under Cloudy Sky Conditions (Point 1A 7/7/89)

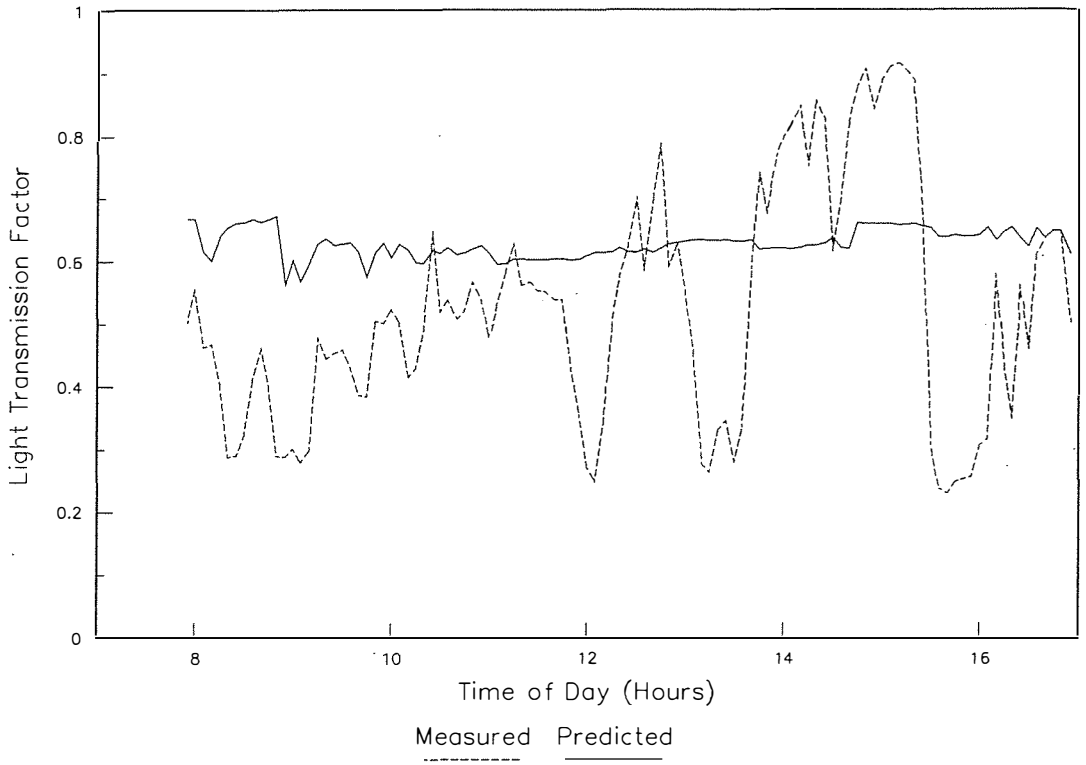

Figure 4.17. Predicted and Measured Light Transmission Factors under Cloudy Sky Conditions (Point 1A 7/7/89)

Initial analysis of predicted versus measured five minute data revealed a considerable amount of scatter (Figures 4.18 to 4.25).

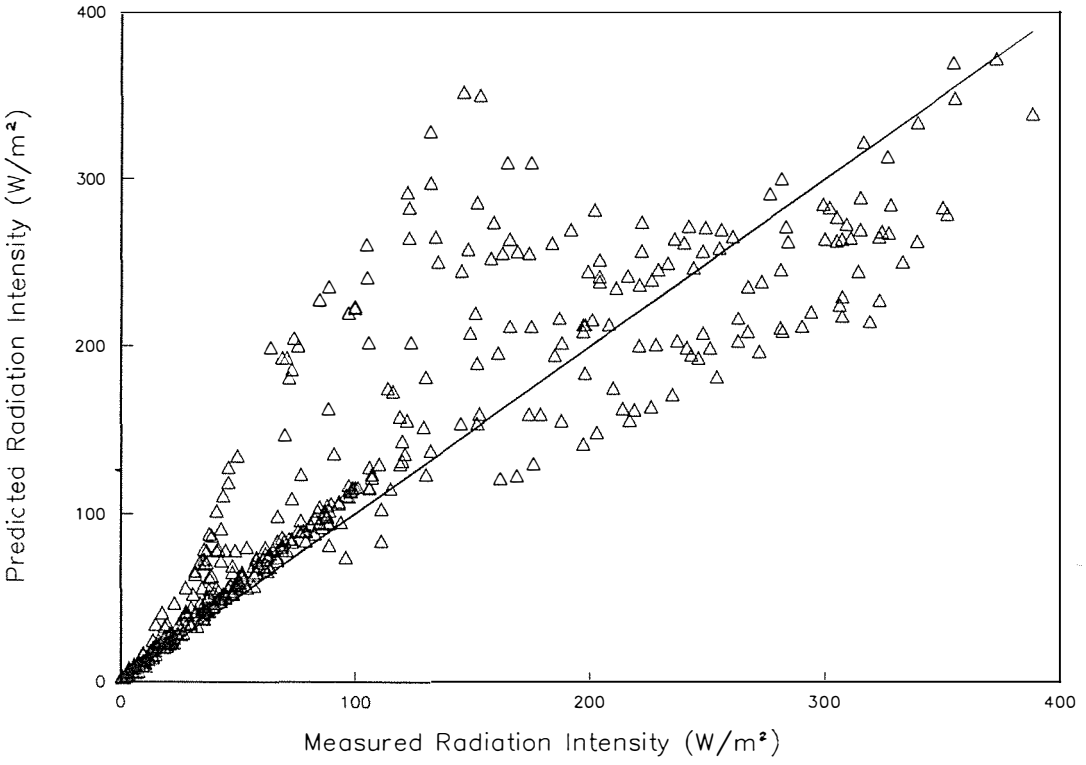

Figure 4.18. Predicted vs Measured Radiation Levels Point 1A

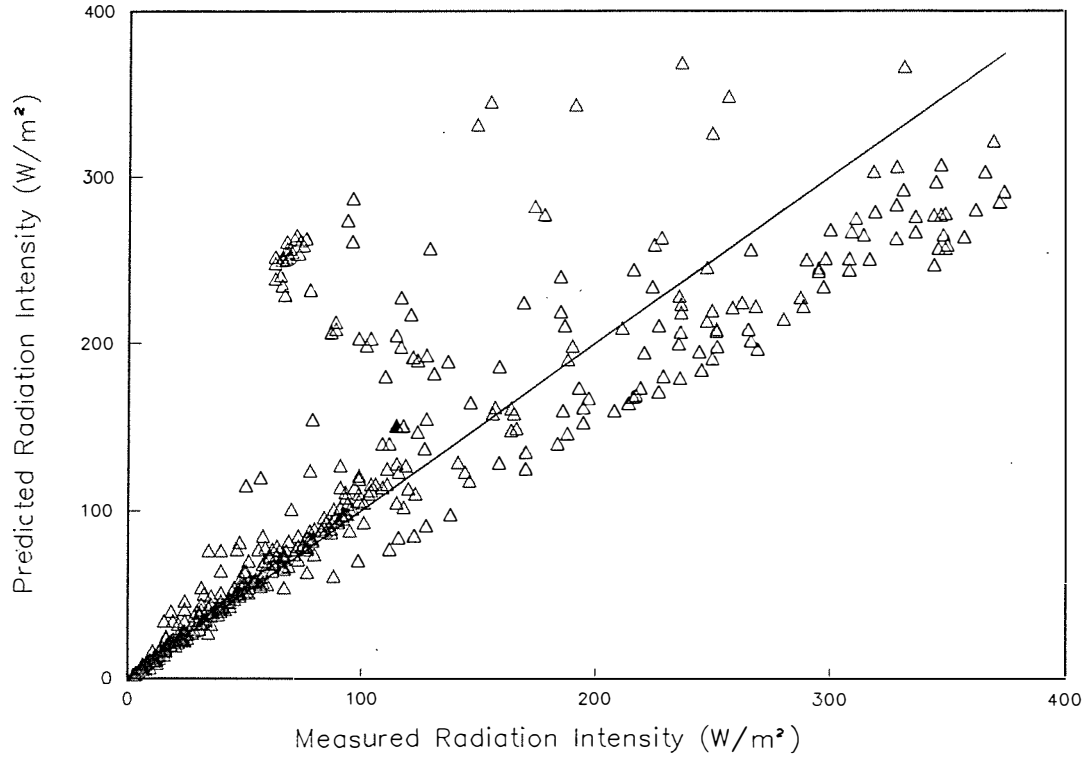

Figure 4.19. Predicted vs Measured Radiation Levels Point 1B

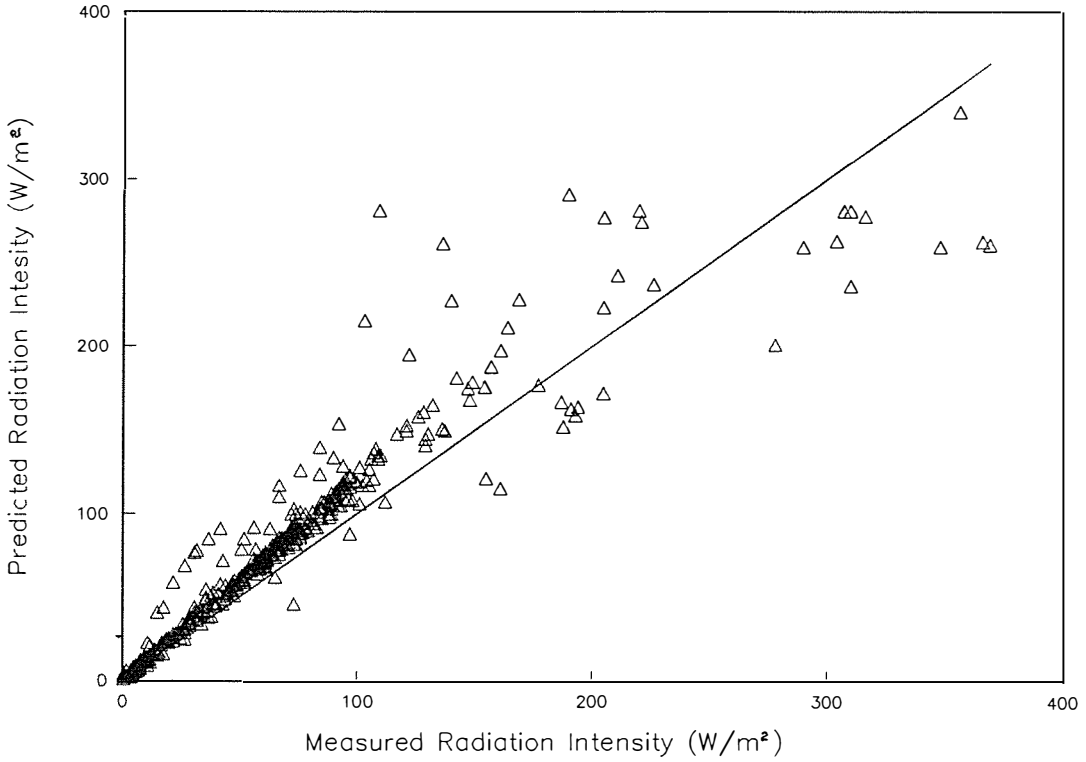

Figure 4.20. Predicted vs Measured Radiation Point 2A

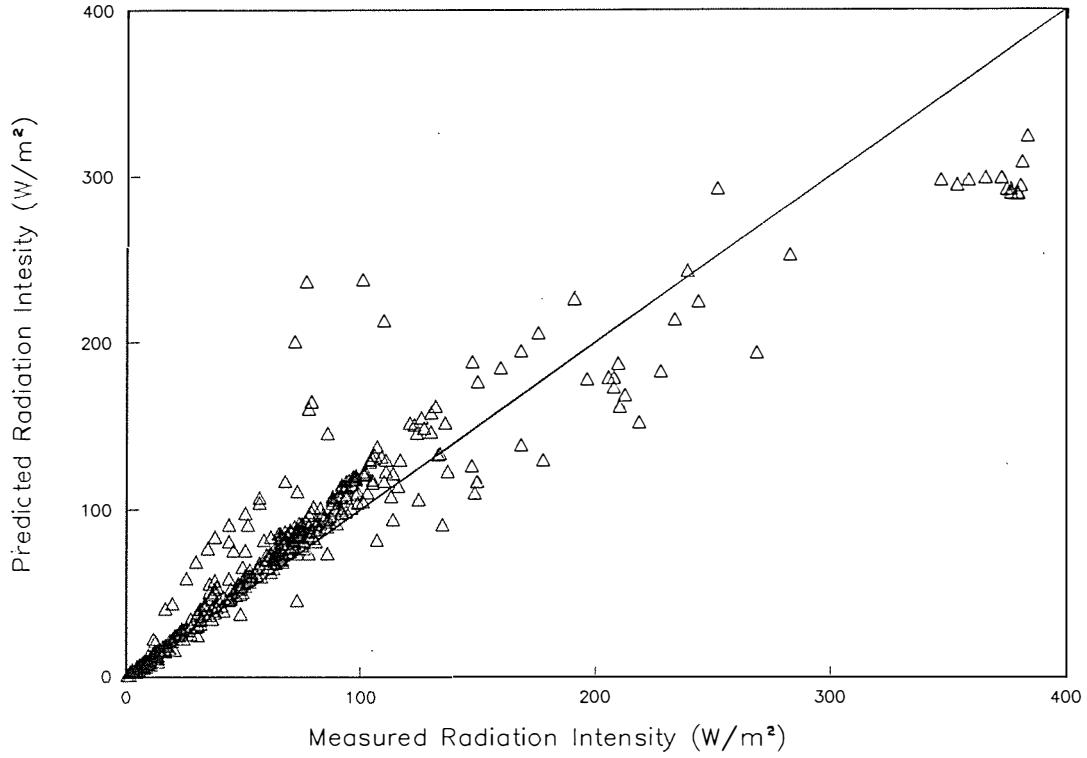

Figure 4.21. Predicted vs Measured Radiation Point 2B

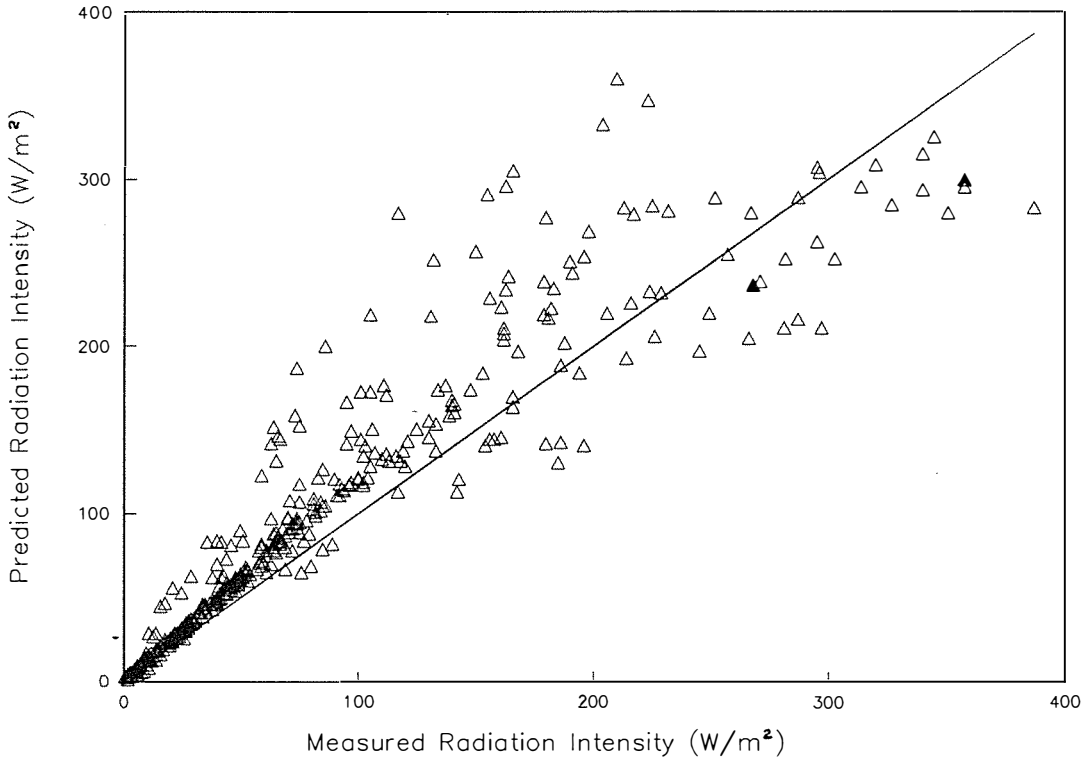

Figure 4.22. Predicted vs Measured Radiation Point 3A

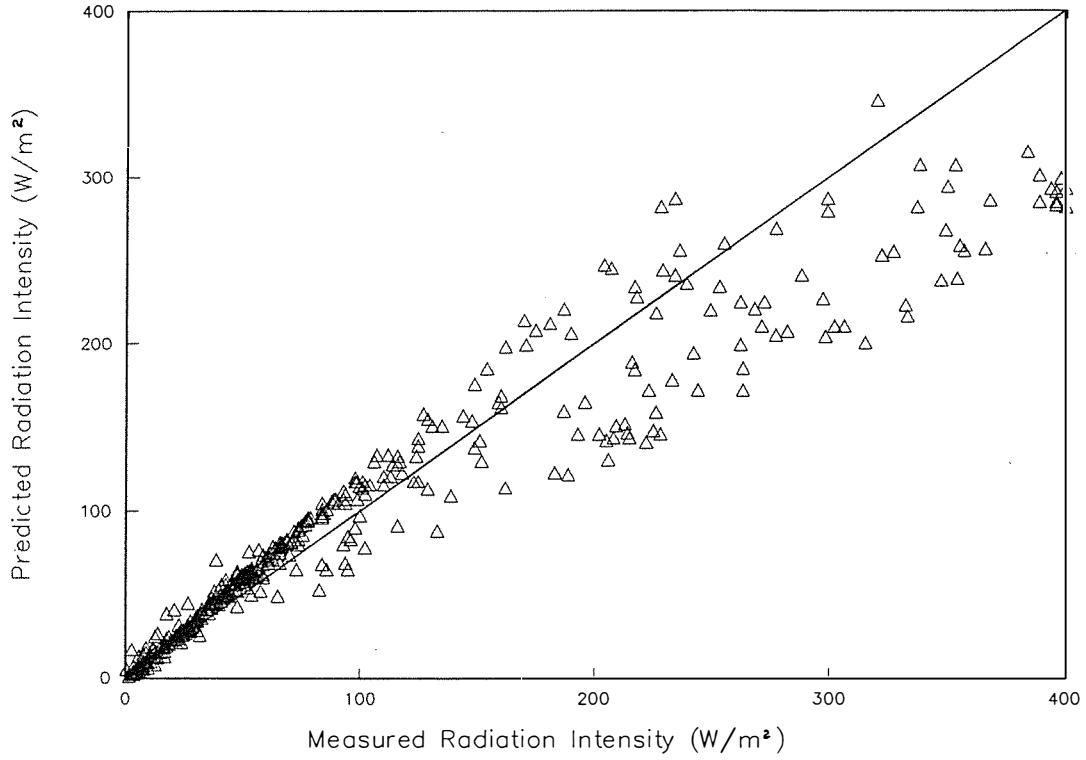

Figure 4.23. Predicted vs Measured Radiation Point 3B

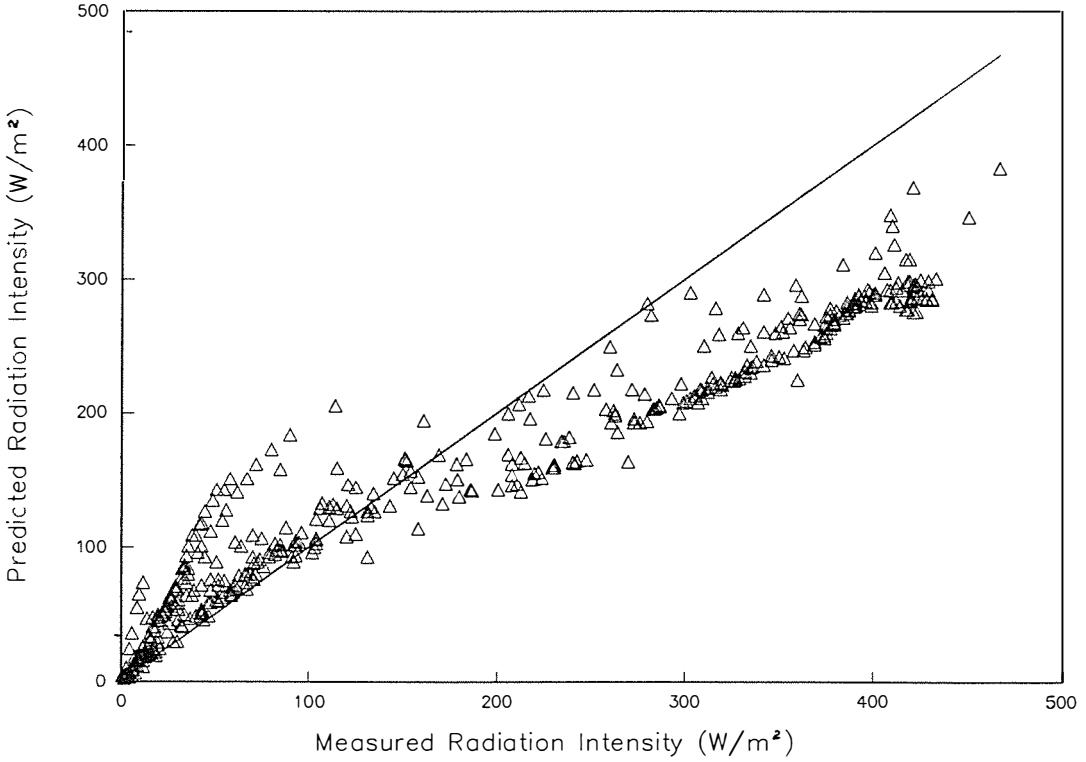

Figure 4.24. Predicted vs Measured Radiation Point 4A

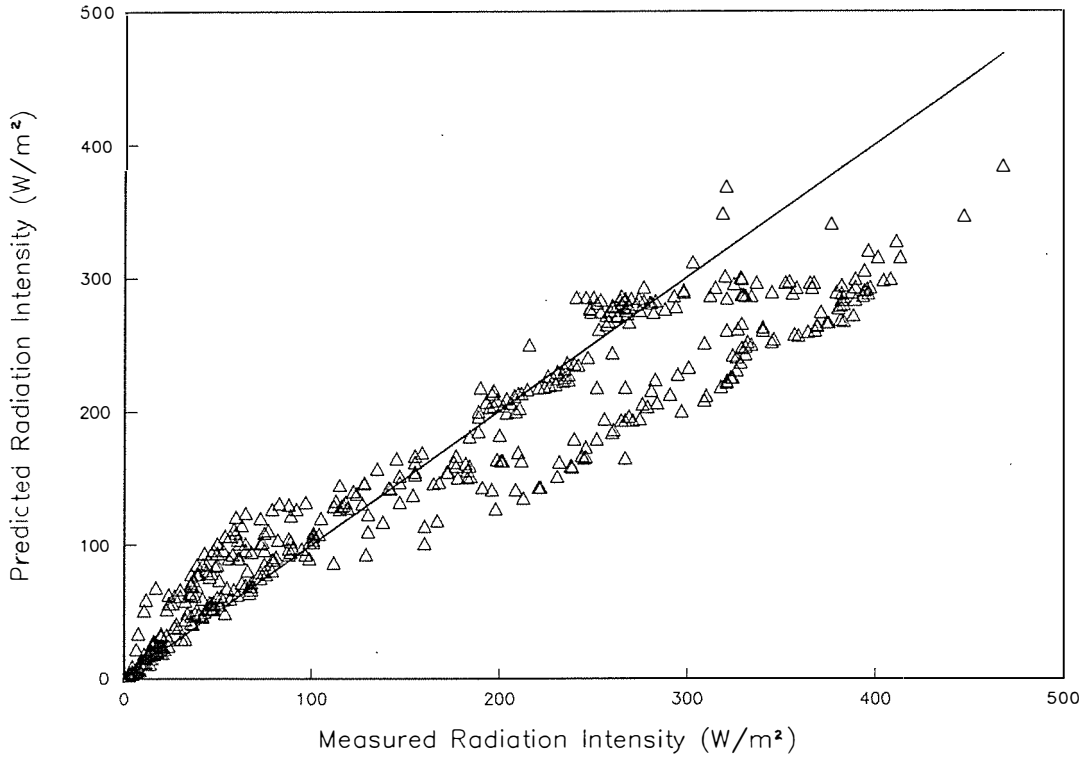

Figure 4.25. Predicted vs Measured Radiation Point 4B

In order to progress, hourly and daily average light transmissions were generated, from the five minute data. The results of the hourly averaging are shown in Figures 4.26 and 4.27, and the daily averaging in Figures 4.28 and 4.29. Reasonable fits were obtained when the North-West perimeter data was removed and treated separately. For the perimeter locations the model predicted the light transmission well for hourly average transmission and slightly over-estimated daily transmission (4%). The light transmission for the internal locations was consistently over-predicted by 38%, for daily averages, and 24%, for hourly averages. These figures are based on the model with clean glass. Inclusion of the effect of dust accumulation reduced these over-estimates considerably.

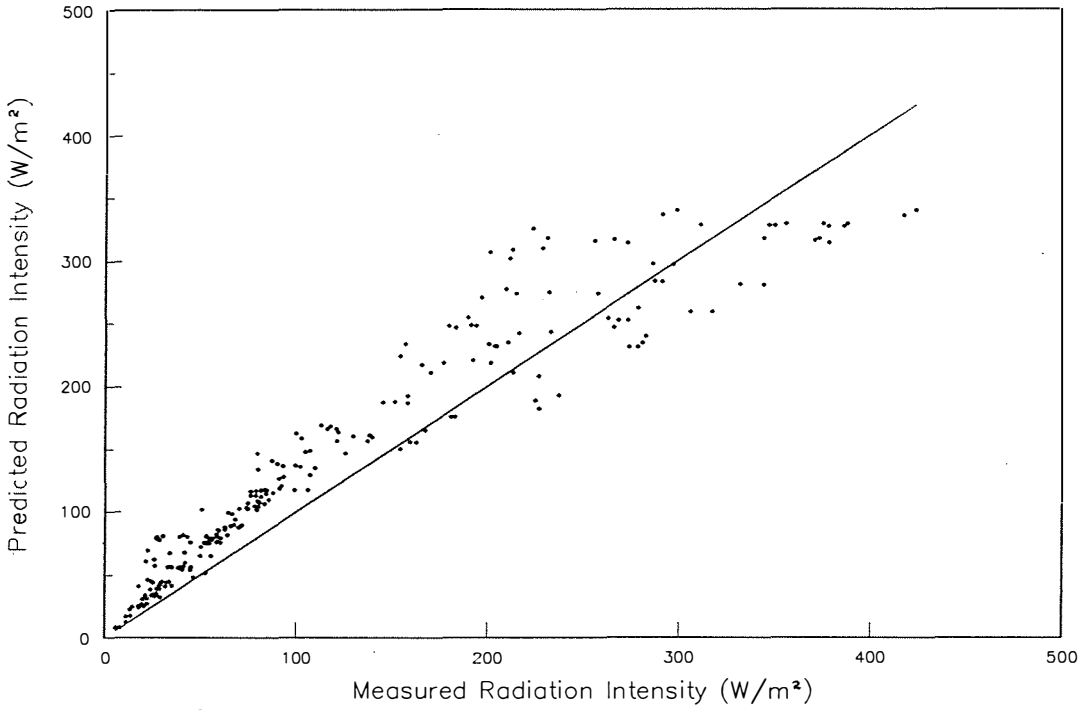

Predicted = 1.24 Measured
R^2 = 0.96

Figure 4.26. Predicted vs Measured Hourly Average Light Intensities Excluding Perimeter Locations.

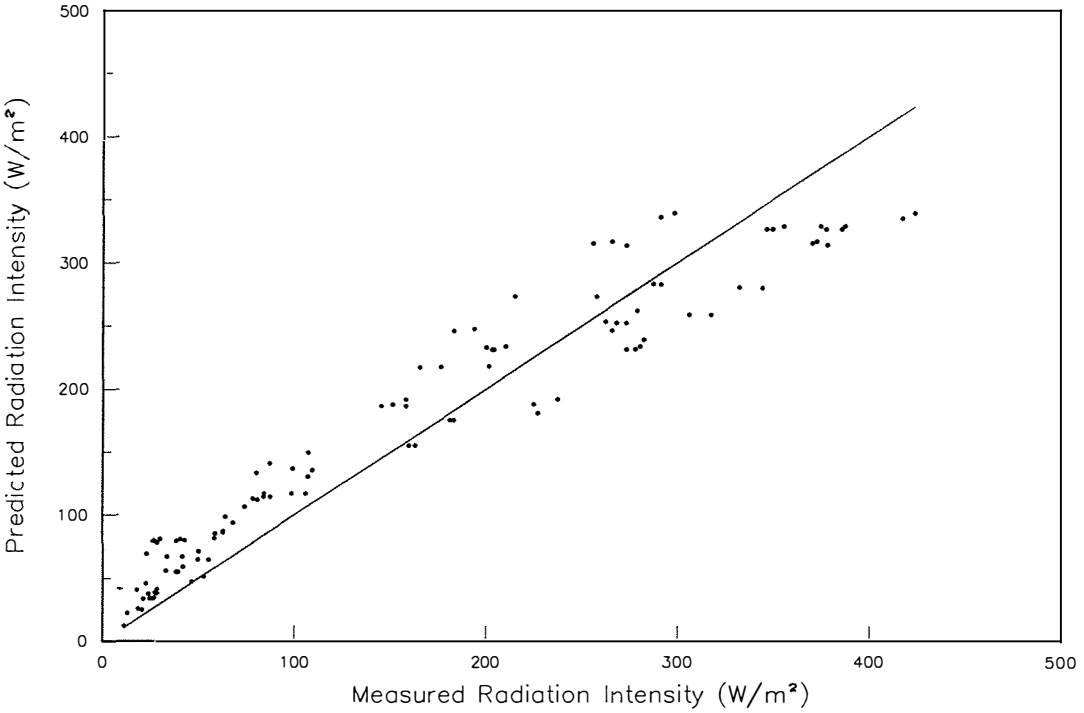

Predicted = 0.99 Measured
R^2 = 0.90

Figure 4.27. Predicted vs Measured Hourly Average Light Intensities Perimeter Locations.

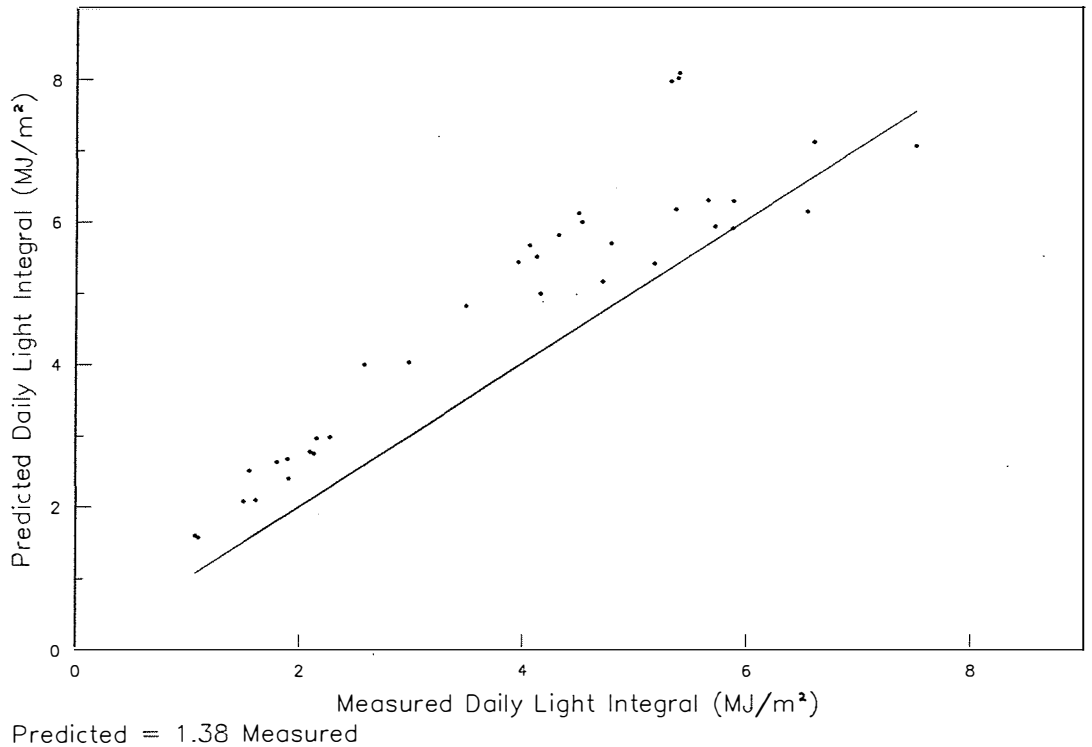

Predicted = 1.38 Measured
R^2 = 0.96

-Figure 4.28. Predicted vs Measured Daily Light Integrals Excluding Perimeter Locations.

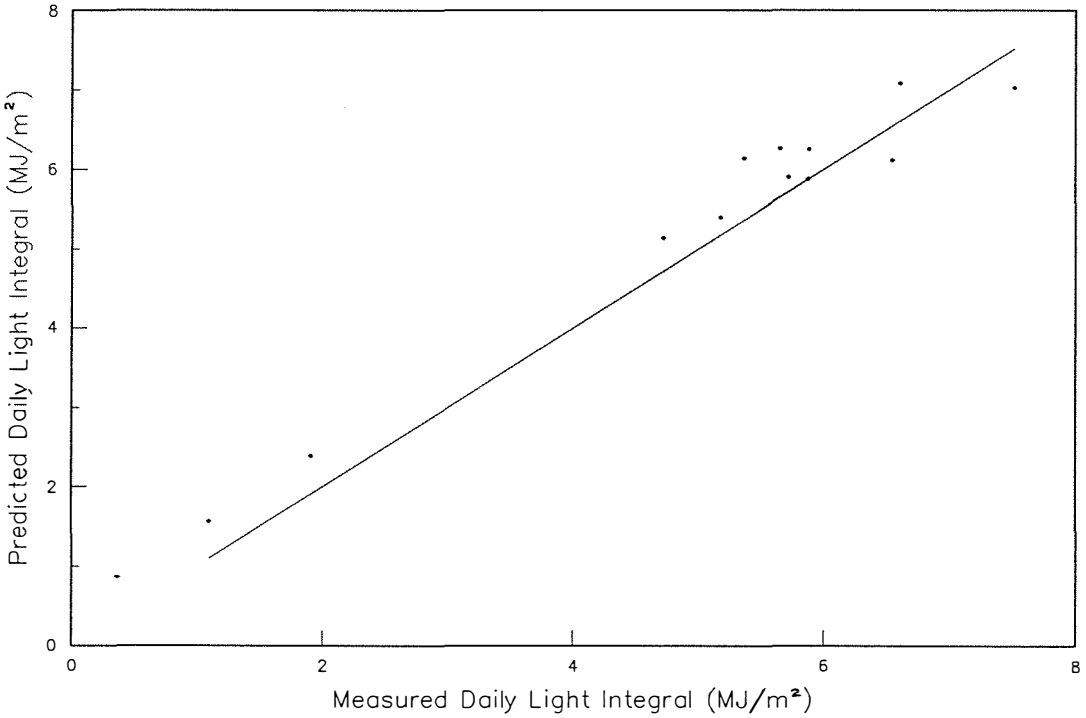

Predicted = 1.04 Measured
R^2 = 0.96

Figure 4.29. Predicted vs Measured Daily Light Integrals Perimeter Locations.

4.3.8 Discussion

The results obtained were as expected, since the model did not realistically account for the effect of dust accumulation, larger size of the gutters compared to other horizontal structural members, or the presence of the overhead heating system. The important finding at this point was that the model had a systematic error of about 24%, for interior locations and hourly average transmission, and 1% for perimeter locations. On the basis that the perimeter locations amounted to 22.7 m², or 22.2% of the floor area, a weighted correction factor, τ_R, was calculated from:

$$\tau_R = \frac{\tau_{Rp} A_{fp} + \tau_{Ri} A_{fi}}{A_{fp} + A_{fi}} \qquad (4.23)$$

where τ_{Rp} and τ_{Ri} are the appropriate transmission reduction factors for the perimeter and interior locations, 1.01 and 0.81 respectively, and A_{fp} and the A_{fi} are the area of floor for perimeter and interior locations, 22.7 m² and 79.6 m² respectively.

To utilize the predictions of the light transmission model in the greenhouse simulation model, the transmission tables, generated with no extra absorption, were used and multiplied by the reduction factor, τ_R. The absorption of the structure and glazing were increased by a factor of $1.0 - \tau_R$. The total absorbed radiation was divided between the glazing and structure by a structural absorption factor, α_{struc} (0.44), based on the relative projected area of the structural members in the greenhouse to the that of all the structural components including the glazing bars.

4.4 SUMMARY

In the first section of this chapter a model has been developed to partition incoming solar radiation into direct and diffuse components, and to further subdivide these into photosynthetically active and near infra-red components, in order to be able to correctly determine the light interception by the crop.

In section 4.2 models of light transmission into greenhouses have been reviewed. The modification and calibration of one of these models has been described in section 4.3. A systematic error was discovered due to the models inherent simplifications of the layout of the structural components. It was found that reduction of transmission by dust would also have a marked effect on transmission. Other trials found that the predictions of light intensity at the floor of the greenhouse could also be used to predict the light intensity at the top of the crop, except at very low sun angles, where errors would not be significant.

A new computer program has been written to calculate the average transmission factor for three different distributions of diffuse sky light. The Uniform Overcast and Standard Overcast distributions produced almost identical results. However, results for a Clear Sky distribution were more variable. When the sun was close to the zenith the results were similar to those obtained from the overcast skies, but when the sun was close to the horizon the transmission factor was 20% higher. To account for the under-prediction of the Uniform Overcast sky distribution during clear or partially cloudy skies the circumsolar fraction of diffuse radiation should be treated as direct radiation.

The calibrated model has been used to develop transmissivity and absorptivity tables for the test greenhouse for diffuse and direct incident radiation. This information has been used subsequently in the greenhouse and crop simulation models (Chapters 5 and 6).

5 THE GREENHOUSE MODEL

In this chapter the development of a model describing the response of the greenhouse environment to external disturbances, and internal control actions, will be discussed. The first section reviews models already published in the literature. The remainder of the chapter is devoted to the development of a dynamic simulation model of the greenhouse environment. In section 5.2 a rationale for the development of a new simulation model is discussed. This is followed by the development of the differential and algebraic equations which describe the greenhouse system. The many parameters used in the model equations are presented in section 5.4, and the practical implementation of the model equations as a computer program, in section 5.5. Results of the simulation model validated against measured data are presented in section 5.6. This is follow by a discussion and a brief summary.

5.1 REVIEW OF EXISTING MODELS

In this section existing models of the response of the greenhouse environment are reviewed. This review has been updated periodically throughout the course of the research, to include some concurrent studies.

During the last thirty years many models of the greenhouse environment system have been developed. The number of models reported in the literature reflects the increasing use of models in the applied sciences. This, in itself, can be traced to the availability of the computing power necessary to solve complex models using numerical techniques. Over this period of time there has been a progression in the complexity of the models produced to describe the response of the greenhouse environment, from simple analytical models with one dependent variable, to highly complex models with many dependent variables, requiring numerical solutions.

In a review of models conducted by Kano and Sadler (1985) for publications up to 1983, five categories of model were identified: time series (i.e. empirical models), steady state single component models, steady state multiple component models, dynamic multiple component models, and models that include the carbon dioxide exchange of the crop. These classes, with some minor modifications, will be used in this review. Table 5.1 is a summary of the many models published in the last thirty years, defined by type, country of origin, and reported use of the model.

Other reviews of greenhouse modelling have been carried out by Takakura et al (1985), Takakura (1989), Kyritsis (1989), and Bot (1989a).

Table 5.1. Models of the Greenhouse Environment				
Author(s)	Date	Type	Country	Use of Model
Schockert & von Zabeltitz	1980	TS	West Germany	Energy consumption prediction
Strom & Amsen	1981	TS	Denmark	Energy consumption prediction
Udink ten Cate	1983	TS	The Netherlands	Controller evaluation
Davis	1984	TS	United Kingdom	Controller evaluation
Hesketh et al	1986	TS	New Zealand	Controller evaluation
Walker	1965	SSS	USA	Simulation of Air Temperature
Garzoli & Blackwell	1971 1973	SSS	Australia	Greenhouse climate under Australian conditions
Price & Peart	1973	SSS	USA	Evaluation of power plant/ greenhouse complex
Bailey	1977	SSS	UK	Energy consumption prediction
Horigushi	1978	SSS	Japan	
Landsberg et al	1979	SSS	United Kingdom/ Australia	Efficacy of evaporative cooler
Rotz et al	1979	SSS	USA	Use of Solar collectors
Garzoli & Blackwell	1981b	SSS	Australia	Nocturnal heat loss (single skin)
Ewen et al	1980	SSS	USA	Coal mine air for heating
Von Elsner	1980	SSS	West Germany	Greenhouse climate study
Breuer	1983	SSS	The Netherlands	Energy consumption prediction
Wass & Barrie	1984	SSS	United Kingdom	Energy consumption prediction
White	1984	SSS	New Zealand	Energy consumption prediction
Shell & Staley	1985	SSS	Canada	Energy consumption prediction
Zhao et al	1985	SSS	USA/Israel	Predict leaf temperature & transpiration

Table 5.1. Models of the Greenhouse Environment (continued)

Author(s)	Date	Type	Country	Use of Model
Santamouris & Lefas	1986	SSS	Greece	Sub-surface heat storage
Garzoli & Blackwell	1987	SSS	Australia	Nocturnal heat loss (double skin)
Jolliet Jolliet & Munday Jolliet et al	1988 1989 1989	SSS	Switzerland	Energy consumption prediction
Businger	1963	SSM	The Netherlands	Greenhouse climate study
Seginer & Levav	1971	SSM	Israel	Greenhouse climate study
Selcuk	1971	SSM		Evaluation of power/desalination/food production facility
Kimball	1973	SSM	USA	Greenhouse climate study
Maher & O'Flaherty	1973	SSM	Ireland	Evaluation of evaporative cooling & plastic covers
Selcuk & Tran	1975	SSM		Greenhouse with solar still
Amdursky	1980	SSM		
Chandra & Albright	1980	SSM	USA	Test thermal screens
Kindelan	1980	SSM	Spain	Greenhouse climate study
Seginer	1980	SSM	Israel	Optimization analysis
Kimball	1981 1983b	SSM	USA	Greenhouse climate studies (The MEBP model)
Lovseth	1981	SSM		
Avissar & Mahrer	1982	SSM	Israel	Greenhouse climate study
Bailey	1984	SSM	United Kingdom	Evaluation of heat-pump de-humidifier
Bellamy & Ward Bellamy	1984 1991	SSM	New Zealand	Evaluation of novel shaped greenhouse. Modified MEBP model
Okada	1985	SSM	Japan	Test thermal screens
Baille et al	1985	SSM	France	Test thermal screens

Table 5.1. Models of the Greenhouse Environment (continued)

Author(s)	Date	Type	Country	Use of Model
Bellamy & Kimball	1986	SSM	USA/New Zealand	CO_2 enrichment Modified MEBP model
Burek et al Burek & Norton	1989 1989	SSM	United Kingdom	Validation of modified MEBP model for air supported greenhouse
Kurata	1989a	SSM	Japan	Effect of thermal screens on solar storage
Takami & Uchijima	1977a 1977b	SSM/D	Japan	Solar heat storage
Levit & Gaspar	1988	SSM/D	Argentina	Greenhouse climate study Energy consumption prediction
Takakura et al	1971	D	Japan/USA	Greenhouse climate study
Froehlich Froehlich et al	1976 1979	D	USA	Greenhouse climate study
Olszewski & Trezek	1976	DS	USA	Use of power plant reject heat
Chandra	1979	D	United States	Greenhouse climate study
Kittas	1980	D	Greece/France	Greenhouse climate study
Chandra et al	1981	D	USA	Energy and moisture requirements
Duncan et al	1981	D	USA	Test thermal screens
Glaub & Trezek	1981a 1981b	D	USA	Energy and mass flows in a solar heated hydroponic greenhouse
Ahmadi & Glockner	1982	D	Canada	Performance of inflated greenhouse
Bot	1983	D	The Netherlands	Greenhouse climate study
Ziv	1983	D	Israel	
Arinze et al	1984	D	Canada	Evaluate solar storage systems
Huang & Kato	1984	D	USA/Japan	Greenhouse climate study
Tross et al	1984	D	Israel	Evaluation of Optical Liquid Filter greenhouse

Table 5.1. Models of the Greenhouse Environment (continued)

Author(s)	Date	Type	Country	Use of Model
Deltour et al	1985	D	Belgium	Greenhouse climate studies
Willits et al	1985	D	USA	Evaluate rock-bed storage
Boulard & Baille	1986a 1986b	D	France	Evaluation of soil heat storage
Alabiso et al	1989	D	Italy	Evaluation of waste heat utilization system
Sorbie & Curry	1973	DC	USA	Greenhouse climate and growth of winter lettuce
Parker et al	1981	DC	USA	Effect of soil heating
Van Bavel et al	1981	DC	France/USA	Fluid-roof greenhouse
Cooper & Fuller	1983	DC	Australia	Greenhouse climate and growth of tomatoes
Hwang et al	1989	DC	USA	Greenhouse climate study with tomato growth model

TS = Time series model
SSS = Steady state single component model
SSM = Steady state multiple component model
SSM/D = Steady state multiple component model with some dynamic components
D = Dynamic model
DC = Dynamic model including carbon exchanges of crop

5.1.1 Time Series Models

In this class of model the system outputs (greenhouse environment responses) are related directly to the system inputs (control actions and weather disturbances), without attempting to explain the internal operation of the system. (See Chapter 2).

Time series models have been developed to determine the heating requirements of greenhouses (Schockert & Von Zabeltitz, 1980, Strom & Amsen, 1981). The model of Schockert & Von Zabeltitz related the energy consumption coefficient to prevailing wind speed for single and double glass structures, while the model of Strom & Amsen related energy usage to mean outside temperature. These two models reflect other similar models of greenhouse energy consumption. They are derived from data collected from real greenhouses in particular climates and are not widely applicable.

Time series models have also been used to study the control characteristics of greenhouses (Udink ten Cate, 1983, Hesketh et al, 1986, Davis, 1984). The model of Udink ten Cate was used to compare the response of conventional PI, modified PI, and adaptive control algorithms for controlling air temperature in a Dutch greenhouse with natural ventilation and pipe heating. The heating, ventilation and solar radiation input processes were modelled as first order functions and the transfer function was derived in the Laplace domain. Experiments were then performed to determine the various parameters of the model of the open loop system, gains, time constants, and dead times. The parameters of the time series model were also related to the parameters (i.e the heat transfer coefficients) of a simple analytical model, which were calculated subsequently, from the time series model. The time series model of the system was used to design and test various control algorithms.

Davis (1984) used ARMAX (auto-regression moving average exogenous variable) and TF (transfer function) models to develop adaptive controllers for a greenhouse ventilation system. These were compared to conventional proportional and PI algorithms and found to be superior. A slightly modified version of the ARMAX model was tested on a real greenhouse and gave satisfactory results.

Hesketh et al (1986) developed a discrete polynomial model of a greenhouse with fan ventilation and forced convection heating. From this a polynomial controller was developed and its performance simulated. It was predicted that this new controller would have markedly better performance than a conventional on/off controller, particularly if the control outputs were allowed to vary continuously.

5.1.2 Steady state Single Component Models

This class of model deals with energy and mass balance of one component of the greenhouse system, and attempts to relate the greenhouse behaviour to the components of these balance equations.

The simplest models in the class consider only the energy balance of the greenhouse air. An early model of this type was set out by Walker (1965) (developed further in Walker et al (1983)) who developed the energy balance of the greenhouse air and the equations describing the various heat fluxes contributing to the energy balance. These were used to relate the greenhouse air temperature to the input variables, solar radiation and outside air temperature.

Several authors have utilised Walker's model since that time. Rotz et al (1979) studied the effects of three different covering systems in conjunction with three different solar collector techniques. Ewen et al

(1980) considered a greenhouse heated with coal mine air. Models similar to Walker's are that of Horigushi (1978) and Von Elsner (1980). Garzoli and Blackwell (1971, 1973, 1981a, 1981b) developed a model for use under Australian conditions. Landsberg et al (1979) studied the efficacy of evaporative cooling using such a model solved at 15 minute intervals, effectively a quasi-static analysis. Santamouris and Lefas (1986) have studied the thermal response and control of a hybrid greenhouse with sub-surface heat storage.

Some authors have based their energy balances on components other than the greenhouse air. Garzoli and Blackwell (1981), in their study of the nocturnal heat loss from a single skin plastic greenhouse, developed the energy balance around the cover. They later extended this to a two cover system (Garzoli & Blackwell, 1987). Zhao et al (1985) considered the energy balance of the crop to predict night time leaf temperatures and transpiration.

Several models of this type have been developed principally to predict the energy consumption of greenhouses. Bailey (1977) developed a model based on degree-day data corrected for solar radiation effects. White (1984) described a model in which hourly weather data was generated from long term monthly averages and used to solve the energy balance for each hour of a theoretical normal month. The energy input requirements were then summed over all hours for the month. Wass & Barrie (1984) described a similar model, using real weather data, validated against fuel consumption figures supplied by four growers in the South-West of England.

Breuer (1983) presented a model developed in the Netherlands, at IMAG (Institute of Agricultural Engineering). This was used by Van de Braak et al (1984) to produce cumulative frequency distributions of heat load, to test the performance of a heat pump. The model was also used to compare energy demands for greenhouses in The Netherlands and in Ohio (Short & Breuer, 1985).

Shell and Staley (1985) developed a modified form of the ASHRAE (American Society of Heating, Refrigerating and Air-conditioning Engineers) steady state building heat loss model (ASHRAE, 1982)), after considering the work of Blom et al (1983) and Walker et al (1983). Their model calculated the energy balance of the greenhouse, and hence the energy consumption, on a monthly basis, based on monthly solar radiation and monthly mean temperature differences. This was used as part of an economic analysis of alternative energy conservation strategies.

Recently Jolliet (1988) (also Jolliet & Munday, 1989, Jolliet et al, 1989) developed a model which separated out the day and night time energy requirements, and accounted for the solar heat storage in the soil, as a

function of potential solar energy storage lost by ventilation. This model used the Solar Energy Utilisation Factor, which is the ratio of useful solar energy to collected solar energy, a concept used in the analysis of solar collectors.

5.1.3 Steady State Multiple Component Models

This class of model considers the energy and mass balances of several sub-systems of the greenhouse simultaneously. This results in a system of simultaneous algebraic equations which, when solved, yield the steady states of the system variables. When these steady states are found for successive time steps, a quasi-steady state solution of the time response of the system results.

Businger (1963) identified many of the energy fluxes in the greenhouse and formulated a model based on the energy balances at the soil surface and the greenhouse cover. This model has been the basis for many subsequent models of this type. Kimball (1973) derived the steady state energy balances for both sides of the greenhouse cover, the crop, the internal air space, six soil layers, an evaporative cooler, and a mass balance for the internal air space. The resulting set of twelve simultaneous algebraic equations was solved for the twelve unknowns, eleven temperatures and one vapour pressure, using a linearized Taylor series method which seeks successive approximations to the solution. The model was validated for a greenhouse without a crop under three different operational conditions: normal operation, evaporative cooling, and cooling with shade in place. Simulations were performed hourly to produce a quasi-steady state analysis.

Maher and O'Flaherty (1973) produced a similar but less detailed model, using energy balances for the cover, air and crop. This model was used to study the likely effect of evaporative cooling and polyethylene as a covering.

Chandra and Albright (1980) developed a model which included an elaborate treatment of long-wave radiation exchanges. This model was used to test the effect of thermal screens.

Kindelan (1980) developed a steady state model of the greenhouse cover, air and crop in conjunction with a dynamic sub-model of the soil. As part of this sub-model, the depth below which heat transfer was insignificant was determined.

Avissar & Mahrer (1982) (also Mahrer & Avissar, 1984) developed a similar model, with a dynamic soil sub-model. A unique feature of their model was the dynamic simulation of moisture movement within the soil profile. This was included since moisture content has a marked effect on the thermal

properties of the soil. Furthermore, there may be significant energy transfer associated with moisture transport in both the liquid and vapour phases. For crops grown in the soil, with high rates of transpiration, diurnal changes in the soil moisture profile can be quite marked. Another feature of this model was the special attention placed on realistic modelling of the stomatal functioning of the crop in response to environmental change within the greenhouse. The model was used to predict the heating and cooling requirements of glass and polyethylene covered greenhouses during the winter and summer in the coastal region of Israel.

Kimball (1981, 1986) produced an improved model with a novel approach to accounting for the heat transfer into and out of the soil. This model formed a sub-model of his Modular Energy Balance Program (MEBP) capable of simulating the performance of several energy related devices connected together such as a greenhouse, solar collector, rock bed, and thermo-stat. In the earlier model the floor was divided into thin layers of presumably negligible heat capacity. However, for this to be true the layers would need to be very thin and thus a large number would be required to represent adequately the effective storage depth of the soil. Furthermore, the time step of the simulation must be reduced to the order of minutes, whereas other parts of the system follow the diurnal weather pattern with a time step of one hour. Thus, accurate simulation of the soil heat fluxes increased the computational time by one order of magnitude (Kimball, 1981). To overcome this problem the soil heat flux at the surface was represented using thermal response factors (Kusuda, 1969, Peavy, 1978, Kimball, 1983a). This method calculated the surface heat flux as a function of the temperature history of the surface. The thermal response factors must be predetermined by solving the standard heat diffusion equation for the appropriate geometry and boundary conditions. The model also included a detailed analysis of long-wave radiation exchanges.

The Modular Energy Balance Program has been used by other workers recently. Bellamy & Ward (1984) used the program to simulate the performance of a greenhouse, with a novel M shaped roof, for New Zealand conditions which is currently being prototype tested (Bellamy, 1991). Bellamy and Kimball (1986) used the program to investigate the effect of climate and location on the ventilation time requirements of greenhouses as part of a study of the potential for carbon dioxide enrichment. Burek et al (1989) have validated the model using an air supported greenhouse. Good results were obtained after a minor alteration was made to the algorithm.

Baille et al (1985) reported on a model similar to that of Kimball's earlier work (Kimball, 1973) which they also used to test the theoretical performance of thermal screens.

Okada (1985) developed a model to analyse the effect of multi-layer thermal screens. Energy balances of the cover, two screen layers, the air, and the floor surface were included.

5.1.4 Dynamic Models

This class of model considers the time dependent energy and mass storage of each sub-system in the greenhouse. This results in systems of simultaneous differential equations, which when solved yield the time response of the system state variables to the time varying boundary values.

Takakura et al (1971) produced one of the first dynamic models of the greenhouse environment. Their model included the dynamic energy balances of the crop, air and soil, but ignored the thermal mass of the glass cover, where a steady state analysis was used. A dynamic mass balance for the greenhouse air was also included. The soil was modelled using a two dimensional network consisting of twenty soil blocks. Thus the horizontal heat loss from the soil under the greenhouse was modelled as well as the vertical movements. At each time interval, three algebraic equations were solved by iteration to find the glass cover temperature, followed by the solution of the twenty five differential equations describing the dynamic parts of the model. A Runge-Kutta numerical integration method was used to solve the dynamic equations. Time variant parameters of the model, such as heat transfer coefficients, were updated at the end of each time step, for use in the next time step of the simulation. Later versions of this model have been implemented in CSMP (Continuous Systems Modelling Program (IBM, 1975)).

Kittas (1980) developed in great detail the energy and mass balance equations for the various surfaces in a greenhouse as part of a study to determine the dynamic characteristics of the energy and mass exchange between the greenhouse air space and the exterior environment. From this, a model of the response of the internal air temperature, cover and soil surface temperatures was created. Included in this thesis was a great deal of information regarding data gathering for model validation, and determination of the various energy and mass exchange parameters. Based on this work Kittas further developed, and statistically tested, a number of semi-empirical relationships to predict inside air and cover temperature.

Duncan et al (1981) developed a dynamic model which only considered the energy balance of the greenhouse air. The time lag of solar heat released from the soil was accounted for by introducing a third order delay of one hour into the model. This was determined by calibration experiments. Simulation was performed using the GASP IV simulation language (Pritsker, 1974).

Glaub and Trezek (1981a, 1981b) developed the equations for a dynamic model of the greenhouse environment as part of a review of heat and mass transfer in the greenhouse environment. They developed dynamic energy balances for the inner and outer covers, air, crop, a floor slab, and a water mass balance for the air. They placed particular emphasis on including the effect of water vapour on the enthalpy of the greenhouse air, a factor ignored by most other researchers.

Parker et al (1981) presented a dynamic model of a greenhouse soil heating system that was attached to the greenhouse environmental simulation model of Sorbie & Curry (1973).

Ahmadi and Glockner (1982) used a dynamic model, with balances at the cover, air, crop, and four soil layers, and a water vapour balance of the air, to study the performance of inflated plastic greenhouses for Southern Canada. Validation of the model was reported in a subsequent paper (Ahmadi et al, 1982).

One of the most rigorous dynamic models of the greenhouse environment yet developed is that of Bot (1983). This model considered all components of the system to be dynamic in nature. The system was represented using the bond graph technique (Karnopp & Rosenberg, 1975, Oster et al, 1973, Van Dixhoorn & Evans, 1974), a procedure similar to the electrical network technique described below (Huang & Kato, 1984). As with the electrical network the bond graph representation was a linearized system. Solution of the bond graph could be accomplished by computer programs such as ENPORT (Rosenberg, 1974) or THT_SIM (Kraan, 1974, Van Dixhoorn, 1977), used by Bot. The linear differential equations could also be extracted from the bond graph and solved using standard numerical techniques or a simulation language. Bot reported that CSMP has been used for this purpose (van Bavel et al, 1985). An extensive part of this work was experimental determination of the relationships governing the various heat and mass fluxes in the greenhouse, in particular solar radiation transmission, natural ventilation, and convective heat and mass transfer coefficients. This work is continuing (Bot, 1988, Pers. Comm.).

Arinze et al (1984) used a dynamic model, solved using a Runge-Kutta predictor-corrector method, to investigate greenhouses with passive and active solar heat storage. Their model considered the greenhouse cover, air, crop and seven soil layers, as well as the water vapour balance of the air. Time steps of 5 and 10 minutes were used. Comparison of simulated with real data collected from a prototype greenhouse showed that the model fit was generally good (within 10% of measured temperature).

Huang and Kato (1984) developed an electrical network analogy of the energy flows in a greenhouse which included thermal capacity effects. Using this technique all energy flow equations were linearized and expressed as current flows in resistors, component temperatures were represented as voltage potentials, and thermal capacities as capacitors. For any combination of specified potentials (temperatures) the circuit could be solved using a circuit analysis program to yield the unknown potentials (temperatures) and currents (heat flows).

Tross et al (1984) used the greenhouse simulation model of Ziv (1983) to study the microclimate of a closed Optical Liquid Filter greenhouse sited in the Negev Desert. In this model the greenhouse cover was divided into 12 separate control volumes.

The models of Van Bavel (Van Bavel et al, 1981), Takakura (Takakura et al 1971) and Bot (Bot, 1983) were all programmed in CSMP and compared using data from Lubbock (Texas), Tokyo (Japan), and Wageningen (The Netherlands) (Van Bavel et al, 1985). The three models produced essentially the same results but with some differences mainly attributable to differences in the determination of convective heat transfer coefficients, stomatal functioning and solar radiation transmission.

Willits et al (1985) used the model of Chandra (1979) (also Chandra et al, 1980, 1981) in a similar study of the performance of a greenhouse attached to a rock-bed storage device. A unique feature of Chandra's model was the use of the Finite Element Method (Huebner, 1975) to solve the soil heat fluxes and temperatures.

Deltour et al (1985) reported on the development of a dynamic model based on eight differential equations solved by a Runge-Kutta technique.

Another, rather unique model, was that of Froehlich (1976) (also Froehlich et al 1979; Albright, 1984). This model was solved analytically (rather than numerically) by assuming that the forcing functions were periodic and could be expressed as Fourier series, and that the dependent variables were also periodic. A closed-form solution was then found for the various temperatures in the system.

Hwang et al (1989) developed a dynamic model of the greenhouse environment, which has been extensively validated. This model was used as a sub-model in a simulation of tomato growth and production (see next section).

5.1.5 Models Including the Carbon Dioxide Balance

This class of model is generally dynamic with the inclusion of the carbon dioxide balance of the greenhouse airspace, and a sub-model simulating crop photosynthesis, and possibly crop growth.

Sorbie and Curry (1973) presented a dynamic energy balance model of the greenhouse which included the plant growth model of Curry (1971) (also Curry & Chen, 1971). The resulting system of differential equations for the energy and mass balances of the greenhouse cover, air, crop and soil layers, was solved using a program written in the CSMP simulation language. The growth of lettuce in response to greenhouse environment was successfully simulated using this model.

Van Bavel et al (1981) presented a dynamic model which was used to simulate the performance of a fluid-roof greenhouse. The results were compared to those for a conventional glass greenhouse. In their model the thermal capacity of the crop was ignored, and treated with a steady state energy balance, and the soil was one dimensional. The carbon dioxide balance of the crop was also simulated (Van Bavel, 1978). The various equations were solved using a program written in CSMP.

Cooper and Fuller (1983) report a dynamic model based on the TRNSYS simulation program (Klein et al, 1975, 1976). Energy and mass balances were developed for the greenhouse cover, air, floor, and separate growing medium. The photosynthetic rate of the crop was modelled using the model of Enoch and Sacks (1978) for a C-3 plant (spray carnations). Validation of some aspects of the model has subsequently been presented (Fuller et al, 1987).

Jones et al (1989c) have combined the tomato growth model TOMGRO (Jones et al, 1989a, 1989b) with the dynamic greenhouse model of Hwang et al (1989) to evaluate the economics of temperature and carbon dioxide control, in Florida.

Shina & Seginer (1989) have also combined TOMGRO with a greenhouse simulation model (Seginer et al, 1986) to evaluate an optimization technique used to derive environmental management strategies for greenhouse tomato.

5.1.6 Summary of Existing Models

It can be seen from the proceeding sections, and Table 5.1, that there has been a great deal of interest in using mathematical models to describe the

response of the greenhouse environment. Approximately ninety percent of the models that have been developed are analytic in nature, as opposed to empirical (time series) models.

Time series models have been used to predict greenhouse energy consumption, and to study the control characteristics of greenhouses. Time series models however have some limitations: they are not generally applicable between different greenhouses, nor do they reveal any information about the internal workings of the system.

More than half of the models reviewed have been used to investigate the energy consumption of greenhouses, and to evaluate new greenhouse technologies for energy conservation or energy substitution. Evaluation of thermal screens and solar energy storage systems, are two prime examples. Most of these models have been developed during the late 1970's and early 1980's when energy prices escalated rapidly. Most of these models were steady state models which gave an acceptable trade-off between complexity, and hence computational power requirements, and accuracy. Steady state models have a definite place in the study of the greenhouse environment when short term effects are not important. Thus they are well suited to energy consumption prediction, and medium to long term evaluation of new greenhouse technologies. The steady state assumption however makes these models unsuitable for control system studies. Increasing the number of greenhouse surfaces modelled adds to the complexity of the resulting model, and the effort required to find solutions to the system of equations, but increases the generality of the model, by reducing the amount and level at which empirical information must be used.

Dynamic models of the greenhouse environment, made up approximately a third of all models reviewed, however they have not been adopted widely. This is most likely a reflection of the computational power required to solve complex dynamic models. Takakura (1989) stated that the increasing availability of 16 and 32-bit personal computers and simulation languages suitable for these machines, should lead to the wider use of dynamic models, not only by researchers, but also those involved in extension and consulting activities.

Very few of the models reviewed included the carbon dioxide balance and predicted the growth of the crop. However, in the last two years, the use of combined greenhouse and crop simulation models has increased. These combinations have been used to study environmental management strategies for optimal crop growth.

5.2 RATIONALE FOR A NEW GREENHOUSE MODEL

After reviewing greenhouse models, as they stood in 1984, and considering the initial aims of the project, in relation to greenhouse control system evaluation (Wells et al, 1985), it was decided that a model of the greenhouse environment should be formulated, based on the most advanced work then available. The initial emphasis on control predisposed the study toward dynamic models, either empirical or analytical. The work of Udink ten Cate (1983) formed a foundation for the possible application of time series modelling techniques, while that of Bot (1983) provided a sound basis for work with analytical models.

In 1986 the aims of the project were revised and as a result more emphasis was placed on the desire to include the crop more fully into the model. By that stage it had become clear that the focus of international greenhouse research was shifting away from purely energy related studies, toward control studies, aimed at optimizing the management of the greenhouse environment. This change in direction was initiated by the relative stability of energy prices, and the increasing availability of computer based control systems. The inclusion of the crop into the greenhouse model would allow the model to be used in studies of optimal control at all three levels of the greenhouse system.

In light of this it was again decided that the project would continue with the use of a dynamic model and that this be analytical in nature. The greenhouse environment model would therefore be a continuation of previous work, rather than something completely new.

Several models were chosen as possible starting points. Bot's (1983) model provided a most valuable starting point, particularly in relation to the natural ventilation sub-model. The model of Cooper & Fuller (1983) was also very valuable since it included a growing crop, and a separate root medium in the model, which was akin to the system used to grow cucumbers in the test greenhouse made available for the validation experiment. Furthermore the TRNSYS implementation of their model was familiar to this author, from previous research on modelling passive solar energy systems (Wells, 1982). The model of Glaub & Trezek (1981a) proved to be particularly useful, since they rigourously presented the derivation of the energy and mass balance of the greenhouse airspace and correctly considered the effect of water vapour on enthalpy. Sorbie & Curry's (1973) model provided a further foundation for the inclusion of the crop. Other useful models were those of Takakura et al (1971), Kittas (1980), Ahmadi & Glockner (1982), and Arinze et al (1984).

Two major criticism of existing models were made at this point. Firstly, many models ignore the effect of water vapour on the thermal capacity of the air. Secondly, and more importantly, it was discovered that a model which did not consider the structure to be separate from the glazing was not capable of correctly simulating the rise in air temperature of an empty greenhouse during the day. The literature search did not reveal any published models in which the temperature of the greenhouse structure had been simulated independently to the glazing. On this basis alone the development of a new model could be justified.

The requirements for the model were summarised as follows.

1. The model should be dynamic. This would provide the best information on the dynamic nature of the greenhouse environmental response and would be useful for control system evaluation.

2. The model should include short term plant dynamics such as stomatal functioning to represent transpiration and water uptake realistically.

3. The model should easily interface to a crop growth model capable of simulating the short term growth processes (photosynthesis, respiration, and partitioning of assimilate), as well as the medium and long term development of the crop (node initiation, leaf expansion, and leaf death).

4. The model should be general, and based on well established physical relationships at the lowest appropriate level of abstraction, and thus maintain the highest possible level of generality.

5. The model should be validated with data obtained from a greenhouse operating under New Zealand conditions.

5.3 ENERGY AND MASS BALANCES

In this section the development of a dynamic model to simulate the greenhouse environment in response to varying boundary conditions is described. The preliminary discussion focuses on the application of the Continuity Equation and the First Law of Thermodynamics to spatially distributed systems. The equations describing the relationship between temperature, mass content, and enthalpy are then developed for each control volume within the greenhouse. In sections 5.3.9 and 5.3.10 the differential equations which describe the rate of change of enthalpy and mass within these control volumes are presented. The various ancillary equations describing the rate of energy and mass flow are developed in sections

5.3.11 to 5.3.17, grouped by heat and mass transfer categories such as conduction, convection, and radiation. The parameters used in the ancillary equations will be discussed in section 5.4.

5.3.1 Preliminaries

The basis of a dynamic model of the greenhouse environment is an energy and mass balance of the various elements or control volumes, which make up the greenhouse system (Takakura et al, 1971). These include the glazing material, the structure, the crop, the root medium, the floor, the underlying soil, and the greenhouse air. All these elements are distributed in space, and therefore should be modelled as distributed sub-systems (Tross et al, 1984). However, due to the increased complexity of modelling distributed systems it is usual to treat the whole as a number of homogeneous sub-systems, in which the states are assumed to be uniform. This gives rise to the 'lumped heat capacity' method (Incropera & De Witt, 1985, Holman, 1986). Figure 5.1 is a schematic representation of the sensible heat flows in a greenhouse relative to the important participating surfaces. Figure 5.2 shows the important mass flows.

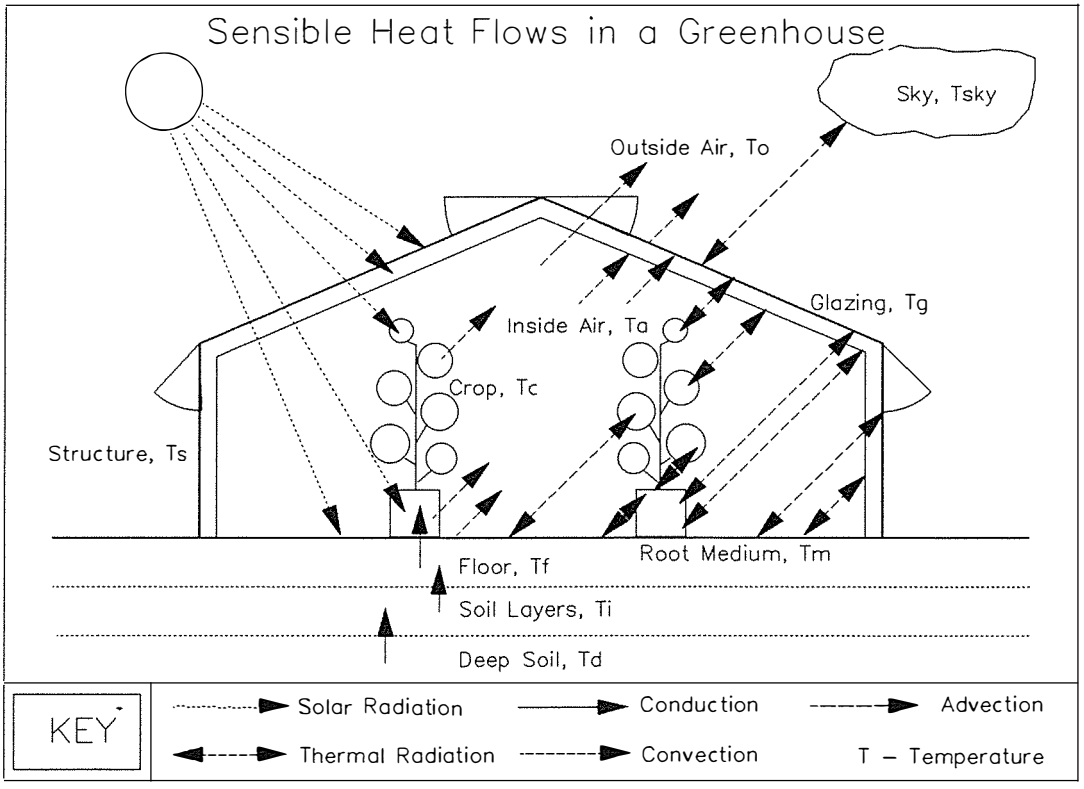

Figure 5.1. Sensible Heat Flows in a Greenhouse.

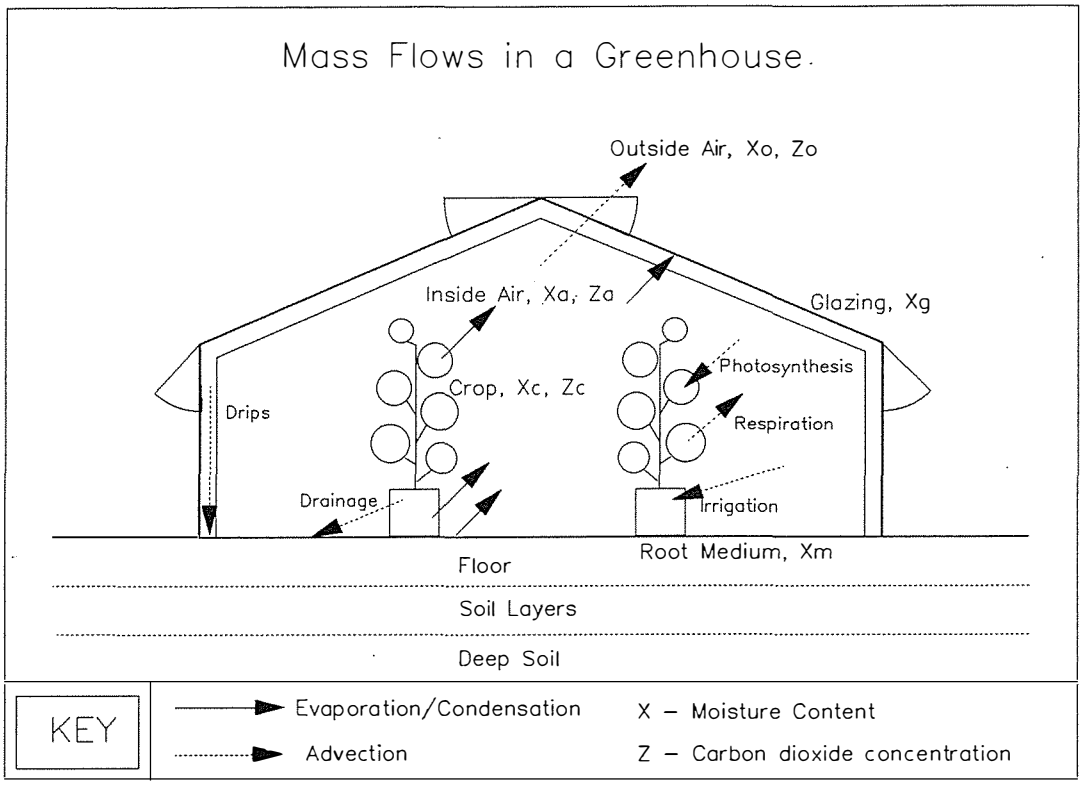

Figure 5.2. Mass Flows in a Greenhouse.

The basis for modelling the energy balance of each sub-system is the First Law of Thermodynamics, (Law of Conservation of Energy). The mass balance is based on the Continuity Equation (Law of Conservation of Mass).

The Continuity Equation can be written for a control volume as (Van Wylen & Sonntag, 1976):

$$\frac{dm}{dt} = \sum \dot{m}_i - \sum \dot{m}_o \qquad (5.1)$$

where dm/dt is the rate of change of mass storage within the control volume, and $\sum \dot{m}_i$ and $\sum \dot{m}_o$ are the net rates of mass input to, and output from the control volume, respectively.

The Continuity Equation can therefore be stated as: 'for a control volume, the rate of change of mass inside the control volume is equal to the rate of mass flowing into the control volume, minus the rate of mass flowing out of the control volume.'

For a control volume the First Law of Thermodynamics can be written as (Van Wylen & Sonntag, 1976):

$$\sum \dot{Q} + \sum \dot{H}_i + \sum \dot{KE}_i + \sum \dot{PE}_i = \frac{dE}{dt} + \sum \dot{H}_o + \sum \dot{KE}_o + \sum \dot{PE}_o + \sum \dot{W} \qquad (5.2a)$$

or

$$\sum \dot{Q} + \sum \dot{m}_i \left(h_i + \frac{v_i^2}{2} + gZ_i \right) = \frac{dE}{dt} + \sum \dot{m}_o \left(h_o + \frac{v_o^2}{2} + gZ_o \right) + \sum \dot{W} \qquad (5.2b)$$

where $\sum \dot{Q}$ is the rate of net heat input, $\sum \dot{W}$ is the rate of net work output, dE/dt is the rate of change of stored energy with time, and $\sum \dot{H}$, $\sum \dot{KE}$, and $\sum \dot{PE}$, are the combined rates of enthalpy, kinetic energy and potential energy movement across the control surface. The subscripts ^{i} and ^{o}, refer to inputs and outputs respectively. Note that h is specific enthalpy, v is velocity, Z is height above datum, and g is the gravitational constant.

The First Law of Thermodynamics can be stated as: 'for a control volume, the rate of heat transfer into the control volume, plus the rate of energy flowing in, as a result of mass transfer, is equal to the rate of change of energy inside the control volume, plus the rate of energy flowing out, as a result of mass transfer, plus the rate of work output.'

For the case where kinetic, potential, and work terms are negligible the equation for the First Law reduces to:

$$\sum \dot{Q} + \sum \dot{m}_i h_i = \frac{dE}{dt} + \sum \dot{m}_o h_o \qquad (5.3)$$

or

$$\frac{dU}{dt} = \sum \dot{Q} + (\dot{m}h)_i - (\dot{m}h)_o \qquad (5.4)$$

since the energy storage term is given by:

$$E = U + KE + PE \qquad (5.5)$$

and the rates of change of kinetic and potential energy, within the control volume, are also negligible.

Often it is convenient to work with the enthalpy, H, of the control volume rather than the internal energy, U. Enthalpy is defined by:

$$H = U + PV \qquad (5.6)$$

where P is the pressure in the control volume, V. For a constant pressure process then:

$$\frac{dH}{dt} = \frac{dU}{dt} \tag{5.7}$$

and therefore:

$$\frac{dH}{dt} = \sum \dot{Q} + (\dot{m}h)_i - (\dot{m}h)_o \tag{5.8}$$

The rate of change of temperature of the control volume is related to the rate of change of enthalpy via the definition of specific heat capacity, C_p.

$$C_p = \frac{dh}{dT} \tag{5.9}$$

It follows then that:

$$h = \int_0^T C_p dT \tag{5.10}$$

Now if C_p is constant over the range 0 to T and $H_{(T=0)}$ is set to be zero then:

$$H = mC_pT \tag{5.11}$$

Therefore, for a control volume containing a single homogeneous material with constant specific heat capacity the energy balance equation can be written as:

$$mC_p\frac{dT}{dt} = \sum \dot{Q} + (\dot{m}h)_i - (\dot{m}h)_o \tag{5.12}$$

where m is the mass in the control volume (g), C_p is the specific heat capacity of the mass ($J.g^{-1}.K^{-1}$), dT/dt is the rate of change of temperature of the mass with time ($K.s^{-1}$), $\dot{Q}$ is the rate of heat transfer across the boundary (W), $\dot{m}$ is the rate of mass transfer across the boundary ($g.s^{-1}$), h is the specific enthalpy ($J.g^{-1}$), and i and o and refer in inflow and outflow respectively. Thus the rate of change of enthalpy, and hence temperature, of the control volume is proportional to the net rate of heat transfer into the system across the boundary, plus the difference between the rates on energy input and output due to advective mass transfer across the boundary.

The assumption of constant specific heat capacity is valid for a number of materials of interest. The specific heat capacity of air increases by less than 0.3% in the range 0°C to 50°C. Over the same temperature range the specific heat capacity of liquid water decreases by less than 0.7%, and the specific heat capacity of water vapour increases by less than 0.1% (Van Wylen & Sonntag, 1976). Over the narrow range of temperatures encountered in the greenhouse it will be assumed that other materials also have constant specific heat capacities.

Where the sub-system in question is not homogeneous, complications arise. If the relative proportions of the constituents of the sub-system remain constant, with time, then the specific heat capacity term used should be the mass weighted average of the specific heat capacities of the constituents.

However, for a sub-system where one, or more, components change their proportions significantly, with time, equation 5.12 can no longer be used. Equation 5.8 or 5.4 should be used to model the change in enthalpy or internal energy, along with the change of the mass fractions, and the new temperature determined subsequently. This technique is usually only applied to the moist air in the greenhouse (Glaub & Trezek, 1981a). In this study it will be applied to all the sub-systems, where water content changes with time.

5.3.2 Greenhouse Glazing

The greenhouse glazing is modelled as a horizontal layer at the top of the greenhouse system. The mass of the glazing sub-system includes the glazing material (glass in this case), and the immediate support structure (the glazing bars). Also included is water condensed on the underside of the cover.

The mass balance of water condensed on the underside of the glazing has upper and lower limits. The lower limit is zero, when the cover is dry. The upper limit is reached when the maximum thickness of water is reached. From this point onward further condensation results in drainage down the underside of the roof to the gutter and down the walls.

To account for the greater area of the glazing, compared to the floor area, a glazing area index, GAI, is introduced.

$$GAI = A_g / A_f \tag{5.13}$$

where A_g is the exposed surface area of the greenhouse glazing for heat transfer (m^2), and A_f is the total floor area of the greenhouse (m^2).

The initial enthalpy of the glazing, per square metre of floor, $\hat{H}_g$ (J.m^{-2}), can be calculated from:

$$\hat{H}_g = \frac{m_{gl}}{A_f} C_{pgl} T_g + \frac{m_{gb}}{A_f} C_{pgb} T_g + \frac{m_{gw}}{A_f} C_{pw} T_g \qquad (5.14a)$$

$$= T_g(\Phi_g + X_g C_{pw}) \qquad (5.14b)$$

where m_{gl} is the mass of the glazing (g), m_{gb} is the mass of the glazing bars (g), m_{gw} is the mass of condensed water on the glazing (g), C_{pgl} is the specific heat capacity of the glazing (J.g^{-1}.$^{\circ}$C^{-1}), C_{pgb} is the specific heat capacity of the glazing bars (J.g^{-1}.$^{\circ}$C^{-1}), Φ_g is the combined thermal capacity of the glazing and glazing bars per unit floor area (J.m^{-2}.$^{\circ}$C^{-1}), and X_g is the moisture content per unit floor area (gH_2O.m$_{-2}$). Note that C_{pw} is the specific heat capacity of water (4.18 J.g^{-1}.$^{\circ}$C^{-1}),

The temperature of the glazing (and associated condensed water) can therefore be found from:

$$T_g = \frac{\hat{H}_g}{\Phi_g + X_g C_{pw}} \qquad (5.15)$$

The rate of change of enthalpy and moisture content are defined by the energy and mass balance equations (sections 5.3.9 and 5.3.10).

Both sides of the glazing are considered simultaneously. Relevant heat exchanges are: conduction to the structure; convective heat transfer to the outside and inside air; radiative heat transfer with the sky, structure, heater, crop, root medium, and floor; absorbed solar radiation; latent heat transfer associated with condensation and evaporation of water on the underside of the glazing. If condensation runs off the glazing then a small amount of energy loss is associated with this process. The relevant mass transfers are: condensation, evaporation, and run-off.

5.3.3 Greenhouse Structure

The greenhouse structure is modelled as a homogeneous layer directly below the glazing and in thermal communion with it. The mass of the structural sub-system includes the portal frames, and the purlins, which support the glazing bars. The surface area of the structural elements, for heat transfer, relative to the floor area is defined by a structural area index, SAI.

$$SAI = A_s / A_f \qquad (5.16)$$

where A_s is the surface area of the structure exposed for heat transfer (m^2).

The initial enthalpy of the structure, per square metre of floor area, $\hat{H}_s$ ($J.m^{-2}$), can be calculated from:

$$\hat{H}_s = \frac{m_s}{A_f} C_{ps} T_s \qquad (5.17a)$$

$$= \Phi_s T_s \qquad (5.17b)$$

where m_s is the mass of the structure (g), C_{ps} is the specific heat capacity of the structure ($J.g^{-1}.^{\circ}C^{-1}$), and Φ_s is the thermal capacity of the structure per unit floor area ($J.m^{-2}.^{\circ}C^{-1}$).

The temperature of the structure can therefore be calculated from:

$$T_s = \frac{\hat{H}_s}{\Phi_s} \qquad (5.18)$$

For the structure the relevant heat exchanges are: convective heat transfer with the inside air; radiative exchanges with the glazing, heater, crop, root medium, and floor; and conduction to the glazing via the glazing bars. If the glazing is transparent to thermal radiation then radiative exchange with the sky must also be considered.

5.3.4 Crop Canopy

The crop is modelled as a series of broken, horizontal layers. The total leaf area is represented by the leaf area index, LAI. Since the leaf area index considers only one side of the leaves, the heat exchanges are multiplied by two.

$$LAI = \frac{A_c}{2A_f} \qquad (5.19)$$

where A_c is the total surface area of the crop (m^2), considering both sides of the leaves.

The initial enthalpy of the crop, per square metre of floor area, $\hat{H}_c$ ($J.m^{-2}$), is calculated from:

$$\hat{H}_c = \frac{m_c}{A_f} C_{pc} T_c + \frac{m_{cw}}{A_f} C_{pw} T_c \qquad (5.20a)$$

$$= T_c(\Phi_c + X_c C_{pw}) \qquad (5.20b)$$

where m_c is the dry mass of the crop (g), m_{cw} is the mass of water in the crop (g), C_{pc} is the specific heat capacity of the crop dry matter ($J.g^{-1}.^{\circ}C^{-1}$), Φ_c is the crop dry matter thermal capacity per unit floor area ($J.m^{-2}.^{\circ}C^{-1}$), and X_c is the moisture content per unit floor area ($gH_2O.m^{-2}$).

The temperature of the crop can therefore be calculated from:

$$T_c = \frac{\hat{H}_c}{\Phi_c + X_c C_{pw}} \qquad (5.21)$$

Relevant heat flows for the crop are: convective heat transfer to the air; radiative heat transfer to the glazing, structure, heater, root medium, and floor; absorption of solar radiation; latent heat transfer associated with evapotranspiration; and the advective enthalpy gain associated with water uptake from the root medium. If the glazing is transparent to thermal radiation then radiative exchange with the sky must also be considered. The relevant mass transfers for the crop are: evapotranspiration and water uptake, and carbon dioxide uptake from the air for photosynthesis, and release by respiration.

5.3.5 Root Medium

Where the plant roots are placed in a separate root medium, such as bags of peat, or an inert material, and water and nutrients are supplied via a hydroponic system, the thermal mass of the root medium may be quiet significant. The root medium temperature may thus be significantly different from that of the air, or floor. For this reason the root medium is modelled separately to the floor and underlying soil. The surface area of the root medium for heat and mass exchanges, relative to the floor area, is introduced via a root medium surface area index, MAI. This is calculated from:

$$MAI = \frac{N_{plant}}{A_f}\left(\frac{\pi D_m^2}{4} + \pi D_m \Delta_m\right) \qquad (5.22)$$

where N_{plant} is the number of plants in the greenhouse, which is equal to the number of bags of root medium. D_m and Δ_m are the bag diameter (m) and depth (m), respectively.

The initial enthalpy of the root medium, $\hat{H}_m$ ($J.m^{-2}$), is given by:

$$\hat{H}_m = \frac{m_m}{A_f} C_{pm} T_m + \frac{m_{mw}}{A_f} C_{pw} T_m \qquad (5.23a)$$

$$= T_m(\Phi_m + X_m C_{pw}) \qquad (5.23b)$$

where m_m is the dry mass of the root medium (g), m_{mw} is the mass of water in the root medium (g), C_{pm} is the average specific heat capacity of the root medium dry matter ($J.g^{-2}.^{\circ}C^{-1}$), Φ_m is the dry matter thermal capacity per unit floor area ($J.m^{-2}.^{\circ}C^{-1}$), and X_m is the moisture content of the root medium per unit floor area ($gH_2O.m^{-2}$).

The temperature of the root medium can be calculated from:

$$T_m = \frac{\hat{H}_m}{\Phi_m + X_m C_{pw}} \qquad (5.24)$$

Relevant heat transfers for the root medium are: convective heat transfer with the inside air; conduction with the floor; radiative exchanges with the other surfaces; evaporative heat loss to the inside air; and advective enthalpy gain from irrigation water, and losses by drainage and crop water uptake. Drainage of the medium occurs to ensure that the moisture content does not rise above the maximum moisture holding capacity. Thus the relevant mass exchanges are: evaporation to the inside air, irrigation, drainage, and uptake by the crop.

5.3.6 Floor

The floor is modelled as a horizontal layer covering the soil. This allows for the floor to be a material other than soil, for example concrete. Where the plant roots are contained in a bagged root medium placed on the floor then the effective area of the floor for convective, evaporative, and radiative exchanges is reduced. In the model this is accounted for by introducing a floor area index, FAI.

$$FAI = 1 - \frac{N_{plant}}{A_f}\left(\frac{\pi D_m^2}{4}\right) \qquad (5.25)$$

The initial enthalpy of the floor per unit area, $\hat{H}_f$ (J.m^{-2}), is given by:

$$\hat{H}_f = \frac{m_f}{A_f} C_{pf} T_f + \frac{m_{fw}}{A_f} C_{pw} T_f \qquad (5.26a)$$

$$= T_f(\Phi_f + X_f C_{pw}) \qquad (5.26b)$$

where m_f is the dry mass of the floor (g), m_{fw} is the mass of water in the floor (g), C_{pf} is the average specific heat capacity of the floor dry matter, Φ_f is the thermal capacity of the floor dry matter per unit area (J.m^{-2}.$^{\circ}$C^{-1}), and X_f is the moisture content of the floor per unit area (gH_2O.m^{-2}).

The temperature of the floor layer can therefore be calculated from:

$$T_f = \frac{\hat{H}_f}{\Phi_f + X_f C_{pw}} \qquad (5.27)$$

The relevant heat exchanges for the floor are: convective heat transfer to the inside air; radiative exchanges with the other surfaces; and conduction to the soil layer immediately below, and the root medium. The floor of the test greenhouse was covered with a layer of heavy black polyethylene, which effectively prevented evaporation from the floor, and entry of drainage water from the root medium.

To satisfy the stability criteria for a numerical solution using the lumped capacitance method (Incropera & De Witt, 1985, Holman, 1986), the thickness of the floor layer was set to one centimetre (0.01 m).

5.3.7 Soil Layers

The soil underlying the floor was divided into five horizontal layers, each increasing in thickness, according to a geometric progression, as suggested by Cormary (1977) (Kittas, 1980). The first layer was twice as thick as the floor (0.02 m), and the second layer was double this again. As a result of this pattern the lower surface of the fifth layer was 63 centimetres below the surface (0.63 m). Below this depth, measurements and theory showed that the diurnal temperature variation was very small. This level was therefore treated as a boundary surface at the deep ground temperature, T_d).

The mass of the soil layers included the solid particles, soil water and air. In this model the water content of the soil was assumed to be constant with time, since irrigation water was prevented from entering, evaporation was prevented from leaving, and there was no crop water uptake. This significantly reduced the amount of detail required to model the soil, and saved on computational time. For a crop grown in the soil this

simplification could not have been made and mass transfer in the soil would needed to have been modelled, possibly using a technique similar to that suggested by Avissar & Mahrer (1982).

The initial enthalpy of the 1st soil layer per unit area, $\hat{H}_1$ ($J.m^{-2}$), is given by:

$$\hat{H}_1 = \frac{m_1}{A_f} C_{p1} T_1 + \frac{m_{1w}}{A_f} C_{pw} T_1 \qquad (5.28a)$$

$$= T_1(\Phi_1 + X_1 C_{pw}) \qquad (5.28b)$$

where m_1 is the dry mass of the first soil layer, m_{1w} is the mass of water in the first soil layer, C_{p1} is the average specific heat capacity of the dry matter, Φ_1 is the thermal capacity of the dry matter per unit floor area ($J.m^{-2}.^{\circ}C^{-1}$), and X_1 is the moisture content of the first soil layer per unit area of floor ($gH_2O.m^{-2}$).

The temperature of the 1st soil layer can therefore be calculated from:

$$T_1 = \frac{\hat{H}_1}{\Phi_1 + X_1 C_{pw}} \qquad (5.29)$$

In an exactly analogous manner the enthalpies, $\hat{H}_2$, $\hat{H}_3$, $\hat{H}_4$, and $\hat{H}_5$, and temperatures, T_2, T_3, T_4, and T_5, of the other soil layers can be found.

Since moisture movement was assumed to be negligible in the soil system, due to the plastic floor cover, the only relevant heat exchanges are conductive heat transfer between the layers.

5.3.8 Inside Air Space

The greenhouse air space is in contact with all the other surfaces in the greenhouse, and therefore acts as a transfer medium for heat and mass exchanges within the system.

The appropriate equation for the enthalpy of moist air per unit floor area, $\hat{H}_a$ ($J.m^{-2}$), is:

$$\hat{H}_a = \frac{m_a}{A_f}[C_{pa} T_a + w(\lambda_0 + C_{pv} T_a)] \qquad (5.30a)$$

$$= \frac{m_a}{A_f} C_{pa} T_a + \frac{m_{aw}}{A_f} \lambda_0 + \frac{m_{aw}}{A_f} C_{pv} T_a \qquad (5.30b)$$

$$= T_a(\Phi_a + X_a C_{pv}) + \lambda_0 X_a \qquad (5.30c)$$

where m_a is the mass of dry air (gDA), w is the humidity ratio of the air ($gH_2O.gDA^{-1}$), λ_0 is the latent heat of vapourization (2501 $J.g^{-1}$ at the reference temperature of 0°C), m_{aw} is the mass of water vapour in the air (gH_2O), Φ_a is the thermal capacity of the dry air per unit floor area ($J.m^{-2}.°C^{-1}$), and X_a is the moisture content per unit floor area ($gH_2O.m^{-2}$). Note that C_{pv} is the specific heat capacity of water vapour (1.87 $J.g^{-1}.°C^{-1}$).

From the preceding the air temperature can be found, if the moisture content is known.

$$T_a = \frac{\hat{H}_a - \lambda_0 X_a}{\Phi_a + X_a C_{pv}} \tag{5.31}$$

The wet bulb temperature, and other psychrometric variables of interest can be found from the dry bulb temperature and absolute humidity according to well known psychrometric relationships.

The absolute humidity of the air, χ_a ($gH_2O.m^{-3}$), is related to the moisture content per unit floor area ($gH_2O.m^{-2}$), via the average depth of air in the greenhouse, Δ_a (m). Thus $\chi_a = X_a/\Delta_a$.

The vapour pressure of the moist air, e_a (Pa), is calculated from:

$$e_a = \frac{\chi_a R(T_a + 273.15)}{M_w} \tag{5.32a}$$

$$= \frac{X_a R(T_a + 273.15)}{\Delta_a M_w} \tag{5.32b}$$

where R is the Universal Gas Constant (8.31 $J.mol_{-1}.K_{-1}$), M_w is the molecular mass of water (18.0 $g.mol^{-1}$), and T_a is in degrees Celsius.

From this the density of the dry air fraction, ρ_a ($gDA.m^{-3}$), can be found from its partial pressure ($P_o - e_a$):

$$\rho_a = \frac{M_a(P_o - e_a)}{R(T_a + 273.15)} \tag{5.33}$$

and the thermal capacity of the dry air per unit floor area, Φ_a ($J.m^{-2}$), is then given by:

$$\Phi_a = \rho_a C_{pa} \Delta_a \tag{5.34}$$

where C_{pa} is the specific heat capacity of dry air (1.01 $J.g^{-1}.^{\circ}C^{-1}$).

The saturation vapour pressure, e_a', can be calculated using the equation of Tetens (1930), as given by Monteith and Unsworth (1989):

$$e'_a = 611 \exp\left[17.27\left(\frac{T_a}{T_a + 237.3}\right)\right] \tag{5.35}$$

where the air temperature T_a is in degrees Celsius.

With this information the relative humidity, RH (%), and wet bulb temperature, T_{aw} ($^{\circ}C$), can be found.

$$RH \approx \frac{100 e_a}{e'_a} \tag{5.36}$$

$$T_{aw} \approx T_a - \left(\frac{e_a' - e_a}{s + \gamma}\right) \tag{5.37}$$

where γ is the psychrometric constant (66 $Pa.K^{-1}$) (Monteith & Unsworth, 1989), and s is the slope of the saturation vapour pressure curve ($Pa.K^{-1}$), at temperature T_a.

The slope of the saturation vapour pressure curve, s, can be estimated from the Clapeyron Equation (Van Wylen & Sonntag, 1976) as:

$$s \equiv \left(\frac{de_a'}{dT}\right) \approx \frac{e_a' \lambda_a M_w}{R(T_a + 273.15)^2} \tag{5.38}$$

where λ_a is the latent heat of vapourization of water at temperature T_a.

The carbon dioxide concentration of the inside air on a mass basis, ξ_a ($mgCO_2.m^{-3}$), is related to the carbon dioxide content per unit floor area, Ξ_a ($mgCO_2.m^{-2}$), via the average depth of air in the greenhouse by:

$$\xi_a = \frac{\Xi_a}{\Delta_a} \tag{5.39}$$

From this the concentration on a volumetric basis, CO_{2a} (vppm or $\mu 1.1^{-1}$), can be found as:

$$CO_{2a} = \frac{1000\xi_a}{\rho_c} \tag{5.40a}$$

$$= \frac{1000\xi_a}{1.52\rho_a} \tag{5.40b}$$

where ρ_c is the density of carbon dioxide ($g.m^{-3}$) which is 1.52 times the density of the dry air, ρ_a, since the molecular mass of carbon dioxide, M_c (44 $g.mol^{-1}$), is 1.52 times the average molecular mass of dry air, M_a (29 $g.mol^{-1}$). The factor of 1000 accounts for the change in volume units.

5.3.9 Energy Balance Equations

The energy balances of the various components can now be written as the sum of the energy transfer terms. All the terms on the right hand side of the following equations will be defined in sections 5.3.11 to 5.3.16. In general, B denotes absorbed solar radiation, C denotes convective heat transfer, R denotes radiative heat transfer, G denotes conductive heat transfer, LE denotes evaporative energy transfer, and E denotes advective energy transfer.

For the glazing:

$$\frac{d\hat{H}_g}{dt} = B_g - C_{go} - C_{ga} + G_{sg} - R_{gsky} + R_{sg} + R_{hg} + R_{cg} + R_{mg} + R_{fg} - LE_{ga} - E_{drip} \tag{5.41}$$

For the structure:

$$\frac{d\hat{H}_s}{dt} = B_s - C_{sa} - G_{sg} - R_{sg} + R_{hs} + R_{cs} + R_{ms} + R_{fs} \tag{5.42}$$

For the crop:

$$\frac{d\hat{H}_c}{dt} = B_c - C_{ca} - R_{cg} - R_{cs} - R_{ch} + R_{mc} + R_{fc} - LE_{ca} + E_{up} \tag{5.43}$$

For the root medium:

$$\frac{d\hat{H}_m}{dt} = B_m - C_{ma} + G_{fm} - R_{mg} - R_{ms} - R_{mh} - R_{mc} + R_{fm} - LE_{ma} - E_{up} + E_{irr} - E_{drain} \tag{5.44}$$

For the floor:

$$\frac{d\hat{H}_f}{dt} = B_f - C_{fa} - G_{fm} - G_{fl} - R_{fg} - R_{fs} - R_{fh} - R_{fc} - R_{fm} \tag{5.45}$$

For the top soil layer:

$$\frac{d\hat{H}_1}{dt} = G_{f1} - G_{12} \tag{5.46}$$

For subsequently deeper layers:

$$\frac{d\hat{H}_2}{dt} = G_{12} - G_{23} \tag{5.47a}$$

$$\frac{d\hat{H}_3}{dt} = G_{23} - G_{34} \tag{5.47b}$$

$$\frac{d\hat{H}_4}{dt} = G_{34} - G_{45} \tag{5.47c}$$

For the deepest soil layer:

$$\frac{d\hat{H}_5}{dt} = G_{45} - G_{5d} \tag{5.48}$$

For the inside air:

$$\frac{d\hat{H}_a}{dt} = C_{ga} + C_{sa} + C_{ha} + C_{ca} + C_{ma} + C_{fa} - C_{ao} + LE_{ga} + LE_{ca} + LE_{ma} - E_{ao} \tag{5.49}$$

The result of deriving the energy balance equations is a set of simultaneous differential equations. As a check on the formulation of the energy balances it will be noticed that the energy exchanges are either internal (between two sub-systems) or external (between an internal sub-system and a boundary surface). Each internal exchanges should be self cancelling, that is it should appear twice in the model, once as a positive quantity (energy gain) and once as a negative quantity (energy loss). Each external exchange should only occur once.

5.3.10 Mass Balance Equations

In a similar fashion to the derivation of the energy balances, the mass balances can be written as the sum of the mass exchange terms. The right hand terms of the following equations will be defined in sections 5.3.15 and 5.3.16.

For the underside of the glazing:

$$\frac{dX_g}{dt} = -f_{ga} - f_{drip} \tag{5.50}$$

For the crop canopy:

$$\frac{dX_c}{dt} = f_{up} - f_{ca} - f_{fruit} \tag{5.51}$$

For the root medium:

$$\frac{dX_m}{dt} = f_{irr} - f_{drain} - f_{ma} - f_{up} \tag{5.52}$$

For the water balance of the inside air:

$$\frac{dX_a}{dt} = f_{ga} + f_{ca} + f_{ma} - f_{ao} \tag{5.53}$$

And also for the carbon dioxide balance of the inside air:

$$\frac{d\Xi_a}{dt} = f_{resp} + f_{growth} - f_{gross} - f_{vent} \tag{5.54}$$

The mass balances give rise to an additional set of simultaneous differential equations. As occurred for the heat transfers, some of the mass transfers are internal to the model. These appear twice in the model and cancel out each other. Other mass transfers are external, that is between the system and a boundary, and occur only once in the formulation.

5.3.11 Solar Radiation Gains

The solar radiation gains are all external energy exchanges, positive in magnitude (energy gains), and expressed in $W.m^{-2}$ of total floor area.

The solar radiation absorbed by the glazing is:

$$B_g = \alpha_{gdr} S'_{dr} + \alpha_{gdf} S'_{df} \tag{5.55}$$

The absorptivities of the glazing for direct and diffuse radiation, α_{gdr} and α_{gdf}, were determined using the corrected results of the light transmission model (Chapter 4). S'_{dr} and S'_{df} are the direct and diffuse solar radiation intensities ($W.m^{-2}$) outside the greenhouse, corrected for circumsolar radiation (see section 4.1.3).

The solar radiation absorbed by the structure is:

$$B_s = \alpha_{sdr} S'_{dr} + \alpha_{sdf} S'_{df} \tag{5.56}$$

The absorptivities of the structure for direct and diffuse radiation, α_{sdr} and α_{sdf}, were determined using the corrected results of the light transmission model (see section 4.3.8).

The solar radiation absorbed by the crop canopy is:

$$B_c = \alpha_{cpdr}\tau_{gdr}S_{pdr} + \alpha_{cpdf}\tau_{gdf}S_{pdf} + \alpha_{cndr}\tau_{gdr}S_{ndr} + \alpha_{cndf}\tau_{gdf}S_{ndf} \quad (5.57)$$

The transmissivities of the glazing for direct and diffuse radiation, τ_{gdr} and τ_{gdf}, were determined using the corrected results of the light transmission model (section 4.3.8). The absorptivities of the crop for the direct and diffuse components of photosynthetically active (PAR), α_{cpdr} and α_{cpdf}, and near infra-red radiation (NIR), α_{cndr} and α_{cndf}, are found from the transmissivities and reflectivities of the crop according to the well known relationship $\alpha_c + \tau_c + \rho_c = 1$. The reflectivity and transmissivity coefficients of the crop, ρ_c and τ_c, for each radiation class, were calculated using the equations developed in sections 6.2.2.5 and 6.2.2.6, where the crop canopy radiation model is developed.

The solar radiation absorbed by the root medium is:

$$B_m = (1 - FAI)[\alpha_{mp}(\tau_{gdr}\tau_{cpdr}S_{pdr} + \tau_{gdf}\tau_{cpdf}S_{pdf}) + \alpha_{mn}(\tau_{gdr}\tau_{cndr}S_{ndr} + \tau_{gdf}\tau_{cndf}S_{ndf})] \quad (5.58)$$

where α_{mp} and α_{mn} are the absorptivities of the root medium for PAR and NIR radiation. The transmissivities of the crop for the direct and diffuse components of photosynthetically active (PAR), τ_{cpdr} and τ_{cpdf}, and near infra-red radiation (NIR), τ_{cndr} and τ_{cndf}, were estimated using the equations developed in section 6.2.2.6. It is assumed that of the radiation arriving below the crop canopy a fraction $(1 - FAI)$ will be incident on the root medium.

The solar radiation absorbed by the floor is:

$$B_f = FAI[\alpha_{fp}(\tau_{gdr}\tau_{cpdr}S_{pdr} + \tau_{gdf}\tau_{cpdf}S_{pdf}) + \alpha_{fn}(\tau_{gdr}\tau_{cndr}S_{ndr} + \tau_{gdf}\tau_{cndf}s_{ndf})] \quad (5.59)$$

where α_{fp} and α_{fn} are the absorptivities of the floor for PAR and NIR radiation. It is assumed that of the radiation arriving below the crop canopy a fraction FAI will be incident on the floor.

5.3.12 Convective Exchanges

All the convective exchanges, C, in the greenhouse system are internal exchanges, except for the external convective exchange between the glazing and the outside air, and are expressed in $W.m^{-2}$ of total floor area. The convective heat transfer coefficients, h_c ($W.m^{-2}.^{\circ}C^{-1}$), are defined in section 5.4.7. Air infiltration and ventilation are dealt with under advective exchanges (see section 5.3.16).

The rate of convection from the glazing to the outside air is:

$$C_{go} = h_{Cgo} GAI(T_g - T_o) \tag{5.60}$$

The rate of convection from the glazing to the inside air is:

$$C_{ga} = h_{Cga} GAI(T_g - T_a) \tag{5.61}$$

The rate of convection from the structure to the inside air is:

$$C_{sa} = h_{Csa} SAI(T_s - T_a) \tag{5.62}$$

The rate of convection from the crop canopy to the inside air is:

$$C_{ca} = h_{Cca} 2LAI(T_c - T_a) \tag{5.63}$$

The rate of convection from the root medium to the inside air is:

$$C_{ma} = h_{Cma} MAI(T_m - T_a) \tag{5.64}$$

The rate of convection from the floor to the inside air is:

$$C_{fa} = h_{Cfa} FAI(T_f - T_a) \tag{5.65}$$

The rate of convection from the heating system to the inside air is:

$$C_{ha} = h_{Cha} HAI(T_h - T_a) \tag{5.66}$$

5.3.13 Radiative Exchanges

The radiative heat transfers, R, in the greenhouse are internal exchanges, except for external exchanges with the sky and the heating system, and are expressed in $W.m^{-2}$ of total floor area.

In general the radiation exchange between two surfaces in an isothermal enclosure can be written as:

$$R_{12} = A_1 \mathcal{F}_{12} \sigma (T_1^4 - T_2^4) \tag{5.67}$$

where σ is the Stephan-Boltzmann constant ($5.67 \times 10_{-8}$ W.m$_{-2}$.K$_{-4}$), and $\mathcal{F}_{12}$ is the combined emissivity view factor, sometimes known as Hottel's Script F (McAdams, 1954), and is defined by:

$$\frac{1}{\mathcal{F}_{12}} = \left(\frac{1 - \epsilon_1}{\epsilon_1} \right) + \frac{1}{F_{12}} + \frac{A_1}{A_2} \left(\frac{1 - \epsilon_2}{\epsilon_2} \right) \tag{5.68}$$

where the two surfaces have areas of A_1 and A_2, and emissivities of ϵ_1 and ϵ_2. The view factor from surface 1 to surface 2 is F_{12}.

A radiative heat transfer coefficient h_{R12}, can be defined such that:

$$R_{12} = A_1 h_{R12} (T_1 - T_2) \tag{5.69}$$

Equating equations 5.67 and 5.69 gives:

$$h_{R12} = \mathcal{F}_{12} \sigma \frac{(T_1^4 - T_2^4)}{(T_1 - T_2)} \tag{5.70a}$$

$$\approx 4 \mathcal{F}_{12} \sigma T_{mean}^3 \tag{5.70b}$$

where T_{mean}, is the mean of T_1 and T_2.

The advantage of defining the radiative heat transfer coefficient in this manner is that the radiative transfers are expressed in terms of the actual temperature differences between the surfaces, rather that the difference between the fourth powers of the absolute temperatures. The radiative heat transfer coefficients, h_R (W.m^{-2}.$^{\circ}$C^{-1}), and the appropriate view factors are discussed in section 5.4.8.

The net radiation exchange between the glazing and the sky is:

$$R_{gsky} = GAI \mathcal{F}_{gsky} \sigma (T_g^4 - T_{sky}^4) \tag{5.71a}$$

$$= h_{Rgsky} GAI (T_g - T_{sky}) \tag{5.71b}$$

The net radiation exchange between the structure and the glazing is:

$$R_{sg} = SAI\mathcal{F}_{sg}\sigma(T_s^4 - T_g^4) \quad (5.72a)$$

$$= h_{Rsg}SAI(T_s - T_g) \quad (5.72b)$$

The net radiation exchange between the heater and the glazing is:

$$R_{hg} = HAI\mathcal{F}_{hg}\sigma(T_h^4 - T_g^4) \quad (5.73a)$$

$$= h_{Rhg}HAI(T_h - T_g) \quad (5.73b)$$

where HAI is the heater surface area index, and is equal to the surface area of the heating system, A_h, divided by the floor area, A_f.

The net radiation exchange between the heater and the structure is:

$$R_{hs} = HAI\mathcal{F}_{hs}\sigma(T_h^4 - T_s^4) \quad (5.74a)$$

$$= h_{Rhs}HAI(T_h - T_s) \quad (5.74b)$$

The net radiation exchange between the crop and the glazing is:

$$R_{cg} = 2LAI\mathcal{F}_{cg}\sigma(T_c^4 - T_g^4) \quad (5.75a)$$

$$= h_{Rcg}2LAI(T_c - T_g) \quad (5.75b)$$

The net radiation exchange between the crop and the structure is:

$$R_{cs} = 2LAI\mathcal{F}_{cs}\sigma(T_c^4 - T_s^4) \quad (5.76a)$$

$$= h_{Rcs}2LAI(T_c - T_s) \quad (5.76b)$$

The net radiation exchange between the crop and the heater is:

$$R_{ch} = 2LAI\mathcal{F}_{ch}\sigma(T_c^4 - T_h^4) \quad (5.77a)$$

$$= h_{Rch}2LAI(T_c - T_h) \quad (5.77b)$$

The net radiation exchange between the root medium and the glazing is:

$$R_{mg} = MAI\mathcal{F}_{mg}\sigma(T_m^4 - T_g^4) \quad (5.78a)$$

$$= h_{Rmg}MAI(T_m - T_g) \quad (5.78b)$$

The net radiation exchange between the root medium and the structure is:

$$R_{ms} = MAI\mathcal{F}_{ms}\sigma(T_m^4 - T_s^4) \quad (5.79a)$$

$$= h_{Rms}MAI(T_m - T_s) \quad (5.79b)$$

The net radiation exchange between the root medium and the heater is:

$$R_{mh} = MAI\mathcal{F}_{mh}\sigma(T_m^4 - T_h^4) \quad (5.80a)$$

$$= h_{Rmh}MAI(T_m - T_h) \quad (5.80b)$$

The net radiation exchange between the root medium and the crop is:

$$R_{mc} = MAI\mathcal{F}_{mc}\sigma(T_m^4 - T_c^4) \quad (5.81a)$$

$$= h_{Rmc}MAI(T_m - T_c) \quad (5.81b)$$

The net radiation exchange between the floor and the glazing is:

$$R_{fg} = FAI\mathcal{F}_{fg}\sigma(T_f^4 - T_g^4) \quad (5.82a)$$

$$= h_{Rfg}FAI(T_f - T_g) \quad (5.82b)$$

The net radiation exchange between the floor and the structure is:

$$R_{fs} = FAI\mathcal{F}_{fs}\sigma(T_f^4 - T_a^4) \quad (5.83a)$$

$$= h_{Rfs}FAI(T_f - T_s) \quad (5.83b)$$

The net radiation exchange between the floor and the heater is:

$$R_{fh} = FAI\mathcal{F}_{fh}\sigma(T_f^4 - T_h^4) \quad (5.84a)$$

$$= h_{Rhf}HAI(T_f - T_h) \quad (5.84b)$$

The net radiation exchange between the floor and the crop is:

$$R_{fc} = FAI\mathcal{F}_{fc}\sigma(T_f^4 - T_c^4) \quad (5.85a)$$

$$= h_{Rfc}FAI(T_f - T_c) \quad (5.85b)$$

The net radiation exchange between the floor and the root medium is:

$$R_{fm} = FAI\mathcal{F}_{fm}\sigma(T_f^4 - T_m^4) \quad (5.86a)$$

$$= h_{Rfm}FAI(T_f - T_m) \quad (5.86b)$$

5.3.14 Conductive Exchanges

Conduction heat transfers occur in the soil, and between the structure and glazing, and between the floor and root medium. All the conductive exchanges, G, are internal, except for conduction at the deep soil boundary, and are expressed in W.m^{-2} of total floor area. The thermal conductances, h_c (W.m^{-2}.°C^{-1}), and thermal conductivities, k (W.m^{-1}.°C^{-1}), are defined in section 5.4.10. The thickness of the various layers are defined in section 5.4.1.

The rate of conduction into the first soil layer from the floor is:

$$G_{f1} = \frac{2}{\left(\frac{\Delta_f}{k_f} + \frac{\Delta_1}{k_1}\right)}(T_f - T_1) \qquad (5.87a)$$

$$= h_{cf1}(T_f - T_1) \qquad (5.87b)$$

The rate of conduction from the 1st layer into the 2nd layer is:

$$G_{12} = \frac{2}{\left(\frac{\Delta_1}{k_1} + \frac{\Delta_2}{k_2}\right)}(T_1 - T_2) \qquad (5.88a)$$

$$= h_{c12}(T_1 - T_2) \qquad (5.88b)$$

In an exactly analogous fashion the rate of conduction between the other soil layers can be defined.

The rate of conduction across the deep ground boundary is:

$$G_{5d} = \frac{2k_5}{\Delta_5}(T_5 - T_d) \qquad (5.89a)$$

$$= h_{c5d}(T_5 - T_d) \qquad (5.89b)$$

The rate of heat conduction from the floor into the root medium is:

$$G_{fm} = h_{cfm}(T_f - T_m) \qquad (5.90)$$

The rate of heat conduction from the structure to the glazing is:

$$G_{sg} = h_{csg}(T_s - T_g) \qquad (5.91)$$

5.3.15 Evaporative Exchanges

Evaporative exchanges occur between the inside air and wet surfaces within the greenhouse. All the evaporative mass transfers, f, are internal

exchanges, and are expressed in $gH_2O.s^{-1}.m^{-2}$ of total floor area. The corresponding evaporative heat transfers, LE, are expressed in $W.m^{-2}$ of total floor area. The mass transfer resistances, r_v, are discussed in section 5.4.11.

The rate of evaporation from the glazing to the inside air is:

$$f_{ga} = \frac{GAI}{r_{vga}}(\chi_g' - \chi_a) \tag{5.92}$$

where χ_g' is the saturated water vapour concentration ($gH_2O.m^{-3}$), at the glazing temperature, T_g, and χ_a is the water vapour concentration of the inside air ($gH_2O.m^{-3}$).

Note that a negative evaporation rate implies that condensation is occurring on the under surface of the glazing when the glazing temperature is below the dew point temperature of the inside air. It must also be pointed out that evaporation can only occur when there is water present on the underside of the glazing. If the glazing is dry then evaporation will be zero. This is discussed in section 5.5.2.

From equation 5.92 is follows that the evaporative heat transfer rate between the glazing and the inside air is:

$$LE_{ga} = \lambda_a f_{ga} \tag{5.93a}$$

$$= \frac{\lambda GAI}{r_{vga}}(\chi_g' - \chi_a) \tag{5.93b}$$

The evapotranspiration rate from the crop is given by

$$f_{ca} = \frac{2LAI}{(r_{vca} + r_{vcl})}(\chi_c' - \chi_a) \tag{5.94}$$

where χ_c' is the saturated water vapour concentration ($gH_2O.m^{-3}$), at the crop canopy temperature T_c and χ_a is the water vapour concentration of the inside air ($gH_2O.m^{-3}$).

Therefore the latent heat loss by evapotranspiration from the crop canopy is:

$$LE_{ca} = \lambda_a f_{ca} \tag{5.95a}$$

$$= \frac{\lambda 2LAI}{(r_{vca} + r_{vcl})}(\chi_c' - \chi_a) \tag{5.95b}$$

The rate of evaporation from the root medium to the inside air is:

$$f_{ma} = \frac{MAI}{r_{vma}}(\chi_m' - \chi_a) \qquad (5.96)$$

where χ_m' is the saturated water vapour concentration ($gH_2O.m^{-3}$), at the root medium temperature T_m, and χ_a is the water vapour concentration of the inside air ($gH_2O.m^{-3}$).

And therefore the evaporative mass flow rate is:

$$LE_{ma} = \lambda_a f_{ma} \qquad (5.97a)$$

$$= \frac{\lambda MAI}{r_{vma}}(\chi_m' - \chi_a) \qquad (5.97b)$$

5.3.16 Advective Exchanges

Advective heat transfers are associated with bulk fluid motions between regions with different enthalpy. An important advective flow for the greenhouse environment is air movement between the inside and the outside of the greenhouses by ventilation or infiltration. Other advective flows include addition of irrigation water to the root medium, drainage of water from the root medium, uptake of water by the crop, and water dripping of the underside of the glazing. All the advective mass flows, except between the root medium and the crop are external exchanges, and are expressed in $gH_2O.s^{-1}.m^{-2}$ of total floor area. Advective heat flows are expressed in $W.m^{-2}$ of total floor area.

The rate of sensible heat loss from the greenhouse by ventilation is given by:

$$C_{ao} = h_{ao}(T_a - T_o) \qquad (5.98)$$

where h_{ao} is the advective heat transfer coefficient and is given in section 5.4.12.

The rate of water vapour transfer from the inside to outside is given by:

$$f_{ao} = \frac{(\chi_a - \chi_o)}{r_{ao}} \qquad (5.99)$$

where χ_a is the water vapour concentration of the inside air ($gH_2O.m^{-3}$), and χ_o is the water vapour concentration of the outside air ($gH_2O.m^{-3}$), and the mass transfer resistance, r_{ao}, is equal to:

$$r_{ao} = \rho_a C_{pa} / h_{ao} \tag{5.100}$$

From this the advective heat exchange, associated with the mass transfer, can be calculated as:

$$E_{ao} = \lambda f_{ao} \tag{5.101a}$$

$$= \frac{\lambda}{r_{ao}} (\chi_a - \chi_o) \tag{5.101b}$$

When irrigation water is added to the root medium enthalpy is also added at a rate according to:

$$E_{irr} = f_{irr} C_{pw} (T_{irr} - T_{ref}) \tag{5.102}$$

where T_{ref} is the reference temperature for zero enthalpy (0°C in this case).

If sufficient water is added during irrigation to saturate the medium completely then drainage will occur. This causes the medium to lose enthalpy at a rate according to:

$$E_{drain} = f_{drain} C_{pw} (T_m - T_{ref}) \tag{5.103}$$

The water uptake rate from the root medium is a function of the water potential of the root medium and the crop.

$$f_{up} = K_c (\psi_m - \psi_c) \tag{5.104}$$

where K_c is the hydraulic conductivity of the crop, and ψ_m and ψ_c are the water potential of the root medium and crop respectively. These are discussed further is section 5.4.12.

Enthalpy will thus be added to the crop at the following rate:

$$E_{up} = f_{up} C_{pw} (T_m - T_{ref}) \tag{5.105}$$

When sufficient water condenses on the under side of the glazing it will begin to drip off the glazing at a rate f_{drip}, which is assumed to be equal to the rate of condensation, $-f_{ga}$. As a result of the this the glazing system loses enthalpy according to:

$$E_{drip} = f_{drip} C_{pw} (T_g - T_{ref}) \tag{5.106}$$

5.3.17 Carbon Dioxide Exchanges

In equation 5.54, four important carbon dioxide fluxes of the inside air space were introduced. These were the production of carbon dioxide by maintenance respiration of the crop, f_{resp}, production by growth respiration of the crop, f_{growth}, removal of carbon dioxide by photosynthesis, f_{gross}, and loss to the outside air, f_{vent}. Maintenance and growth respiration are discussed in section 6.2.4. Photosynthesis is dealt with in section 6.2.3.

The loss of carbon dioxide per unit floor area due to ventilation ($mgCO_2.s^{-1}.m^{-2}$ of total floor area) is given by:

$$f_{vent} = \frac{(\xi_a - \xi_o)}{r_{ao}} \tag{5.107}$$

where ξ_a is the concentration of carbon dioxide inside the greenhouse ($mgCO_2.m^{-3}$), and ξ_o is the concentration of carbon dioxide outside the greenhouse ($mgCO_2.m^{-3}$).

5.4 DETERMINATION OF ANCILLARY PARAMETERS

The ancillary equations 5.55 to 5.107 contain many parameters which must be estimated before the differential equations can be solved. Some of the parameters are fixed, for example the various surface areas and component masses. Others, particularly the heat and mass transfer coefficients vary in response to the changing state of the system, and must be regularly updated. In the following sections the various parameters in the ancillary equations are defined.

5.4.1 Greenhouse Dimensions

Since the areas and volumes of all the components in the system were fixed, (except for the crop), the dimensions of the greenhouse and the root medium bags were read into the model in the initialization phase and the surface areas calculated. Other parameters read in at this time were the thickness of the glazing, the depth of the floor and soil layers, the volume of the glazing bars and structural elements, and the exposed surface areas of the structure and the heating system. These are given in Table 5.2.

Table 5.2. Greenhouse Dimensions

Parameter	Symbol	Value	Units
Length of Greenhouse		15.5	m
Width of Greenhouse		6.6	m
Height to Gutter		2.1	m
Height to Ridge		4.0	m
Diameter of Root Medium Bags	D_m	0.2	m
Height of Root Medium Bags	Δ_m	0.2	m
Exposed Surface Area of Structure	A_s	112.8	m_2
Exposed Surface Area of Heating System	A_h	10.0	m^2
Volume of Glazing Bars	V_{gb}	0.074	m_3
Volume of Structural Elements	V_s	0.165	m_3
Thickness of Glazing	Δ_{gl}	0.003	m
Depth of Floor Layer	Δ_f	0.01	m
Depth of 1st Soil Layer	Δ_1	0.02	m
Depth of 2nd Soil Layer	Δ_2	0.04	m
Depth of 3rd Soil Layer	Δ_3	0.08	m
Depth of 4th Soil Layer	Δ_4	0.16	m
Depth of 5th Soil Layer	Δ_5	0.32	m

Table 5.3 shows the surface areas of the greenhouse components which were determined from the data in Table 5.2.

Table 5.3. Calculated Surface Areas

Parameter	Symbol	Value	Units
Area of Glazing	A_g	223.1	m^2
Total Area of Floor	A_f	102.3	m_2
Exposed Surface Area of Root Medium	A_m	22.0	m_2

5.4.2 Densities and Specific Heat Capacities

The density and specific heat capacity of the glazing, glazing bars, and structure were read into the model during the initialization phase. Other values were specified as constants. The densities are given in Table 5.4 and the specific heat capacities in Table 5.5.

Table 5.4. Density of Greenhouse Components

Component	Material	Symbol	Density ($g.m_{-3} \times 10_{-6}$)
Glazing	Glass	ρ_{gl}	2.7
Glazing Bars	Aluminium	ρ_{gb}	2.7
Structure	Steel	ρ_{s}	7.8
Floor and Soil	Water	ρ_{w}	1.0
"	Organic Matter	ρ_{om}	1.3
"	Quartz Minerals	ρ_{q}	2.66
"	Clay Minerals	ρ_{cl}	2.65

Table 5.5. Specific Heat Capacity of Greenhouse Components			
Component	Material	Symbol	Specific Heat Capacity ($J.g_{-1}.^{\circ}C_{-1}$)
Glazing	Glass	C_{pgl}	0.84
Glazing Bars	Aluminium	C_{pgb}	0.89
Structure	Steel	C_{ps}	0.44
Floor and Soil	Water	C_{pw}	4.18
"	Organic Matter	C_{pom}	1.92
"	Quartz Minerals	C_{pq}	0.8
"	Clay Minerals	C_{pcl}	0.9
Air	Water Vapour	C_{pv}	1.88
"	Dry Air	C_{pa}	1.01

5.4.3 Composition of the Floor and Soil Layers

The composition of the soil was determined by taking samples at various depths and analyzing the fraction of quartz, and clay minerals present, as well as organic matter and water content. The water content on a volumetric basis was found to be relatively uniform in time and depth down to one metre. The soil in the top 30 cm was quiet high in organic matter as a result of previous crops being grown in the soil. Below this the organic fraction was very small. The soil was very compact and nearly saturated resulting in negligible air being present. Table 5.6 shows the composition of the floor and soil layers on a volumetric basis.

Table 5.6. Composition of the Floor and Soil by Volume Fraction				
Layer	Quartz	Clay	Organic Matter	Water
Floor	0.20	0.15	0.30	0.35
Soil 1-4	0.20	0.15	0.30	0.35
Soil 5	0.30	0.30	0.05	0.35

5.4.4 Composition of the Root Media

The root media used during the trials were made up of mixtures of pumice and bark. Samples of all the various mixtures were analysed to determine the volumetric fractions of the media in terms of composition of organic matter and inert material, which was assumed to be quartz type minerals. The void fraction of the media ranged between 0.63 and 0.8 with a mean of approximately 0.7. It was therefore assumed for all further calculations that the solid fraction of the media was 0.3. Therefore, for calculations of specific heat capacity it was assumed that the volume fraction of quartz minerals in the root medium, x_{qm}, would be $0.3(1-x_b)$, and the volume fraction of organic material, x_{omm}, would be $0.3x_b$, where x_b was the fraction of bark in the mixture.

Regression analysis revealed the maximum water holding capacity, WHC_m ($gH_2O.gDM^{-1}$), of a root media to be a function of the fraction of bark in the mix on a volumetric basis, x_b.

$$WHC_m = 0.55 - 0.6x_b + 2.6x_b^2 \qquad (5.108)$$

From this it can be seen that the water holding capacity varied from 0.55 $gH_2O.gDM^{-1}$ for a medium with no bark to 2.55 $gH_2O.gDM^{-1}$ for one with 100% bark. For the simulations an average mixture of 50% pumice and 50% bark was assumed. Thus the assumed water holding capacity was 0.9 $gH_2O.gDM^{-1}$.

The volume fraction of water at field capacity of a media could then be calculated from:

$$Field = WHC_m \frac{(x_{qm}\rho_q + x_{omm}\rho_{om})}{\rho_w} \qquad (5.109)$$

For the average mixture of pumice and bark this gave a volume fraction of water at field capacity of 0.53.

The maximum moisture content per unit floor area, X_m' ($gH_2O.m^{-2}$ of total floor area), was determined from:

$$X_m' = \frac{WHC_m V_m}{A_f}(x_{qm}\rho_q + x_{omm}\rho_{om}) \qquad (5.110)$$

where V_m is the total volume occupied by the root medium (m^3).

5.4.5 Thermal Capacities of the Greenhouse Components

The thermal capacity of each component per unit floor area, Φ ($J.m^{-2}.^{\circ}C^{-1}$), was calculated from the information presented in the previous sections. The thermal capacity of the structure, Φ_s, floor, Φ_f, and soil layers, Φ_1 to Φ_5, remained constant throughout the simulation. The thermal capacity of the dry fraction of the root medium, Φ_m, and the glazing, Φ_g, also remained constant but their overall thermal capacities varied with water content, X_m and X_g. As the crop grew its volume and hence thermal capacity increased. Table 5.7 shows the fixed thermal capacities used in the simulations as well as the likely range in the case of the crop.

Table 5.7. Thermal Capacity of Greenhouse Components

Component	Volume (m^3)	Mass ($g \times 10^{-6}$)	Thermal Capacity per Unit Floor Area ($J.m^{-2}.^{\circ}C^{-1} \times 10^{-3}$)
Glass	0.67	1.81	14.9
Glazing Bars	0.07	0.20	1.7
Total Glazing	0.74	2.01	16.6
Structure	0.17	1.29	5.5
Air (Average)	310.9	0.37	3.7
Crop (LAI = 0.1)	0.02	0.02	0.8
Crop (LAI = 3)	0.61	0.62	25.0
Root Medium (Dry)	0.88	0.52	6.0
Root Medium (Saturated)	0.88	0.99	25.2
Floor	1.02	1.67	29.3
Soil 1	2.05	3.34	58.7
Soil 2	4.09	6.68	117.3
Soil 3	8.18	13.36	234.6
Soil 4	16.37	26.72	469.2
Soil 5	32.74	65.73	940.8

5.4.6 Solar Radiation Parameters

At the beginning of each call to the energy and mass balance model the solar radiation parameters were determined, as discussed in section 5.3.11. The transmission and absorption of the greenhouse were read from a data

array depending on the solar azimuth and elevation. This array was generated in the initialization phase from data read from the input files SKY.DAT and DIFF.DAT (See Appendix 3).

The transmission values were then multiplied by the reduction factor, τ_R, as explained in section 4.3.8, to account for the systematic error in the light transmission model. Correspondingly, the absorption of the structure and glazing were increased by a factor of $1.0-\tau_R$. The total absorbed radiation was divided between the glazing and structure by a structural absorption factor, α_{struc} (0.44), based on the relative projected area of the structural members in the greenhouse to that of all the structural components including the glazing bars.

The transmission and absorption parameters for the crop were calculated using the relationships detailed in section 6.2.2, as discussed in section 5.3.11. The absorption of radiation at each surface was then computed.

5.4.7 Convective Heat Transfer Coefficients

Based on the initial temperatures of the surfaces the convective heat transfer coefficients were determined using well known empirical correlations, (Monteith, 1973, Holman, 1986, Incropera & De Witt, 1985) taking into account the nature of the convective processes.

Firstly the dimensionless boundary layer parameters are determined at the mean boundary layer temperature, T_{mean} from:

$$T_{mean} = \frac{(T_{surface} + T_a)}{2} \tag{5.111}$$

From this the thermal diffusivity, κ_a ($m^2.s^{-1}$), and kinematic viscosity, ν_a ($m^2.s^{-1}$), of the air can be calculated according to:

$$\kappa_a = 18.1 \times 10^{-6}(1 + 0.007 T_{mean}) \tag{5.112}$$

and

$$\nu_a = 13.3 \times 10^{-6}(1 + 0.007 T_{mean}) \tag{5.113}$$

The Reynolds number, Re, and Grashof number, Gr, are now determined from:

$$\mathrm{Re} = \frac{u_a d}{\nu_a} \tag{5.114}$$

and

$$Gr = \frac{g\beta_{mean} D_c^3 |T_{surface} - T_a|}{\nu_a^3} \tag{5.115}$$

where u_a is the air speed across the surface ($m.s_{-1}$), d is the characteristic dimensional length of the surface (m), g is the gravitational constant (9.81 $m.s^{-2}$), and β_{mean} is the bouyancy parameter of the boundary layer (K^{-1}). Note that $\beta_{mean} = 1/(T_{mean} + 273.15)$.

The boundary between free, forced and mixed convection are defined by:

FORCED $$0 < \frac{Gr}{Re^2} < 0.33 \tag{5.116a}$$

MIXED $$0.33 \leq \frac{Gr}{Re^2} \leq 10.0 \tag{5.116b}$$

FREE $$10.0 < \frac{Gr}{Re^2} < \infty \tag{5.116c}$$

For forced convection in air the dimensionless heat transfer coefficient, (Nusselt number Nu), is given by:

$$Nu_{forced} = ARe^n \tag{5.117}$$

Values for the parameters A and n are given in Table 5.8.

Table 5.8. Parameters for Forced Convection Correlations

Flow Regime	Criteria	A	n
Laminar	$Re \leq 2 \times 10^4$	0.60	0.5
Turbulent	$Re > 2 \times 10^4$	0.032	0.8

For free convection stable conditions occur on the underside of an horizontal surface when the temperature of the surface is greater than the air temperature, and on the top side of a horizontal surface when the surface temperature is less than the air temperature. The Nusselt number is given by:

$$Nu_{free} = BGr^m \tag{5.118}$$

Values for the parameters B and m are given in Table 5.9.

Table 5.9. Parameters for Free Convection Correlations

Flow Regime	Criteria	B	m
Vertical Laminar	$Gr \leq 1 \times 10^9$	0.58	0.25
Vertical Turbulent	$Gr > 1 \times 10^9$	0.11	0.33
Stable Horizontal	All Gr	0.23	0.25
Unstable Horizontal Laminar	$Gr \leq 1 \times 10^5$	0.50	0.25
Unstable Horizontal Turbulent	$Gr > 1 \times 10^5$	0.13	0.33

For the case of mixed free and forced convection the appropriate value of the Nusselt number can be found from:

$$Nu^3 = Nu^3_{forced} + Nu^3_{free} \tag{5.119}$$

Finally the convective heat transfer coefficient is found from:

$$h_c = \frac{Nu \kappa_a \rho_a C_{pa}}{d} \tag{5.120}$$

For the outside surface of the glazing the heat transfer coefficient was calculated from the outside wind speed, and the glazing to outside air temperature difference. The characteristic dimension used was the average of the width and length of the greenhouse, that is 11.05 m. Test calculations showed that if either the length (15.5 m) or width (6.6 m) was used then the heat transfer coefficient would only change by ±5% with a 10°C temperature difference and a wind speed of 1 $m.s^{-1}$, and by ±0.1% at the same temperature difference and 5 $m.s^{-1}$ wind speed. Therefore, the selection of the exact characteristic dimension was not critical, as long as the order of magnitude was correct.

For the calculation of convective heat transfer coefficients of the internal surfaces a constant air velocity of 0.2 $m.s^{-1}$ was assumed. This was based on the average of measurements made with the hot-wire anemometer. For the surfaces in the greenhouse with large characteristic dimensions, the selection of air speed is not critical as the flow regime will always

be free convection, or if in the mixed region the Reynolds number will not be large and thus has little effect on the combined Nusselt number. The inside of the glazing was assumed be a vertical wall with a characteristic dimension equal to the sum of the height from the floor to the gutter plus half the sloping length of the roof. This was done to allow for the fact that the vertical convection pattern can develop over the full height of the greenhouse. Once again it was discovered that small variations in the characteristic dimension had little effect on the heat transfer coefficient. For the floor, the average of the length and width of the greenhouse was used as a characteristic dimension. The exact value used also proved not to be critical as long as it was of the correct order of magnitude. The heat transfer coefficient of the root medium was assumed to be equal to that of the floor. For the structural members two estimates of the heat transfer coefficient were made and averaged. The first was for vertical members with a characteristic length of 2 m, and the second was for horizontal members with a characteristic diameter of 0.1 m.

The convective heat transfer coefficient of the crop leaves was calculated by first estimating the average leaf length from the simulated number of leaves, and the total leaf area. This was done each time the leaf area was updated (once a day). Due to the largely horizontal nature of cucumber leaves a heat transfer coefficient was estimated for both sides of the leaf and then these were averaged. The rationale behind this was that the flow regime is usually mixed convection, and one side of the leaf will always have stable free convection. Since the characteristic dimension of a cucumber leaf is of the same order of magnitude as the air speed, variations in air speed can have a considerable effect on the heat transfer coefficient. For a leaf length of 0.2 m, and a 5°C temperature difference, the likely variation in air speed (0.05 $m.s^{-1}$ to 0.5 $m.s^{-1}$) will cause the heat transfer coefficient to vary between 3 and 6 $W.m^{-2}.°C^{-1}$. Since it was not possible to find suitable relationships between the measured air speed and other parameters, such as outside wind speed, or ventilation rate, the compromise, of assuming a constant average air speed of 0.2 $m.s^{-1}$, seemed reasonable. For the conditions mentioned above this would yield a heat transfer coefficient of around 4 $W.m^{-2}.°C^{-1}$.

5.4.8 Radiation Heat Transfer Coefficients

In section 5.3.13 is was shown that in general the radiative heat transfer coefficient, h_{R12}, is a function of the combined emissivity view factor, $\mathcal{F}_{12}$, and the mean temperature of the two participating surfaces.

$$h_{R12} \approx 4\mathcal{F}_{12}\sigma T^3_{mean} \qquad (5.121)$$

The combined emissivity view factor in turn can be determined from the emissivity of the two surfaces, ϵ_1 and ϵ_2, the surface areas, A_1 and A_2, and the view factor, F_{12}.

$$\frac{1}{\mathcal{F}_{12}} = \left(\frac{1-\epsilon_1}{\epsilon_1}\right) + \frac{1}{F_{12}} + \frac{A_1}{A_2}\left(\frac{1-\epsilon_2}{\epsilon_2}\right) \tag{5.122}$$

Based on the geometry and size of the surfaces in the greenhouse the various view factors were calculated using standard reciprocity relationships (Holman, 1986). These were updated whenever the leaf area index changed (once per day in the combined model). The emissivities of the surfaces were gleaned from standard sources and are given in Table 5.10.

Table 5.10. Emissivity of Greenhouse Surfaces

Surface	Material	Symbol	Emissivity	Source
Glazing	Glass	ϵ_g	0.94	2
Structure	Painted Steel	ϵ_s	0.92	2
Heating System	Painted Steel/ Oxidized Copper	ϵ_h	0.92 / 0.78 Average 0.85	2
Crop Canopy	Vegetation	ϵ_c	0.95	3
Root medium	Bark /Pumice	ϵ_m	0.95	1
Floor	Black Polyethylene	ϵ_f	0.67	4

Sources:
1 Assumed
2 Holman (1986)
3 Monteith & Unsworth (1990)
4 Newman (1991)

The procedures followed to calculate the view factors for radiation exchanges are outlined in the following sections.

5.4.8.1 Thermal Radiation Transmission of the Crop

The transmission factor of the crop for thermal radiation, τ_{cb}, is calculated on the assumption that the leaves are perfect emitters and absorbers of thermal radiation.

$$\tau_{cb} = e^{(-K_{bdf} LAI)} \tag{5.123}$$

where LAI is the leaf area index, and K_{bdf} is the extinction coefficient for diffuse radiation in a canopy of "black" leaves. This was found to be a function of the leaf angle distribution and the leaf area index (for further discussion of radiation transmission through leaf canopies see section 6.2.2.)

5.4.8.2 Self View Factor of the Crop

The self view factor of the crop can be found by considering a crop canopy distributed horizontally in space between two very large flat plates. The area of the plates are A_1 and A_2 respectively and are equal, and the total surface area of the crop, including both sides of the leaves is A_c. By definition the leaf area index is:

$$LAI = \frac{A_c}{2A_1} \tag{5.124}$$

It follows then that the total surface area of the crop is:

$$A_c = 2LAI\,A_1 = 2LAI\,A_2 \tag{5.125}$$

In the absence of the crop the view factors from one plate to the other would be approximately one. However, with the crop canopy present the view factors will be reduced according to the transmission of the crop canopy.

$$F_{12} = \tau_{cb} \tag{5.126}$$

and

$$F_{21} = \tau_{cb} \tag{5.127}$$

The view factor from each plate to the crop is therefore equal to the absorptivity of the crop.

$$F_{1c} = 1 - \tau_{cb} \tag{5.128}$$

and

$$F_{2c} = 1 - \tau_{cb} \tag{5.129}$$

Applying the reciprocity relationship to equations 5.128 and 5.129 gives the view factors from the crop to the two plates.

$$F_{c1} = F_{1c}\frac{A_1}{A_c} \tag{5.130a}$$

$$= \frac{(1-\tau_{cb})}{2LAI} \tag{5.130b}$$

and

$$F_{c2} = F_{2c}\frac{A_2}{A_c} \tag{5.131a}$$

$$= \frac{(1-\tau_{cb})}{2LAI} \tag{5.131b}$$

Thus the self view factor of the crop can be calculated from:

$$F_{cc} = 1 - F_{c1} - F_{c2} \tag{5.132a}$$

$$= 1 - \frac{(1-\tau_{cb})}{LAI} \tag{5.132b}$$

5.4.8.3 Self View Factor of the Root Medium

The self view factor of the root medium bags, F_{mm}, was estimated from relationships found in Rohsenow & Hartnett (1973) for cylinders at known spacing. The diameter and height of the bags were both 0.2 m. The spacing between bags in the row was 0.44 m and between the rows was 1.4 m. For the 1989 trial there were 14 bags in a row across the greenhouse, and 10 rows along the length of the house. From this information it was possible to estimate view factors between the sides of a bag and other bags.

The minimum view factor (0.24) was for a corner bag, which would see the least number of other bags. The maximum view factor (0.38) occurred for a bag in the centre of the greenhouse. Averaging over all bags produced a view factor of approximately 0.30 between the side of a bag and any other bag. The self view factor of all the bags of root medium also needed to take amount of the total surface area of the medium including sides of the bags and the top surface, which would not see any other side or top surface. The total side area of all bags was 17.6 m² and the area of all the top surfaces was 4.4 m², giving a total exposed area of 22.0 m², of which the side area accounted for 80%. The average self view factor, F_{mm}, for the root medium bags was therefore estimated to be 0.24.

5.4.8.4 View Factor Root Medium to Floor

The view factor between the root medium and the floor, F_{mf}, was estimated in the following manner. The fraction of radiation leaving the side of a bag which arrives at another bag is given by:

$$F_{\text{side side}} = \left(\frac{A_m}{A_{\text{side}}}\right) F_{mm} \tag{5.133}$$

Therefore the fraction of radiation leaving the side of a bag which arrives at the floor will be:

$$F_{\text{side f}} = \frac{1}{2}\left(1 - \frac{A_m F_{mm}}{A_{\text{side}}}\right) \tag{5.134}$$

assuming that half of the radiation fraction goes directly upwards, and the other half goes to the floor.

To obtain the view factor between the root medium and the floor the previous equation must be multiplied by the ratio of side area to total surface area of the root medium to account for the top surface which does not see the floor. Therefore:

$$F_{mf} = \frac{1}{2}\left(\frac{A_{\text{side}}}{A_m}\right)\left(1 - \frac{A_m F_{mm}}{A_{\text{side}}}\right) \tag{5.135a}$$

$$= \frac{1}{2}\left(\frac{A_{\text{side}}}{A_m} - F_{mm}\right) \tag{5.135b}$$

5.4.8.5 View Factor Root Medium to Crop

The view factor from the root medium to the crop is given by:

$$F_{mc} = (1 - F_{mm} - F_{mf})(1 - \tau_{cb}) \tag{5.136}$$

where $(1 - F_{mm} - F_{mf})$ is the fraction of radiation leaving the root medium which is travelling upwards towards the crop, and $(1 - \tau_{cb})$ is the absorptivity of the crop.

5.4.8.6 View Factor Root Medium to Heating System

The view factor from the root medium to the heating system is given by:

$$F_{mh} = (1 - F_{mm} - F_{mf})\tau_{cb}\zeta_h \tag{5.137}$$

where ζ_h is the heating system radiation interception coefficient. This was estimated to be 0.02 by determining the area of the sky obstructed by the heating system when viewed from the floor.

5.4.8.7 View Factor Root Medium to Structure

The view factor from the root medium to the greenhouse structure is given by:

$$F_{ms} = (1 - F_{mm} - F_{mf})\tau_{cb}\zeta_s \tag{5.138}$$

where ζ_s is the radiation interception coefficient of the structure. This was estimated to be 0.15 by determining the area of the sky obstructed by the greenhouse structural members when viewed from the floor.

5.4.8.8 View Factor Root Medium to Glazing

Since glass is opaque to thermal radiation all upward radiation from the root medium bags which is not intercepted by the crop, the heating system, or the structure, will be incident on the glazing. The view factor from the root medium to the glazing will therefore be:

$$F_{mg} = (1 - F_{mm} - F_{mf})\tau_{cb}(1 - \zeta_h - \zeta_s) \tag{5.139}$$

5.4.8.9 View Factors for the Floor

The view factor from the floor to the root medium bags can be found by applying the reciprocity relationship to the result of equation 5.135. Note that the effective floor area for radiation exchanges is reduced by the area occupied by the bags of root medium. Thus:

$$F_{fm} = F_{mf}\left(\frac{MAI}{FAI}\right) \tag{5.140}$$

In a manner similar to that used for the root medium the view factors from the floor to the crop, heating system, structure, and glazing can be calculated according to the following relationships:

$$F_{fc} = (1 - F_{fm})(1 - \tau_{cb}) \tag{5.141}$$

$$F_{fh} = (1 - F_{fm})\tau_{cb}\zeta_h \tag{5.142}$$

$$F_{fs} = (1 - F_{fm})\tau_{cb}\zeta_s \tag{5.143}$$

and

$$F_{fg} = (1 - F_{fm})\tau_{cb}(1 - \zeta_h - \zeta_s) \quad (5.144)$$

5.4.8.10 View Factors for the Crop

The view factors from the crop to the floor and root medium can be found by applying the reciprocity relationship to the results of equations 5.141 and 5.136 respectively. Thus:

$$F_{cf} = F_{fc}\left(\frac{FAI}{2LAI}\right) \quad (5.145)$$

and

$$F_{cm} = F_{mc}\left(\frac{MAI}{2LAI}\right) \quad (5.146)$$

The view factors between the crop and the heating system, structure and glazing can now be found by considering relevant interceptions of the upward fraction of radiation emitted by the crop. Therefore:

$$F_{ch} = (1 - F_{cc} - F_{cm} - F_{cf})\zeta_h \quad (5.147)$$

$$F_{cs} = (1 - F_{cc} - F_{cm} - F_{cf})\zeta_s \quad (5.148)$$

and

$$F_{cg} = (1 - F_{cc} - F_{cm} - F_{cf})(1 - \zeta_h - \zeta_s) \quad (5.149)$$

5.4.8.11 View Factors for the Heating System

The view factors from the heating system to the floor, root medium, and crop can be found by applying the reciprocity relationship to the results of equations 5.142, 5.137, and 5.147 respectively. Thus:

$$F_{hf} = F_{fh}\left(\frac{FAI}{HAI}\right) \quad (5.150)$$

$$F_{hm} = F_{mh}\left(\frac{MAI}{HAI}\right) \quad (5.151)$$

and

$$F_{hc} = F_{ch}\left(\frac{2LAI}{HAI}\right) \tag{5.152}$$

The view factors between the heating system and the structure, and glazing can now be found by considering relevant interceptions of the upward fraction of radiation emitted by the heating system. Therefore:

$$F_{hs} = (1 - F_{hh} - F_{hc} - F_{hm} - F_{hf})\zeta_s \tag{5.153}$$

and

$$F_{hg} = (1 - F_{hh} - F_{hc} - F_{hm} - F_{hf})(1 - \zeta_s) \tag{5.154}$$

5.4.8.12 View Factors for the Structure

The view factors from the structure to the floor, root medium, crop, and heating system can be found by applying the reciprocity relationship to the results of equations 5.143, 5.138, 5.148, and 5.153, respectively. Thus:

$$F_{sf} = F_{fs}\left(\frac{FAI}{SAI}\right) \tag{5.155}$$

$$F_{sm} = F_{ms}\left(\frac{MAI}{SAI}\right) \tag{5.156}$$

$$F_{sc} = F_{cs}\left(\frac{2LAI}{SAI}\right) \tag{5.157}$$

and

$$F_{sh} = F_{hs}\left(\frac{HAI}{SAI}\right) \tag{5.158}$$

The view factor between the structure and glazing can now be found by determining the upward fraction of radiation emitted by the structure. Hence:

$$F_{sg} = 1 - F_{ss} - F_{sh} - F_{sc} - F_{sm} - F_{sf} \tag{5.159}$$

5.4.8.13 View Factors for the Glazing

The view factors from the inside of the glazing to the other surfaces inside the greenhouse can all be calculated by applying the reciprocity

relationship to the previously calculated view factors from those surfaces to the glazing. Since all possible radiation exchanges are covered in previous sections, these view factors were not required for the model.

The view factor of the outside of the glazing to the sky was estimated to be 0.6 by calculating the individual view factors between the greenhouse walls and roof and the ground and the adjacent buildings. The radiant exchanges with these surfaces were ignored on the basis that they would have very similar temperatures to that of the greenhouse glazing.

5.4.8.14 Combined Emissivity View Factors

From the preceding information the combined emissivity view factors can be calculated. Only those factors used in the model are presented.

$$\mathcal{F}_{gsky} = \epsilon_g F_{gsky} \tag{5.160}$$

$$\frac{1}{\mathcal{F}_{sg}} = \left(\frac{1-\epsilon_s}{\epsilon_s}\right) + \frac{1}{F_{sg}} + \left(\frac{SAI}{GAI}\right)\left(\frac{1-\epsilon_g}{\epsilon_g}\right) \tag{5.161}$$

$$\frac{1}{\mathcal{F}_{hg}} = \left(\frac{1-\epsilon_h}{\epsilon_h}\right) + \frac{1}{F_{hg}} + \left(\frac{HAI}{GAI}\right)\left(\frac{1-\epsilon_g}{\epsilon_g}\right) \tag{5.162}$$

$$\frac{1}{\mathcal{F}_{hs}} = \left(\frac{1-\epsilon_h}{\epsilon_h}\right) + \frac{1}{F_{hs}} + \left(\frac{HAI}{SAI}\right)\left(\frac{1-\epsilon_s}{\epsilon_s}\right) \tag{5.163}$$

$$\frac{1}{\mathcal{F}_{cg}} = \left(\frac{1-\epsilon_c}{\epsilon_c}\right) + \frac{1}{F_{cg}} + \left(\frac{2LAI}{GAI}\right)\left(\frac{1-\epsilon_g}{\epsilon_g}\right) \tag{5.164}$$

$$\frac{1}{\mathcal{F}_{cs}} = \left(\frac{1-\epsilon_c}{\epsilon_c}\right) + \frac{1}{F_{cs}} + \left(\frac{2LAI}{SAI}\right)\left(\frac{1-\epsilon_s}{\epsilon_s}\right) \tag{5.165}$$

$$\frac{1}{\mathcal{F}_{ch}} = \left(\frac{1-\epsilon_c}{\epsilon_c}\right) + \frac{1}{F_{ch}} + \left(\frac{2LAI}{HAI}\right)\left(\frac{1-\epsilon_h}{\epsilon_h}\right) \tag{5.166}$$

$$\frac{1}{\mathcal{F}_{mg}} = \left(\frac{1-\epsilon_m}{\epsilon_m}\right) + \frac{1}{F_{mg}} + \left(\frac{MAI}{GAI}\right)\left(\frac{1-\epsilon_g}{\epsilon_g}\right) \tag{5.167}$$

$$\frac{1}{\mathcal{F}_{ms}} = \left(\frac{1-\epsilon_m}{\epsilon_m}\right) + \frac{1}{F_{ms}} + \left(\frac{MAI}{SAI}\right)\left(\frac{1-\epsilon_s}{\epsilon_s}\right) \tag{5.168}$$

$$\frac{1}{\mathcal{F}_{mh}} = \left(\frac{1-\epsilon_m}{\epsilon_m}\right) + \frac{1}{F_{mh}} + \left(\frac{MAI}{HAI}\right)\left(\frac{1-\epsilon_h}{\epsilon_h}\right) \tag{5.169}$$

$$\frac{1}{\mathcal{F}_{mc}} = \left(\frac{1-\epsilon_m}{\epsilon_m}\right) + \frac{1}{F_{mc}} + \left(\frac{MAI}{2LAI}\right)\left(\frac{1-\epsilon_c}{\epsilon_c}\right) \tag{5.170}$$

$$\frac{1}{\mathcal{F}_{fg}} = \left(\frac{1-\epsilon_f}{\epsilon_f}\right) + \frac{1}{F_{fg}} + \left(\frac{FAI}{GAI}\right)\left(\frac{1-\epsilon_g}{\epsilon_g}\right) \tag{5.171}$$

$$\frac{1}{\mathcal{F}_{fs}} = \left(\frac{1-\epsilon_f}{\epsilon_f}\right) + \frac{1}{F_{fs}} + \left(\frac{FAI}{SAI}\right)\left(\frac{1-\epsilon_s}{\epsilon_s}\right) \tag{5.172}$$

$$\frac{1}{\mathcal{F}_{fh}} = \left(\frac{1-\epsilon_f}{\epsilon_f}\right) + \frac{1}{F_{fh}} + \left(\frac{FAI}{HAI}\right)\left(\frac{1-\epsilon_h}{\epsilon_h}\right) \tag{5.173}$$

$$\frac{1}{\mathcal{F}_{fc}} = \left(\frac{1-\epsilon_f}{\epsilon_f}\right) + \frac{1}{F_{fc}} + \left(\frac{FAI}{2LAI}\right)\left(\frac{1-\epsilon_c}{\epsilon_c}\right) \tag{5.174}$$

$$\frac{1}{\mathcal{F}_{fm}} = \left(\frac{1-\epsilon_f}{\epsilon_f}\right) + \frac{1}{F_{fm}} + \left(\frac{FAI}{MAI}\right)\left(\frac{1-\epsilon_m}{\epsilon_m}\right) \tag{5.175}$$

5.4.9 Determination of the Effective Sky Temperature

The radiant temperature of the sky was estimated using the relationships proposed by Berdahl and Fromberg (1982), for clear skies, and modified for cloud cover as suggested by Monteith (1973) with an average cloud base temperature of eight degrees below ambient.

For the a clear day the emissivity of the sky is assumed to be:

$$\epsilon_{sky}(0) = 0.741 + 0.0062T_{od} \tag{5.176}$$

and during a clear night:

$$\epsilon_{sky}(0) = 0.727 + 0.006T_{od} \tag{5.177}$$

The dew point temperature of the outside air, T_{od} (°C), can be calculated from the outside vapour pressure, e_o (Pa), by:

$$T_{od} = \frac{237.3\,\mathrm{Ln}(e_o/611.0)}{17.27 - \mathrm{Ln}(e_o/611.0)} \tag{5.178}$$

The outside vapour pressure can be determined from measurements of the outside dry bulb temperature, T_o (°C), and wet bulb temperature, T_{ow} (°C).

$$e_o = 611 \exp\left(\frac{17.27 T_{ow}}{T_{ow} + 237.3}\right) - \gamma(T_o - T_{ow}) \quad (5.179)$$

where γ is the psychrometric constant (66 $Pa.K^{-1}$).

During cloudy conditions the emissivity of the sky was increased according to:

$$\epsilon_{sky}(C) = \epsilon_{sky}(0) + Cloud\left[1 - \epsilon_{sky}(0) - \left(\frac{T_o - T_{cloud}}{T_o + 273.15}\right)\right] \quad (5.180)$$

where $Cloud$ is the fraction of the sky covered with clouds, and T_{cloud} is the cloud base temperature and is assumed to be 8°C below the outside air temperature, T_o, on average (Monteith, 1973).

Cloud cover fraction was estimated from the clearness index, K_t, when the solar elevation was above 10°. For values of K_t less than 0.2 the sky was assumed to be overcast, and for values greater than 0.75 the sky was assumed to be clear. Between these limits a linear change in cloud cover was calculated. The rationale for these choices is based on Figure 4.1 which shows that below 20% clearness index solar radiation is almost entirely diffuse, and above 75% clearness index a minimum fraction of diffuse radiation is realised. During the night the cloud cover fraction existing just before sunset was maintained. This is sometimes unrealistic as the passage of a frontal system during the night can have a marked effect on cloud cover.

5.4.10 Conductive Heat Transfer Coefficients

The thermal conductivity of the soil and floor was estimated using the method set out by ten Berge (1986). A subroutine to perform these calculations was included as part of the initialization routine. This allowed the soil characteristics to be altered easily, if so desired, by changing the composition and water content of the soil layers. However, these were assumed to be constant throughout the simulation. The thermal conductivity was 1.38 $W.m^{-1}.°C^{-1}$ for the floor and first four soil layers, and 1.37 $W.m^{-1}.°C^{-1}$ for the fifth soil layer, using the compositions given in Table 5.6.

The conductivity of the root medium was calculated at the beginning of each call to the energy and mass balance model to account for the changing water content of the medium. For the 50/50 bark/pumice root medium the thermal conductivity varied from 0.45 $W.m^{-1}.^{\circ}C^{-1}$ for a completely dry condition to 0.97 $W.m^{-1}.^{\circ}C^{-1}$ for a completely saturated condition. For 100% bark the range of thermal conductivity was 0.33 to 0.87 $W.m^{-1}.^{\circ}C^{-1}$, and for 100% pumice the range was 0.57 to 1.13 $W.m^{-1}.^{\circ}C^{-1}$. On the basis that the bags of root medium where kept well watered, the assumption that all bags were 50/50 mix would not have introduced any large errors.

The thermal conductance between the root medium and the floor, h_{Cfm}, was estimated from the thermal conductivities and the half thickness of the two layers according to:

$$h_{Cfm} = \frac{2}{\left(\frac{\Delta_m}{k_m} + \frac{\Delta_f}{k_f}\right)} \qquad (5.181)$$

Conductance between the structure and the glazing bars, h_{Csg}, was estimated, based on contact areas, and entered as a constant parameter, 0.6 $W.m^{-2}.^{\circ}C^{-1}$, based on the total surface area of the floor.

5.4.11 Evaporative Mass Transfer Resistances

The evaporative mass transfer resistances, r_v ($s.m^{-1}$), were estimated from the appropriate convective coefficients via the Lewis number, Le, (Monteith, 1976).

For the underside of the glazing:

$$r_{vga} = Le^{0.67}\left(\frac{\rho_a C_{pa}}{h_{Cga}}\right) \qquad (5.182)$$

For the crop boundary layer:

$$r_{vca} = Le^{0.67}\left(\frac{\rho_a C_{pa}}{h_{Cca}}\right) \qquad (5.183)$$

and for the root medium:

$$r_{vma} = Le^{0.67}\left(\frac{\rho_a C_{pa}}{h_{Cma}}\right) \qquad (5.184)$$

where $Le^{0.67}$ is equal to 0.93, ρ_a is the density of the dry air ($g.m^{-3}$), and C_{pa} is the specific heat capacity of the air (1.01 $J.g^{-1}.^{\circ}C^{-1}$).

The internal leaf resistance to water vapour transfer, r_{vci}, was estimated using the empirical correlation derived in Appendix 2.

5.4.12 Advective Heat and Mass Transfer Coefficients

The ventilation rate was calculated at the beginning of each simulation call based on the model derived in Appendix 1, which predicted the air exchange rate per hour, N_v (hr^{-1}). From this the advective heat transfer coefficient, h_{ao} ($W.m^{-2}.^{\circ}C^{-1}$), can be found from:

$$h_{ao} = \left(\frac{N_v}{3600}\right)\left(\frac{m_a C_{pa}}{A_f}\right) \qquad (5.185a)$$

$$= \frac{N_v \Phi_a}{3600} \qquad (5.185b)$$

where m_a is the mass of dry air in the greenhouse (g), C_{pa} is the specific heat capacity of the air (1.01 $J.g^{-1}.^{\circ}C^{-1}$), and Φ_a is the thermal capacity of the air per unit floor area ($J.m^{-2}.^{\circ}C^{-1}$). The factor 3600 converts the time units from hours to seconds, and the area of the floor, A_f, is included in order that the rate of advective heat transfer be per unit floor area.

The equivalent advective mass transfer resistance is:

$$r_{ao} = \frac{\rho_a C_{pa}}{h_{ao}} \qquad (5.186)$$

The rate of addition of irrigation water, f_{irr} ($gH_2O.s^{-1}.m^{-2}$ of total floor area) was calculated from the irrigation watering information read in from the boundary value data files.

When the moisture content of the root medium was greater than or equal to the maximum root medium moisture content, X_m' (equation 5.110), then the rate of drainage from the medium, f_{drain}, was set equal to the rate of irrigation, f_{irr}. At all other times f_{drain} was set to zero.

To simulate the effect of dripping of condensed water from the underside of the glazing, it was assumed that when the average depth of water spread across the glazing was greater than 0.2 mm, and condensation was occurring, then the rate of dripping, f_{drip}, would equal the rate of condensation, $-f_{ga}$. At all other times f_{drip} was set to zero. Note that $-f_{ga}$ is the rate of condensation, and $+f_{ga}$ is the rate of evaporation from the underside of the glazing.

The water potential of the crop, ψ_c (bars), was linearly related to the relative water content, RWC_c, (Behboudian, 1977, Bruggink et al 1988). The relative water content was defined as the water content of the plant relative to the maximum water content of the plant, when the water potential was zero. Therefore:

$$\psi_c = -\frac{(1 - RWC_c)}{\Omega_c} \qquad (5.187a)$$

$$= -\frac{\left(1 - \frac{X_c}{X_c'}\right)}{\Omega_c} \qquad (5.187b)$$

where X_c is the moisture content of the crop per unit floor area ($gH_2O.m^{-2}$), and X_c' is the maximum moisture content of the crop per unit floor area ($gH_2O.m^{-2}$). This was calculated from the water holding capacity of the crop, WHC_c ($gH_2O.gDM^{-1}$), multiplied by the total dry matter content of the crop, DM_c (gDM), and the number of plants in the greenhouse, N_{plant}, divided by the floor area, A_f. The water holding capacity of the crop was determined to be 19.0 $gH_2O.gDM^{-1}$ based on maximum water content measurements of around 95%.

From the data of Behboudian (1977) and Marcelis (1989) a representative value for the hydraulic capacitance of the crop, Ω_a, was determined to be 0.014 bar^{-1}. From the same sources, a representative value of the hydraulic conductivity of the crop, K_c, was found to be 0.004 $gH_2O.m^{-2}.s^{-1}.bar^{-1}$.

The water potential of the root medium was determined from experiments using gypsum blocks to measure water potential, and gravimetric weighing to determine the corresponding water content. In a similar manner to that described above for the crop, the water potential, ψ_m (bar), was related to the relative water content of the root medium, WHC_m.

$$\psi_m = -\frac{(1 - RWC_m)}{\Omega_m} \qquad (5.188a)$$

$$= -\frac{\left(1 - \frac{X_m}{X_m'}\right)}{\Omega_m} \qquad (5.188b)$$

where X_m is the moisture content of the root medium per unit floor area ($gH_2O.m^{-2}$), and X_m' is the maximum moisture content of the crop per unit floor area ($gH_2O.m^{-2}$) (see equation 5.110). From the data the hydraulic capacitance of the root medium, Ω_m, was found to be 0.4 $gH_2O.m^{-2}.s^{-1}.bar^{-1}$.

5.5 IMPLEMENTATION OF THE MODEL

The differential equations 5.41 to 5.54, the ancillary equations, 5.55 to 5.107, and the various ancillary parameters described in section 5.4, form the basis of the greenhouse energy and mass balance model. The equations, along with various support routines to handle data input and output were coded in ESL (European Simulation Language, Hay et al, 1988). Boundary value data, for the outside weather and control inputs were available, from the data logging phase, at 5 minute intervals. This data was used to drive the model.

Three versions of the greenhouse energy and mass balance model (GEMB) were developed. Initially the energy and mass balances were developed for an empty greenhouse with no plants or bags of root medium. After a few trial runs with this model, the complete model including the crop and medium was developed and tested. In this second model the leaf area index was held constant throughout the simulation period. Later a third version was developed which incorporated the growing plants (see Chapter 6). Results from the second and third versions of the model are reported in this thesis.

5.5.1 Integration Technique

The simulation language used provided a number of procedures which could be selected to solve the differential equations. After some experimentation it was found that the fixed step second order Runge-Kutta routine could be used during the night, so long as the step length was not more than 30 seconds long. This allowed the simulation to progress fairly rapidly without becoming unstable when the heating system switched on and off.

During the day, when ventilators opened and closed, and the crop began transpiring it was necessary to use the default simulation method. This is a 4/5 order, 6 stage, variable step, pseudo-iterative method due to Sarafyan (Hay et al, 1988). This technique calculates two solutions, one at fourth order, and one at fifth order, and the difference is used to estimate the truncation error. If the truncation error is large the solution is rejected, the step length will be reduced and a new pair of solutions determined. This procedure is repeated until the truncation error is within acceptable limits. If the error is small then the step length for the next step may be increased.

The ability of this method to vary its step length means that when rapid changes are occurring in the system the differential equation solver will take a large number of small steps, which increases the simulation run time, but prevents the solution from becoming unstable. During times of

slow rates of change the step length will grow and the solution will speed up. Thus an acceptable trade-off between stability, accuracy, and simulation time can be achieved.

5.5.2 Discontinuities

A discontinuity is an event which causes a step change in the algebraic or differential equations describing the system, and hence in one or more state variables. In the presence of a discontinuity the Taylor series representation of the integration step is invalid, and thus all numerical integration techniques based on this will give erroneous results.

One of the main advantages of programming the model in ESL was that the language has inbuilt capabilities to deal with discontinuities. At the end of each time step the discontinuity conditions are tested to see if a discontinuity occurred in the step. If so the step length is adjusted, by interpolating the discontinuity function, until the point of discontinuity lies between two time steps. The system parameters are then adjusted, to reflect the effect of the discontinuity, and the simulation resumed.

Several discontinuities occur in the model, in relation to the mass balance equations for the underside of the glazing and the root medium. Condensation will occur on the glazing whenever the saturation vapour pressure of the glazing is below the vapour pressure of the air. This corresponds to a concentration gradient between the air and the glazing which will cause water vapour to migrate toward the glazing and condense there. Evaporation from the glazing, on the other hand, is not a continuous process. There will be times when the vapour pressure gradient between the glazing and air is such that evaporation should occur, but will not because the glazing is dry. Thus a discontinuity is introduced to equations 5.41, 5.49, and 5.50, which include the latent heat transfer term.

Another discontinuous process at the glazing is dripping of condensate. This will only occur when a critical mass of condensed water is reached. Beyond this dripping will occur at a rate which keeps the weight of water at this critical level. Thus there is an upper bound for the amount of condensed water that can form on the underside of the glazing. This introduces a discontinuity to equations 5.41 and 5.50.

A similar upper bound exists for the amount of water that may be present in the root medium. If sufficient irrigation water is applied, to bring the water status to field capacity, then further addition will cause drainage from the medium to occur. In fact this was the deliberate watering policy pursued throughout the experiments, to ensure that no plant was under-watered. Field capacity is determined by the physical nature of the medium, with organic matter content and void ratio being of prime

importance. A discontinuity may also occur if the medium becomes completely dry. In this case, evaporation from the medium will cease, even though the vapour pressure gradient may be favourable. Therefore, discontinuities must be considered in equations 5.44 and 5.52.

In theory, a similar upper bound exists for the moisture content of the crop. When a plant takes up more water than it transpires, or stores in new tissue, then the crop may expel liquid water directly by guttation. In practice, cucumbers, with their low dry matter content, large leaves, low stomatal resistance, and rather poor root systems are unlikely ever to exceed their maximum water holding capacity.

5.6 RESULTS OF THE SIMULATION

In this section the results of the simulations of the cropped greenhouse are presented. In section 5.6.1 results from the second version of the model, with a crop present but not growing, are presented. In section 5.6.2 long term correlations between simulated and measured variables, from the third version of the model with a growing crop, are presented.

5.6.1 Sample Results of the Greenhouse Simulation with Static Crop

The main validation of the energy and mass balance model, incorporating the crop at fixed leaf area index, was performed using data from the 15th week of the crop (8/11/89 - 14/11/89). During this period the actual leaf area index was relatively constant, at 2.2 $m^2.m^{-2}$, which corresponded to the period of maximum leaf area. Figure 5.3 shows the levels of the important outside meteorological boundary variables, dry bulb temperature, wet bulb temperature, global radiation, and wind speed for the 8th of November 1989. Figures 5.4 to 5.13 show the values of important simulated state variables, compared to the measured values.

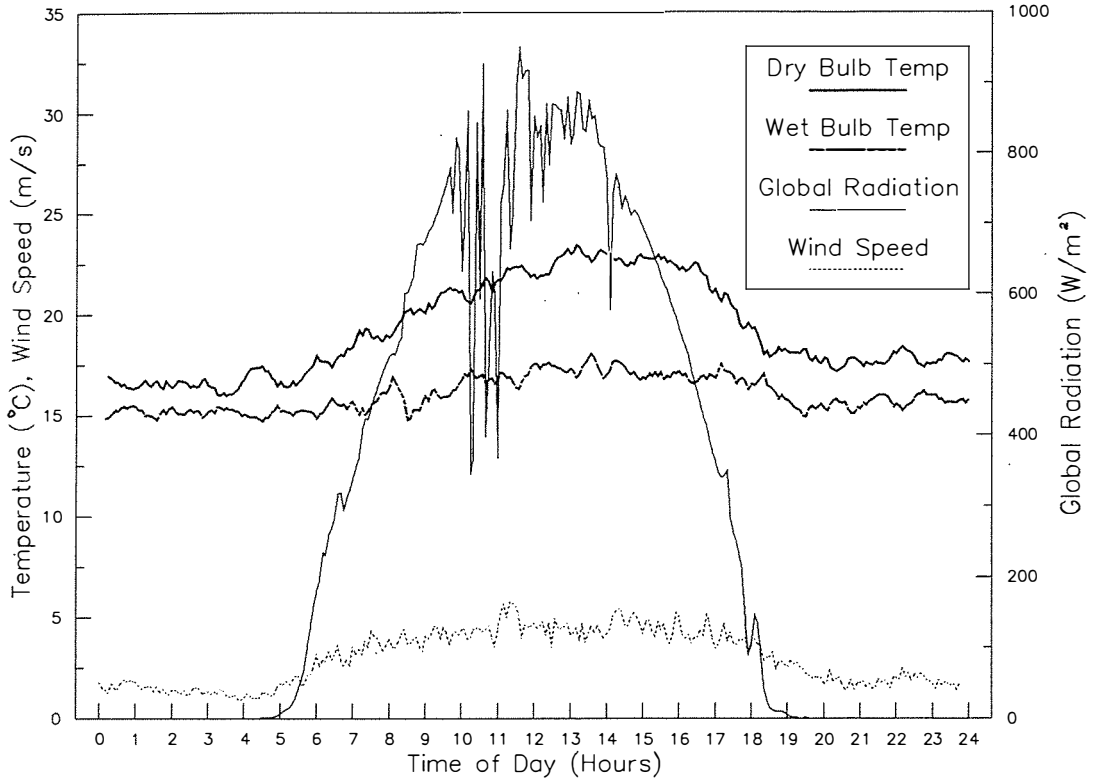

Figure 5.3. Prevailing weather conditions on 8/11/89.

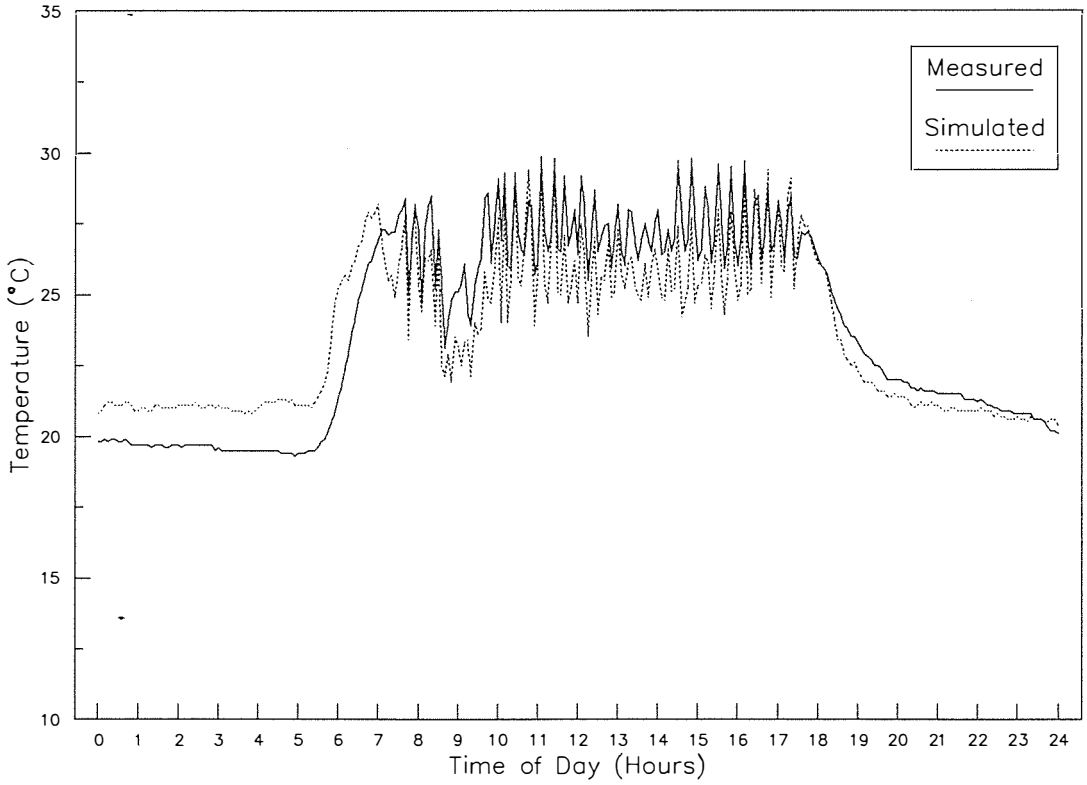

Figure 5.4. Measured and Simulated Air Temperature on 8/11/89.

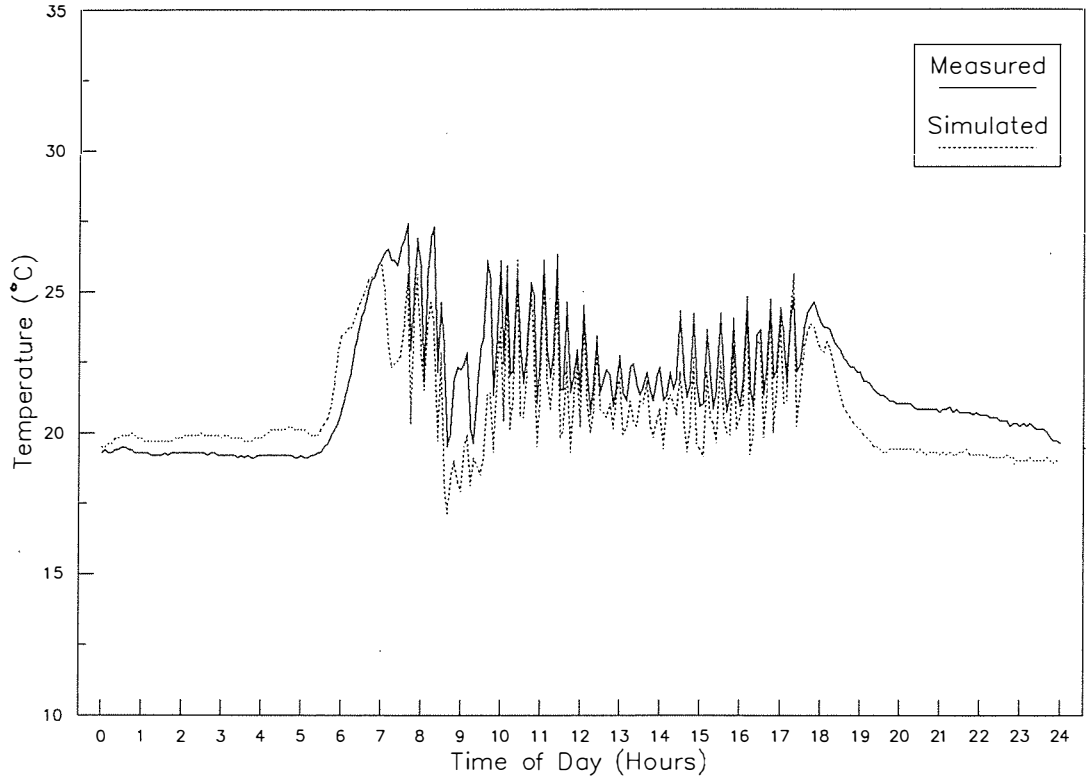

Figure 5.5. Measured and Simulated Wet Bulb Temperature on 8/11/89.

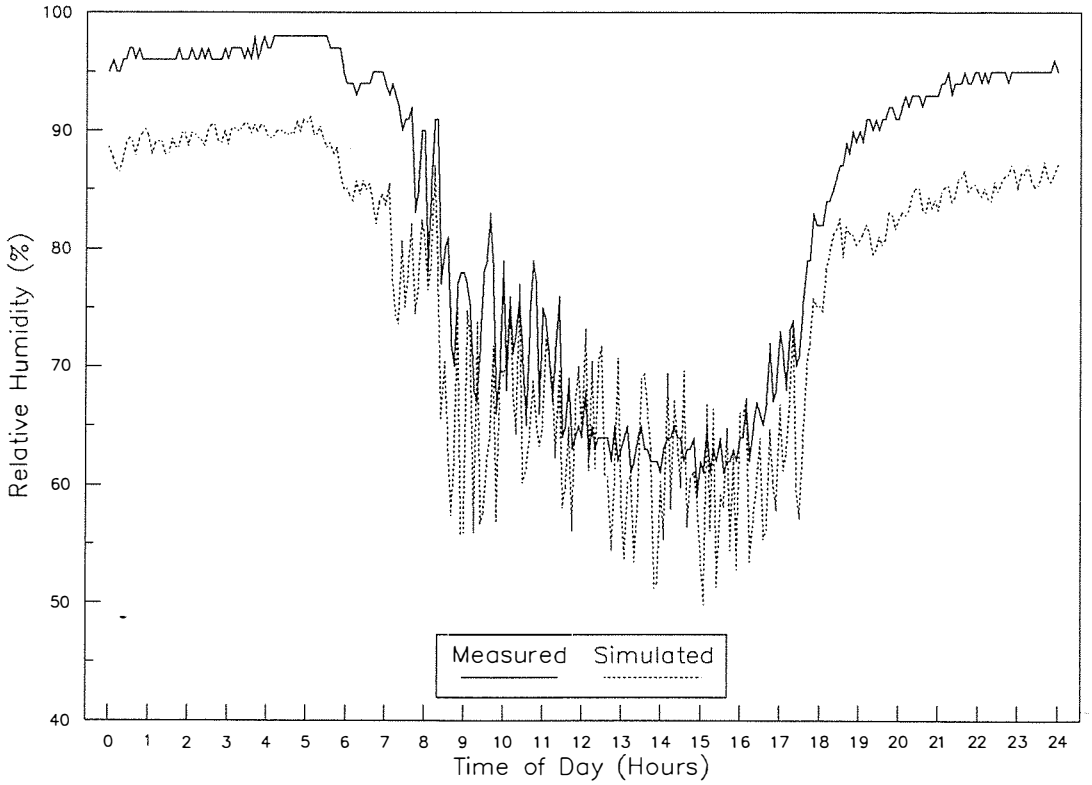

Figure 5.6. Measured and Simulated Relative Humidity on 8/11/89.

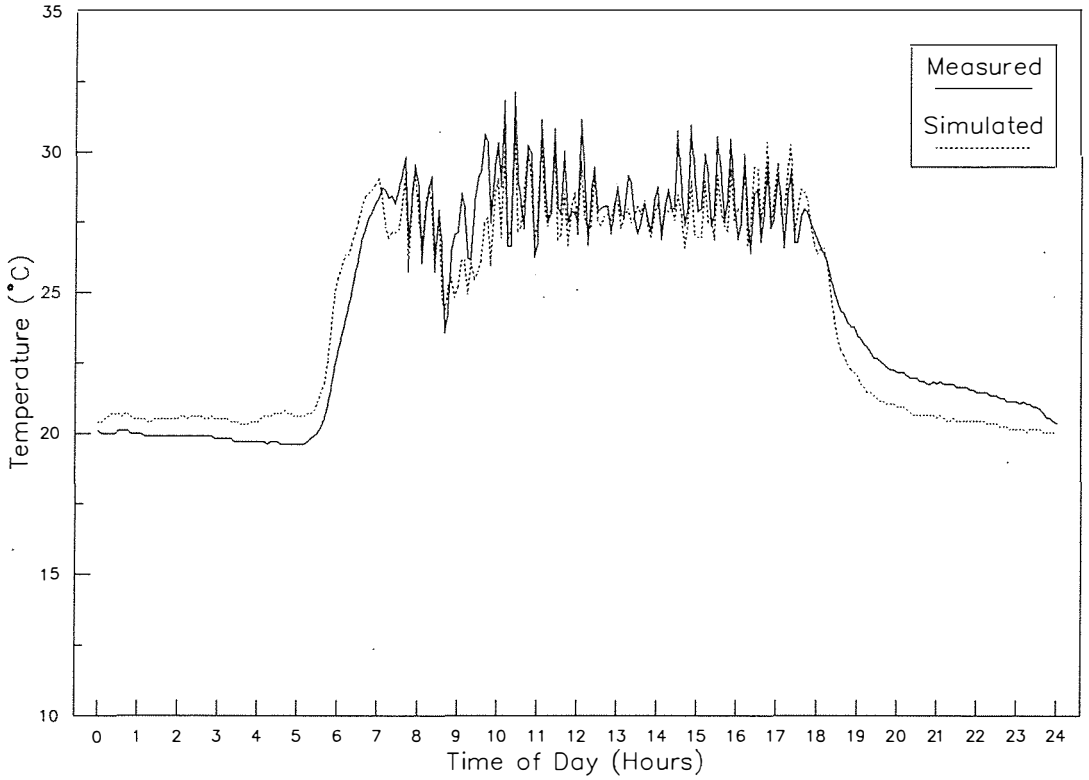

Figure 5.7. Measured and Simulated Leaf Temperature on 8/11/89.

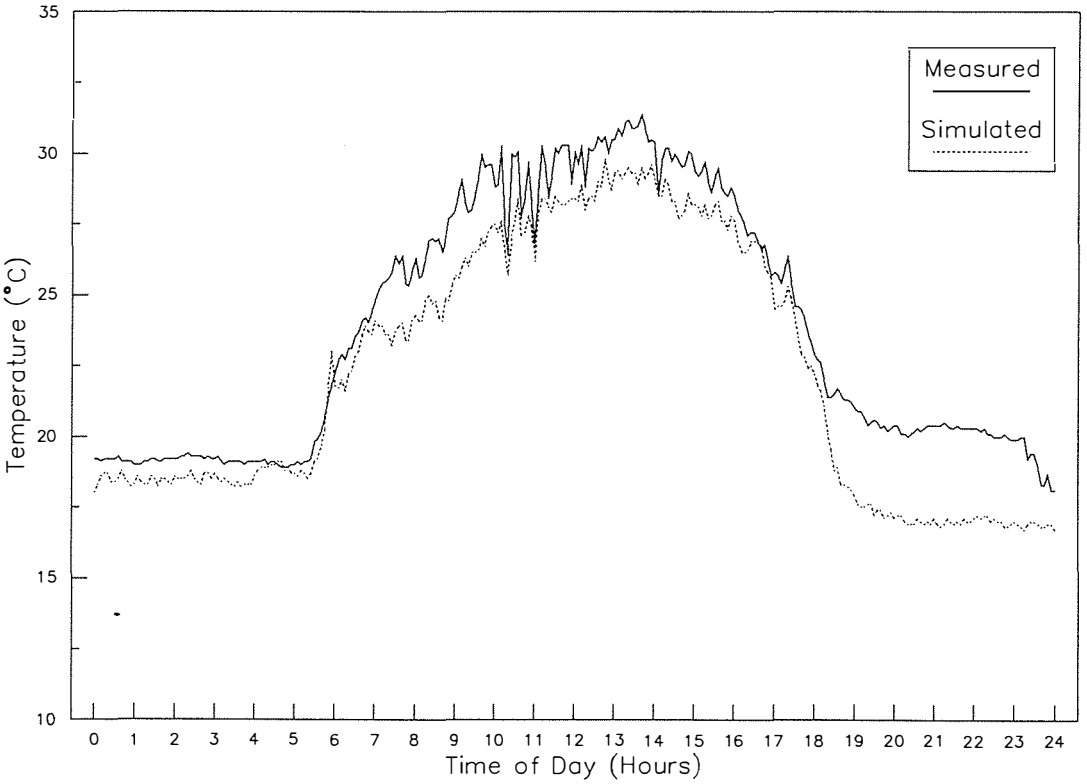

Figure 5.8. Measured and Simulated Glazing Temperature on 8/11/89.

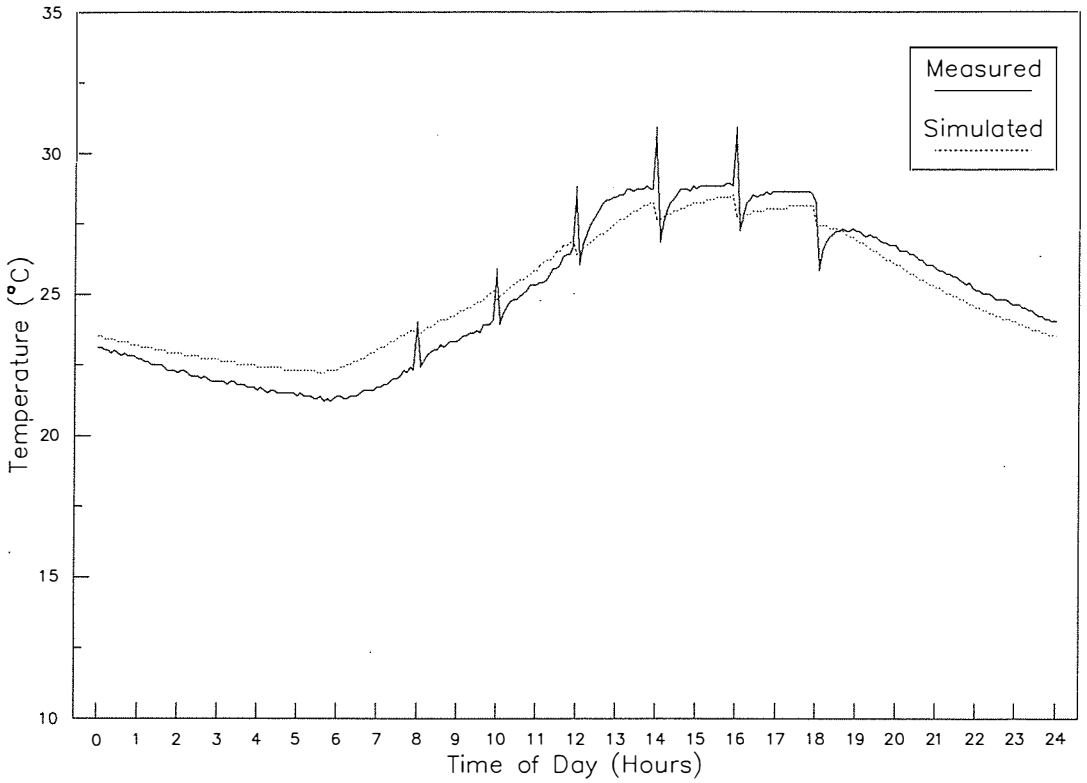

Figure 5.9. Measured and Simulated Root Medium Temperature on 8/11/89.

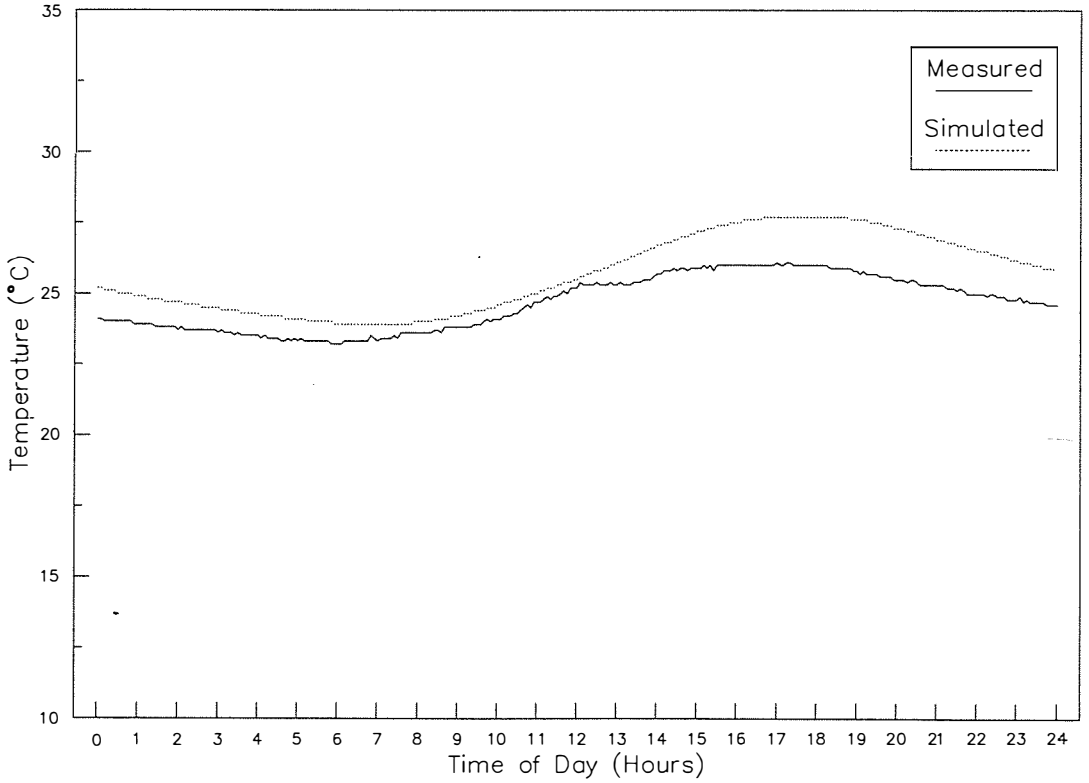

Figure 5.10. Measured and Simulated Soil Temperature (5 cm) on 8/11/89.

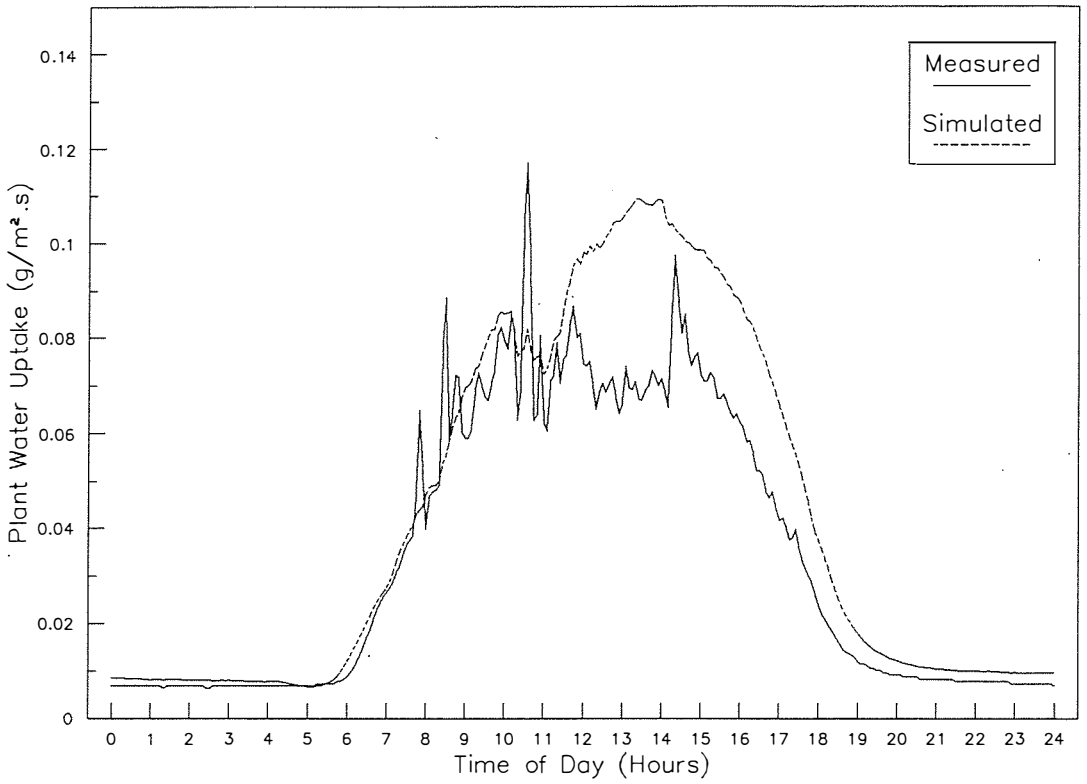

Figure 5.11. Measured and Simulated Water Uptake Rate on 8/11/89.

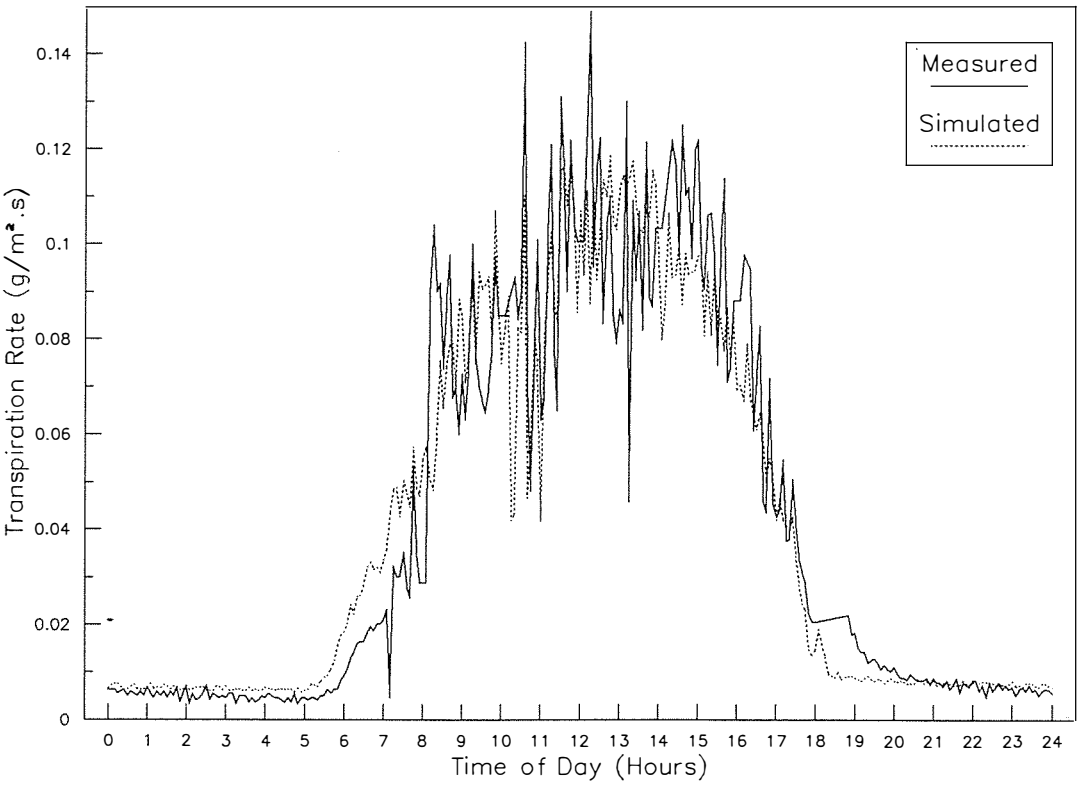

Figure 5.12. Measured and Simulated Transpiration Rate on 8/11/89.

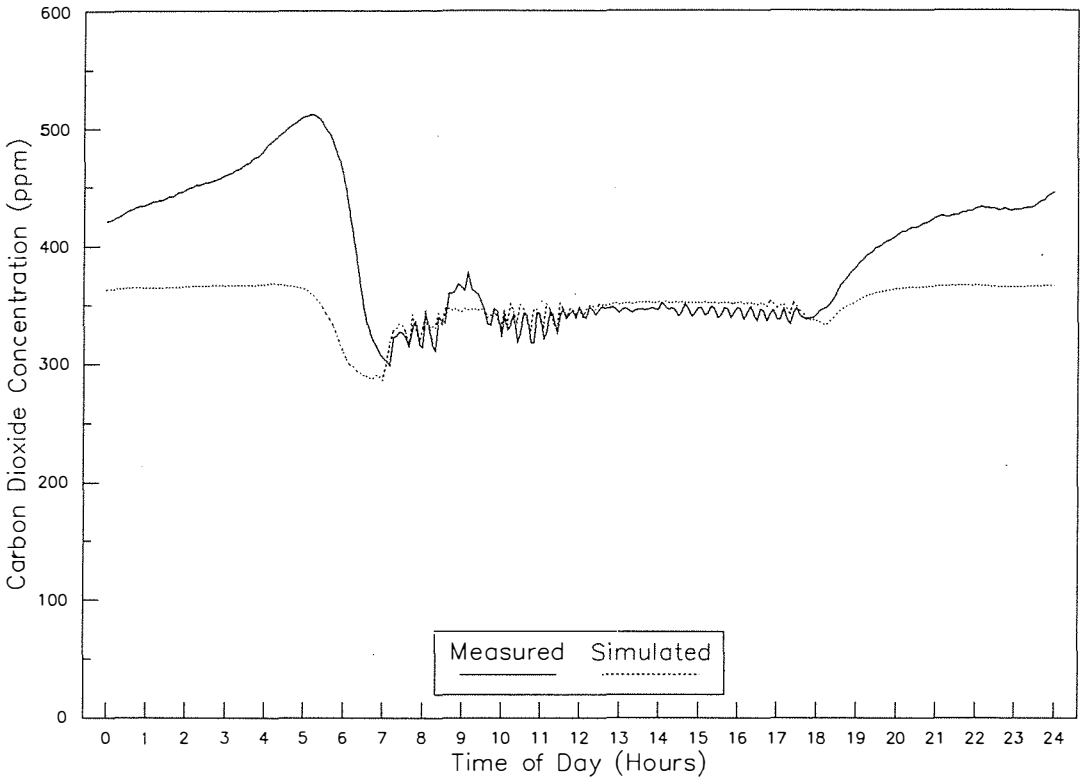

Figure 5.13. Measured and Simulated CO_2 concentration on 8/11/89.

It can be seen that the fit between simulated and measured variables was generally good, with all the simulated temperatures being within a few degrees of the measured values. Simulation of relative humidity was not as good, with the simulated value generally being lower than the measured value at night (Figure 5.6). Most of this error can be attributed to the relatively large over-estimate of air temperature (Figure 5.4) compared to that for wet bulb temperature (Figure 5.5).

Figure 5.4 shows a typical pattern of temperature offset during the night period from midnight to 0500 hrs. Note that during this period the outside temperature and wind speed were fairly constant (Figure 5.3), and that the heater did not operate. Since the glazing and leaf temperatures (Figures 5.7 and 5.8) for this period were also fairly constant, a period of near steady state heat transfer may have occurred. Since the simulated air temperature was greater than the measured air temperature, but the simulated glazing temperature was slightly below the measured glazing temperature, an error in estimating the heat transfer coefficients is implied. The outside heat transfer coefficients were under-estimated and the inside heat transfer coefficients were over-estimated.

During the day the simulation managed to track the measured inside air temperature despite large fluctuation in temperature due to ventilation.

Careful examination of Figure 5.4 shows that the air temperature was slightly under-predicted. This was most likely due to over-estimation of the ventilation rate.

The simulation of leaf temperature was encouragingly good, (Figure 5.7), as this is an important parameter for the determination of photosynthesis, respiration and development within the crop model. As with the prediction of air temperature, there is an offset at night indicating errors in determining the exact value for the heat transfer coefficients. However, during the day the rapidly changing pattern of leaf temperature, due to ventilation and solar radiation disturbances, was followed adequately.

The results for the glass surface were not as good as for the leaf temperature (Figure 5.8). Generally the model under-predicted the glass temperature. Glass temperature was strongly influenced by the sky temperature, and hence the assumed level of cloud cover. However, the error in predicting the glazing temperature appears not to have affected the leaf temperature greatly.

Simulation of the root medium temperature was also good (Figure 5.9). The sharp glitches in the measured temperature are due to the addition of irrigation water. Initially the temperature of the medium tends to rise due to the enthalpy added, but then falls due to increased cooling by evaporation from the wet surface. The model predicted the cooling effect but not the warming. This was due to the assumption that the irrigation water would be at the deep ground temperature, which was probably lower than the actual water temperature.

Figure 5.10 shows that the soil temperature was also well predicted, although there is evidence to suggest that the simulation lagged behind the measured temperature by about two hours. Also the slightly greater amplitude of the simulated temperature curve suggests that thermal conductance down from higher layers was too great, or that the thermal capacity at this level was too low.

Water uptake by the plant, and transpiration were generally well modelled (Figures 5.11 and 5.12). This was rather surprising, considering the number of assumptions that had to be made about the water relations of the plants. The cause of the over-prediction of water uptake rate in the afternoon could not be explained, except to assume that the hydraulic conductivity of the plant, which was assumed to be constant, did in fact decrease.

The simulation of carbon dioxide concentration was not at all good during night hours. Possible sources of error leading to this situation could have been, an over-estimate of the air exchange rate, or an under-estimate of respiration. In light of the fact, that the predicted relative humidity was

also generally low at night, it may well be, that the former case was true. Also in this, the second version of the model, there was no carbon dioxide production due to growth respiration, as the crop was assumed to be static. It was later discovered, when running the final model with a growing crop, that growth respiration produced significantly greater quantities of carbon dioxide than did maintenance respiration, and this would explain a large part of the discrepancy.

The prevailing outside weather conditions on the 29th of October 1989, 18 weeks after seed sowing, are shown in Figure 5.14. By this day the leaf area index of the crop had reduced to 1.9. The simulated and measured profiles of inside dry bulb, wet bulb, glazing, leaf and root medium temperatures are shown in Figures 5.15 to 5.19.

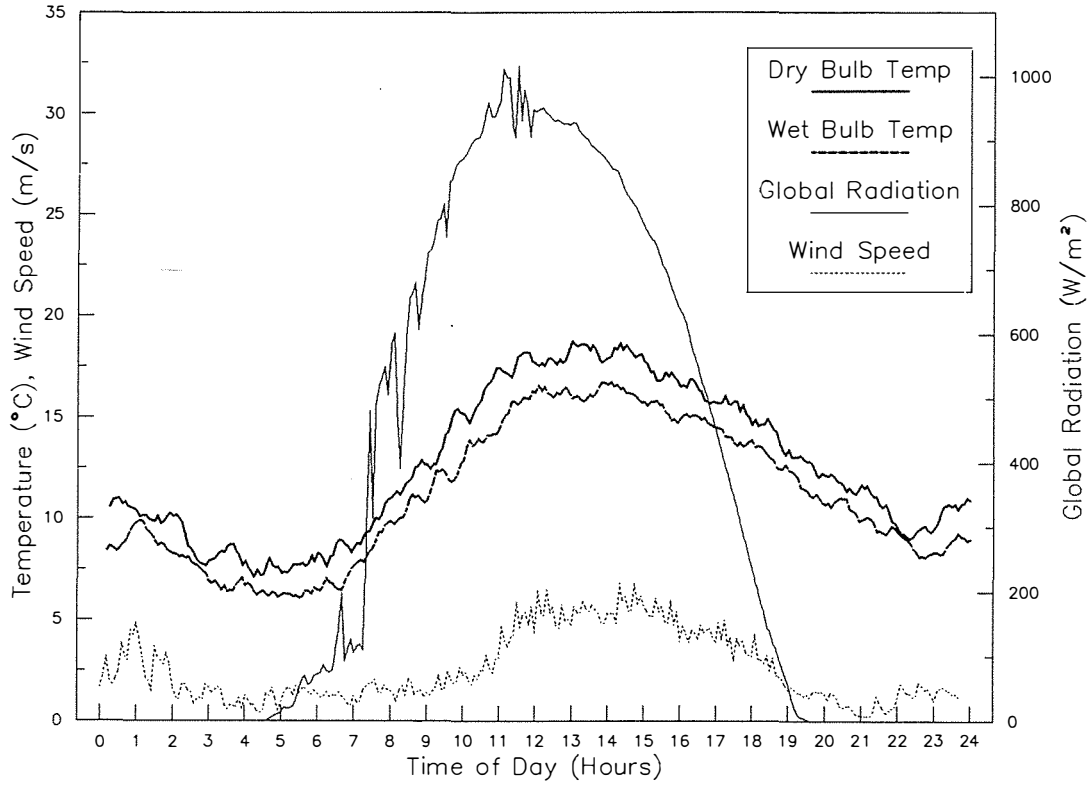

Figure 5.14. Prevailing Weather Conditions on 29/11/89.

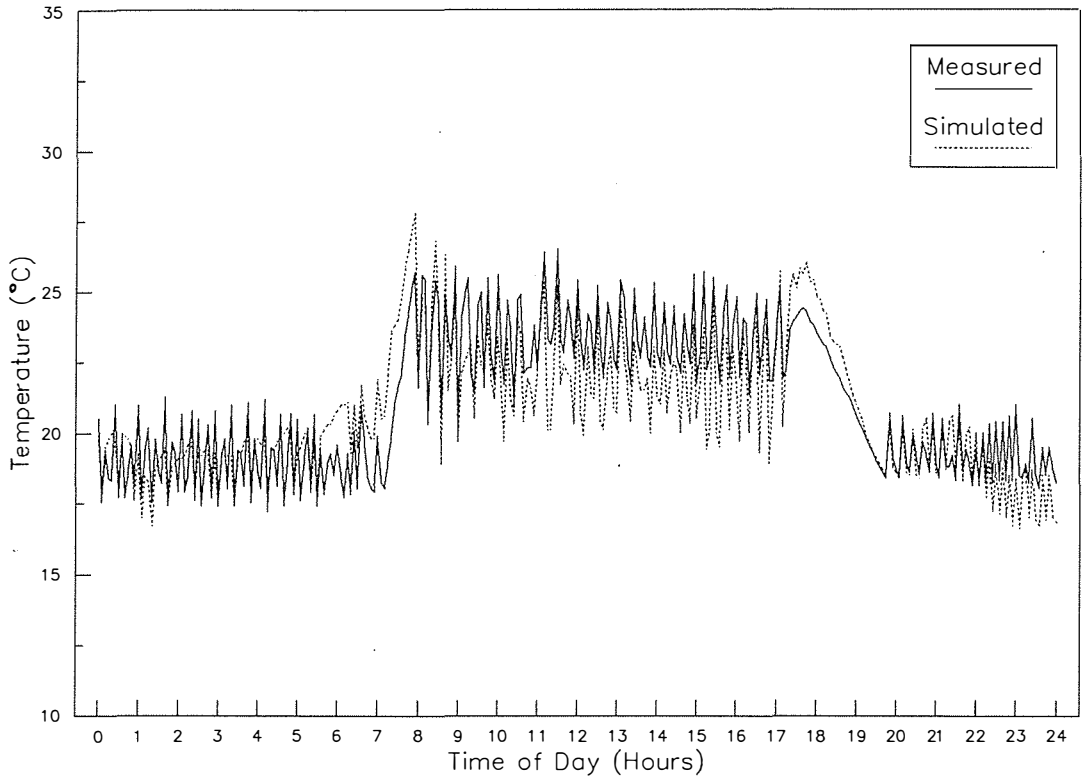

Figure 5.15. Measured and Simulated Air Temperature on 29/11/89.

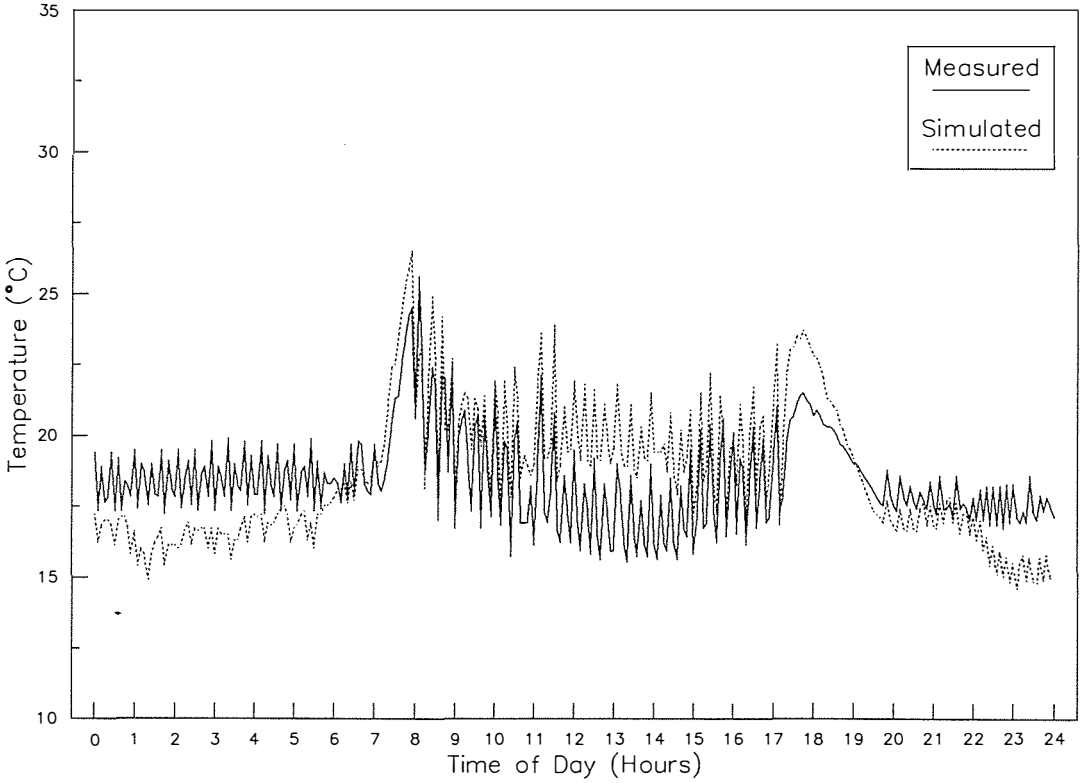

Figure 5.16. Measured and Simulated Wet Bulb Temperature on 29/11/89.

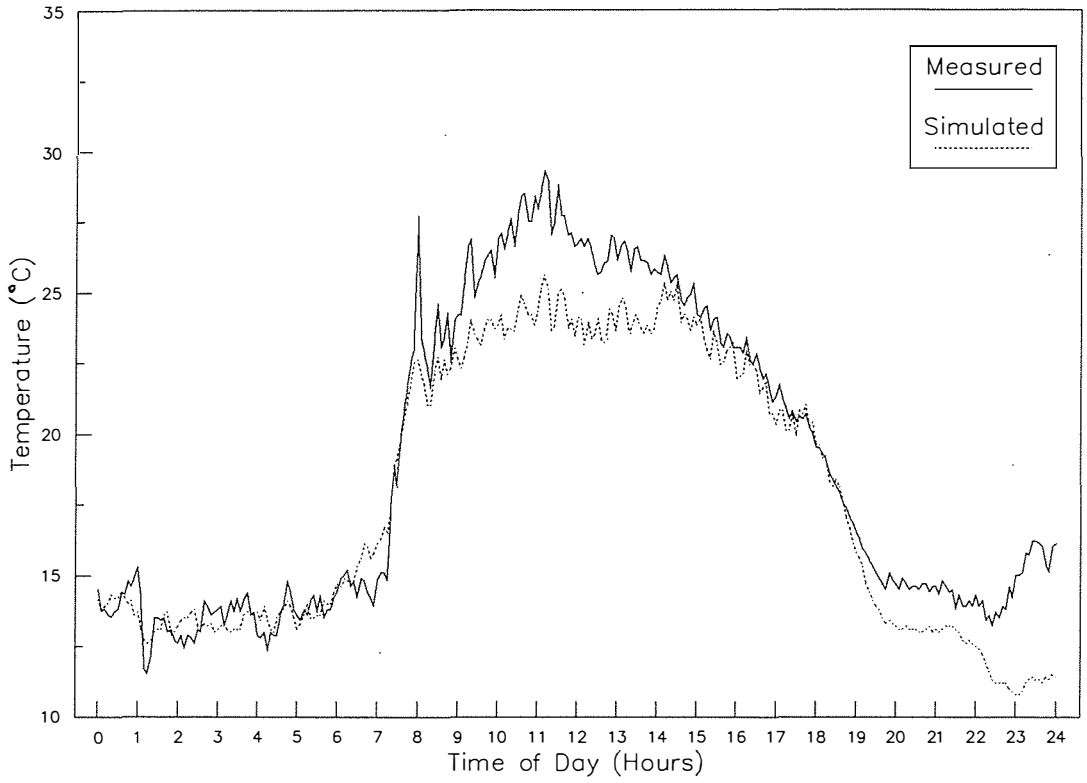

Figure 5.17. Measured and Simulated Glazing Temperature on 29/11/89.

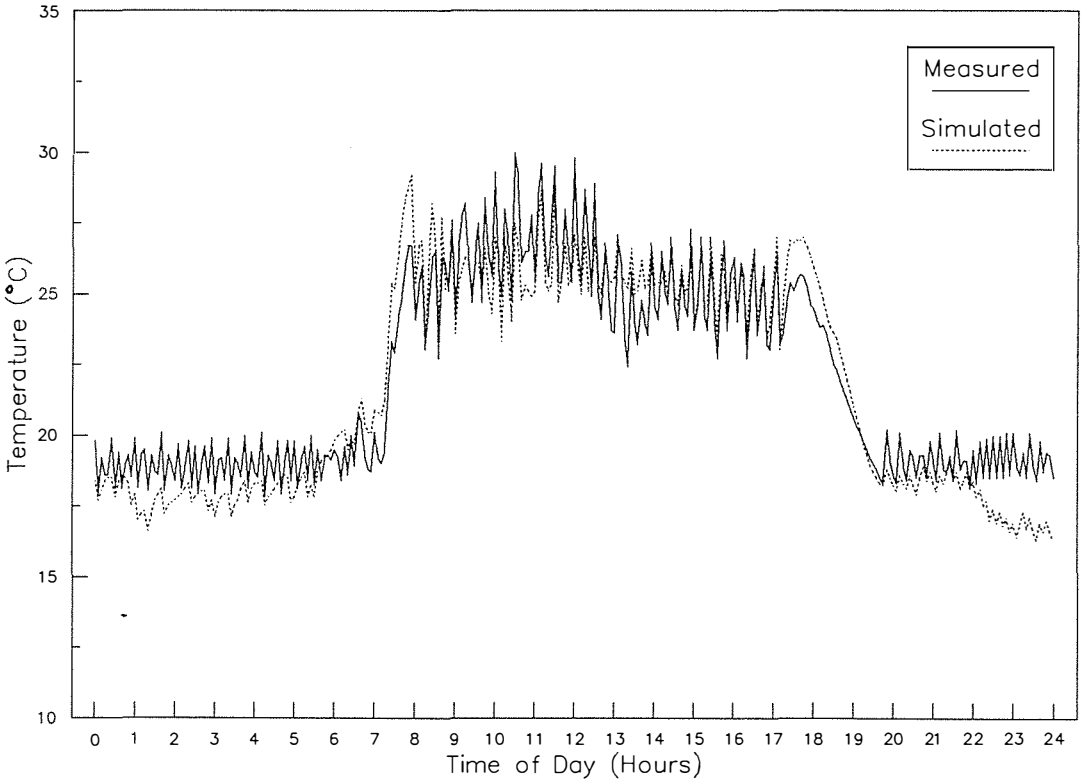

Figure 5.18. Measured and Simulated Leaf Temperature on 29/11/89.

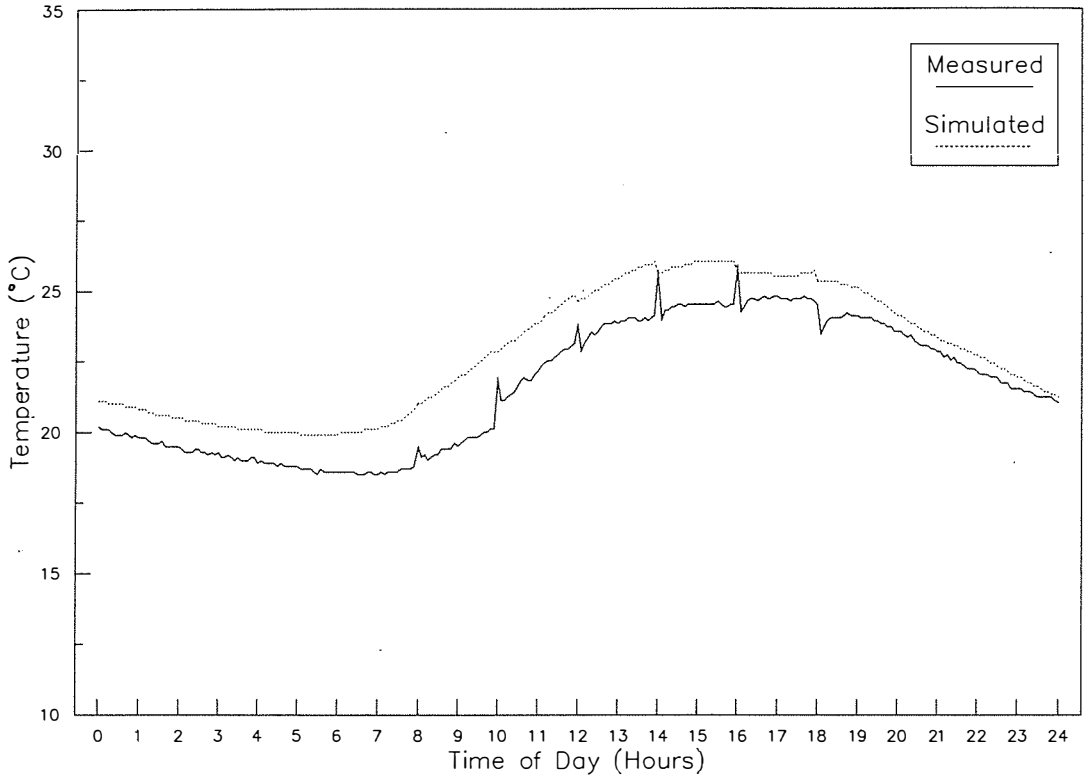

Figure 5.19. Measured and Simulated Root Medium Temperature on 29/11/89.

Again it can be seen that there was good general agreement between simulated and measured values of temperatures within the greenhouse. The outside temperatures were lower for this night and caused the heaters to operate. The model was capable of tracking the quiet large fluctuations in temperature caused by the on-off operation of the heaters which were generously sized.

The prevailing weather conditions on the 20th of September, 8 weeks after seed sowing, are shown in Figure 5.20. Figures 5.21 to 5.25 show the measured and simulated profiles of inside dry and wet bulb temperature, relative humidity, glazing and root medium temperatures. Leaf temperature was not recorded at this time. The plants at this stage had only 6 or 7 leaves and the leaf area index was between 0.1 and 0.2.

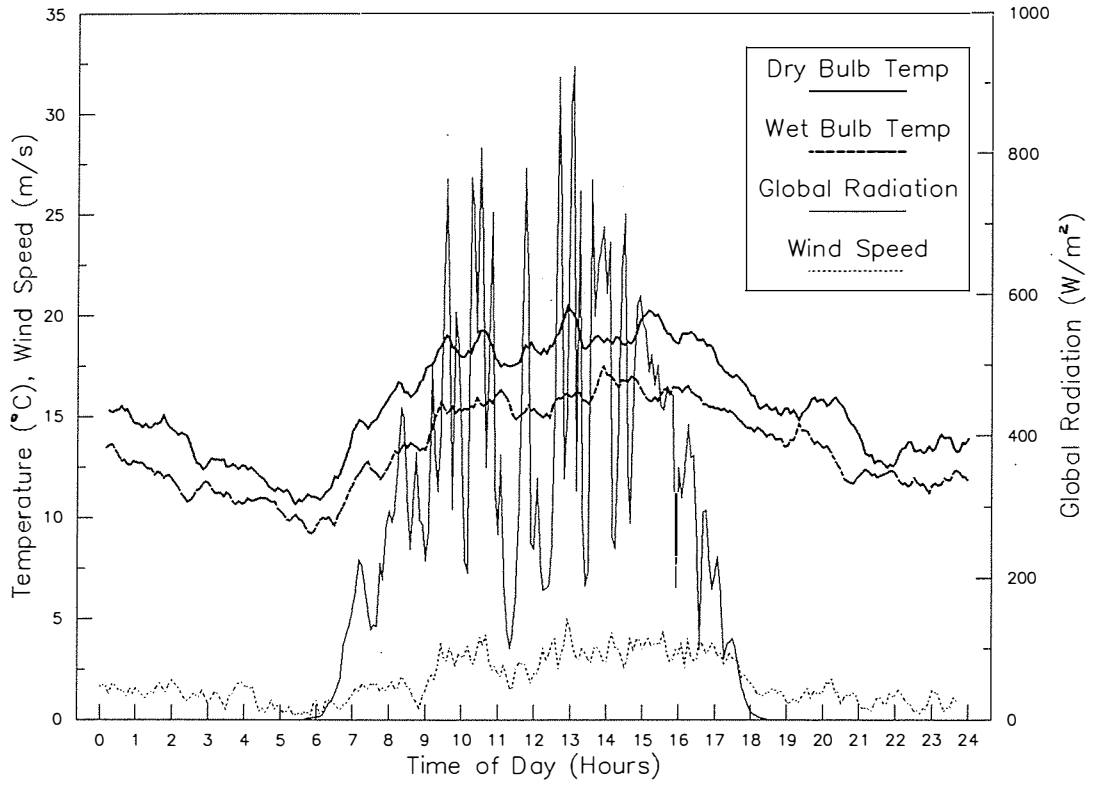

Figure 5.20. Prevailing Weather Conditions on 20/9/89.

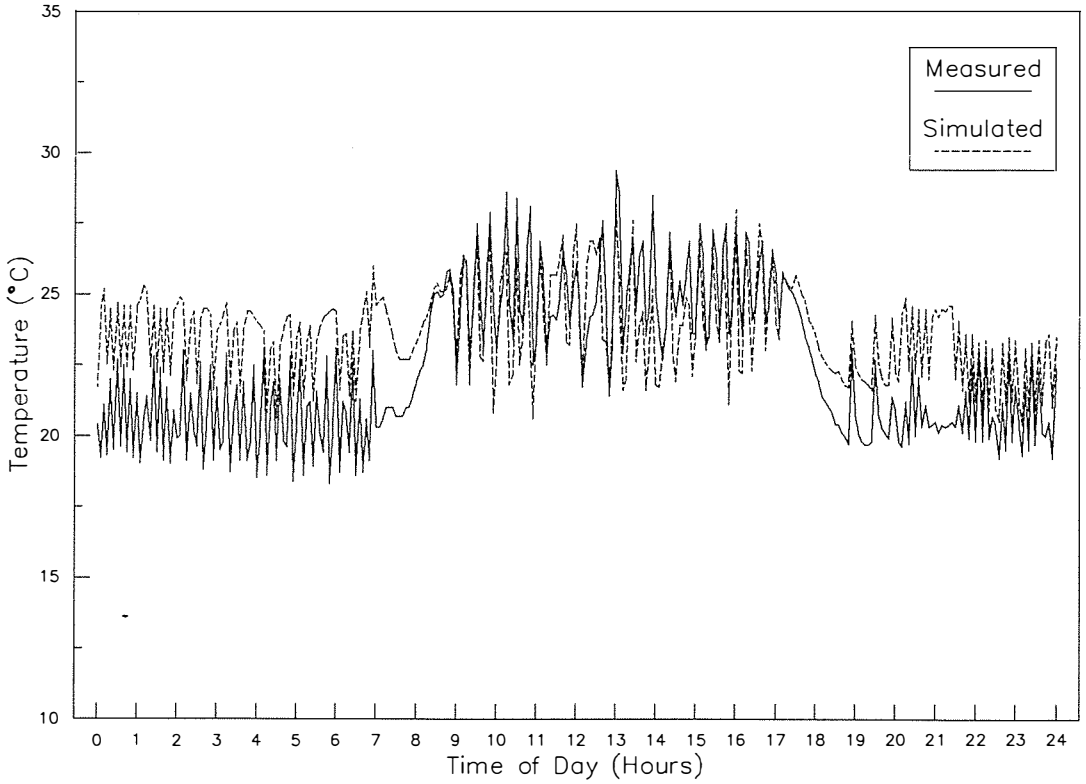

Figure 5.21. Measured and Simulated Air Temperature on 20/9/89.

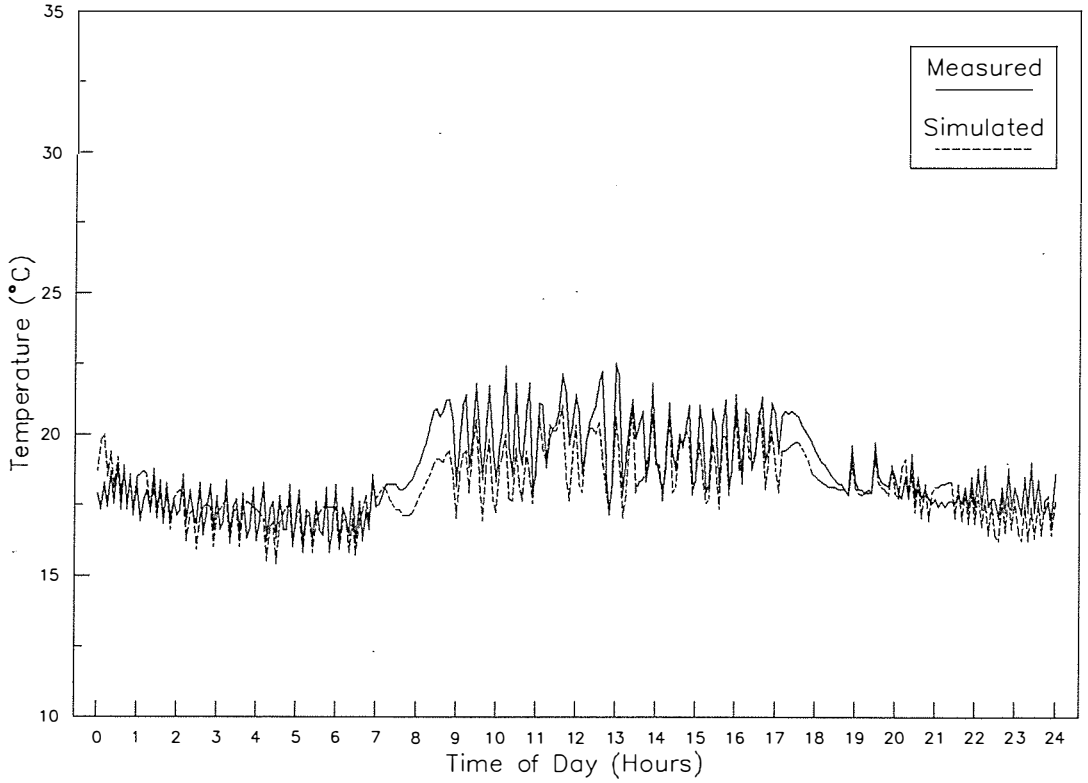

Figure 5.22. Measured and Simulated Wet Bulb Temperature on 20/9/89.

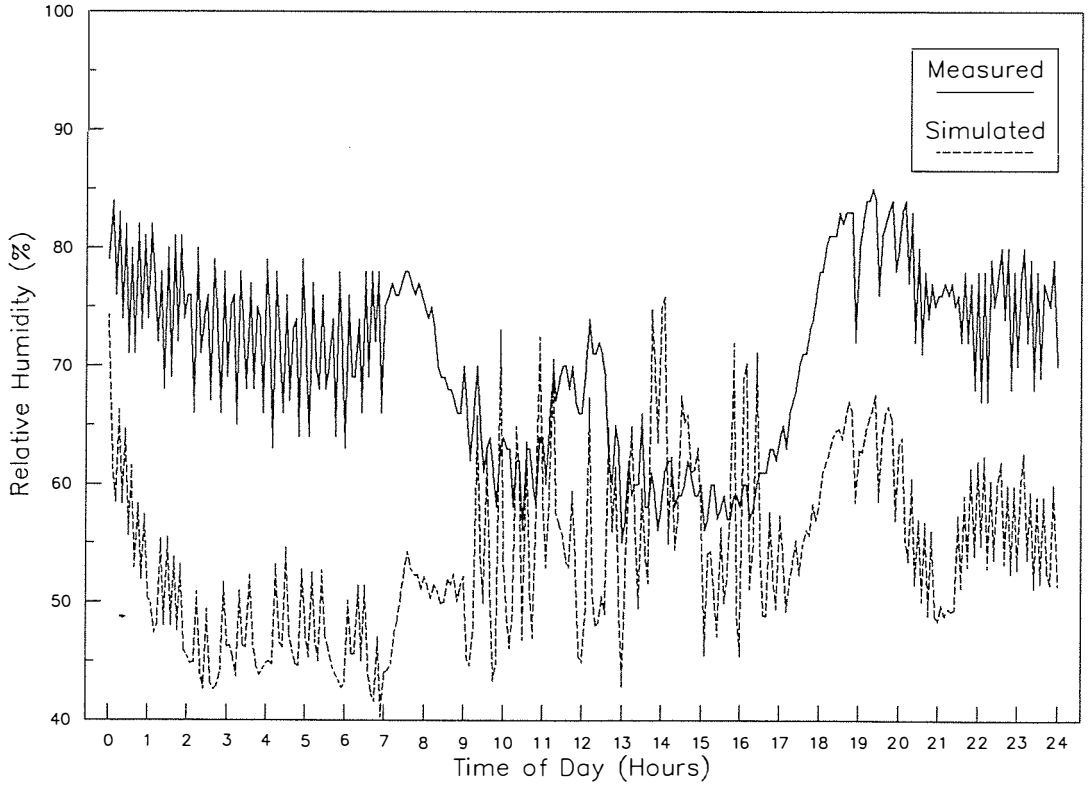

Figure 5.23. Measured and Simulated Relative Humidity on 20/9/89.

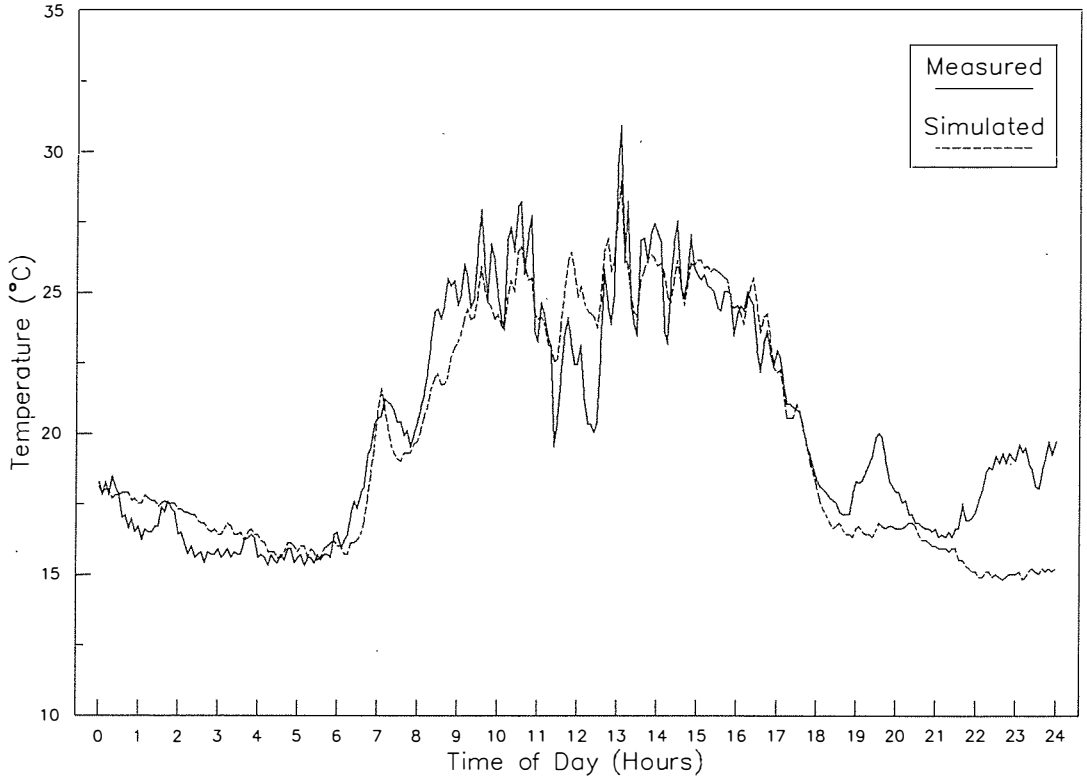

Figure 5.24. Measured and Simulated Glazing Temperature on 20/9/89.

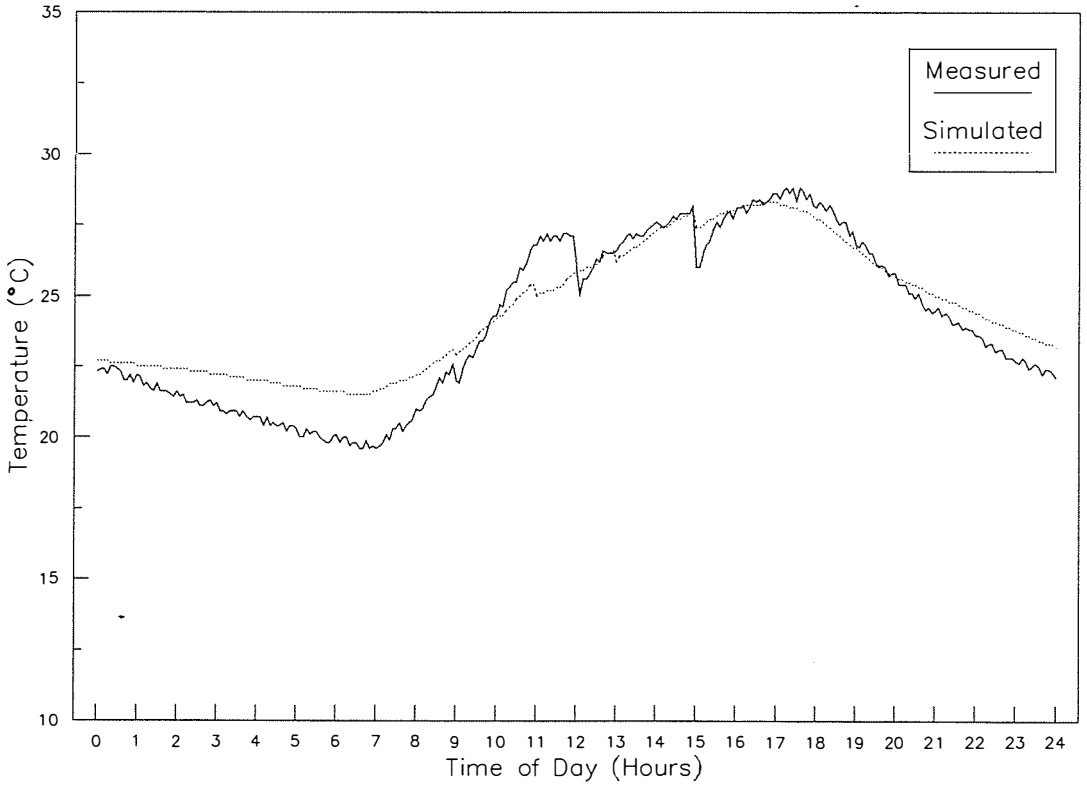

Figure 5.25. Measured and Simulated Root Medium Temperature on 20/9/89.

Due to the relatively low outside temperature the heating system operated for a large portion of the night time period. During this time the air temperature inside the greenhouse was over-predicted. Once again this suggests errors in the prediction of the heat transfer coefficients between the inside air and the glazing. During the day, passing clouds caused the solar radiation levels to vary widely. This caused the ventilation system to work hard to try and maintain the temperature. As a result the air temperature fluctuated considerably, but on the whole the model was capable of predicting these variations.

As a result of the low leaf area index at this time, most of the solar radiation entering the greenhouse would have been absorbed by the floor and the root medium. The consequence of this is that the root medium temperature cycle (Figure 5.25) had a slightly larger amplitude than for the previous sets of results. The model did not predict the low temperature point, just before sunrise, because of the over-prediction of air temperature. Also, at this time the crop watering was being hand operated, at irregular intervals. It can be seen that two watering events occurred at about 1200 hrs and 1500 hrs. It can be assumed that these were of quite long duration as the temperature of the root medium fell significantly. However, in the boundary input file for this period three regular watering times were assumed. The effect of these can be seen from the small perturbations in the simulated curves at 1100 hrs, 1300 hrs and 1500 hrs.

The prediction of internal relative humidity at night was once again rather poor due to the over-estimate of the air temperature.

Although some trends became obvious from running the model for selected days, no real indication was given of the long term performance of the simulations. However, this information became available when the model was modified to include the growing crop and simulations were performed over an extended period of the crop's life, from 20/9/89 to 15/12/89, when the last harvest was made (see Chapter 6 for more details).

5.6.2 Long Term Correlations

In order to test the fit of the model for air and leaf temperature over an extended simulation, the mean error, the RMS error, and the correlation coefficient between the measured and simulated states were calculated on a daily basis. Figure 5.26 shows the course of the mean daily error for the air temperature prediction. The RMS error, which gives an indication of variability between the signals, is shown in Figure 5.27. The correlation coefficient is plotted in Figure 5.28.

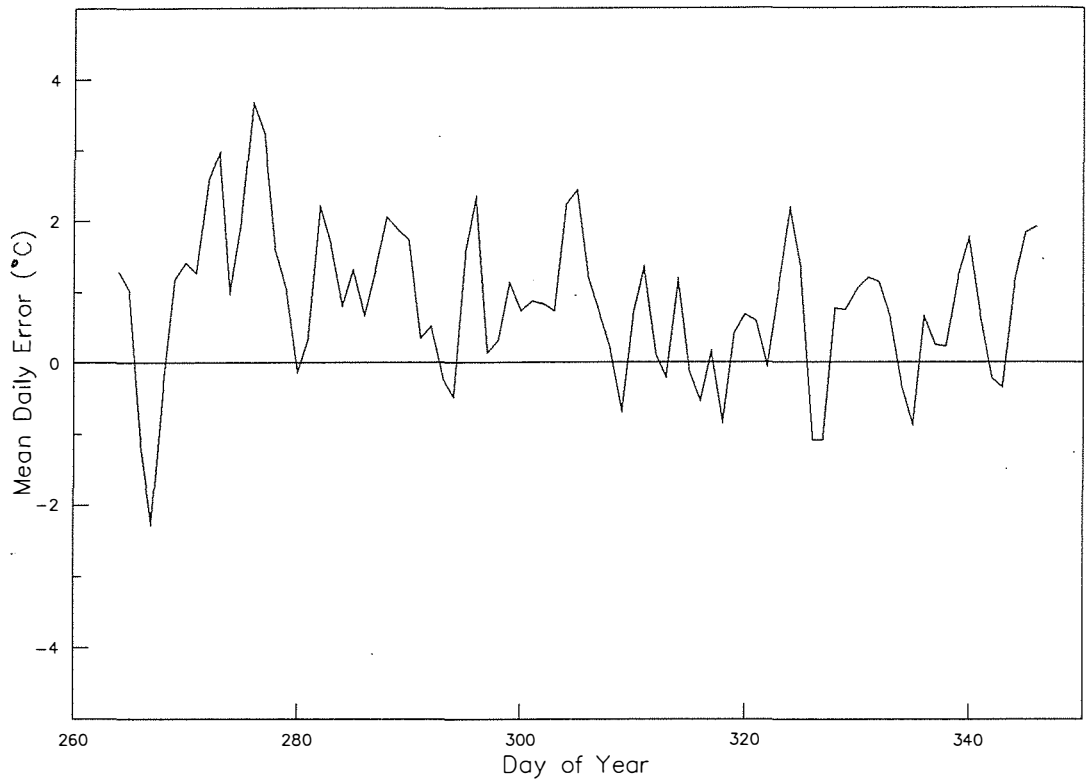

Figure 5.26. Daily Mean Error of Air Temperature Prediction for 1989 Season.

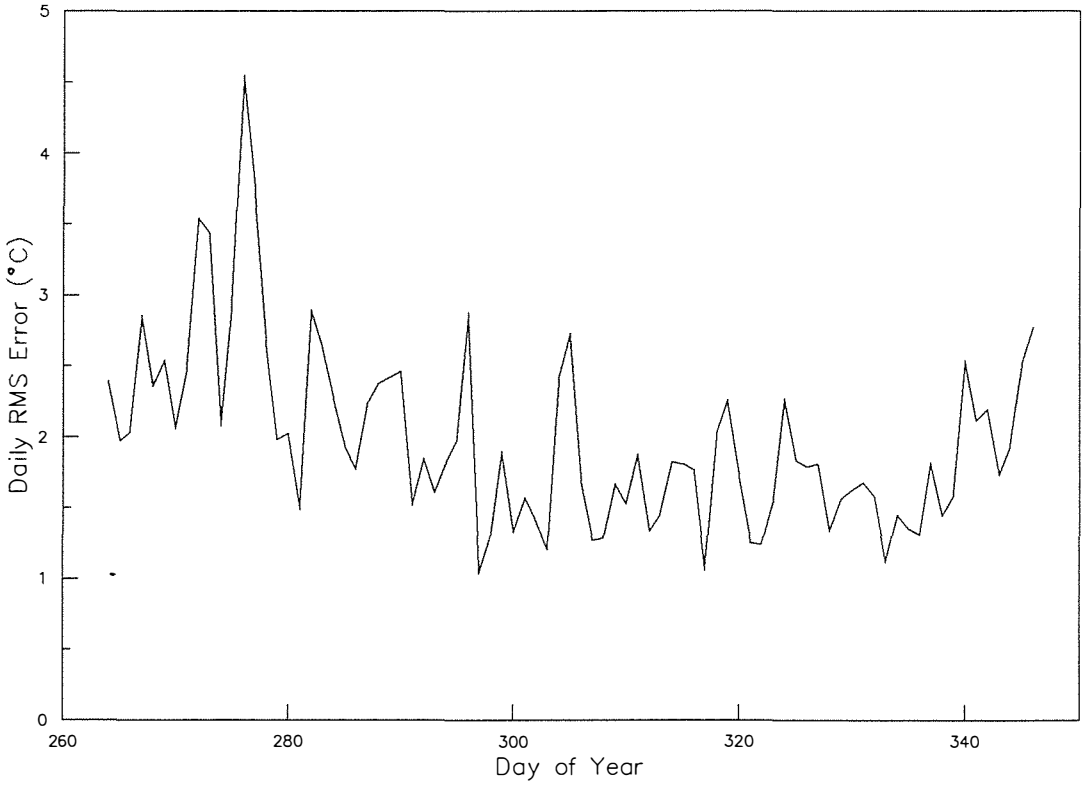

Figure 5.27. Daily RMS Error of Air Temperature Prediction for 1989 Season.

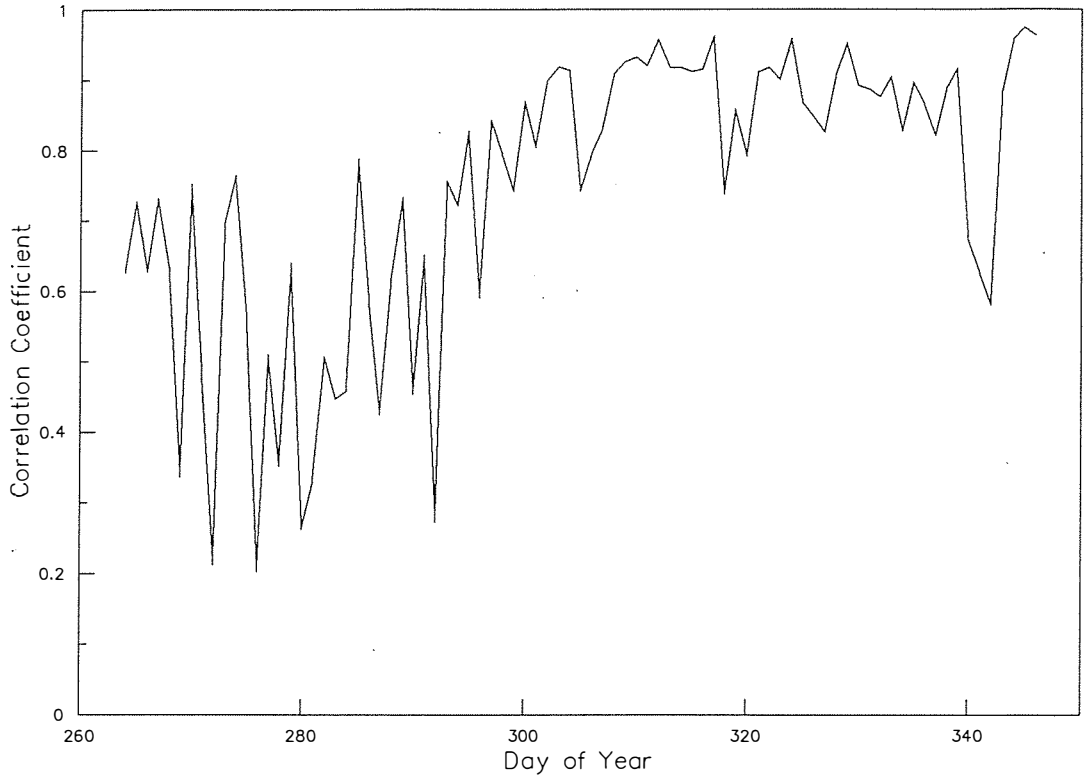

Figure 5.28. Daily Correlation Coefficient of Air Temperature Prediction for 1989 Season.

The long term correlations show that the accuracy of the air temperature prediction varied with time. Both the mean error, and the RMS error, and thus variance, improved as the experiment proceeded (Figures 5.26, 5.27 & 5.28). Early in the simulation run the air temperature was generally over-predicted at night and under-predicted during the day. This was most likely due to errors in predicting the internal glazing heat transfer coefficients. The improvement in the RMS error of air temperature prediction with time was due most likely to the increasing thermal capacity of the crop. This has a stabilizing effect on all temperatures within the system by absorbing a large part of the incoming solar radiation and converting it to latent rather than sensible heat. Thus temperature swings in the greenhouse are reduced.

The leaf temperature prediction was relatively more consistent with time (Figures 5.29, 5.30, & 5.31). The consistently high correlation coefficient was particularly pleasing to note. It should be noted that these results do not cover the early period of the crop when the plants were small. Since small leaves tend to have higher convective heat transfer coefficient than larger leaves it would be expected that the temperature of young plants would follow air temperature much more closely. Thus the poorer results obtained for air temperature, in the early phase, would probably have occurred for the crop.

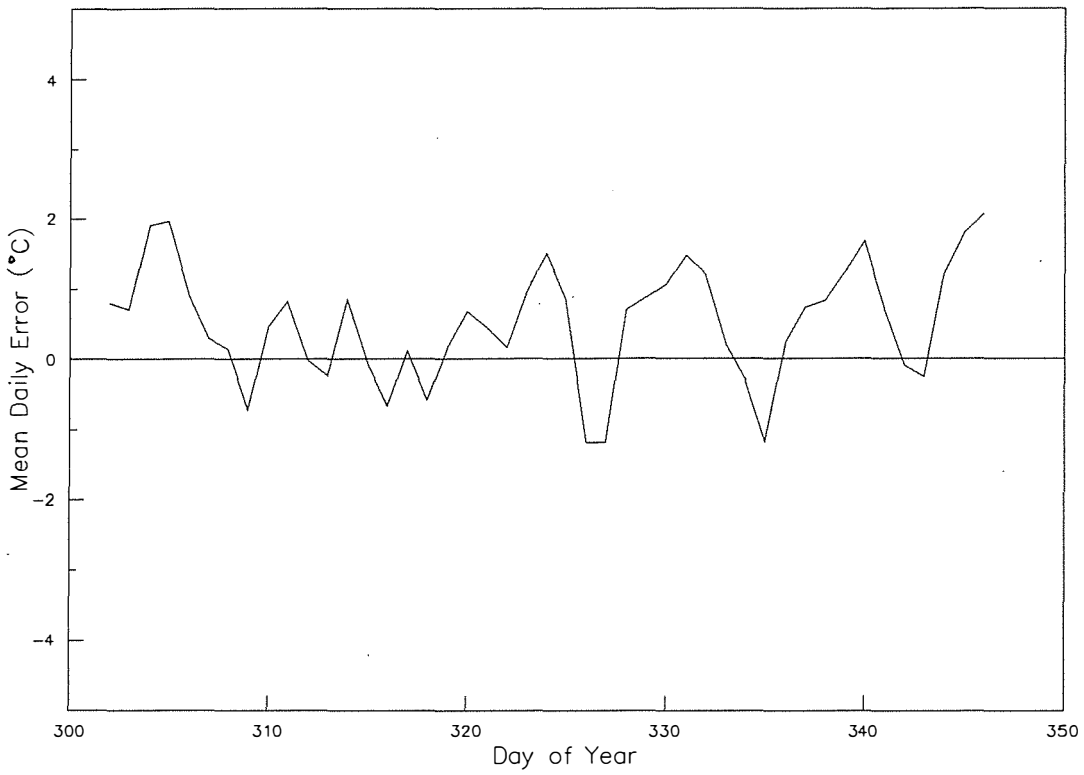

Figure 5.29. Daily Mean Error of Leaf Temperature Prediction for 1989 Season.

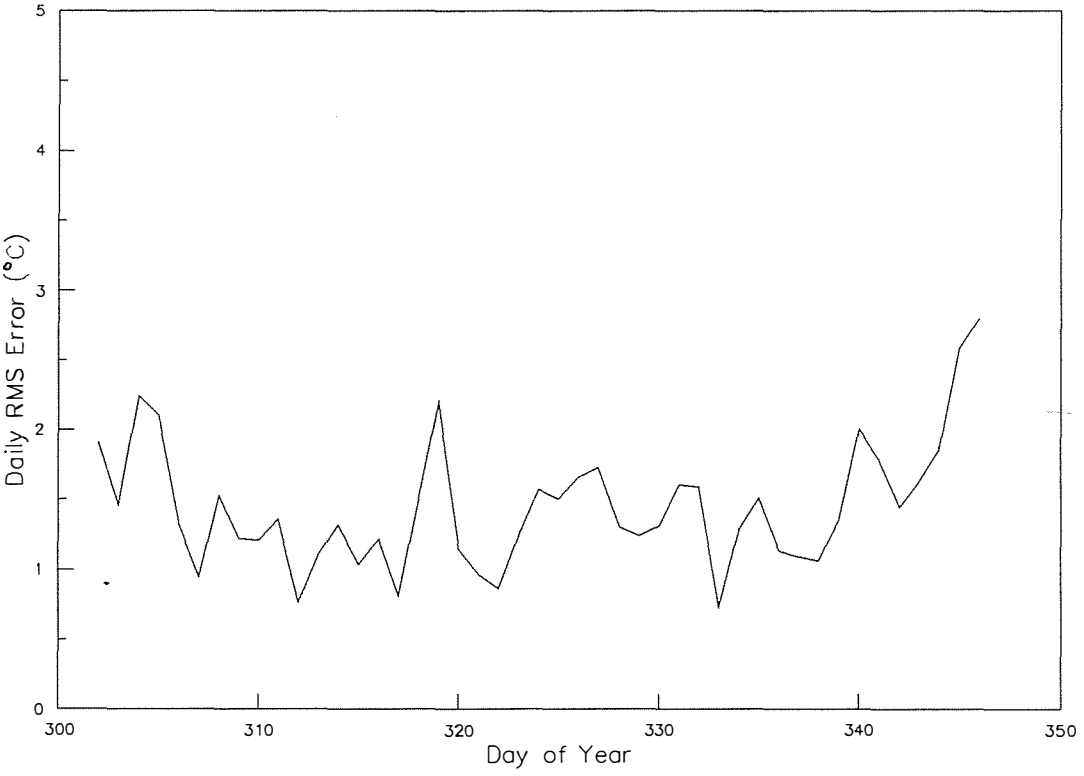

Figure 5.30. Daily RMS Error of Leaf Temperature Prediction for 1989 Season.

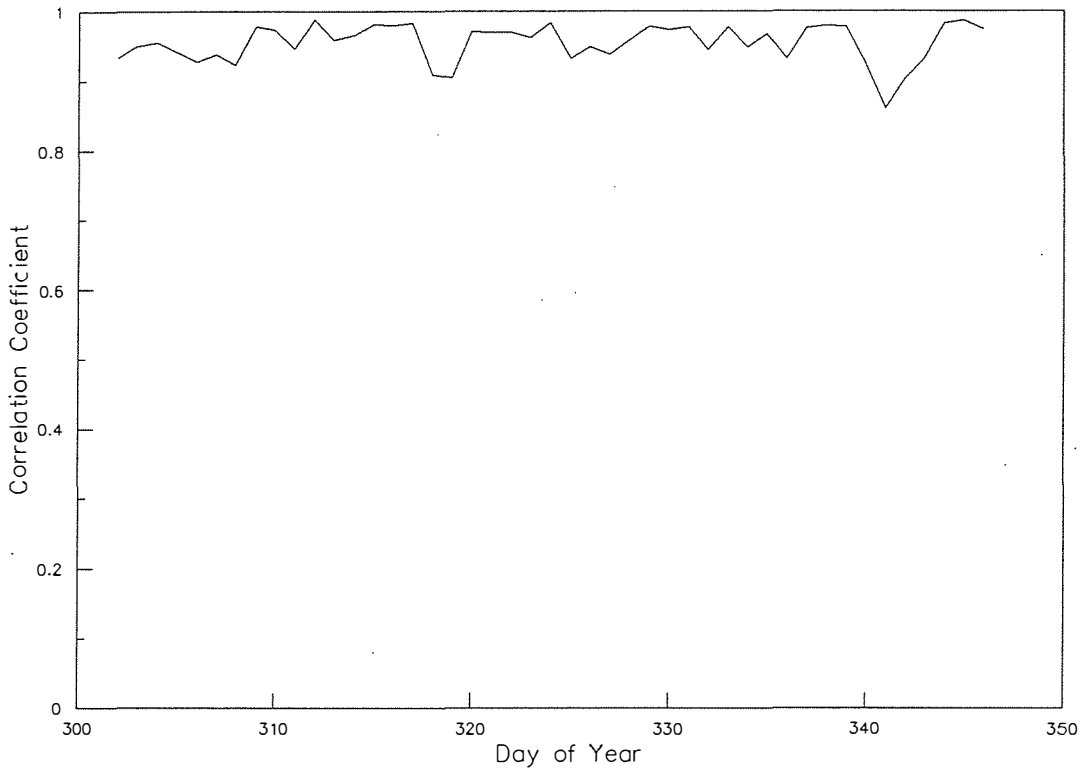

Figure 5.31. Daily Correlation Coefficient of Leaf Temperature Prediction for 1989 Season.

5.7 DISCUSSION

After reviewing the large amount of literature on greenhouse modelling it was decided that a new model would be developed. The rationale for this revolved around the fact that only 5 out of the approximately 70 models reviewed incorporated the carbon dioxide balance of the greenhouse air space, or made any attempt to simulate the long term development and growth of a crop in response to the greenhouse environment. Furthermore, it was discovered from the literature that many modellers had made simplifications without justifying them. For instance, only the work of Glaub & Trezek (1981a) rigorously considered the effect of water vapour on the enthalpy of the greenhouse air.

An omission in all the models reviewed was the independent treatment of the greenhouse structure. In a conventional glasshouse the surface area and light interception of the structure is significant, but its temperature will not be the same as the glazing, because it is not in direct thermal contact with the outside air. Furthermore, due to the relatively low thermal capacity of the structure compared to the glazing it temperature will rise much faster. During preliminary work, a model was developed in which the thermal mass, and light interception, of the structural components was combined with the glazing. This model was not capable of simulating the rise in air temperature of an empty greenhouse during the

day. The main reason for this was that a large portion of the solar radiation absorbed by the structure was not allowed to transfer to the greenhouse air. This was due to the temperature of the structural mass being at the same temperature as the glazing, which is generally lower than inside air temperature due to the influence of the colder outside air. Therefore, in this trial model, a disproportionate amount of solar radiation was lost to the outside, resulting in low inside air temperatures.

When the structure was treated independently to the glazing system the situation was very different. Since the thermal communication between the structure and glazing bars was fairly low, and the structure absorbed a significant fraction of the radiation (44% of all radiation absorbed by the glazing & structure) the structure temperature was generally higher than inside air temperature during the day. The simulations showed that during the night the temperature of the structure would be a few degrees below the inside air temperature, which was held at around 18°C by the heating system, but that after sunrise the temperature of the structure would rapidly rise to around 35°C, under clear sky conditions. Therefore, the structure added a significant amount of sensible heat to the greenhouse airspace. The only other way to get a realistic simulation of air temperature was to assume that the air absorbed about 20% of the incoming radiation directly. This, of course, is physically impossible because the extinction coefficient of air is only about 0.01 km^{-1}. Thus the absorption of a 3 m depth of air would only be about 0.003%. From this it can be assumed that previous authors have either had to apply arbitrary correction factors, or have not tested their models on empty uncontrolled houses. Therefore models which do not treat the structure separately to the greenhouse will give an inaccurate picture of the overall energy balance of the structure, and may well give erroneous results under conditions of high solar radiation and low outside temperature.

The greenhouse simulation model finally developed was very complex, even though simplifying assumptions were made to avoid simulating the water contents of the floor and soil layers, which where found to be fairly constant. The states of the greenhouse were described by 16 differential equations (11 enthalpy balances, 4 water balances, and 1 carbon dioxide balance). In total 45 heat fluxes were considered, solar radiation absorbed at 5 surfaces, 8 convective heat transfers, 8 conductive heat transfers, 19 radiative transfers, 3 evaporative transfers, and 5 advective transfers. Eight water fluxes were included, 4 in the vapour phase and 4 in the liquid phase. In addition four carbon dioxide fluxes, were included to simulate the carbon dioxide concentration of the inside air. These fluxes in turn were determined from approximately 130 ancillary equations involving an even larger number of parameters.

As a consequence of the complexity of the model, it was not possible to investigate the effect of all possible parameters, within the time frame available for the study. However, it was pleasing to be able to develop a model which simulated temperatures to within a few degrees without having to assume values for many parameters. Wherever possible the parameters were derived from standard data, or calculated from a knowledge of the physical system. This led to a model with a reasonably high degree of generality, which could be used, with caution, to simulate the performance of other greenhouses.

The main areas where significant parameters had to be estimated for the particular greenhouse were the ventilation rate, and the calibration factors for the light transmission model. It was also necessary to develop an empirical model for the stomatal functioning of the cucumber crop. However, beside these limitations, there is some confidence that the resulting model is reasonably general. Since the necessity for calibration factors for the light transmission model results from the model's inability to deal completely with interception by structural components, and loss of light due to dust, it is predicted that a range of calibration factors could be derived for particular types of greenhouses, given sufficient measurements. Hence, when running the environmental simulation model it would only be necessary to supply the appropriate calibration factors for the type of greenhouse being studied.

Estimation of natural ventilation rates would remain a problem unless a predictive sub-model was to be introduced. For a fan ventilated greenhouse this would not be problem as in this case the air change rate could be accurately predicted from fan performance data.

5.8 SUMMARY

In this chapter a dynamic model to simulate the state of the greenhouse environment in response to varying boundary conditions has been presented. The review of the literature (section 5.1) revealed that nearly 70 different greenhouse models have been reported on in the last 25 years. Simulation models have tended to become more complex during that time. However, of all these models only five attempted to incorporate the carbon dioxide balance of the greenhouse, or simulate the concurrent growth of the crop.

In section 5.2 the requirements of the model to meet the aims of the project have been outlined. Due to the requirements for a dynamic model incorporating the crop responses on both short and longer time scales, it was decided to develop a new model, but to build on existing work.

The energy and mass balances describing the rate of change of enthalpy and mass in the greenhouse environment have been developed in section 5.3 after considering the underlying physical principles of the greenhouse environment. This resulted in a system of differential and ancillary algebraic equations which have been solved to reveal the time course of the greenhouse environment, in response to varying boundary conditions (the outside weather). Due to the complexity of the model there were many parameters in the ancillary algebraic equations. The determination of these parameters has been described in section 5.4.

The model has been implemented on a personal computer using the simulation language ESL. Sample results of these simulation runs have been presented in section 5.6.1, for a greenhouse with a static crop. In general the results of the simulation fitted the measured greenhouse environmental states well, although there were some areas of weakness, particularly in the prediction of relative humidity and carbon dioxide concentration at night. In section 5.6.2 long term correlations between the simulated and measured states have been presented, for a version of the model which included the dynamic crop growth model which is described in Chapter 6.

6 THE CROP MODEL

Modelling crop growth and development is a relatively new aspect of the biological sciences. A search of the literature reveals that the majority of crop modelling work has occurred in the last twenty years, and predominantly in the last ten. As with greenhouse simulation models the main reason for the increasing popularity of crop modelling would appear to be the availability of computing equipment of the right power and price to enable such models to be implemented as management tools and not simply as academic curiosities.

In this chapter existing crop models are reviewed briefly followed by the development of a cucumber crop simulation model.

6.1 SHORT REVIEW OF EXISTING CROP MODELS

Many existing crop models have been reviewed by Joyce and Kickett (1987) as part of a major review of plant growth modelling edited by Wisiol & Hesketh (1987). This follows an earlier review of modelling of photosynthesis edited by Hesketh and Jones (1980). Of the models reviewed by Joyce and Kickett (1987), 20 were grazing-land models, 15 were for forestry species, and 38 were for single-crop species (17 species). However, of these models only three were for greenhouse crops. One model simulated tomato yield (Cooper & Fuller, 1983,) and the other two were for lettuce production (Sorbie & Curry, 1973, Sweeney et al, 1981).

To date the greatest efforts with crop simulation have been directed to economically significant arable species such as cotton (Baker et al 1983, Jackson & Arkin, 1984a), maize (Jones & Kiniry, 1986, Stapper & Arkin, 1980, Wright & Keener, 1982, Jackson & Arkin, 1984b, Shaffer et al, 1984), potatoes (Ingram & McCloud, 1984, Ng & Loomis, 1984), rice (van Ittersum, 1972), sorghum (Arkin et al, 1976, Vanderlip & Arkin, 1977, Maas & Arkin, 1978, Maas & Arkin, 1980a), soybean (Acock et al 1985, Meyer et al, 1979, Meyer et al 1980, Wilkerson et al 1983), and wheat (Baker et al 1981, Maas & Arkin, 1980b, van Keulen et al, 1982). A feature of all these models, with the notable exception of those for soybean, is that they are all for annual determinate crops, and therefore do not address some of the important aspects of modelling indeterminate greenhouse crops such as tomatoes and cucumber. A determinate plant is one in which each stem, or tiller, will eventually terminate with a reproductive organ (flower/fruit) (e.g. wheat). An indeterminate plant, on the other hand, is one in which each stem will continue to grow indefinitely, and produce new vegetative organs (leaves) at successive nodes (e.g. cucumber). Reproductive organs will form at some or all nodes depending on the particular plant.

More recently models for greenhouse vegetable crop production have been developed, mainly in Northern Europe. Species modelled include cucumbers (Augustin, 1984, Schapendonk & Gaastra, 1984a, 1984b, Liebig, 1989b), kohlrabi, lettuce, radish, and tomatoes (Jones et al, 1989a, 1989b, Biemond, 1989b). Amongst these models the two distinct approaches of empirical and analytical modelling can be observed.

6.1.1 Empirical Models of Greenhouse Crops

The models developed by the Institute of Greenhouse Vegetable Crops, at the University of Hannover, are a good example of the empirical model type. By performing successive trials under controlled environment conditions, statistical models of crop production have been developed, for radish, lettuce, kohlrabi, cucumber, and tomato (Krug & Liebig, 1988, Liebig, 1989a). Non-linear regression functions, with multiplicative terms were fitted to the data, to find mean growth rates, and thereby growth periods, as a function of environmental conditions. To achieve this the life cycle of the crop was divided into physiologically meaningful stages, (e.g. sowing to emergence, emergence to start of tuberization, etc) (Krug, 1985). These models have proved useful in greenhouse production planning, as a major emphasis in the modelling process was predicting the effect of environment on the timing of crop development processes, as well as overall yields. This has led to the conception, by the Hannover group, of bio-economic models, as tools for greenhouse management (Bögemann, 1984, Biemond, 1989a, 1989b, Liebig, 1989a, Krug, 1989). However, these models make no attempt to predict the actual course of growth and development of the crop. Also, because of the high level of abstraction involved, the models could not safely be extrapolated to conditions beyond those under which they were developed.

6.1.2 Analytical Models of Greenhouse Crops

Analytical modelling of greenhouse crop production, at various levels of abstraction, has been centred on the Agricultural University of The Netherlands. Starting with the pioneering work of de Wit et al (1970) various researchers have developed increasingly more sophisticated models of crop growth. The predominant approach has been to study specific aspects of plant physiology such as photosynthesis, respiration, and transpiration, as distinct sub-systems. As well as the processes just listed, which all have short term responses to changes in the greenhouse environment, there are processes, such as partitioning of assimilate, and morphological changes, such as organogenesis and leaf expansion, which respond over the medium term and long term, (that is hours and days).

Analytical models, based on the most up-to-date physiological research, have been used to increase the quantitative knowledge of the processes involved in the plant and how they interact with each other, and the environment. These sub-models have been integrated into crop models capable of predicting the time course of plant growth and development (Penning de Vries & van Laar, 1982, Spitters et al, 1988, Penning de Vries et al, 1989, Jones et al, 1989).

The usefulness of these models for the greenhouse engineer is that they predict the response of the plant to environmental changes in the short term, and therefore give an understanding of the feed-back processes connecting the plant and the environment. Additionally analytical models predict the long term effect of particular environmental control strategies on the crop yield. A crop simulation model of this type used in conjunction with a greenhouse environment simulation model and modern optimization techniques, would allow the selection of optimal control trajectories for the greenhouse environment, based on prevailing weather conditions, costs, expected market prices, and the state of the crop (Enoch, 1978a, 1978b, Seginer, 1980).

Models of the photosynthetic sub-system have been developed and tested for several greenhouse crops (Schapendonk & Brouwer, 1985, Nederhoff et al, 1988, Gijzen and ten Cate, 1988, Nederhoff et al, 1989, Marcelis, 1989), based on models previously developed for field crops (de Wit et al, 1970, Goudriaan, 1982). Similar models for photosynthetic production have been reported by Enoch & Sacks (1978), Acock et al (1978), and Oikawa (1986).

Models of maintenance and growth respiration of greenhouse crops have been presented by Schapendonk and Challa (1980), and Schapendonk, (1984). Other relevant work on respiration is that of Penning de Vries & van Laar, (1982), and Gent & Enoch, (1983).

Partitioning of assimilates between the different organs of a crop is a major factor affecting the final yield of crops. This is particularly true for indeterminate crops such as cucumbers and tomatoes where the partitioning of dry matter growth is dynamic, and depends in part on the relative sink strengths of the organs present. Models of partitioning of assimilate have been developed for cucumber by Schapendonk and Brouwer (1984), Marcelis et al (1989) and Heuvelink and Marcelis (1989).

The water relations of greenhouse crops were studied by Behboudian (1977), and transpiration in response to greenhouse environment has been modelled in detail by Stanghellini (1987). Bruggink et al (1988) and Marcelis (1989) modelled plant water potential in relation to plant water uptake and transpiration losses. The response of stomata to environmental conditions

and plant water status have also been studied using a number of models (Penning de Vries, 1972, Takakura et al, 1975, Bell, 1982, Avissar et al, 1985, Tantau, 1987).

6.2 A CROP MODEL FOR GREENHOUSE CUCUMBER

The basic outline of the cucumber crop simulation model is shown schematically in Figure 6.1. Inputs to the model are the levels of radiation, temperature, humidity, and carbon dioxide in the aerial environment of the crop, and the root environment water status. The model can be divided into six sub-models, namely plant development, photosynthesis, respiration, assimilate reserve, partitioning and growth, and transpiration.

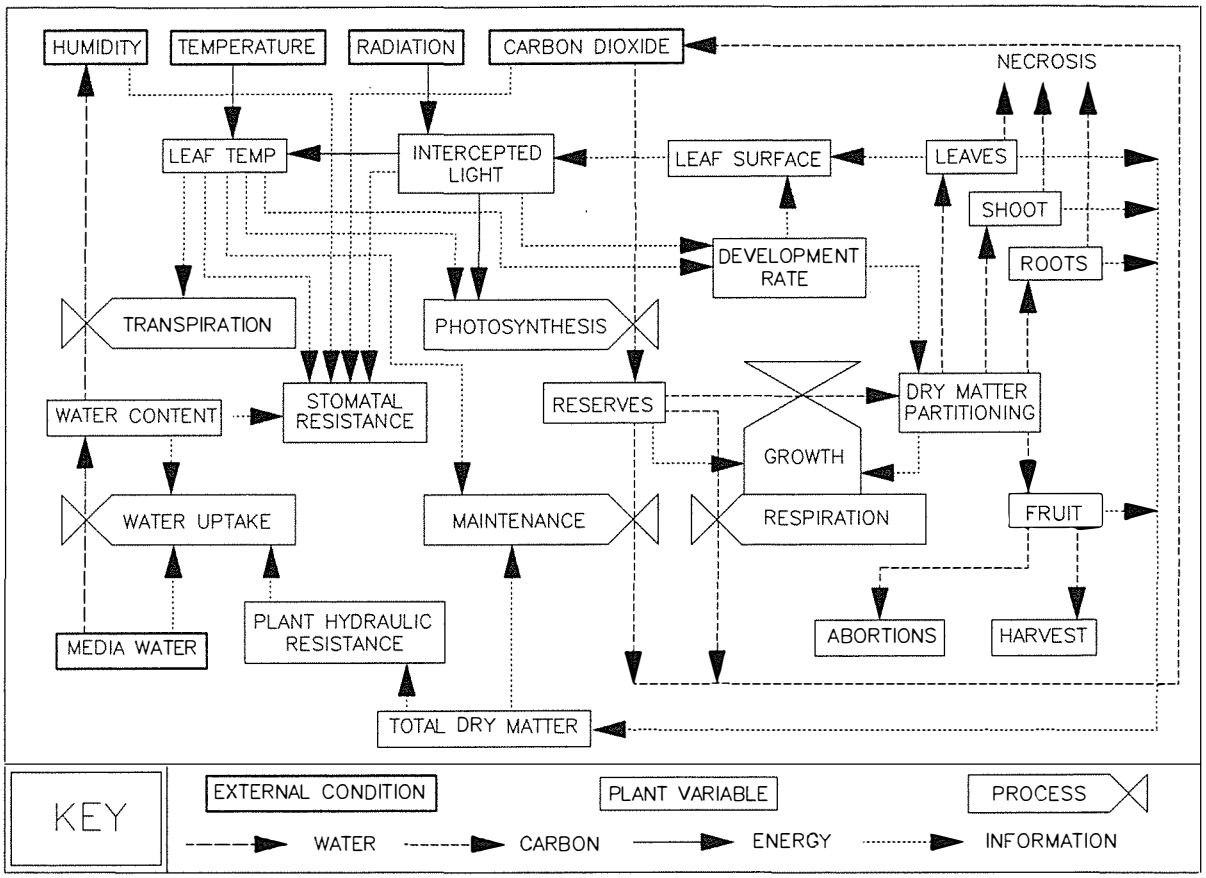

Figure 6.1. Schematic of a Crop Model for Greenhouse Cucumber

The developmental rate of the crop refers to the rate of production of new nodes, and hence leaves, fruit, and possible lateral growths (tillers). This is developed in more detail in section 6.2.1.

The photosynthetic apparatus converts carbon dioxide to carbohydrate reserves. Photosynthesis is governed by the carbon dioxide gradient existing between the air and leaf, the amount of available photosynthetically active radiation (PAR), leaf temperature, leaf boundary

layer and stomatal resistance, and the availability of photosynthetic sites (leaf area and nutrition). Since photosynthesis is strongly influenced by stomatal resistance, this process is closely coupled to transpiration. Radiation absorption of the crop canopy is discussed in section 6.2.2, and photosynthesis in section 6.2.3.

Carbohydrate reserves are initially held in the leaves as sugars, or are converted to starch, which is also held in leaves. Some of these reserves are used for maintenance respiration, which is a function of total dry matter and plant temperature. Remaining reserves are available for growth processes, the formation of structural carbohydrates and lipids, and in association with nitrogen, proteins and organic acids, at various points within the plant. All these growth processes require energy, both to transport the sugar and amino-acid building blocks in the phloem system, and to synthesize the final products. The energy consumed in these processes is commonly referred to as growth respiration. Maintenance and growth respiration combine to reduce the efficiency of the plant as a converter of carbon dioxide to useful dry matter. The sub-models for maintenance and growth respiration are developed in section 6.2.4. The assimilate reserve balance in discussed in section 6.2.5.

Growth of the plant occurs as a result of reserve carbohydrates translocating to other organs within the plant and synthesizing with nitrogen and other minerals to form new plant dry matter. Partitioning of the assimilate between all the organs on a plant is primarily governed by the availability of reserve assimilates from the photosynthetic sources (leaves) compared to the relative strengths of individual growth organs (including leaves), to attract assimilates. This is discussed in more detail in section 6.2.6, where a sub-model for growth is described.

The flow of water through the plant is governed by the water potential difference which exists between the root media and the greenhouse air. Within this, two major mechanisms can be identified. Firstly, the water uptake rate is governed by the water potential difference between the root media and the plant, and the hydraulic resistance of the xylem system, and the root epidermis. Secondly, the transpiration rate is governed by the vapour pressure difference between the leaf and the air, and the internal resistance of the leaves. The saturation vapour pressure of the leaf is a function of leaf temperature. The vapour pressure of the air is a function of air temperature and absolute humidity. Stomatal resistance is affected by the water content of the plant as well as vapour pressure deficit, leaf temperature, radiation and carbon dioxide concentration. This aspect of the plant model was developed in Chapter 5, due to the close coupling between the plant and the environment, at this level (see also Appendix 2).

6.2.1 Development of the Plant and Expansion of the Leaf Surface

An important part of any crop model which is to be used for predictive purposes is the simulation of the time course of leaf canopy expansion and architecture since this is a governing factor in light interception (see section 6.2.2). Plant canopy growth, form and function has been reviewed recently by Russell et al (1989). Leaf area expansion of a whole plant is the result of two processes, leaf initiation and individual leaf growth.

From the literature it is possible to distinguish three major methods of determining leaf area expansion with increasing levels of abstraction, (Jones & Hesketh, 1980): models of cellular division, growth and differentiation (Thornley, 1976); models of individual leaf initiation and growth (Hackett, 1973, Horie et al 1979, Jones et al, 1989); and models of whole plant leaf expansion based on traditional growth analysis and degree-day methods. For studies where it is desirable to study the effect of variable environment on the plant the medium level of abstraction appears to be the best, since it avoids the problems of working with cellular models, and avoids the problem of extrapolating with empirical models of high abstraction level. For this study the model of Horie et al (1979) was adapted to fit measured data.

The expansion of the leaf surface of cucumbers has been studied extensively by several authors. The most useful information can be obtained from a series of papers from the University of Nottingham (Milthorpe, 1959, Newton, 1963, Milthorpe & Newton, 1963, Hopkinson, 1964, Wilson, 1966, Hopkinson, 1966). In these papers the effect of temperature, light intensity and duration, and other leaves, on the initiation, surface expansion, cell division and carbon economy of individual leaves and the whole plant were investigated. Based on this work, and other similar trials, Horie et al (1979) (also Horie, 1978) developed a model which described the development of individual leaves of a cucumber plant in the vegetative phase. They referred to this as a template, which by definition is a pattern for testing the accuracy of form.

A feature of this model was that the expansion of the leaf surface was treated independently of weight growth. This avoided the necessity to estimate the specific leaf area, or leaf thickness, which is known to be the result of complex environmental interactions.

Horie's model is based on the common observation that the relative growth rates of different plant dimensions at the same stage of growth are linearly related, and that as a consequence plant form is preserved despite overall differences in size or chemical composition. So called allometric relationships are often used to describe the form of a plant.

6.2.1.1 Allometric Relationships

For a leaf the characteristic dimensions are length and width. When length is measured from petiole to tip and width across the widest part, it is found that a constant allometric relationship exists. For the cultivar 'Spouro', Horie et al (1979) found that the area of the leaf was given by:

$$A = 0.75LW \tag{6.1}$$

and that the width, W, was related to length, L, by:

$$W = 1.18(L - 0.5) \tag{6.2}$$

Robbins and Pharr (1987) analysed the allometric relations of six fresh-market and nine pickling cultivars grown outside and 'Calypso', grown in a greenhouse, both in soil and in a hydroponic system. They presented a number of linear regression equations for area, based on linear combinations of length and width.

Although their results are similar to those obtained in this study, it is difficult to compare directly because their relationships all include a constant term. While this may lead to the best least squares fit, it means that the equations will not predict accurately the size of small leaves.

Robbins and Pharr (1987) state the no lack of fit problems were apparent from residual plots. However analysis of the data collected from a crop of 'Sandra' revealed significant lack of fit problems if a single regression was used to represent all leaf sizes. For this reason a separate relationship for small leaves was developed. A physical basis for the change point can be justified by the observation that small leaves below about 10 cm in length have a more oblong shape.

Regression analysis of measurements of leaves of 'Sandra' gave the following allometric relations:

$$W = 1.08L \tag{6.3}$$

with a regression coefficient of 0.80.

$$A = 52 + 0.74(LW - 100) \qquad LW > 100\text{cm}^2 \tag{6.4a}$$

and:

$$A = 0.52LW \qquad LW \leq 100\text{cm}^2 \tag{6.4b}$$

The regression coefficients for equations 6.4a and 6.4b were 0.92 and 0.96 respectively.

A similar tendency for younger leaves was observed by Heij and de Lint (1984) for 'Farbio'. They found relationships of, $A = 0.85L^2$, for larger leaves, and $A = 0.70L^2$ for smaller leaves, which are generally observed to be more oblong than larger leaves. They also observed that the first leaves on a stem tend to be rounder than later leaves, and may thus have slightly greater areas than that predicted by the foregoing relationships. However, since these leaves are smaller than average, and therefore form only a small portion of the total leaf area, any errors can be ignored. Observations confirm this phenomenon occurred with the leaves of 'Sandra' both on the main stem and on laterals.

6.2.1.2 Plastochron Index

The concept of plastochron index is useful to describe the development rate of plants. A plastochron is broadly defined as the time interval between corresponding developmental stages of successive leaves (or nodes) of a plant (Erickson & Michelini, 1957). Usually a reference length is chosen, which can be determined readily. When the length of the i-th leaf of the plant exactly equals the reference length then the plant is defined to be i plastochrons old. The plastochron index is defined in such a way as to provide a continuous indicator of the developmental stage of the plant in between the discrete plastochronic events.

For the purposes of this study the plastochron index, P, is as defined by Erickson and Michelini (1957).

$$P = i + \frac{\ln(L_i) - \ln(L_R)}{\ln(L_i) - \ln(L_{i+1})} \qquad (6.6a)$$

$$= i + \frac{\ln(L_i / L_R)}{\ln(L_i / L_{i+1})} \qquad (6.6b)$$

where i is the leaf number of the leaf which is just longer than the reference length L_R. L_i and L_{i+1} are the lengths of the i-th and i+1-th leaf respectively.

6.2.1.3 Leaf Production Rate

The rate of leaf initiation at the apex, q, has been found to be a function of light and temperature (Milthorpe, 1959, Newton, 1963, Schapendonk & Challa, 1980, Schapendonk et al, 1984), and of the mass of fruit present, and can be described by:

$$q = f(\overline{T}_c) f(\overline{S}_p) f(\text{fruit sinks}) \qquad (6.7)$$

where $\overline{T}_c$ is the average daily crop temperature and $\overline{S}_p$ is the average daily PAR intensity.

The relationships of Milthorpe (1959) and Newton (1963) were used for the developmental sub-model, as they predicted rates of leaf unfolding close to that observed for the trial crops.

The development rate, q, can also be expressed in terms of the plastochron index, by differentiation of equation 6.6. Thus:

$$q = \frac{dP}{dt} = \frac{\ln(L_i/L_{i+1})d\ln(L_i/L_R)/dt - \ln(L_i/L_R)d\ln(L_i/L_{i+1})/dt}{\ln^2(L_i/L_{i+1})} \quad (6.8a)$$

$$= \left[\frac{1}{\ln(L_i/L_{i+1})}\right]\left[\frac{d\ln(L_i)}{dt}\right] - \left[\frac{\ln(L_i/L_R)}{\ln^2(L_i/L_{i+1})}\right]\left[\frac{d\ln(L_i/L_{i+1})}{dt}\right] \quad (6.8b)$$

At the point where the length of the i-th leaf is equal to the reference length the last term of equation 6.8b is zero. Therefore at this point:

$$\frac{d\ln(L_i)}{dt} = \left(\frac{1}{L_i}\right)\left(\frac{dL_i}{dt}\right) \quad (6.9)$$

which is the relative length growth rate on a time basis, RGR_t. Thus:

$$q = \frac{RGR_t}{\ln(L_i/L_{n+1})} \quad (6.10)$$

The relative length growth rate on a plastochron basis is defined as:

$$RGR_p = \frac{d\ln(L_i)}{dP} \quad (6.11)$$

or

$$RGR_p = \frac{RGR_t}{q} \quad (6.12)$$

Equations 6.10 and 6.12 can be combined to give:

$$RGR_p = \ln(L_i/L_{i+1}) \quad (6.13)$$

Equation 6.13 is of great importance since it relates the time variable RGR_p to the position variable $\ln(L_i/L_{i+1})$.

Horie et al (1979) found that the leaf production rate, q, was also a function of plastochron age of the plant. In particular the rate of production was slightly slower than expected in young plants. This lag was modelled as an exponential decay. Thus:

$$q = \frac{dP}{dt} = (1 - \exp(-P/\theta_p))q_s \qquad \text{for } P > 1 \qquad (6.14)$$

where θ_p is the plastochron constant of adaptation (found to be 3 plastochrons for a reference length of 1 mm), and q_s is the stationary value of q as determined by the prevailing environment (Equation 6.7).

Equations 6.7 and 6.14 thus form the basis for determining the development of the plant. For the prevailing environmental conditions the stationary value of q is determined, the actual rate is then found from equation 6.14. When the differential equation (6.14) is integrated with respect to time the Plastochron Index, P, and hence the stage of development is obtained.

Equation 6.14 can be integrated analytically to find the Plastochron index, $P(t)$ after time t.

$$P(t) = \theta_p \ln\{\exp(q_s/\theta_p)[\exp(P(0)/\theta_p) - 1] + 1\} \qquad (6.15)$$

where $P(0)$ is the initial plastochron index at time zero.

6.2.1.4 Growth of Successive Leaves

It has been observed for many species that during the rapid growth phases linear relationships result when the logarithm of successive leaf lengths are plotted against leaf number (Figure 6.2). Based on this it is possible to identify three distinct phases of growth.

a) The primordial phase, from initiation within the apical bud to unfolding is characterised by this logarithmic relationship between successive leaves. During this phase the relative rate of cell division is equal to the relative length growth rate and is thus proportional to the leaf initiation rate. Unfolding occurs when the critical unfolding length is reached. This is a function of length number.

b) The expanding phase starts at leaf unfolding and is characterised by a change in the slope of the logarithmic relationship between successive leaf lengths. During this phase it appears that the relative rate of cell division is the same as that before unfolding but the fraction of dividing cells decreases. This decrease is related to light levels.

Higher light levels extend the period over which cell division continues and thus larger leaves result. The cessation of cell division heralds the end of the expanding phase.

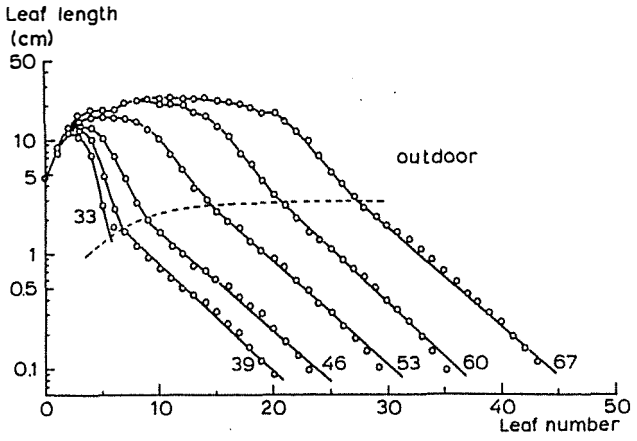

Figure 6.2. Leaf Pattern Curves for Leaf Length (from Horie et al, 1979).

c) The maturing phase occurs for a brief time after the expanding phase. Final leaf size is attained as the last cells expand to their final sizes (approximately four times the size of dividing cells (Milthorpe and Newton, 1963)). The final size of the cells is hardly affected by environment. Thus it is only cell number and hence the duration of the expanding phase which determines final leaf size.

Figure 6.3 shows a typical leaf length distribution curve for a plant at plastochron P. The slope of the straight segment of the curve from P to U (primordial phase) is a, and from U to M (expanding phase) is b. The vertical distance between this and the successive curve (at $P+1$) is the logarithm of length increase for each leaf.

For the primordial phase:

$$\ln(L_i) = \ln(L_R) + a(P-i) \qquad U \le i \le P \tag{6.16}$$

Now the relative length growth rate on a plastochron basis for the i-th leaf will be:

$$RGR_{pl} = \frac{d\ln(L_i)}{dP} = a + \frac{da}{dP}(P-i) \tag{6.17}$$

and the relative length growth rate of the i-th leaf on a time basis will be:

$$RGR_{ti} = q\left[\alpha + \frac{d\alpha}{dP}(P - i)\right] \qquad (6.18)$$

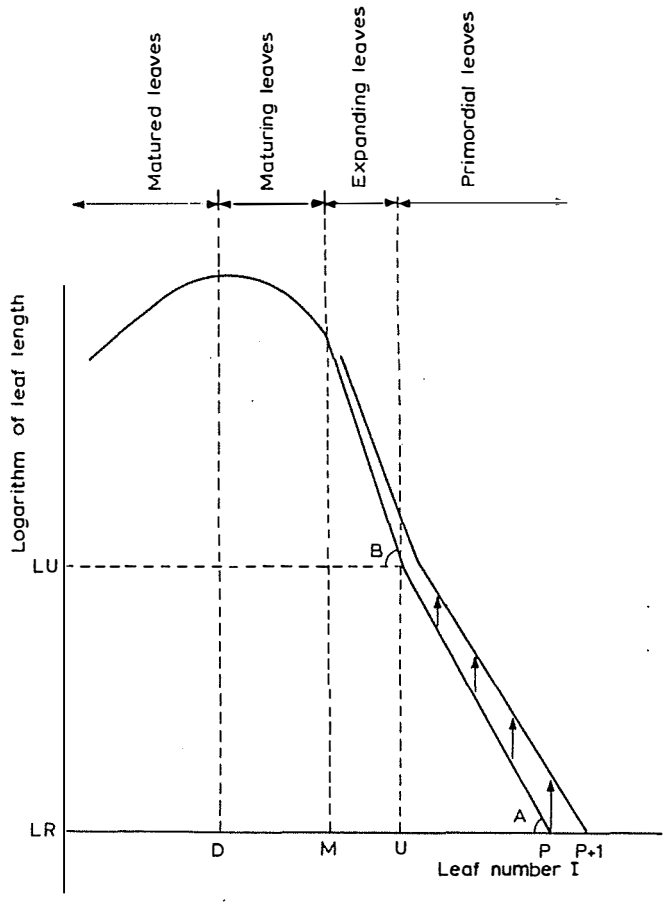

Figure 6.3. A Typical Leaf Pattern Curve (from Horie et al, 1979)

Now α is found be a decreasing exponential function of plastochron age, reaching a stationary value in old plants. Thus:

$$\alpha = \alpha_s + \alpha_d \exp(-P/\theta_a) \qquad (6.19)$$

where α_s is the stationary value of α, α_d is a delay variable, and θ_a is the exponential decay constant.

Similarly for the expanding phase :

$$\ln(L_i) = \ln(L_R) + a(P - U) + b(U - i) \qquad M \le i < U \qquad (6.20)$$

Now the relative length growth rate on a plastochron basis will be:

$$RGR_{pi} = a + \frac{da}{dP}(P-U) + \frac{db}{dP}(U-i) + \frac{dU}{dP}(b-a) \qquad (6.21)$$

and the relative length growth rate on a time basis will be:

$$RGR_{ti} = q\left[a + \frac{da}{dP}(P-U) + \frac{db}{dP}(U-i) + \frac{dU}{dP}(b-a) \right] \qquad (6.22)$$

As with a so also b is found to decrease exponentially with plastochron age of the plant. Thus:

$$b = b_s + b_d \exp(-P/\theta_b) \qquad (6.23)$$

The number of the leaf which is at unfolding U can be found by setting i equal to U and rearranging equation 6.16. Now:

$$U = P - \frac{\ln(L_U/L_R)}{a} \qquad (6.24)$$

The value of $\ln(L_U/L_R)$ is also found to be a function of plastochron age.

$$\ln(L_U/L_R) = c = c_s - c_d \exp(-P/\theta_c) \qquad (6.25)$$

Thus U is found from P by:

$$U = P - \frac{c_s - c_d \exp(-P/\theta_c)}{a_s + a_d \exp(-P/\theta_a)} \qquad (6.26)$$

Horie et al (1979) have estimated the parameters to be:

$a_s = 0.22$	$a_d = 1.17$	$\theta_a = 5.7$
$b_s = 0.34$	$b_d = 2.07$	$\theta_b = 8.0$
$c_s = 3.30$	$c_d = 3.30$	$\theta_c = 10.0$

Since the relative rates of cell division and length growth are equal in the primordial phase then c is also the logarithm of the ratio of the number of cells at unfolding to the number of cells present at the reference length.

Under constant environmental conditions the fraction of dividing cells, F, decreases linearly with time. Therefore:

$$F = 1 \qquad U - i \leq 0 \qquad (6.27a)$$

$$F = 1 - \frac{(U-i)}{n} \qquad 0 < U - i \leq n \qquad (6.27b)$$

$$F = 0 \qquad n < U - i \qquad (6.27c)$$

where n, the time span of linear decrease, is expressed as a number of leaves or plastochrons. The value of n is equal to the number of leaves immediately below the unfolding leaf in which cell division is decreasing.

Under variable light conditions the fraction of dividing cells, F, decreases at a variable rate given by:

$$\frac{dF}{dU} = -\frac{1}{n} \qquad (6.28)$$

This can be expressed on a plastochron basis as:

$$\frac{dF}{dP} = -\left(\frac{1}{n}\right)\frac{dU}{dP} \qquad (6.29)$$

or on a time basis:

$$\frac{dF}{dt} = -\left(\frac{q}{n}\right)\frac{dU}{dP} \qquad (6.30)$$

The time course of F can be found by integration of dF/dt.

Horie et al (1979) have determined the relationship between n, light levels, and the number of the unfolding leaf.

$$n = \mathrm{f}(i)(2.9 + 0.49\overline{S}_p) \qquad (6.31)$$

Values of $\mathrm{f}(i)$ plotted against leaf number are shown in Figure 6.4, for the main stem and laterals.

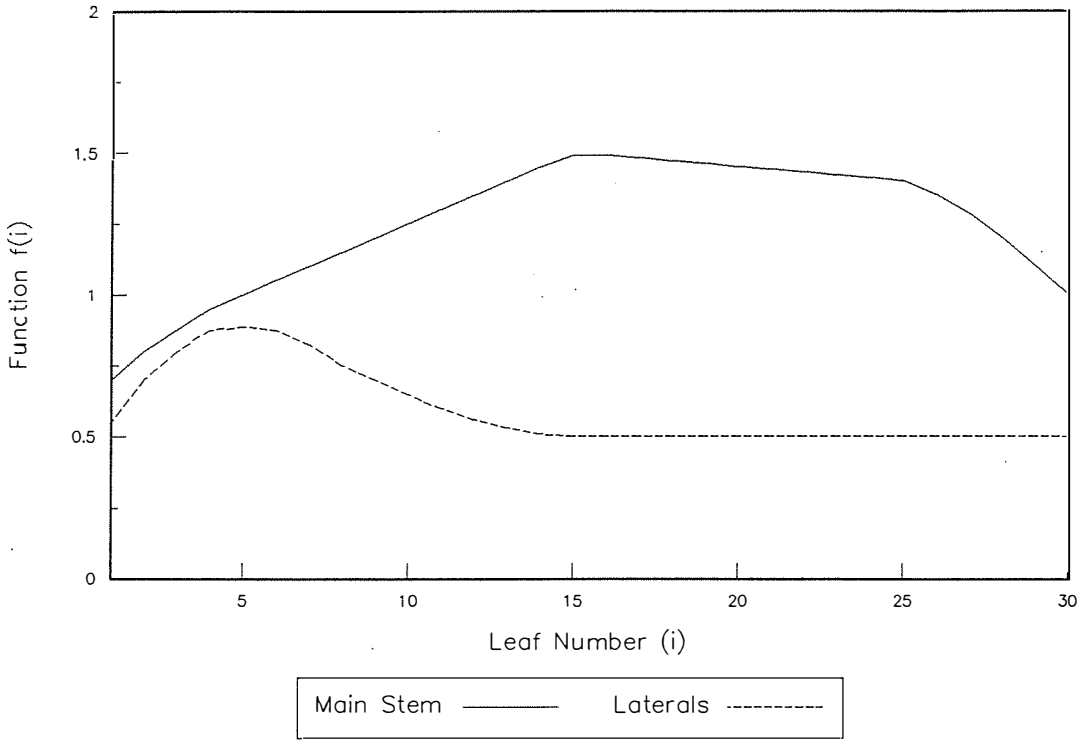

Figure 6.4. Function f(i) for Leaf Expansion versus Leaf Number.

The time course of leaf length can thus be found by integrating the following equation:

$$\frac{dL_i}{dt} = RGR_{ti} L_i \tag{6.32}$$

from leaf initiation to unfolding, and then until F becomes zero, at which point final leaf length is assumed to be attained.

In order to facilitate a smooth transition from the expanding to the maturing phase, Horie et al (1979) applied a somewhat cosmetic reduction function to equation 6.32.

$$\frac{dL_i}{dt} = RGR_{ti} L_i RF \tag{6.33}$$

Where the reduction factor is:

$$RF = (1 - 1/4)^{-1/3}(1 - L_i/4NC_i)^{1/3} \tag{6.34}$$

The factor NC_i is the number of epidermal cells along the mid-rib of the i-th leaf relative to the number at the reference length L_R. During the primordial phase the relative growth rates of the leaf length and cell number are the same and therefore $NC_i = L_i$, and the reduction factor equals

one. During the expanding and maturing phases the leaf length increases more rapidly than the number of cells, because the fraction of dividing cells is decreasing, and therefore the reduction factor reduces to zero. This occurs when the leaf length is four times the relative number of cells, i.e. the expanded cells are four times as long as dividing cells.

The relative number of cells present along the mid-rib of a leaf is also found by integration, since:

$$\frac{dNC_i}{dt} = RGR_{ci} NC_i F \qquad (6.35)$$

The relative growth rate of cell numbers, RGR_{ci}, is equal to the relative growth rate of leaf length on a time basis, RGR_{ti}.

To find the expansion of the leaf surface Horie et al (1979) integrated equation 6.14 numerically to find the time course of the plastochron index, then equations 6.30, 6.33, and 6.35 were integrated for each leaf to find the new length, relative number of cells and fraction of dividing cells.

To reduce the number of differential equations that had to be solved, Horie's model has been simplified slightly. Firstly the fraction of dividing cells is assumed to decrease in a linear manner with plastochron time, i.e. according to equation 6.27. This removes the need to integrate equation 6.30. Secondly, it was discovered that the application of an alternative smoothing function removed the need to use the reduction factor (equation 6.34). Only equation 6.35 was integrated, to yield the time course of relative cell number, NC_i. From this the leaf length was calculated directly according to:

$$L_i = L_R NC_i (4 - 3F) \qquad (6.36)$$

This assumes that once cells stop dividing they immediately attain their fully expanded state of four times their size while dividing (Milthorpe & Newton, 1963).

In order to find the relative number of cells along the mid-rib of the leaf at time t, equation 6.35 was integrated analytically to yield:

$$NC_i(t) = NC_i(0) \exp(RGR_{ti} F) \qquad (6.37)$$

where $NC_i(0)$ is initial relative cell number of the i-th leaf at time zero.

It was found that, using the parameters found by Horie et al (1979), the expansion of the leaf surface on the main stem of a cucumber could be modelled satisfactorily. In order to model lateral leaves some adjustment of the parameters was required. The rate of leaf initiation was found to be lower than that of the main stem. Also the value of n had to be reduced to satisfactorily simulate the smaller leaves typical of laterals.

6.2.1.5 Leaf Senescense

In order to simulate the leaf area development of the cucumber crop over an extended period of time, it was also necessary to consider the rate at which older leaves died off. Observations of the crop over two years revealed that the lower leaves on the main stem of the cucumber plants started dying off when the plastochron age was around 40 (approximately 25 unfolded leaves) which roughly corresponded to the time when the apex of the plant reached the cropping wire (2.2 m above the floor). The rate of senescence was approximately one third the rate of development (increase in plastochron index). Leaf senescence occurred earlier for laterals, at plastochron age 20 (approximately 5 unfolded leaves) but the rate of senescence was slower, only being one quarter of the rate of development.

6.2.1.6 Validation of Leaf Growth and Development

The leaf growth and stem development model was programmed in ESL, and simulations performed using measured average daily solar radiation and air temperature data as boundary conditions. Separate equations were developed for the plastochron age of the main stem and a typical lateral. The lateral was set to initiate when the main stem reached a plastochron age of 49. The development of 30 leaves on the main stem, and 20 leaves on the lateral, were individually followed by integration, using equation 6.37. Each plant was assumed to develop three identical laterals.

Data collected from the cucumber crop of 1989 on leaf sizes and numbers was then compared to the predictions from the model. This is shown in Figures 6.5 and 6.6. On the 31st of October, 90 days after sowing, all main stems were cut back to on average 27 nodes. On the 30th of November, all remaining leaves on the main stem, and approximately the first three leaves on the laterals, were removed, in order to allow more light to penetrate to the new lateral leaves growing down toward the floor. These events were also considered in the model. It can be seen that the predictions of the model for leaf area and leaf numbers agreed well with the measured data. On this basis it was decided to accept the model as suitable for inclusion into the overall crop model.

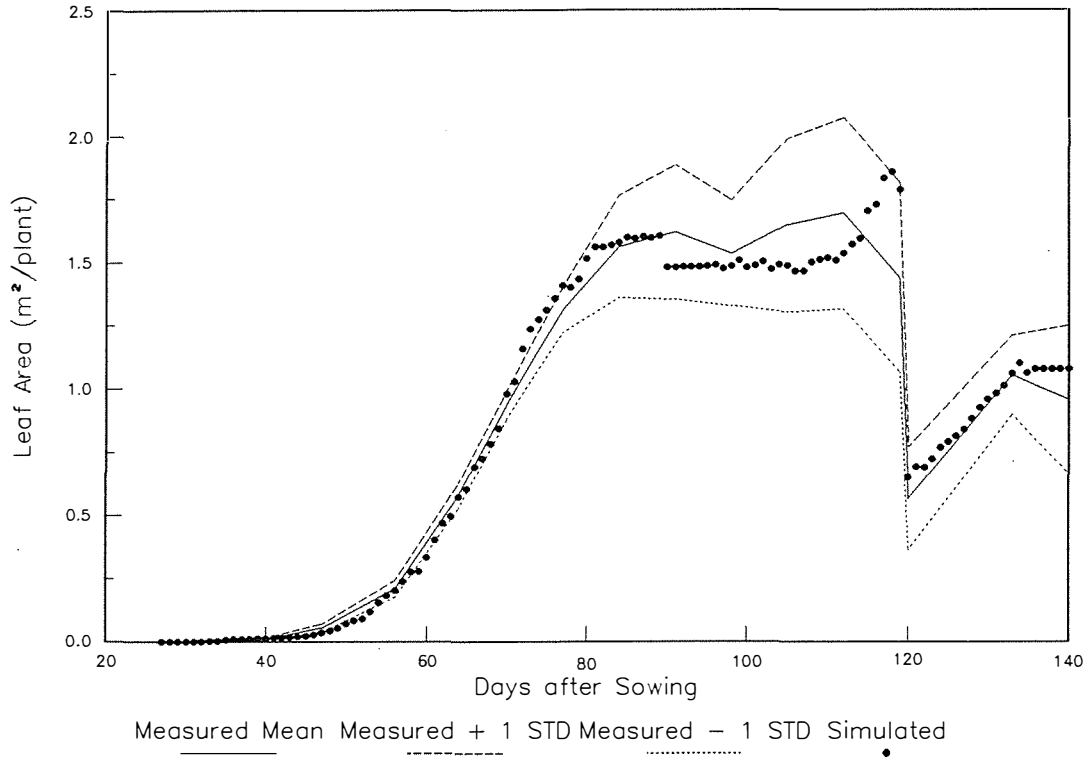

Figure 6.5. Predicted versus Measured Leaf Area

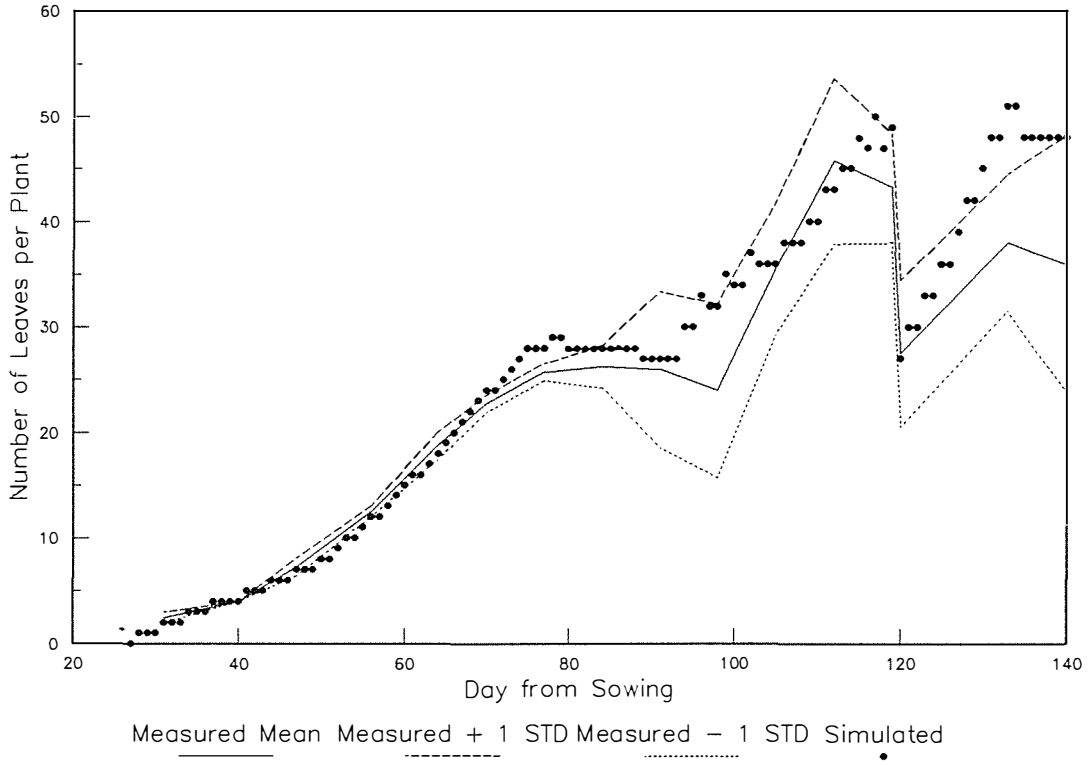

Figure 6.6. Predicted versus Measured Number of Leaves

6.2.2 Radiation in the Crop Canopy

The amount of radiation absorbed or transmitted by a plant canopy is the result of many complex factors which determine the path of photons in the canopy through multiple scattering processes before either being absorbed in a leaf, reflected back from the top of the canopy, or transmitted through to the ground below. The original direction of the radiation relative to the inclination angle and spatial distribution of the leaves is important, as well as the radiative properties of the leaves themselves.

Monsi & Saeki (1953) introduced the idea that radiation intensity in a plant canopy decreases according to an exponential extinction law (Beer's Law). Since then many researchers have applied both analytical and numerical methods to the problem of predicting the radiation absorbed at any level within the canopy.

The main features of these models are: the estimation of leaf reflectance and transmittance in the PAR and NIR bands, the determination of the leaf angle distribution, the determination of canopy reflectivity, and the determination of the extinction coefficient for direct and diffuse radiation.

If a fraction of the incident radiation, ρ, is reflected from the crop canopy then the fraction, $1-\rho$, penetrates the canopy and is available for photosynthesis.

As light travels down through the crop canopy it is attenuated according to Beer's Law. From this the transmissivity of the crop can be found.

$$\tau = \frac{I_L}{I_o} = (1-\rho)\exp(-KLAI) \tag{6.38}$$

where I_o is the intensity above the canopy, I_L is the intensity below leaf area index LAI, ρ is the reflectivity of the crop canopy, and K is the extinction coefficient.

6.2.2.1 Radiative Properties of Leaves

The principle features of the radiative properties of a green leaf are strong absorption in the PAR band, (except for a slight variation in the green region of the spectrum), low absorption in the far-red region of the NIR, with increasing absorption throughout the NIR region, and almost complete absorption in the FIR region (Monteith & Unsworth, 1990) (Table 6.1).

The scattering coefficient, σ, is defined as the sum of the transmissivity, τ, and the reflectivity, ρ.

Table 6.1 Average Radiative Properties of Green Leaves

	PAR	NIR	Total Solar	FIR
Reflectivity ρ	0.09	0.51	0.30	0.03
Transmissivity τ	0.06	0.34	0.20	0.00
Scattering σ	0.15	0.85	0.50	0.03
Absorptivity α	0.85	0.15	0.50	0.97

6.2.2.2 Leaf Angle Distribution

The penetration of radiation into a plant canopy is largely determined by the orientation of the leaves relative to the incoming radiation. The orientation of the leaves relative to the plant is described by the leaf inclination angle density function (Ross, 1975, Goudriaan, 1977). It is usual to assume that the leaves have no azimuthal preference, since measurements indicate that canopies approximate this (Lemeur, 1973, Ross, 1981). Thus only the leaf inclination from the horizontal, Θ, need be considered.

The leaf inclination angle density function (Campbell, 1986, 1990), $g(\theta)$ is the fraction of the canopy which have leaf area with inclination angle, relative to the horizontal, between Θ and $\theta + d\theta$. The density function is such that:

$$\int_0^{\frac{\pi}{2}} g(\theta) d\theta = 1 \tag{6.39}$$

If the leaves have random inclination, as well as random azimuth, as was assumed earlier, then they can be arranged on the surface of a sphere. The surface inclination density function of a sphere is well known:

$$g(\theta)_s = \sin(\theta) \tag{6.40}$$

Two extreme distributions may also be considered. If all leaves are horizontal then the leaf angle distribution is an impulse function at $\theta = 0$. If all the leaves are vertical then they can be projected onto a cylinder, whose leaf angle distribution is an impulse function at $\theta = \pi/2$. Between these extreme distributions exist a series of distributions corresponding

to oblate and prolate ellipsoids. Campbell (1986, 1990) has analyzed the properties of ellipsoidal distributions in detail. The leaf angle density function is given by:

$$g(\theta) = \frac{2X^3 \sin(\theta)}{Y[\cos^2(\theta) + X^2 \sin^2(\theta)]^2} \tag{6.41}$$

where $X = x/y$ and x is the length of the horizontal semi-axis of the ellipsoid, and y is the length of the vertical semi-axis. Thus X is a measure of the eccentricity of the distribution. Values greater than 1 imply an oblate distribution which tends toward the horizontal distribution as $X \to \infty$. Values less than 1 imply a prolate distribution which tends toward the vertical distribution as $X \to 0$.

Now when $X < 1$:

$$Y = X + \frac{\sin^{-1}(\sqrt{1 - X^2})}{\sqrt{1 - X^2}} \tag{6.42}$$

When $X > 1$:

$$Y = X + \ln\left[\frac{(1 + \sqrt{1 - X^{-2}})/(1 - \sqrt{1 - X^{-2}})}{2X\sqrt{1 - X^{-2}}}\right] \tag{6.43}$$

When $X \to 1$ $Y \to 2$ and we have the spheroidal distribution.

6.2.2.3 Extinction Coefficient for Direct Radiation

The extinction coefficient for beam radiation, and canopies composed of non-scattering "black" leaves, has been defined by several authors. Ross (1975) defined a G-function, which is the average projection of canopy elements onto a surface normal to the direction of the solar beam. Other authors (Warren-Wilson, 1967, Monteith, 1973) have defined the K-function, which is the average projection of canopy elements onto the horizontal. The G and K functions are related by:

$$G(\beta) = K(\beta)\sin(\beta) \tag{6.43}$$

Based on Campbell and Norman (1989) the following equations for finding the extinction coefficient for direct radiation attenuation in a stand of "black" leaves, K_{bdf}, can be derived from the K-function for various common angle distributions.

For the horizontal distribution:

$$K_{bdr} = 1 \tag{6.44}$$

For the vertical distribution:

$$K_{bdr} = 2\cot(\beta)/\pi \tag{6.45}$$

For the ellipsoidal distribution:

$$K_{bdr} = \frac{\sqrt{X^2 + \cot(\beta)^2}}{Y} \tag{6.46}$$

which reduces to the well known extinction coefficient for a spherical distribution:

$$K_{bdr} = \frac{\sin(\beta)}{2} \tag{6.47}$$

when $X = 1$.

For real leaves Goudriaan (1977) has shown that the extinction coefficient is:

$$K_{dr} = K_{bdr}\sqrt{(1-\tau)^2 - \rho^2} \tag{6.48}$$

or when the simplification is used that $\tau = \rho = \sigma/2$ then:

$$K_{dr} = K_{bdr}\sqrt{(1-\sigma)} \tag{6.49}$$

Thus for photosynthetically active radiation (PAR) and near infra-red radiation (NIR) the extinctions coefficients will be:

$$K_{pdr} = K_{bdr}\sqrt{(1-\sigma_p)} \tag{6.50}$$

and

$$K_{ndr} = K_{bdr}\sqrt{(1-\sigma_n)} \tag{6.51}$$

respectively.

6.2.2.4 Extinction Coefficient for Diffuse Radiation

The extinction coefficient for diffuse radiation can be found, at least in theory, by integrating the canopy transmission with respect to the elevation of the incoming radiation from the horizon to the zenith.

$$\exp(-K_{df}LAI) = \int_0^{\pi/2} \exp(-K_{dr}LAI)dS \tag{6.52}$$

where dS for a Uniform Overcast Sky is given by:

$$dS = 2S_{df}'\sin(\beta)\cos(\beta)d\beta \tag{6.53}$$

It can be seen that K_{df} will depend on the total leaf area index, the scattering coefficient and the shape of the leaf angle distribution.

Goudriaan (1982) has suggested that for the spherical leaf angle distribution the following approximation is applicable:

$$K_{df} = 0.8\sqrt{(1-\sigma)} \tag{6.54}$$

To test this, equation 6.52 was integrated numerically and K_{df} was found for values of X between 0.6 and 1.8, and values of σ between 0 and 1.0. Analysis of the results showed that K_{df} could be approximated by:

$$K_{df} = K_{bdf}\sqrt{(1-\sigma)} \tag{6.55}$$

where K_{bdf} is the extinction coefficient for diffuse radiation in a canopy of "black" leaves and was found to be approximated by:

$$K_{bdf} = 0.83 + 0.1115\ln(X) - 0.077\ln(LAI) + 0.053\ln(X)\ln(LAI) \tag{6.56}$$

which approaches Goudriaan's estimate when the leaf angle distribution is spherical and leaf area index is approximately 1.

The extinction coefficients for diffuse PAR and NIR radiation will thus be:

$$K_{pdf} = K_{bdf}\sqrt{(1-\sigma_p)} \tag{6.57}$$

and

$$K_{ndf} = K_{bdf}\sqrt{(1-\sigma_n)} \tag{6.58}$$

respectively.

6.2.2.5 Reflectance of the Plant Canopy

Since leaves are not black in the short-wave region of the spectrum there will always be some PAR and NIR reflected from the plant canopy which is unavailable for photosynthesis. The reflectivity of a closed canopy with horizontal leaf angle distribution for direct radiation is given by Goudriaan (1977) as:

$$\rho_{hor} = \frac{1 - \sqrt{1 - \sigma}}{1 + \sqrt{1 - \sigma}} \tag{6.59}$$

Thus the reflectivity for PAR and NIR radiation from a canopy of horizontal leaves will be:

$$\rho_{phor} = \frac{1 - \sqrt{1 - \sigma_p}}{1 + \sqrt{1 - \sigma_p}} \tag{6.60}$$

and

$$\rho_{nhor} = \frac{1 - \sqrt{1 - \sigma_n}}{1 + \sqrt{1 - \sigma_n}} \tag{6.61}$$

respectively.

An exact mathematical expression for non-horizontal leaves is not possible (Goudriaan, 1988). However a reasonable approximation is given by:

$$\rho_{dr} = \left(\frac{2K_{dr}}{1 + K_{dr}} \right) \rho_{hor} \tag{6.62}$$

Thus the reflectivity for PAR and NIR radiation from a canopy of non-horizontal leaves will be:

$$\rho_{pdr} = \left(\frac{2K_{pdr}}{1 + K_{pdr}} \right) \rho_{phor} \tag{6.63}$$

and

$$\rho_{ndr} = \left(\frac{2K_{ndr}}{1 + K_{ndr}} \right) \rho_{nhor} \tag{6.64}$$

respectively.

For diffuse light the canopy reflectivity can be found by integration over the sky vault as was done for the diffuse extinction coefficient. This results in the following empirical relationship:

$$\rho_{df} = [0.90 + 0.075\ln(X)]\rho_{hor} \tag{6.65}$$

or

$$\rho_{pdf} = [0.90 + 0.075\ln(X)]\rho_{phor} \tag{6.66}$$

and

$$\rho_{ndf} = [0.90 + 0.075\ln(X)]\rho_{nhor} \tag{6.67}$$

for the reflectivity of diffuse PAR and NIR radiation from a leaf canopy of non-horizontal leaves, respectively.

Reflectance of the canopy is complicated by the presence of a reflecting boundary below the crop (soil or floor). Goudriaan (1977) and Monteith and Unsworth (1990) have shown that the effective reflectivity of the canopy soil system is:

$$\rho_{cf} = \rho_c - (\rho_c - \rho_f)\exp(-2KLAI) \tag{6.68}$$

where ρ_c represents the appropriate crop reflectivity, ρ_f is the reflectivity of the underlying floor or soil, and K is the appropriate extinction coefficient. Thus ρ_{cf} has obvious limits of ρ_f and ρ_c as leaf area index varies from zero to infinity.

The effect of floor reflectivity is most noticeable when the product $KLAI$ is less than 2.

From this the effective reflectivities for the direct and diffuse components of PAR and NIR radiation can be found.

For direct PAR radiation:

$$\rho_{cpdr} = \rho_{pdr} - (\rho_{pdr} + \alpha_{fp} - 1)\exp(-2K_{pdr}LAI) \tag{6.69}$$

For direct NIR radiation:

$$\rho_{cndr} = \rho_{ndr} - (\rho_{ndr} + \alpha_{fn} - 1)\exp(-2K_{ndr}LAI) \tag{6.70}$$

For diffuse PAR radiation:

$$\rho_{cpdf} = \rho_{pdf} - (\rho_{pdf} + \alpha_{fp} - 1)\exp(-2K_{pdf}LAI) \quad (6.71)$$

And for diffuse NIR radiation:

$$\rho_{cndf} = \rho_{ndf} - (\rho_{ndf} + \alpha_{fn} - 1)\exp(-2K_{ndf}LAI) \quad (6.72)$$

6.2.2.6 Transmission of Radiation

The transmission of radiation through the total crop canopy can be found by applying equation 6.38 to each component of the incoming radiation.

For the direct component of PAR radiation the transmissivity is:

$$\tau_{cpdr} = (1 - \rho_{cpdr})\exp(K_{pdr}LAI) \quad (6.73)$$

For the direct component of NIR radiation the transmissivity is:

$$\tau_{cndr} = (1 - \rho_{cndr})\exp(K_{ndr}LAI) \quad (6.74)$$

For the diffuse component of PAR radiation the transmissivity is:

$$\tau_{cpdf} = (1 - \rho_{cpdf})\exp(K_{pdf}LAI) \quad (6.75)$$

For the diffuse component of NIR radiation the transmissivity is:

$$\tau_{cndf} = (1 - \rho_{cndf})\exp(K_{ndf}LAI) \quad (6.76)$$

6.2.2.7 Absorption of Photosynthetically Active Radiation by a Leaf

The photosynthetically active radiation absorbed by a leaf is made up of three components: direct beam radiation, I_{pdr}, which strikes the leaf unattenuated by the canopy above and therefore at the same intensity as the direct radiation above the canopy, I_{opdr}, direct beam radiation which arrives at the leaf indirectly having been scattered by the leaf canopy (either by reflection, transmission or a combination of both), I_{psc}, and diffuse radiation, I_{pdf}. The scattered radiation is found by considering the difference between the total incident radiation of direct origin, I_{ptot}, and the non-scattered radiation.

Absorption of radiation can be found by differentiation of the transmission equation (equation 6.38).

$$I_a = I_o(1-\rho)K\exp(-KLAI) \tag{6.77}$$

Thus the absorbed fractions of diffuse PAR radiation and total direct PAR radiation are:

$$I_{pdf} = I_{opdf}(1-\rho_{cpdf})K_{pdf}\exp(-K_{pdf}LAI) \tag{6.78}$$

and:

$$I_{ptot} = I_{opdr}(1-\rho_{cpdr})K_{pdr}\exp(-K_{pdr}LAI) \tag{6.79}$$

For non scattered direct radiation a fraction $(1-\sigma_p)$ is available for absorption. Thus the absorbed direct radiation is:

$$I_{pdr} = I_{opdr}(1-\sigma_p)K_{bdr}\exp(-K_{bdr}LAI) \tag{6.80}$$

and the absorbed scattered radiation is:

$$I_{psc} = I_{ptot} - I_{pdr} \tag{6.81}$$

6.2.2.8 Sunlit and Shaded Leaves

It is now possible to distinguish between areas of leaf which are in shade or are sunlit. At any level in the canopy the fraction of sunlit leaf area is:

$$F_{sun} = \exp(-K_{bdr}LAI) \tag{6.82}$$

and thus the fraction of shaded leaf area is $(1-F_{sun})$. The shaded areas absorb diffuse and scattered radiation, while the sunlit area absorbs diffuse, scattered, and direct radiation. Thus:

$$I_{shd} = I_{pdf} + I_{psc} \tag{6.83a}$$

$$= I_{pdf} + I_{ptot} - I_{pdr} \tag{6.83b}$$

and:

$$I_{sun} = I_{shd} + (1-\sigma_p)I_{opdr}K_{bdr} \tag{6.84}$$

Note that in equation 6.84 the intensity of the direct component is averaged over the sunlit area only, as opposed to equation 6.80 where the averaging is done over the combined shaded and sunlit leaf area. However, a more accurate estimate of photosynthesis of sunlit leaves will be obtained if proper account is taken of leaf inclination and thus illumination intensity. In the model this is done by calculating the absorption of beam radiation and integrating the resulting photosynthesis across all leaf inclination angles using Gaussian integration (see next section). The component of absorbed beam radiation is given by:

$$I_{pbeam} = (1 - \sigma_p)\frac{I_{opdr}}{\sin(\beta)} \tag{6.85}$$

and therefore the total absorbed PAR radiation on a sunlit leaf is:

$$I_{sun} = I_{shd} + I_{pbeam}\cos(\iota) \tag{6.86}$$

where ι is the angle of incidence between the solar beam and the leaf.

6.2.3 Photosynthesis

The model of the photosynthetic rate of the crop canopy was derived from the model SUCROS (Simple and Universal Crop Simulator, Spitters et al, 1988). Individual leaf photosynthesis was calculated using the summary model of Gijzen and ten Cate (1988) which is based on a biochemical theory of leaf photosynthesis (Farquhar et al, 1980, von Caemmerer & Farquhar, 1981). The two key parameters of this summary model are the efficiency of light use at low light intensities, η, and the rate of photosynthesis at light saturation, P_{gmax}, both of which are influenced by carbon dioxide concentration and temperature.

6.2.3.1 Maximum Rate of Gross Photosynthesis

The maximum gross rate of photosynthesis P_{gmax} for a single leaf is calculated according to:

$$P_{gmax} = P_{nmax} + R_d \tag{6.87}$$

The maximum rate of photosynthesis P_{nmax} is given by:

$$P_{nmax} = P_{en}\left[1 - \exp\left(\frac{-P_{co_2}}{P_{en}}\right)\right] \tag{6.88}$$

The endogenous rate of photosynthesis, P_{en}, is a function of temperature, as shown in Figure 6.7. The carbon dioxide limited rate of photosynthesis, P_{CO_2}, is governed by the carbon dioxide gradient between the air surrounding the leaf and the inter-cellular concentration, and the resistances in the carbon diffusion pathway.

$$P_{CO_2} = 1.83\left(\frac{CO_{2a} - \Gamma}{r_m + 1.6r_{Vci} + 1.36r_{Vca}}\right) \qquad (6.89)$$

The factor 1.83 converts between $mgCO_2.m^{-3}$ and $\mu l.l^{-1}$.

The mesophyll resistance, r_m, is the reciprocal of mesophyll conductance which is a function of leaf temperature, as shown in Figure 6.8. The internal leaf resistance r_{Vcl} is a function of light intensity, vapour pressure deficit, carbon dioxide concentration, and leaf water status (see Appendix 2). The factor 1.6 relates resistance for carbon dioxide diffusion to that of water vapour. The boundary layer resistance r_{Vca} is a function of leaf size and internal air movement. The factor 1.36 relates the diffusion of carbon dioxide to that of water vapour in a convective process. The compensation point carbon dioxide concentration, Γ, is discussed in the next section.

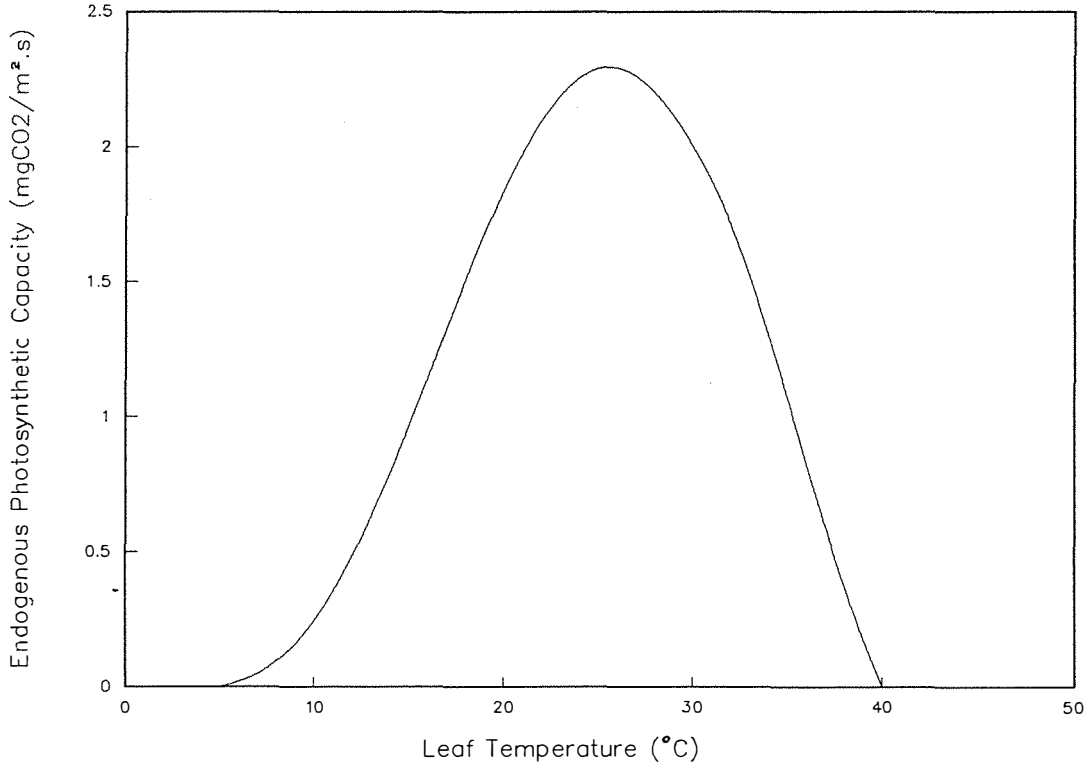

Figure 6.7. Endogenous Photosynthetic Capacity of a Leaf

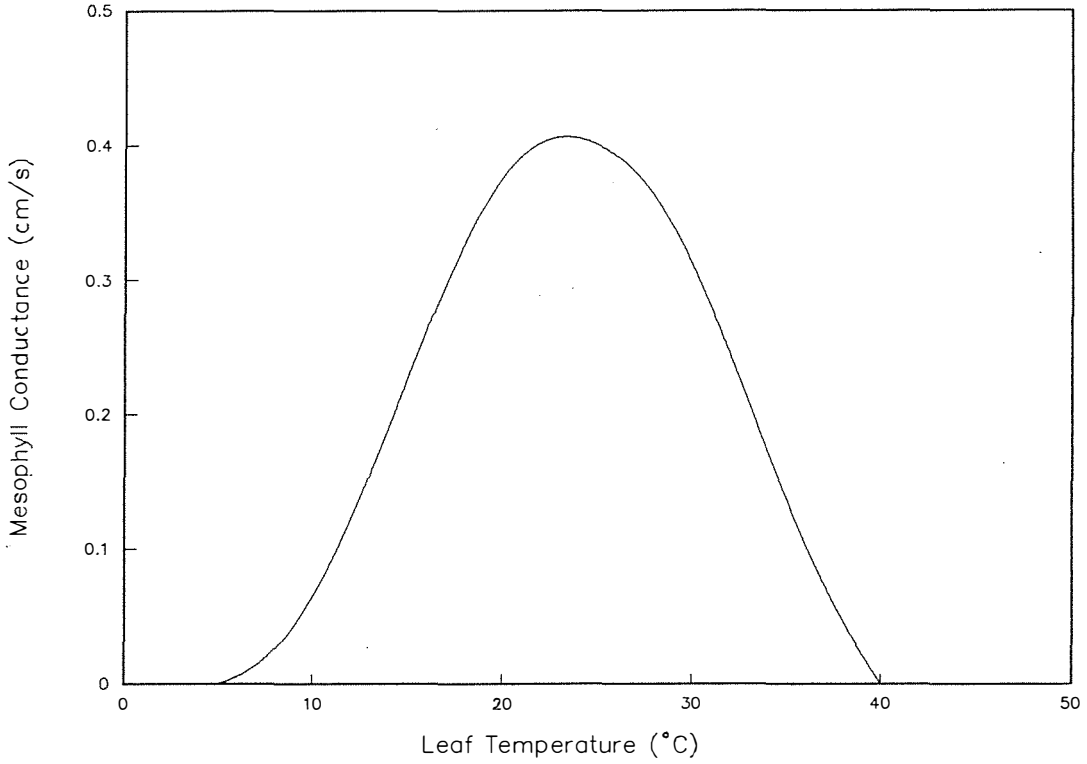

Figure 6.8. Mesophyll Conductance of a Leaf

The rate of dark respiration R_d is given by:

$$R_d = R_{d20} Q_{10}^{(T_c-20)/10} \tag{6.90}$$

where the dark respiration at 20°C, R_{d20}, is assumed to be 0.05 and Q_{10} is 2.

6.2.3.2 Light Use Efficiency Factor

The light use efficiency factor, η, is a function of the temperature and carbon dioxide concentration.

$$\eta = \eta_{pot}\left(\frac{CO_{2a} - \Gamma}{CO_{2a} + 2\Gamma}\right) \tag{6.91}$$

The compensation point carbon dioxide concentration, Γ, is a function of temperature:

$$\Gamma = \Gamma_{25} Q_{10}^{(T_c-25)/10} \tag{6.92}$$

where Γ_{25} is assumed to be 40 μl.l$_{-1}$ and Q_{10} is 1.7. The potential initial light use efficiency, η_{pot}, for cucumber leaves was taken to be 0.017 (Gijzen, 1988, Pers. Comm.).

6.2.3.3 Gross Photosynthesis

The rate of gross photosynthesis is calculated according to the well known asymptotic exponential equation.

$$P_g = P_{gmax}\left[1 - \exp\left(-\frac{\eta I_a}{P_{gmax}}\right)\right] \tag{6.93}$$

The absorbed photosynthetically active radiation, I_a, is calculated according to the method described in section 6.2.2.7, and thus the assimilation rate of shaded leaves is:

$$P_{shd} = P_{gmax}\left[1 - \exp\left(\frac{-\eta I_{shd}}{P_{gmax}}\right)\right] \tag{6.94}$$

For the sunlit leaves the assimilation rate is:

$$P_{sun} = P_{gmax}\left[1 - \exp\left(\frac{-\eta I_{sun}}{P_{gmax}}\right)\right] \tag{6.95}$$

The assimilation rate of any leaf layer can now be found as the weighted sum of the shaded and sunlit assimilation rates: Thus

$$P_t = F_{sun}P_{sun} + (1 - F_{sun})P_{shd} \tag{6.96}$$

6.2.3.4 Canopy Photosynthesis

In order to determine the photosynthesis of a crop canopy equation 6.96, which describes the rate of photosynthesis at one level in the canopy, must be integrated throughout the depth of the canopy. Furthermore, it should be noted that the assimilation of sunlit leaves (equation 6.95) should be integrated over the leaf angle distribution to account for the variable intensity of direct radiation on inclined leaves (equation 6.86).

The integrations are conveniently performed using the Gaussian integration method (Goudriaan, 1986, Spitters, 1986), as was implemented by Spitters et al (1988) for the canopy photosynthesis model SUCROS87. Using this technique the gross photosynthesis, f_{gross} ($mgCO_2.s^{-1}.m^{-2}$ floor area), and the assimilation rate per plant, *Assim* ($mgCO_2.s^{-1}$), were calculated (see section A3.1.10 in Appendix 3).

6.2.4 Respiration

Although respiration has been studied for nearly 200 years (Steward & Bidwell, 1983) the regulatory mechanisms of the process are not very well understood. Respiration can be divided into two distinct parts, associated with maintenance and growth processes.

6.2.4.1 Maintenance Respiration

Maintenance respiration is necessary in order to provide energy for maintaining concentration differences across cell membranes, the continuous re-synthesis of proteins, and overall metabolic activity (idle respiration). In all maintenance can consume 15-30% of the assimilates produced over a season (Penning de Vries et al, 1989). The first two parts of maintenance are quite well quantified in terms of energy cost, but the rates and regulatory mechanisms involved are largely unknown. Estimates for the leaves of field grown crops vary from 30-80 $mgCO_2.gDM^{-1}.day^{-1}$, at 20°C, for temperate crops. Values for non-leaf tissue are more scarce with values ranging from 5-90 $mgCO_2.gDM^{-1}.day^{-1}$. Penning de Vries et al (1989) recommend using 15 $mgCO_2.gDM^{-1}.day^{-1}$ for roots and 10 $mgCO_2.gDM^{-1}.day^{-1}$ for stem tissue.

Several authors have suggested that maintenance respiration should be estimated on the basis of protein content of the tissue, (Thornley, 1977, Schapendonk, 1984) since protein turnover will normally be proportional to content.

Measurements on cucumbers by Challa (1976) arrived at a level of 6 $mgCO_2.g^{-1}protein.hr^{-1}$ for leaves, at 22°C. Schapendonk (1984) estimated the changing protein content of cucumber leaves on the basis of temperature sum to arrive at better estimates of the maintenance respiration. The data of Challa (1976) suggest that the protein content of cucumber leaves is initially about 50% in newly unfolded leaves but that this reduces gradually to about 15%, as the organic acid and mineral fractions increase more rapidly in the leaves than protein, carbohydrate or lipids. Based on these estimates the maintenance respiration coefficient for leaves will change from 3 $mgCO_2.gDM^{-1}.hr^{-1}$ (72 $mgCO_2.gDM^{-1}.day^{-1}$) to 1 $mgCO_2.gDM^{-1}.hr^{-1}$ (22 $mgCO_2.gDM^{-1}.day^{-1}$). In the model a fixed average rate of 1.2 $mgCO_2.gDM^{-1}.hr^{-1}$ was assumed.

From data for cucumber fruit (Schapendonk & Challa, 1980) values of 4-9 $mgCO_2.g^{-1}protein.hr^{-1}$ (22°C) can be determined depending on fruit size. With an average protein content of 12% this corresponds to 1 $mgCO_2.gDM^{-1}.hr^{-1}$ (24 $mgCO_2.gDM^{-1}.day^{-1}$) for new fruit and 0.4 $mgCO_2.gDM^{-1}.hr^{-1}$ (10 $mgCO_2.gDM^{-1}.day^{-1}$) for mature fruit (9 gDM). Since the protein content remains relatively constant in cucumber fruit, it would

appear that the protein turnover decreases with age, suggesting that protein in fruits becomes less active with age (c.f. Penning de Vries et al, 1989). In the model the respiration rate for fruit was set constant at 0.5 $mgCO_2.gDM^{-1}.hr^{-1}$.

Data for stems and roots of cucumber are more scarce. Based on the data of Challa (1976) for the organic N content of roots and stems (about 26% and 17% respectively) respiration coefficients of 1.2 $mgCO_2.gDM^{-1}.hr^{-1}$ and 1.1 $mgCO_2.gDM^{-1}.hr^{-1}$ were selected.

Table 6.2 summarizes the maintenance respiration coefficients used in the model. Note that the units are $mgCO_2.mgDM^{-1}.s^{-1}$.

Table 6.2. Maintenance Respiration Coefficients

Organ Class	Symbol in Model	Maintenance Respiration Rate $mgCO_2.mgDM_{-1}.s_{-1} \times 10_6$
Roots	MainRoot	0.333
Stems	MainStem	0.306
Leaves	MainLeaf	0.333
Fruit	MainFru	0.139

Maintenance respiration is highly dependent upon temperature. It is generally accepted that for every 10°C rise in temperature the respiration rate doubles.

During the day, at high light intensities, the photosynthetic response curve deviates considerably from the initial light use efficiency, due to limitation of carbon dioxide supply. Excess energy (ATP, NADPH reduced) produced by the light reactions can then be channelled into maintenance processes.

The rate of production of carbon dioxide by maintenance respiration, f_{resp} ($mgCO_2.s^{-1}.m^{-2}$ floor area), was calculated by multiplying the dry mass of each class of organ by its appropriate respiration coefficient, and adjusting for temperature. This figure was then multiplies by the total number of plants in the greenhouse, and divided by the floor area (see section A3.1.11, in Appendix 3).

6.2.4.2 Growth Respiration

Growth respiration is the carbon dioxide production from growth processes, synthesis of glucose into other organic components, and the translocation of glucose (and organic and amino-acids) in the phloem system. Both the

glucose requirement and carbon dioxide evolution for the production of organic materials can be estimated with considerable accuracy by considering the stoichiometry of the appropriate biochemical pathways (Penning de Vries, 1975). Transport costs are less well defined but can be estimated by considering the number of membranes involved in the transfer (Penning de Vries et al, 1989). Table 6.3 shows the values used to calculate the growth respiration coefficients.

Table 6.3 Glucose Requirements and Carbon dioxide Evolution from Formation of Organic Compounds and Related Transport.

Organic Compound	Glucose Used ($gCH_2O.gDM_{-1}$)	CO_2 Evolved ($gCO_2.gDM_{-1}$)
Carbohydrates	1.275	0.216
Proteins*	1.887	0.817
Lipids	3.189	1.840
Lignins	2.231	0.740
Organic Acids	0.954	0.025
Minerals	0.120	0.176

* synthesis via amides
From Penning de Vries et al, 1989.

Using the figures in Table 6.2 and the data of Challa (1976) estimates of the growth respiration coefficients were obtained.

For roots the composition of the dry weight accretion was assumed to be 0.30, 0.22, 0.03, 0.10, 0.07 and 0.28 for carbohydrate, protein, lipids, lignins, organic acids, and minerals respectively. Since the data of Challa (1976) did not distinguish between lignins and other carbohydrates it was assumed that lignins would form 25% of the total carbohydrate (Penning de Vries, 1975). This leads to an overall conversion factor of 1.217 $gCH_2O.gDM^{-1}$ formed, or a conversion efficiency of 0.822. Furthermore for every gram of root dry matter formed 0.425 $gCO_2.gDM^{-1}$ will be evolved.

Similarly the composition of the dry weight accretion of the stems was assumed to be 0.30, 0.19 0.02, 0.10, 0.09, 0.30, which gives a conversion factor of 1.150 $gCH_2O.gDM^{-1}$ formed or a conversion efficiency of 0.870, and carbon dioxide formation of 0.386 $gCO_2.gDM^{-1}$.

The fraction of dry weight accretion of cucumber leaves changes with time (Challa, 1976). Initially the accretion is predominantly protein and carbohydrate, however with age this changes to organic acids and minerals.

From Challa's data it can be estimated that at unfolding the respective fractions are 0.29, 0.48, 0.06, 0.03, 0.06, 0.08. In this case the lignin fraction was assumed to be approximately 10% of the total carbohydrate. These figures are assumed to apply for the leaf before unfolding as well. Challa's data also suggests that, excluding the mineral and organic acid fractions, which increase rapidly with age, the carbohydrate, protein, lipid, and lignin contents remain at constant ratios of 0.33, 0.56, 0.08, and 0.03 of the remaining dry matter, and thus of the dry weight accretion. Challa's data also reveals that the ratio of mineral accretion to organic acid accretion is around 1.2. Furthermore the time course of organic acid accretion is related to leaf age expressed on a plastochron basis. At unfolding organic acid accretion is 0.06, by the time of the unfolding of the next leaf this has risen to 0.11, by the second leaf 0.23, by the third leaf 0.35, and by the fourth and subsequent leaves 0.45. Using this information the time course of the composition of the accretion of each leaf can be traced and the conversion factors calculated. The average conversion efficiency was assumed to 0.795 $gCH_2O.gDM^{-1}$, and the average carbon dioxide production to be 0.243 $gCO_2.gDM^{-1}$ formed.

Data for the organic composition of cucumber fruit was very scarce. No complete data sets, giving the proportions of all the organic compounds, were available. Instead values for the glucose consumption and carbon dioxide formation were obtained from Gijzen (Pers. Comm., 1989).

Table 6.4 summarizes the growth respiration coefficients used in the model.

Table 6.4 Growth Respiration Coefficients for Formation of Plant Organs and Related Transport.

Organ Class	Symbol Used in Model	Glucose Used ($mgCH_2O.mgDM^{-1}$)	Symbol Used in Model	CO_2 Evolved ($mgCO_2.mgDM^{-1}$)
Roots	ARroot	1.217	CO2root	0.425
Stem	ARstem	1.150	CO2stem	0.386
Leaves	ARleaf	0.795	CO2leaf	0.243
Fruit	ARfruit	1.515	CO2fruit	0.458

6.2.5 Carbohydrate and Starch Reserves

The carbohydrate levels in the plant were modelled via a mass balance of glucose. All photosynthesis (assimilation) was assumed to contribute to the reserve pool of glucose and all respiration and growth occurred from this pool. If the reserves became zero then all growth processes were stopped. Maintenance respiration was allowed to continue at the expense of dry

matter (protein) breakdown from the leaves, stems, and roots. For breakdown of protein to carbohydrate the conversion efficiency was assumed to be 1/1.887 or 0.53 $mgDM.mgCH_2O^{-1}$.

Some authors have postulated that as starch accumulates in the leaves there is a negative effect on the maximum rate of photosynthesis, although the mechanisms by which this might occur are not well understood. In line with the recommendations of Penning de Vries et al (1989) this effect was built into the model. When the ratio of free carbohydrate to structural dry matter in the plant reached 20% the maximum rate of photosynthesis was reduced linearly until photosynthesis was completely suppressed at levels of 25%.

6.2.6 Partitioning

One of the main difficulties facing the plant growth modeller is deciding how the available assimilate (reserve pool), should be divided out amongst the various plant organs. In plants which have distinct vegetative and reproductive phases it is usual to assume that during the vegetative phase assimilate is partitioned between the shoot and root according to a fixed ratio, or one which varies with age of the plant, according to some previously known scheme which is environmentally independent. It is then further assumed that once reproductive initiation occurs, all vegetative growth ceases. For indeterminate crops, however, these assumptions are not valid and a scheme of dynamic partitioning must be formulated.

Recently several authors have proposed models for dynamic partitioning of assimilates in cucumbers and tomatoes, based on the potential growth rate of organs (Schapendonk & Brouwer, 1984, Jones et al, 1989, Marcelis et al, 1989, Heuvelink & Marcelis, 1989). A sink function, based on the potential growth rate of an organ with time, can be developed by non-destructive measurement of organ size, and hence estimation of weight, for organs with non-limiting assimilate supply. This is assumed when all but one fruit (or truss of tomatoes) is removed from a mature plant. Using this technique Marcelis et al (1989) determined the maximum growth rate of cucumber fruits to be 5 gDM per day, with a growth period of 25 days. Measurements from the crop grown in the test greenhouse gave a maximum growth rate of 4 gDM per day with a growth period of 30 days.

The function for the potential growth rate of the fruit at the i-th node was modified from that given by Schapendonk & Brouwer (1984) and is:

$$PGR(i)_f = 4PGR_f \frac{\exp(-0.6(Age(i)-15))}{1+\exp(-0.6(Age(i)-15))} \qquad (6.97)$$

where PGR_f' is the maximum potential growth rate (0.06 mgDM.s^{-1}), and $Age(i)$ is the age of the i-th fruit, in days from unfolding of the leaf. The factor 15 accounts for the observation that peak growth was attained 15 days after unfolding of the leaf node.

The sink strength of leaves can be estimated by considering the expansion rate of the leaf and the potential specific leaf area, SLA, that would be attained under non-limiting conditions. From the data of Lorenz (1980), Schapendonk & Brouwer (1984) developed the following relationship for specific leaf area, SLA (m^2.kgDM^{-1}):

$$SLA = 3.364\overline{T}_c + 2774\overline{S}_p - 34.53 \qquad (6.98)$$

Given a maximum daily sum of PAR of 500 J.cm^{-2} the minimum specific leaf area will be

$$SLA_{min} = 3.364\overline{T}_c - 29.5 \qquad (6.99)$$

Given a average minimum daily temperature of 20°C then the minimum specific leaf area will be 37.8 m^2.kgDM^{-1} (0.378 cm^2.mgDM^{-1}). Therefore the maximum potential growth rate of leaves can be estimated to be 2.6 mgDM.cm^{-2} of leaf growth.

Heuvelink and Marcelis (1989) have shown that the vegetative parts of cucumber remain in constant ratios regardless of the number of fruit sinks present. The dry weight of the leaves, stem, and roots form 77%, 10% and 13% respectively of the dry weight of the combined vegetative organs. Thus the potential growth rates of root and stem can be estimated from the potential growth rate of the combined leaf area.

The technique for partitioning was to assume that the sink strength of any particular organ was proportional to its potential growth rate. Thus larger fruit would have more power to attract assimilate at the expense of smaller fruit. If the combined sink strength (potential growth rate) of all plant organs exceeded the reserve assimilate availability (taking into account the effect of growth respiration) then each organ had call on the assimilate according to its relative sink strength.

Using the calculated growth rates for each organ class the consumption of glucose and production of carbon dioxide were calculated using the coefficients calculated in section 6.2.4.2. The rate of carbon dioxide production, f_{growth} (mgCO_2.s^{-1}.m^{-2} floor area), was determined by multiplying by the number of plants in the greenhouse, and dividing by the floor area (see section A3.1.11, in Appendix 3).

When the dry weight of a fruit was greater than a threshold picking weight of 14400 mgDM (360 g fresh weight) at a set time of the day it was assumed to be picked. However, if a fruit did not grow to within 20% of this target weight within 12 days of the node unfolding the fruit was aborted. After 20 days from unfolding (5 days past peak growth) all fruit were removed. At this point if a fruit had attained a dry weight of over 10000 mgDM (250 g fresh weight) it was assumed to be harvested. Any fruit not reaching this minimum size was discarded, and added to the number of aborted fruit.

When fruit were removed from the plant, either as harvested fruit or abortions, the mass of water contained in then was calculated from the dry weight, assuming a dry matter content of 4%. This figure was verified by drying fruit samples (see section 3.4.2). This lost water, f_{fruit}, was removed from the plant in the water mass balance equation for the crop (see section 5.3.10).

6.3 IMPLEMENTATION OF THE MODELS

The leaf growth model described in section 6.2.1 was programmed in ESL (Hay et al, 1988) and the results were compared with measurements (section 6.2.1.6). After successfully testing the greenhouse energy balance model with fixed leaf area index (section 5.6.1), a combined model including the leaf growth was developed. Once this was successfully compiled and run, the sub-models for photosynthesis, respiration, and partitioning of assimilates were added. This combined model solved the dynamic greenhouse energy and mass balance sub-model for a 5 minute period and calculated the photosynthetic production and respiration rates in response to changing light levels and leaf temperature. The carbohydrate reserve level was tracked, in response to inputs from photosynthesis and demand for growth and respiration. If the reserves were ever depleted then the leaves, stems, and roots could be used as substrate for maintenance respiration and all growth would cease.

Assimilates were partitioned according to the scheme suggested in section 6.2.6. When the fruit reached a threshold weight they became available for harvesting at the next designated harvest time. Those fruits which had not reached a minimum weight after 12 days of growth were aborted. Fruit which remained on the plant for more than 20 days were removed and either considered to be harvested or aborted depending on weight.

To simulate 12 weeks of the crop's life, from the seven leaf stage, just before the first fruit emerged, till the final harvest, required considerable processing time (48 hours on a 80286 based machine running at 12MHz, and 16 hours on a 80386 based machine running at 33MHz). Due to this constraint, and problems with input data files, only two full runs of the combined model were completed.

6.4 RESULTS OF THE COMBINED MODEL

From the combined model two validation test were carried out. The first involved the long term validation of the energy and mass balance model. This has already been described in Chapter 5. To validate the crop growth model the numbers and weights of picked fruit produced by the simulation were compared to data recorded from the crop during the growing season.

Figure 6.9 shows the results of the simulation for the number of fruit harvested. In the model, only one representative plant is considered, and no attempt was made to account for likely variations between plants. Therefore the model predicts that the output will be discrete, whereas the actual harvest data is almost continuous, because of variations within a quite large population.

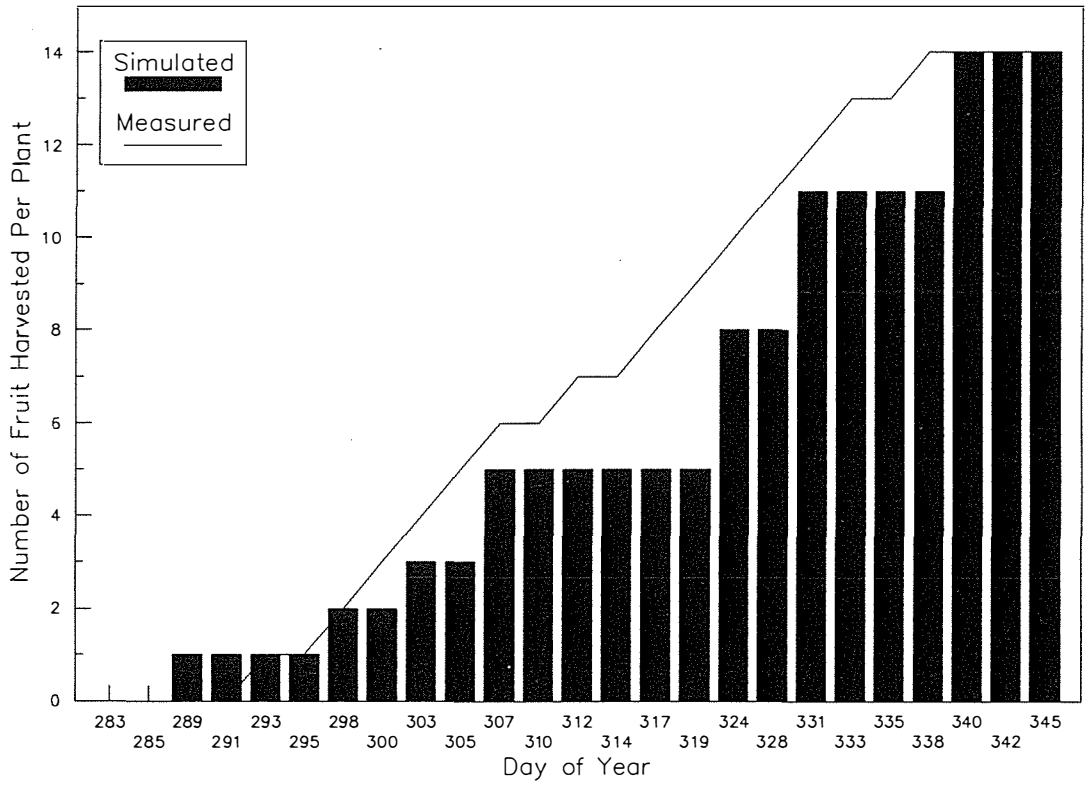

Figure 6.9. Predicted versus Measured Number of Fruit Picked per Plant

The simulated cumulative weight of picked fruit is presented in Figure 6.10. It can be seen that the prediction significantly lags behind the recorded results. This is due to the fact that average picking weight achieved in the model, does not correspond well to what happened for the real crop, where the average picked weight varied considerably over the season.

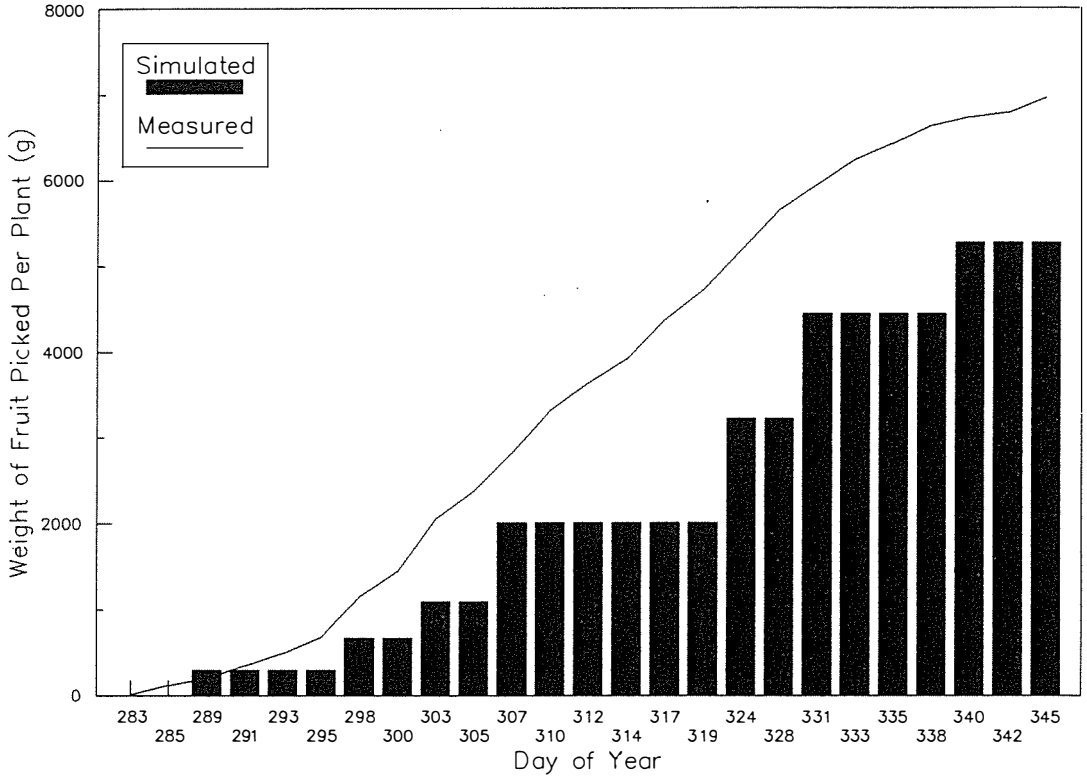

Figure 6.10. Predicted versus Measured Weight of Fruit Picked per Plant

6.5 DISCUSSION

A feature of this model is that it predicted the number and size of leaves present on a cucumber plant independently of the growth of structural dry weight due to photosynthesis and partitioning. The existing model was fitted to data measured from the trial crops with a minimum of alteration to the existing parameters. Minor additions were necessary in order to account for the development of side laterals, and the senescense of older leaves. This was important as by the end of the season there were no leaves left on the main stem. The rate of senescense of leaves was approximately one third of the rate of unfolding of new leaves for the main stem and began when the 25th leaf was unfolding. For the laterals the rate of senescense was one quarter of the rate of development but began much earlier when the 5th leaf was unfolding. Without these additions, and the ability to account for pinching out of the main stem and pruning of older leaves, it would have been impossible to simulate the leaf area of the plant accurately. A simpler model which determined leaf area from a prediction of specific leaf area and assimilate accumulation in the vegetative organs would have been totally inadequate to deal with all the dynamic factors involved.

The model was found to be capable of predicting the leaf area of a cucumber plant to within plus or minus one standard deviation of the measured leaf area throughout the life of the crop. Prediction of leaf numbers was not as accurate, particularly late in the life of the crop, when all the leaves present were on laterals. This was primarily caused by the decision to model only one lateral per plant, to reduce computations, and assume that three identical laterals were allowed to form on each plant. This could potentially have caused problems because as well as over-predicting leaf numbers, fruit numbers were also over-predicted. Fortunately this was not a serious problem, as the inaccuracies only became large at the end of the crops life, when most useful production had already occurred. If the model was to be used over a longer growing season then this problem would need to be addressed by simulating each lateral independently.

The model of absorption of solar radiation within the crop canopy developed in section 6.2.2 is predominantly an amalgamation of existing work. However, by taking this approach, a new correlation to estimate the extinction coefficient for diffuse radiation in crop canopies of arbitrary leaf inclination has been developed based on numerical integration of equation 6.49 across the sky vault. The advantage of this correlation is that is can be used to assess quickly the effect of leaf geometry on the interception of diffuse solar radiation and thermal radiation within a crop canopy. The similar exercise carried out to estimate the effective reflectivity of a crop canopy for diffuse light also provides an easy way to assess the effects of canopy architecture on light utilisation.

On the question of partitioning of assimilates between the various organs in the cucumber plant, this thesis has introduced a novel approach to dealing with the question of dynamic partitioning between vegetative and reproductive organs. The potential growth rate function concepts of Schapendonk & Brouwer (1984) have been extended to include the leaves, stems and roots, as well as the fruit. Experiments conducted to determine the potential growth rate function of the cucumber fruit revealed similar results to other researchers (Heuvelink & Marcelis, 1989, Marcelis et al, 1989). This was particularly encouraging and points towards the wider applicability of the technique. The potential growth rates of the leaves, stems, and roots, have been estimated on the basis of the simulated expansion of the leaf surface and a minimum specific leaf area, determined by average daily temperature. This allows for more realistic modelling of competition between vegetative and reproductive organs, and is an area of the model which would seem to warrant further investigation.

Due to the large amount of computer time required to simulate a crop throughout a full season only limited results were available for analysis. However, these results were promising, with the number of fruit harvested being accurately predicted despite complications arising from variations in

average picking weight throughout the season. Although not fully analysed and presented here, early indications from subsequent runs of the model suggested that the predictions may be improved by increasing the average picking weight. In order to support fruit of increased size the restriction of assimilate reserve levels on photosynthesis needed to be reduced, as it was observed that the critical reserve level was often reached by mid-day and subsequent predictions of gross photosynthetic rate were unrealistically low.

6.6 SUMMARY

In this chapter a model of a cucumber crop growing in a greenhouse has been developed. Existing models were briefly reviewed in section 6.1, and this was followed by an outline of the basic components of an analytical model capable of describing the development of the plant as well as the processes of photosynthesis, respiration and the resulting growth of individual classes of organs.

In section 6.2.1 an existing model describing the development and leaf surface expansion of young cucumber plants has been developed further, in order to model accurately the development and leaf area of fully mature plants.

Equations to evaluate the interception of radiation by the crop canopy have been presented in section 6.2.2. Included in this were new correlation to deal with diffuse light in canopies with ellipsoidal leaf angle distributions.

The equations for photosynthesis of individual leaves and the whole canopy have been presented in section 6.2.3. These were based entirely on the work of the crop modelling group in Wageningen, The Netherlands.

In section 6.2.4 a respiration sub-model has been developed. Maintenance and growth respiration coefficients have been estimated from data published by Penning de Vries et al (1989), based on information about the structural composition of the various cucumber organs gleaned from the literature.

Dynamic partitioning of carbohydrate between the vegetative and reproductive organs of a cucumber plant has been developed in section 6.2.6. The model accurately predicted the number of fruit harvest from the plant over the growing season but underestimated the weight of the fruit. However, modification to the model to improve the simulation have shown early signs of being able to rectify this problem.

7 OVERVIEW AND CONCLUSIONS

In this concluding chapter a summary of the thesis work is presented, together with recommendations for further research. This is followed by a short discourse on the implications to the greenhouse industry, in New Zealand and world wide, and overall conclusions.

7.1 SUMMARY AND RECOMMENDATIONS

The starting point of this thesis was a summary of the historical development of the greenhouse. It became clear that the greenhouse industry has always been reasonably innovative, and has adopted new technologies, and adapted them to its own purposes.

Perhaps more than any other sector of Horticulture, the protected cultivation industry has rapidly entered the age of digital electronics and computer control systems. It should also be recalled that the high energy cost of growing under cover has made the greenhouse industry susceptible to escalating fuel prices. As a consequence of these factors, a great deal of research has been undertaken to assess the viability of energy conservation and substitution systems, and ways of optimizing greenhouse productivity.

Many of the studies of greenhouse design, operation, and productivity, have been carried out using mathematical models of the greenhouse environment. Such models, regardless of type, are valuable tools to aid the engineer and the horticulturalist, since they allow predictions to be made, over a range of conditions, which could not be achieved in reality, except over many years of experimentation.

With this in mind a research programme was put in place to develop suitable mathematical models of the greenhouse environment and the growth of a typical greenhouse crop. These models could then be used to test the performance of proposed greenhouse control systems, alternative energy technologies, and crop management strategies.

The literature review yielded many examples of greenhouse environment models but only a few that included the growth of the plants. Crop models for greenhouse grown species were also not very numerous, although there was a reasonable amount of literature on growth models for arable farm crops such as cotton, and wheat.

Due to the desire to use the model eventually for controller design studies it was decided that a dynamic model of the greenhouse environment should be

developed. Special emphasis was also placed on including the growth of the crop in a realistic manner, in order that the model could also be used to test the long term performance of control and management systems.

The principle parts of this study then were to develop the models and to validate them under local conditions. For the validation phase a glass greenhouse was available in which cucumbers were grown each year. This provided for a number of validation experiments to be performed. In reality the first experiment became a trial run for the following year's experiments. The second and third year's experiments were used to develop and validate the models.

Based on the work of previous researchers, the energy and mass balance equations for the various components making up the greenhouse system were developed. Balances were written for the glazing, the structure, the crop, the root media, the floor and deeper soil layers and the greenhouse air. A unique feature of this model was the separation of the internal structure from the glazing system. This was done when it become clear that the structure contained a significant proportion of the thermal mass of the greenhouse, but that its temperature could be very different to the glazing. Unfortunately no separate measurements of structural temperature were made, as this point was not appreciated until the data-logging phase was completed. ***Recommendation one*** therefore is that the importance of structural thermal mass, and the way that it is modelled, should be investigated more fully.

Light transmission into the greenhouse was modelled using a ray tracing model. Validation of the model uncovered a constant systematic error, which was attributed to the model's failure to include miscellaneous structural components, or to handle realistically the effect of dust accumulation. Validation of the model was hampered by problems with using point measurements which were subject to regular shading by structural components, under all but completely diffuse skies. Averaging the results over time allowed the systematic error to be assessed, and the transmission factors used in the greenhouse model were adjusted accordingly, as this appeared to be the only way to progress beyond the solar radiation model. Given the importance of solar radiation to greenhouse production ***recommendation two*** is that light transmission models be assessed to determine the level of accuracy warranted for various end uses.

An important point to emerge from experimenting with the light transmission model was that, within the limits of applicability of the model, the prediction of light levels at the ground could be safely extrapolated to the top of the crop canopy, except at low sun angles. The model could also be used to determine the relative contribution to light interception by the various components of the greenhouse glazing system.

The results of the validation phase showed that the greenhouse environment model was generally very good at predicting the temperatures of the greenhouse system. Predictions of crop, media, and glazing temperature were highly correlated to the measured values. However the glazing temperature was consistently under-predicted. Errors between predicted and measured air temperature were quite variable, and appeared to be influenced by the leaf area of the crop. Prediction of relative humidity was generally better during the day than at night, when under-prediction frequently occurred. This could have been the result of infiltration rates being too great, or excessive condensation on the underside of the glass due to under-prediction of glass temperature, which is strongly influenced by sky temperature. ***Recommendation three*** is therefore that the effect of outside radiation balance on the glazing temperature be re-evaluated. This may require a more realistic model of sky temperature, or direct measurement of downward radiant flux.

Also following from this is ***recommendation four***, that the infiltration rate model be tested more fully. The results of including the crop model showed that carbon dioxide levels were poorly predicted at night, suggesting that either the respiration rates were too low, or again that the infiltration rate was too high.

An encouraging result of the work with the greenhouse environment model was the good agreement obtained between simulated and measured leaf temperature. Since this parameter strongly influences the growth and development processes of the plant it is important that crop temperature be predicted accurately, if the crop growth model is to be successful.

The results of using the leaf expansion model were also very encouraging. The real difficulties with this model occurred when dealing with leaf senescence and growth of the laterals. In order to make the model work a rather arbitrary assumption was made about the relationship between plant age and senescence and lateral initiation processes. ***Recommendation five*** is therefore that the leaf development and expansion model should be more rigorously tested with respect to leaf senescence and lateral initiation.

The fruit growth model did not give very accurate results over the whole season. While the average number of fruit picked at the end of the season was predicted exactly, the average picking weights were low. This led to an under-estimate of the total weight of fruit picked per plant of around 30%. Obviously this is a problem if accurate prediction of yield and hence income is required. ***Recommendation six*** therefore is that the fruit development and picking aspects of the model be tested in more detail. Particularly important are the assumptions made about the threshold weight at which fruit are considered suitable for picking, and below which abortion occurs.

With the resources available for the project it was not possible to validate the lower levels of the crop simulation model, i.e. photosynthesis, and respiration. ***Recommendation seven*** therefore is that in future experiments measurements of photosynthesis and respiration be performed on a regular basis.

Unfortunately, due to the length of time required to complete a simulation, using the currently available hardware and software, there was insufficient time to complete enough simulations to assess the significance of important parameters within the model. ***Recommendation eight*** therefore is that a full sensitivity analysis be performed on the model in order to locate areas of the model that could be simplified, and thus reduce the execution time.

7.2 IMPLICATIONS FOR THE INDUSTRY

It was stated in section 1.2 of this thesis that the original justifications for the study were to add to the quantitative knowledge of the dynamics of the greenhouse system and to provide a framework for the evaluation of control and management systems and new technologies. The motivation for this was provided by contact with growers and scientists within the greenhouse industry in New Zealand. Most of these people were struggling with the large volume of sometimes conflicting information being supplied by research in the Northern Hemisphere.

The aim of the project then was to develop and test mathematical model of the dynamic response of the greenhouse environment and a crop growing within that environment. This would then form a tool with which to evaluate the effects of applying the new technologies and management strategies being proposed, within a simulated environment. This method of testing, while perhaps not altogether conclusive, could be performed very rapidly, and with minimum cost, compared to the alternative of performing full-scale experiments.

The modelling has been based, wherever possible, on non-empirical techniques to preserve the generality of the results. This means that the resulting model should be amenable to modifications to other types of greenhouses, and possibly other crops. In each case the empirical parts of the model, such as natural ventilation, would have to be evaluated beforehand, or these aspects of the model will need to be re-evaluated at a lower level of abstraction, in order to improve their generality.

The implications for the New Zealand greenhouse industry are firstly that there now exists a model, albeit an imperfect model, of a cucumber crop growing within a greenhouse that can be used to evaluate the operation of proposed greenhouses, or alterations to environmental management practices.

Secondly, a great deal of information regarding the underlying working of the greenhouse system has been collected and synthesized into the model. This information will became available to the industry via the extension, teaching and research activities of Massey University.

Thirdly, the development of this model has involved the co-operation of a number of other researchers from within New Zealand, and particularly overseas countries, such as The Netherlands. This has drawn the attention of key scientists and engineers, working on the problems associated with greenhouse cultivation technology, to the efforts being made to advance the subject here in New Zealand. In the long term this could serve to benefit the industry in New Zealand by initiating closer contacts with researchers in other countries, and also allow New Zealand researchers to have an input to the global knowledge base.

Now that the model has been developed the sort of performance tests described previously can be initiated. The model is currently being modified to include a refrigeration cooling system, in order to evaluate the feasibility of continuously enriching a greenhouse with carbon dioxide. Furthermore, in co-operation with researchers in Florida, and The Netherlands, it is proposed to modify the crop model to be able to simulate a tomato crop. This will make the model more useful to a larger sector of the greenhouse industry. Also, during the development of the full dynamic model, a simpler steady-state model has been developed (Newman, 1991). This model was used successfully to evaluate the justifiable expenditure on thermal screens for New Zealand greenhouses, which was seen as an important question being asked by many growers in New Zealand. It is hoped that many more such questions can be answered logically by the use of the model described in this thesis, and those that will be generated from it.

7.3 CONCLUSION

In conclusion it can be stated that the greenhouse environment model performed with an acceptable degree of accuracy, and could thus be used to study the performance of alternative greenhouse technologies and control systems. It should be emphasised at this point that the major points of difficulty with the model lie in areas where parameters were estimated by empirical means, or assumed (for example the ventilation sub-model, and the sky temperature). It would appear that the model could therefore be improved, if more rigorous analysis was applied to these areas. Overall, however, the greenhouse environment model performed satisfactorily without recourse to excessive parameter estimation.

The results of the crop modelling exercise were somewhat mixed. The leaf expansion model performed reasonably well, although it was necessary to make some assumptions about senescence and lateral initiation which would

affect the model's ability to predict under different circumstances. The total number of harvested fruit was predicted exactly. However, there was some discrepancy during the middle part of the growing period. This situation could most likely be improved by simulating the growth of individual laterals rather than assuming that there are a number of identical laterals, all at exactly the same stage of growth, and therefore in direct competition with one another for carbohydrate supplies. The total weight of fruit harvested was under-predicted. This occurred as a result of the average weight of the real fruit at harvest being higher than that predicted by the model. Some further thought has already been given to this problem and preliminary modifications to the model indicate that a solution has been found. However, further development and testing of the crop model will be required before accurate predictions about overall yield can be made. This process is continuing and will be reported on at a later date.

Overall the model performed in a satisfactory manner, and is seen to be a valuable tool to aid in the rational evaluation of the many and varied options available in the design and operation of greenhouse systems. The primary aim of developing and testing a dynamic model of the greenhouse environment, and a crop growing within that environment, has been fulfilled.

"A cucumber should be well sliced and dressed with pepper and vinegar, and then thrown out as good for nothing."

Samual Jonson (1709-1784)

8 REFERENCES

Acock, B., Charles-Edwards, D.A., Fitter, D.J., Hand, D.W., Ludwig, L.J., Warren-Wilson, J. & Withers A.G., 1978. The contribution of leaves from different levels within a tomato crop to canopy net photosynthesis: An experimental examination of two canopy models. *J. Exp. Bot.*, 29:815-827.

Acock, B., Reddy, V.R., Whisler, F.D., Baker, D.N., McKinion, J.M., Hodges, H.F. & Boote, K.J., 1985. The soybean crop simulator GLYCIM: Model Doc. 1982. PB85 171163/AS, *National Technical Information Service*, Springfield, VA.

Ahmadi, G. & Glockner, P.G., 1982. Dynamic simulation of the performance of an inflatable greenhouse in the southern part of Alberta. I. Analysis and average winter conditions. *Agric. Meteorol.*, 27:155-180.

Ahmadi, G., Kessey, K.O. & Glockner, P.G., 1982. Dynamic simulation of the performance of an inflatable greenhouse in the southern part of Alberta. II. Comparisons with experimental data. *Agric. Meteorol.*, 27:181-190.

Alabiso, M., Parrini, F., Vitale, S., Biondo, A., Licata, R. & Cicero, R.L., 1989. Greenhouse simulation model "ARCEL" applied to a double-layer inflated polyethylene tunnel using low temperature waste heat. *Acta Hort.*, 245:356-362.

Albright, L.D., 1984. Modelling thermal mass effects in commercial greenhouses. *Acta Hort.*, 148:359-368.

Amdursky, V., 1980. Computer models for climate conditions and short-wave radiation in greenhouses. *Acta Hort.*, 106:147-148.

Arinze, E.A., Schoenau, G.J. & Besant, R.W., 1984. A dynamic thermal performance simulation model of an energy conserving greenhouse with thermal storage. *Trans. Amer. Soc. Agric. Eng.*, 27:508-519.

Arkin, G.F., Vanderlip, R.L. & Ritchie, J.T., 1976. A dynamic grain sorghum growth model. *Trans. Amer. Soc. Agric. Eng.*, 19:622-.

ASHRAE, 1982. Environment for animals and plants. Part II, Plants. In: *Applications Handbook*. American Society of Heating, Refrigeration and Air Conditioning Engineers, New York, NY, pp 21.7- 21.20.

Augustin, P., 1984. Ein modell der Ertragsbildung der Gewächshausgurke (*Cucumis sativis* L.). *Arch. Gartenbau,* 32:1-18.

Avissar, R. & Mahrer, Y., 1982. Verification study of a numerical greenhouse microclimate model. *Trans. Amer. Soc. Agric. Eng.,* 25:1711-1719.

Avissar, R., Avissar, P., Mahrer, Y. & Bravdo, B.A., 1985 A model to simulate response of plant stomata to environmental conditions. *Agric. For. Met.,* 34:21-29.

Bailey, B.J., 1977. The calculation of glasshouse fuel requirements using degree-day data corrected for solar heat gain. DN/G/798/04013, *N.I.A.E.,* Silsoe.

Bailey, B.J., 1984. Limiting the relative humidity in insulated greenhouses at night. *Acta Hort.,* 148:411-419.

Baille, A., Aries, F., Baille, M. & Laury, J.C., 1985. Influence of thermal screen optical properties on heat losses and microclimate of greenhouses. *Acta Hort.,* 174:111-118.

Baker, D.N., Smika, D.E., Black, A.L., Willis, W.O. & Bauer, A., 1981. Winter wheat: A model for the simulation of growth and yield in winter wheat. *AgRISTARS,* Publ. No. YM-U2-04281, JSC-18229, Lyndon B. Johnson Space Center, Houston.

Baker, D.N., Lambert, J.R. & McKinion, J.M., 1983. GOSSYM: a simulation of cotton crop growth and yield. *S.C. Agric. Exp. Stn. Tech. Bull.,* 1908.

Baker, J.M. & Van Bavel, C.H.M., 1987. Measurement of mass flow of water in the stems of herbaceous plants. *Plant, Cell and Environment,* 10:777-782.

Basiaux, P., Deltour, J. & Nisen, A., 1973. Effect of diffusion properties of greenhouse covers on light balance in the greenhouse. *Agric. Meteorol.,* 11:357-372.

Baytorun, A.N. & von Zabeltitz, Chr., 1987. Die Wirkung bautechnischer Einflussgrossen auf den Luftwechsel gelufteter Gewachshauser. [Effect of construction parameters on air exchange of ventilated greenhouses.] *Gartenbauwissenschaft,* 52:233-239. [In German].

Behboudian, M.H., 1977. Water relations of cucumber, tomato, and sweet pepper. Thesis, *Agricultural University,* Wageningen, 77-6, 84pp.

Bell, C.J., 1982. A model of stomatal control. *Photosynthetica*, 16:486-495.

Bellamy, L.A., 1991. An investigation into the energy balance of solar greenhouses. PhD Dissertation, *Lincoln University*, New Zealand.

Bellamy, L.A. & Ward, G.T., 1984. The development of passive solar greenhouse designs optimized for the New Zealand glasshouse industry. Draft Report, *Agricultural Engineering Dept.*, Lincoln College, New Zealand.

Bellamy, L.A. & Kimball, B.A., 1986. CO_2 enrichment duration and heating credit as determined by climate. In: Enoch, H.Z. & Kimball, B.A., (Eds.), *Carbon dioxide enrichment of greenhouse crops. II. Physiology, Yield, and Economics*. CRC Press, Boca Raton, Florida.

Berdahl, P. & Fromberg, R., 1982. The thermal radiance of clear skies. *Solar Energy*, 29:299-314.

Biemond, T., 1989a. A glasshouse climate model as part of a bio-economic model. *Acta Hort.*, 260:275-284.

Biemond, T., 1989b. A tomato growth model as part of a bio-economic model. *Acta Hort.*, 260:285-293.

Blom, T., Ingratta, F. & Hughes, J., 1983. Energy conservation in Ontario greenhouses. Publ. 65, *Ontario Ministry of Agriculture and Food*, Ontario.

Bögemann, B., 1984. Ein bio-ökonomisches Simulationsmodell zur Produktionsplanung und -steuerung im Unterglasanbau. I. Konzeption des Grundmodells. [A bio-economic model for production and control in greenhouse production. I. Conception of the basic models]. *Gartenbauwissenschaft*, 49:145-148. [In German].

Bot, G.P.A., 1983. Greenhouse climate: from physical processes to a dynamic model. PhD Dissertation, *Agricultural University*, Wageningen.

Bot, G.P.A., 1989a. Greenhouse simulation models. *Acta Hort.*, 245:315-325.

Bot, G.P.A., 1989b. A validated physical model of greenhouse climate. *Acta Hort.*, 245:389-396.

Boulard, T. & Baille, A., 1986a. Simulation and analysis of soil heat storage systems for a solar greenhouse: I. Analysis. *Energy in Agric.*, 5:175-184.

Boulard, T. & Baille, A., 1986b. Simulation and analysis of soil heat storage systems for a solar greenhouse. II. Simulation. *Energy in Agric.*, 5:285-293.

Boulard, T. & Baille, A., 1987. Analysis of thermal performance of a greenhouse as a solar collector. *Energy in Agric.*, 6:17-26.

Bowman, G.E., 1970. The transmission of diffuse light by a sloping roof. *J.A.E.R.*, 15:100-105.

Breuer, D.R., 1985. Energy in New Zealand greenhouses. Report No. 120, *New Zealand Energy Research and Development Committee*, Auckland.

Breuer, J.J.G., 1983. Rekenmodel energiebehoefte in kassen (2e uitgave). Deel 1. Handleiding. [Computer model of energy requirements in greenhouses (2nd Edition) Part 1. A guide.] Report No. 49, *IMAG*, Wageningen, 72pp. [In Dutch]. (Also available as Translation 532 by G. Bateman, N.I.A.E., Wrest Park, Silsoe, November 1989.)

Britton, C.M. & Dodd, J.D., 1976. Relationships of photosynthetically active radiation and short-wave radiation. *Agric. Meteorol.*, 17:1-8.

Brockett, B.L. & Albright, L.D., 1987. Natural ventilation of single airspace buildings. *J.A.E.R.*, 37:141-154.

Bruce, J.M., 1973. Natural ventilation by stack effect. *Farm Building Progress*, 32:23-27.

Bruce, J.M., 1977. Thermal buoyancy - a comparison of theory and experiment. *Farm Building Progress*, 47:23-25.

Bruce, J.M., 1978. Natural convection through openings and its application to cattle building ventilation. *J.A.E.R.*, 23:151-167.

Bruce, J.M., 1982. Ventilation of a model livestock building by thermal buoyancy. *Trans. Amer. Soc. Agric. Eng.*, 25:1724-1726.

Brugginḳ, G.T. & Heuvelink, E., 1987. Influence of light on the growth of young tomato, cucumber and sweet pepper plants in the greenhouse: Effect on relative growth rate, net assimilation rate and leaf area ratio. *Scientia Hort.*, 31:161-174.

Bruggink, G.T., Schouwink, H.E., & Gieling, Th., 1988. Modelling of water potential and water uptake rate of tomato plants in a greenhouse: Preliminary results. *Acta Hort.*, 229:177-185.

Bruno, R., 1978. A correction procedure for separating direct and diffuse insolation on a horizontal surface. *Solar Energy,* 20:97-100.

Bugler, J.W., 1977. The determination of hourly insolation on an inclined plane using a diffuse irradiance model based on hourly measured global horizontal radiation. *Solar Energy,* 19:477-491.

Burek, S.A.M., Norton, B. & Probert, S.D., 1989. Experimental validation for an air supported structure of a high-level simulation model for greenhouse thermal environment. *Acta Hort.,* 245:331-338.

Burek, S.A.M. & Norton, B., 1989. The effect of structural and operational parameters on effective overall heat loss coefficients for greenhouses. *Acta Hort.,* 245:141-147.

Burtin, M.B., Carels, M.R., Crommelynck, M.D. & Lemoine, M., 1981. Distribution spectrale du rayonnement solaire a Uccle, 2e semestre 1980. [Spectral distribution of solar radiation at Uccle, second half of 1980]. *Inst. Royal Meteor. Belgique,* Misc, Serie B, No 53. [In French].

Businger, J.A., 1963. The glasshouse (greenhouse) climate. In: van Wijk, W.R. (Ed.). *Physics of plant environment*. North-Holland Publishing Co., Amsterdam.

Campbell, G.S., 1986. Extinction coefficients for radiation in plant canopies calculated using an ellipsoidal inclination angle distribution. *Agric. For. Met.,* 36:317-321.

Campbell, G.S., 1990. Derivation of an angle distribution function for canopies with ellipsoidal leaf angle distributions. *Agric. For. Met.,* 49:173-176.

Campbell, G.S. & Norman, J.M., 1989. The description and measurement of plant canopy structure. In: Russell, G., Marshall, B. & Jarvis, P.G., (Eds.). *Plant canopies: their growth, form and function*. Cambridge University Press, Cambridge.

Challa, H., 1976. An analysis of the diurnal course of growth, carbon dioxide exchange and carbohydrate reserve content of cucumbers. PhD Thesis, *Agricultural University,* Wageningen.

Challa, H., 1978. Programming of night temperature in relation to the diurnal pattern of the physiological status of the plant. *Acta Hort.,* 76:147-150.

Challa, H., Bakker, J.C, Bot, G.P.A., Udink ten Cate, A.J. & Van den Vooren, J., 1981. Economical optimization of energy consumption in an early cucumber crop. *Acta Hort.*, 118:191-199.

Challa, H., Bot, G.P.A., Nederhoff, E.M. & van de Braak, N.J., 1988. Greenhouse climate control in the nineties. *Acta Hort.*, 230:459-470.

Chandra, P., 1979. A time-dependent analysis of thermal energy and moisture exchanges in greenhouses. PhD Thesis, *Cornell University*, Ithaca, New York.

Chandra, P. & Albright, L.D., 1980. Analytical determination of the effect on greenhouse heating requirement of using night curtains. *Trans. Amer. Soc. Agric. Eng.*, 23:994-1000.

Chandra, P., Albright, L.D. & Scott, N.R., 1981. A time dependent analysis of greenhouse thermal environment. *Trans. Amer. Soc. Agric. Eng.*, 24:442-449.

Cooper, P.I., 1969. The absorption of solar radiation in solar stills. *Solar Energy*, 12:333-346.

Cooper, P.I. & Fuller, R.J., 1983, A transient model of the interaction between crop, environmental and greenhouse structure for predicting crop yield and energy consumption. *J.A.E.R.*, 28:401-417.

Copet, B. & Videau, J.A., 1981. Digital control systems for greenhouses. *Acta Hort.*, 115:327-334.

Cormary, Aubert & Galland, 1977. Modèles mathemématiques pour serre avec chauffage par tuyau enterré ou par gaine. Internal Report, *E.D.F.* [In French].

Critten, D.L., 1983a. A computer model to calculate the daily light integral and transmissivity of a greenhouse. *J.A.E.R.*, 28:61-76.

Critten, D.L., 1983b. The evaluation of a computer model to calculate the daily light integral and transmissivity of a greenhouse. *J.A.E.R.*, 28:545-563.

Critten, D.L., 1984. The effect of geometric configuration on the light transmission of greenhouses. *J.A.E.R.*, 29:199-206.

Critten, D.L., 1985a. The effect of house length on the light transmissivity of single and multi-span greenhouses. *J.A.E.R.*, 32:163-172.

Critten, D.L., 1985b. A theoretical assessment of the transmissivity of conventional symmetric rooted multi-span E-W greenhouses compared with vertical south roofed greenhouses under natural irradiance conditions. *J.A.E.R.*, 32:173-183.

Critten, D.L., 1986. A general analysis of light transmission in greenhouses. *J.A.E.R.*, 33:289-302.

Critten, D.L., 1987a. Light transmission losses due to structural members in multi-span greenhouses under diffuse skylight conditions. *J.A.E.R.*, 38:193-207.

Critten, D.L., 1987b. Light transmission losses due to structural members in multi-spans under direct light conditions. *J.A.E.R.*, 38:209-215.

Critten, D.L., 1987c. A design guide for calculating light transmission losses in multi-span greenhouses and plastic tunnels. Report No 53, *AFRC Institute of Engineering Research,* Wrest Park, Silsoe.

Critten, D.L., 1989 An approximate theory for predicting the light transmission distribution across a greenhouse. *J.A.E.R.*, 42:301-311.

Critten, D.L. & Legg, B.J., 1987. A general theory of light transmittance of complete structures. *J.A.E.R.*, 36:125-140.

Curry, R.B., 1971. Dynamic simulation of plant growth. I. Development of a model. *Trans. Amer. Soc. Agric. Eng.*, 14:946-949,959.

Curry, R.B. & Chen, L.H., 1971. Dynamic simulation of plant growth. II. Incorporation of actual daily weather and partitioning of net photosynthesis. *Trans. Amer. Soc. Agric. Eng.*, 14:1170-1174.

Curry, R.B., Baker, C.H. & Streeter, J.G., 1975. SOYMOD I: A dynamic simulator of soybean growth and development. *Trans. Amer. Soc. Agric. Eng.*, 18:963-968,974.

Davis, P.F., 1984. A technique of adaptive control of the temperature in a greenhouse using ventilator adjustments. *J.A.E.R.*, 29:241-248.

de Jong, J.B.R.M., 1980. Een karakterisering van de zonnerstraking in Nederland. [Characterisation of solar radiation in The Netherlands]. PhD Dissertation, *Technical University,* Eindhoven. 97+66pp. [In Dutch].

de Wit, C.T., Brouwer, R. & Penning de Vries, F.W.T., 1970. The simulation of photosynthetic systems. In: Setlik, I. (Ed.) *Prediction and measurement of photosynthetic productivity*. Proceedings of the IBP/PP Technical Meeting, Trebon, Czechoslovakia. PUDOC, Wageningen.

Deltour, D. & Nisen, A., 1970. Les verres diffusants en couvertures des serres. *Bull. Rech. Agron.*, Gembloux, NSV, 1:232-235. [In French].

Deltour, J., de Halleux, D., Nijskens, J., Coutisse, S. & Nisen, A., 1985. Dynamic modelling of heat and mass transfer in greenhouses. *Acta Hort.*, 174:119-126.

Dennis, J.E. & Woods, D.J., 1987. New computing environments: Microcomputers in large-scale computing. Ed: Wouk, A., SIAM, 116-122.

Duffie, J.A. & Beckman, W.A., 1980. *Solar engineering of thermal processes*. Wiley & Sons, New York.

Duncan, G.A., Loewer, O.J. & Colliver, D.G., 1981. Simulation of energy flows in a greenhouse: magnitudes and conservation potential. *Trans. Amer. Soc. Agric. Eng.*, 24:1014-1021.

Edwards, R.I. & Lake, J.V., 1964. Transmission of solar radiation in a large-span east-west glasshouse. *J.A.E.R.*, 9:245-249.

Edwards, R.I. & Lake, J.V., 1965a. Transmission of solar radiation in a large-span east-west glasshouse. II. Distinction between the direct and diffuse components of the incident radiation. *J.A.E.R.*, 10:125-131.

Enoch, H.Z., 1978a. A theory for optimalization of primary production in protected cultivation. I. Influence of aerial environment upon primary production. *Acta Hort.*, 76:31-43.

Enoch, H.Z., 1978b. A theory for optimalization of primary production in protected cultivation. II. Primary plant production under different outdoor light regimes. *Acta Hort.*, 76:45-57.

Enoch, H.Z. & Sacks, J.M., 1978. An empirical model of CO_2 exchange at a C3 plant in relation to light, CO_2 concentration and temperature. *Photosynthetica*, 12:150-157.

Erbs, D.G., Klein, S.A. & Duffie, J.A., 1982. Estimation of the diffuse radiation fraction for hourly, daily and monthly-average global radiation. *Solar Energy*, 28:293-302.

Erickson, R.O. & Michelini, F.J., 1957. The Plastochron Index. *Amer. J. of Botany*, 44:297-305.

Ewen, L.S., Walker, J.N. & Buxton, J.W., 1980. Environment in a greenhouse thermally buffered with ground-conditioned air. *Trans. Amer. Soc. Agric. Eng.*, 23:985-989,993.

Farquhar, G.D., von Caemmerer, S. & Berry, J.A., 1980. A Biochemical Model of Photosynthetic CO_2 Assimilation in Leaves of C3 Species. *Planta*, 78-90.

Foster, M.P. & Down, M.J., 1987. Ventilation of livestock buildings by natural convection. *J.A.E.R.*, 37:1-13.

Froehlich, D.P., 1976. Steady-periodic analysis of the greenhouse thermal environment. PhD Thesis, *Cornell University*, Ithaca, NY.

Froehlich, D.P., Albright, L.D., Scott, N.R. & Chandra, P., 1979. Steady-periodic analysis of glasshouse thermal environment. *Trans. Amer. Soc. Agric. Eng.*, 22:387-399.

Fuller, R.J., Meyer, C.P. & Sale, P.J.M., 1987. Validation of a dynamic model for predicting energy use in greenhouses. *J.A.E.R.*, 38:1-14.

Garzoli, K.V. & Blackwell, J., 1971. The heat balance of a glasshouse in summer. *Agric. Eng. Aust.*, 2:6-18.

Garzoli, K.V. & Blackwell, J., 1973. The response of a glasshouse to high solar radiation and ambient temperature. *J.A.E.R.*, 18:205-216.

Garzoli, K.V. & Blackwell, J., 1981a. An analysis of the nocturnal heat loss from a single skin plastic greenhouse. *J.A.E.R.*, 26:203-214.

Garzoli, K.V. & Blackwell, J., 1981b. Thermal analysis of Australian greenhouses. *Acta Hort.*, 115:125-131.

Garzoli, K.V. & Blackwell, J., 1987. An analysis of the nocturnal heat loss from a double skin plastic greenhouse. *J.A.E.R.*, 36:75-85.

Gent, M.P.N. & Enoch, H.Z., 1983. Temperature dependence of vegetative growth and dark respiration: A mathematical model. *Plant Physiol.*, 71:562-567.

Germing, G.H., 1985. (Ed.). *Symposium Greenhouse Climate and its Control*. Published as *Acta Horticulturae*, 174.

Giacomelli, G.A., Ting, K.C. & Panigrahi, S., 1988. Solar PAR vs. Solar total radiation transmission in a greenhouse. *Trans. Amer. Soc. Agric. Eng.*, 31:1540-1543.

Gijzen, H. & ten Cate, J.A., 1988. Prediction of the response of greenhouse crop photosynthesis to environmental factors by integration of physical and biochemical models. *Acta Hort.*, 229:251-258.

Glaub, J.C. & Trezek, G.J., 1981a. Heat and mass transfer analysis of greenhouses. *Paper A.S.A.E.*, 81-4031.

Glaub, J.C. & Trezek, G.J., 1981b. Investigation of solar-heated hydroponic greenhouses. *Paper A.S.A.E.*, 81-4040.

Goudriaan, J., 1977. *Crop micrometeorology: a simulation study*. Simulation Monographs, PUDOC, Wageningen.

Goudriaan, J., 1982. Potential production processes. In: Penning de Vries, F.W.T. & van Laar, H.H. (Eds.) *Simulation of plant growth and crop production*. Simulation Monographs, PUDOC, Wageningen.

Goudriaan, J., 1986. A simple and fast numerical method for the computation of daily totals of crop photosynthesis. *Agric. For. Met.*, 38:249-254.

Goudriaan, J., 1987. Simulation of micrometeorology of crops, some methods and their problems, and a few results. *Agric. For. Met.*, 47:239-258.

Goudriaan, J., 1988. The bare bones of leaf angle distribution in radiation models for canopy photosynthesis and energy exchange. *Agric. For. Met.*, 43:155-169.

Grace, J., 1971. The directional distribution of light in natural and controlled environment conditions. *J. Appl. Ecol.*, 8:155-165.

Hackett, C., 1973. An exploration of the carbon economy of the tobacco plant. I. Inferences from a simulation. *Aust. J. Biol. Sci.*, 26:1057-.

Hay, J.L., Pearce, J.G., Tunball, L. & Crosbie, R.E., 1988. ESL - Software User Manual. CS-1019/04-SUM. ISIM Simulation, Salford University Business Services Ltd, Salford.

Heuvelink, E. & Marcelis, L.F.M., 1989. Dry matter distribution in tomato and cucumber. *Acta Hort.*, 260:149-157.

Heij, G. & de Lint, P.J.A.L., 1984. Glasshouse cucumber, effects of planting date and night temperature on leaf development. *Acta Hort.*, 156:165-176.

Hesketh, J.D. & Jones, J.W., 1980. (Eds.) *Predicting photosynthesis for ecosystem models. Vols. I & II.* CRC Press, Boca Raton, Florida.

Hesketh, T., Skilton, R.A. & Studman, C.J., 1986. Advanced digital control for New Zealand greenhouses. *J.A.E.R.*, 34:207-218.

Holman, J.P., 1986. *Heat Transfer.* (6th Ed.). McGraw-Hill Book Co., New York.

Hopkinson, J.M., 1964. Studies on the expansion of the leaf surface: IV The carbon and phosphorous economy of a leaf. *J. Exp. Bot.*, 15:125-137.

Hopkinson, J.M., 1966. Studies on the expansion of the leaf surface: VI Senescence and the usefulness of old leaves. *J. Exp. Bot.*, 17:762-770.

Horie, T., 1978. A simulation model for cucumber growth to form basis for managing the plant-environment system. *Acta Hort.*, 87:215-223.

Horie, T., de Wit, C.T., Goudriaan, J. & Bensink, J., 1979. A formal template for the development of cucumber in its vegetative stage. Parts I, II, & III. *Proceedings of the Koninklijke Nederlandse Akademie van Wetenschappen,* Series C 82:433-479.

Horigushi, I., 1978. The variation of heating load coefficient for the greenhouse. *Acta Hort.*, 87:95-101.

Horn, H-H., 1985. Untersuchung der frein Luftung von Gewachshausern und Vorschlage zur Anwendung in der Zierpflanzenproduktion. [Studies on natural ventilation in greenhouses and proposals for use in ornamental plant production]. *Arch. Gartenbau,* 33:149-169. [In German].

Horn, H-H., 1989. Untersuchungen zum Massenaustausch bei der frein Gewächshauslüftung. [Studies of the exchange of air masses under natural ventilation of greenhouses]. *Arch. Gartenbau,* 37:305-315.

Hottel, H.C., 1976. A simple model for estimating the transmittance of direct solar radiation through clear atmospheres. *Solar Energy,* 18:129-134.

Huang, B.K. & Kato, A., 1984. Dynamic simulation of greenhouse thermal behaviour. *Paper A.S.A.E.*, 84-4030.

Huebner, J., 1975. *The finite element method for engineers*. John Wiley and Sons, Inc., New York.

Hwang, Y., Jones, P. & Jones, J.W., 1989. A dynamic model for Florida greenhouses. In: Jones, J.W., Dayan, E., Jones, P., Seginer, I., Allen, L.H. & Zipori, I. (Eds.). *On-line computer control system for greenhouses under high radiation and temperature zones*. Final Research Report BARD Project US-871-84.

IBM, 1975. *Continuous system modeling program III. General system information manual (GH19-7000) and users manual (SH19-7001-2)*. IBM Data Processing Division, White Plains, New York.

Incropera, F.P. & De Witt, D.F., 1985. *Fundamentals of heat and mass transfer*. (2nd Ed.) Wiley & Sons, New York.

Ingram, K.T. & McCloud, D.E., 1984. Simulation of potato crop growth and development. *Crop Sci.*, 24:21-.

Iqbal, M., 1980. Prediction of hourly diffuse solar radiation from measured hourly global radiation on a horizontal surface. *Solar Energy*, 24:491-503.

Jackson, B.S. & Arkin, G.F., 1984a. Cotton fruiting model: Calibration and testing, *Paper A.S.A.E.*, 84-4542.

Jackson, B.S. & Arkin, G.F., 1984b. *User's guide to CORN-AP: A maize growth model for an Apple computer*. Mp-1571 Texas Agric. Exp. Stn., College Station, TX.

Jolliet, O., 1988. Modelisation du comportment thermique d'une serre horticole. [A model of thermal behaviour of a horticultural greenhouse.] PhD Thesis No. 713, *Ecole Polytechnique Federale de Lausanne*, Lausanne. [In French].

Jolliet, O. & Munday, G.L., 1989. A 2nd generation static model of greenhouse energy requirements (HORTICERN): a comparison with dynamic models. *Acta Hort.*, 245:346-335.

Jolliet, O., Gay, J-B. & Munday, G.L., 1989. A 2nd generation static model for predicting greenhouse energy inputs as an aid for production planning. *Acta Hort.*, 248:121-128.

Jones, J.W. & Hesketh, J.D., 1980. Predicting leaf expansion. In: Hesketh, J.D. & Jones, J.W. (Eds.), *Predicting photosynthesis for ecosystem models*. CRC Press, Boca Raton, FL.

Jones, J.W. & Kiniry, J.R., 1986. (Eds.) *CERES-Maize*. Texas A & M University Press, College Station, TX.

Jones, J.W., Dayan, E., Allen, L.H., van Keulen, H. & Challa, H., 1989a. A dynamic tomato growth and yield model. In: Jones, J.W., Dayan, E., Jones, P., Seginer, I., Allen, L.H. & Zipori, I. (Eds.). *On-line computer control system for greenhouses under high radiation and temperature zones*. Final Research Report, BARD Project US-871-84.

Jones, J.W., Dayan, E., van Keulen, H. & Challa, H., 1989b. Modelling tomato growth for optimizing greenhouse temperatures and carbon dioxide concentrations. *Acta Hort.*, 248:285-294.

Jones, P., Hwang, Y. & Jones, J.W., 1989c. Economics of temperature and CO_2 control under Florida conditions. In: Jones, J.W., Dayan, E., Jones, P., Seginer, I., Allen, L.H. & Zipori, I. (Eds.). *On-line computer control system for greenhouses under high radiation and temperature zones*. Final Research Report, BARD Project US-871-84.

Joyce, L.A. & Kickett, R.N., 1987. Applied plant growth models for grazing-land, forests, and crops. In: Wisiol, K. & Hesketh, J.D. (Eds). *Plant growth modelling for resource management. Volume I. Current models and methods*. CRC Press, Boca Raton, Florida.

Kano, A. & Sadler, E.J., 1985. Survey of greenhouse models. *J. Ag. Met. (Japan)*, 41:75-81.

Karnopp, D.C. & Rosenberg, R.C., 1975. *System dynamics: A unified approach*. Wiley, New York.

Kimball, B.A., 1973. Simulation of the energy balance of a greenhouse. *Agric. Meteorol.*, 11:243-260.

Kimball, B.A., 1981. A versatile model for simulating many types of solar greenhouse. *Paper A.S.A.E.*, 81-4038.

Kimball, B.A., 1983a. Conduction transfer functions for predicting heat fluxes in various soils. *Trans. Amer. Soc. Agric. Eng.*, 26:211-218.

Kimball, B.A., 1983b. *A Modular Energy Balance Program including subroutines for greenhouses and other latent heat devices*. Ag. Res. Service, U.S.Dept. of Agriculture, Phoenix, Arizona.

Kindelan, M., 1980 Dynamic modelling of greenhouse environment. *Trans. Amer. Soc. Agric. Eng.*, 23:1232-1239.

Kingham, H.G. & Smith, C.V., 1971. Calculated light transmission: the effect of orientation of single glasshouses. *Expl. Hort.*, 22:1-8.

Kittas, C., 1980. Contribution théorique et expérimental a l'etude du bilan d'énergie des serres. Application á l'analyse du déterminisme des températures de la paroi et de l'air intérieur de la serre. [Theoretical and experimental contribution to the study of the energy balance of greenhouses. Application of the analysis to determining the temperatures of the cover and the interior air of the greenhouse]. PhD Thesis, *University of Perpignan,* Montpellier. [In French].

Kirsten, W., 1973. Die natürliche Einstrahlung in Gewächshäuser in Abhängigkeit von deren Form und Aufstellungsrichtung sowie der Beschaffenheit des Hüllstoffes. PhD Thesis, *Technical University,* Hannover. [In German].

Klein, S.A., Cooper, P.I., Freeman, T.L. & others, 1975. A simulation of solar processes and its application. *Solar Energy,* 17:29-37.

Klein, S.A., Beckman, W.A., Cooper, P.I. & others, 1976. *TRNSYS: A transient simulation program*. Solar Energy Lab., Eng. Expt. Station Report 38, University of Wisconsin.

Klucher, T., 1978. *Evaluation of models to predict insolation on tilted surfaces*. N.A.S.A., TM-78842.

Kozai, T., 1973. Numerical experiments on light transmission into greenhouses (1). *J. Ag. Met. (Japan),* 29:179-187. [In Japanese].

Kozai, T., 1974. Numerical experiments on light transmission into greenhouses (2). *J. Ag. Met. (Japan),* Tokyo, 29:239-248. [In Japanese].

Kozai, T., 1975. A computer program for the calculation of the direct solar irradiation in single-span greenhouse. *J. Ag. Met. (Japan),* Tokyo, 31:89-94. [In Japanese].

Kozai, T., 1977. Direct solar light transmission into single-span greenhouses. *Agric. Meteorol.*, 18:327-338.

Kozai, T., 1988. High Technology in Protected Cultivation. Paper presented at Special Lectures 'Horticulture in High Technology Era', May 10-11, Tokyo, Japan.

Kozai, T., & Kimura, M., 1977. Direct solar light transmission into multi-span greenhouses. *Agric. Meteorol.*, 18:339-349.

Kozai, T. & Sase, S., 1978. A simulation of natural ventilation for a multi-span greenhouse. *Acta Hort.*, 87:39-49.

Kozai, T., Goudriaan, J. & Kimura, M., 1978. Light transmission and photosynthesis in greenhouses. PUDOC, Wageningen.

Kozai, T., Sase, S. & Nara, M., 1980. A modelling approach to greenhouse ventilation. *Acta Hort.*, 106:125-136.

Kraan, R.A., 1974. THT-SIM: A conversational simulation program on a small digital computer. *Journal A.*, 15:186-190.

Krug, H., 1985. Growth models for production planning. *Acta Hort.*, 174:241-246.

Krug, H., 1989a. Conception of bio-economic models. *Acta Hort.*, 248:19-26.

Krug, H., 1989b. Growth models as an aid for planning vegetable production in greenhouses. *Acta Hort.*, 260:391-400.

Krug, H. & Liebig, H-P., 1988. Static regression models for planning greenhouse production. *Acta Hort.*, 230:427-433.

Krug, H. & Liebig, H-P., 1989. (Eds.) *International Symposium on Models for Plant Growth, Environmental Control and Farm Management in Protected Cultivation*. Published as *Acta Horticulturae*, 248.

Kurata, K., 1989a. Simulation of inside air temperature, humidity and crop temperature in an energy conserving greenhouse. *Acta Hort.*, 245:339-345.

Kurata, K., 1989b. Model of light environment in greenhouses with emphasis on the role of reflection. *Acta Hort.*, 248:109-114.

Kusuda, T., 1969. *Algorithms for calculating the transient heat conduction by thermal response factors for multi-layer structures of various heat conduction systems (theories, computer programs, and sample calculations)*. National Bureau of Standards Report 10 108.

Kyritsis, K., 1989. Greenhouse simulation modelling progress in Europe. *Acta Hort.*, 245:326-330.

Landsberg, J.J, White, B. & Thorpe, M.R., 1979. Computer analysis of the efficacy of evaporative cooling for greenhouses in high energy environments. *J.A.E.R.*, 24:29-39.

Larsen, R., 1977. (Ed.) *Symposium on more profitable use of energy in protected cultivation*. Published as *Acta Horticulturae*, 76.

Lawrence, W.J.C., 1950. *Science and the glasshouse*. Oliver and Boyd, Edinburgh.

Lawrence, W.J.C., 1963. *Science and the glasshouse*. (3rd Ed.). Oliver and Boyd, Edinburgh.

Lemeur, R., 1973. A method for simulating the direct solar radiation regime in sunflower, Jerusalem artichoke, corn and soybean canopies using actual stand structure data. *Agric. Meteor.*, 12:229-247.

Levit, H.J. & Gasper, R., 1988. Energy budget for greenhouses in humid-temperate climate. *Agric. For. Met.*, 42:241-254.

Liebig, H-P., 1989a. Growth and yield models as an aid for decision making in protected crop production control. *Acta Hort.*, 260:99-113.

Liebig, H-P., 1989b. Model of cucumber growth and prediction of yields. *Acta Hort.*, 260:187-192.

Lorenz, H.P., 1980. Modelluntersuchungen zur Klimareaktion von Wachstumskomponenten am Beispel Salatgurkenpflanzen (*Cucumis sativus* L.) - Ein Beitrag zur Temperaturführung in Gewächshäusern. Thesis. *Technical University*, Hannover.

Lovseth, J., 1981. A greenhouse system with energy storage and high level CO_2 atmosphere. *Acta Hort.*, 115:605-615.

Maas, S.J. & Arkin, G.F., 1978. User's guide to SORGF: A dynamic grain sorghum growth model with feedback capacity. Program and Model Doc. No. 78-1, *Texas Agric. Exp. Stn.*, Blackland Res. Center, Temple, TX.

Maas, S.J. & Arkin, G.F., 1980a. Sensitivity analysis of SORGF, a grain sorghum model. *Trans. Amer. Soc. Agric. Eng.*, 23:671-.

Maas, S.J. & Arkin, G.F., 1980b. TAMW: A wheat growth and development simulation model. Program and Model Doc. No. 80-3. *Texas Agric. Exp. Stn.*, Blackland Res. Center, Temple, TX.

McAdams, W., 1954. *Heat Transmission*. (3rd Ed.). McGraw-Hill Book Co., New York.

MacKenzie, D.W., 1984. Greenhouses in the Auckland and Christchurch Districts, Energy and Economics, 1983. *Agricultural Engineering Department,* Lincoln College.

MacKenzie, G.S., 1812. On the form which the glass of a forcing house ought to have. *Trans. Hort. Soc.,* 2:171-177.

Maher, M.J. & O'Flaherty, T., 1973. An analysis of greenhouse climate. *J.A.E.R.,* 18:197-203.

Mahrer, Y. & Avissar, R., 1984. A numerical simulation of the greenhouse microclimate. *Mathematics and Computers in Simulation,* 26:218-228.

Manbeck, H.B. & Aldrich, R.A., 1967. Analytical determination of direct visible solar energy transmitted by rigid plastic greenhouses. *Trans. Amer. Soc. Agric. Eng.,* 10:564-567,572.

Marcelis, L.F.M., 1989. Simulation of plant-water relations and photosynthesis of greenhouse crops. *Scientia Hort.,* 41:9-18.

Marcelis, L.F.M., Heuvelink, E. & de Koning, A.N.M., 1989. Dynamic simulation of dry matter distribution in greenhouse crops. *Acta Hort.,* 248:269-276.

MathWorks, 1989. *MATLAB for MS-DOS Personal Computers. User's Guide.* The MathWorks, Inc., South Natick, MA.

Meek, D.W., Hatfield, J.L. & Howell, T.A., 1982 A generalized relationship between photosynthetically active radiation and solar radiation. *Agron. Abstracts,* 28 November-3 December 1982, Anaheim, CA.

Meerman, J.W., 1982. *APPLE TUTSIM: Interaktieve simulatie taal gebruikers handeleiding.* Technical University, Twente. [In Dutch].

Meyer, G.E., Curry, R.B., Streeter, J.G. & Mederski, H.J., 1979. SOYMOD/OARDC: A new dynamic simulator of indeterminate soybean growth, development and seed yield. I. Theory, structure and validation. Res. Bull. No. 1113, *Ohio Agric. Res. Dev. Center,* Wooster.

Meyer, G.E., Curry, R.B., Streeter, J.G. & Baker, C.H., 1981. Simulation of reproductive processes and senescence in indeterminate soybeans. *Trans. Amer. Soc. Agric. Eng.,* 24:421-429,435.

Milthorpe, F.L., 1959. Studies on the expansion of the leaf surface. I. The influence of temperature. *J. Exp. Bot.,* 10:233-249.

Milthorpe, F.L. & Newton, P. 1963. Studies on the expansion of the leaf surface. III. The influence of radiation on cell division and leaf expansion. *J. Exp. Bot.*, 14:483-495.

Monsi, M. & Saeki, T., 1953. Über den Lichtfaktor in den Pflanzengesellschaften und seine Bedeutung für die Stoffproduktion. *Jap. J. Bot.*, 14:22-52.

Monteith, J.L., 1973. *Principles of environmental physics*. Edward Arnold, London.

Monteith, J.L. & Unsworth, M.H., 1990. *Principles of environmental physics*. (2nd Ed.) Edward Arnold, London.

Moon, P. & Spencer, D.E., 1942. Illumination from a non-uniform sky. *Trans. Illum. Engng. Soc.*, 37:707-712.

Nederhoff, E.M., van de Vooren, J. & Udink ten Cate, A.J., 1985. A practical tracer gas method to determine ventilation in greenhouses. *J.A.E.R.*, 31:309-319.

Nederhoff, E.M., Gijzen, J.G. & Vegter, J., 1988 Measurement and simulation of crop photosynthesis of cucumber (*Cucumis sativus* L.) in greenhouses. *Neth. J. Ag. Sci.*, 36:253-264.

Nederhoff, E.M., Gijzen, H. & Vegter, J. 1989. A dynamic simulation model for greenhouse cucumber (*Cucumis sativus* L.): Validation of the sub-model for crop photosynthesis. *Acta Hort.*, 248:255-263.

Newman, T.L., 1991. *Evaluating the economic feasibility of thermal screens in New Zealand using a mathematical model*. Masters Thesis, *Massey University*, Palmerston North, New Zealand.

Newton, P., 1963. Studies on the expansion of the leaf surface. II. The influence of light intensity and daylength. *J. Exp. Bot.*, 14:458-482.

Ng, E. & Loomis, R.S., 1984. *Simulation of growth and yield of the potato crop*. Simulation Monographs, PUDOC, Wageningen.

Nisen, A., 1962. Calcul de l'éclairement naturel des constructions horticoles. *Proc. XVIth Hort. Congress*, 16:383-389. [In French].

Norman, J.M., 1980. Interfacing leaf and canopy light interception models. In: Hesketh J.D. & Jones, J.W., (Eds.). *Predicting photosynthesis for ecosystem models. Volume II*. CRC Press, Boca Raton, Florida.

O'Flaherty, T.O. & van der Borg, H.H., 1981. (Eds.). *Symposium on more profitable use of energy in protected cultivation*. Published as *Acta Horticulturae*, 115.

Oikawa, T., 1986. A simulation study of surplus productivity as influenced by the photosynthesis and respiration rates of a single leaf. *J. Ag. Met. (Japan)*, 42:207-216.

Okada, M., 1985. An analysis of thermal screen effects on greenhouse environment by means of a multi-layer screen model. *Acta Hort.*, 174:139-144.

Olszewski, M. & Trezek, G.J., 1976. Performance evaluation of an evaporative pad greenhouse system for utilization of power plant reject heat. *J. Env. Qual.*, 5:259-269.

Orgill, J.F. & Hollands, K.G.T., 1977. Correlation equation for hourly diffuse radiation on a horizontal surface. *Solar Energy*, 19:357-359

Oster, G.F., Perelson, A.S. & Katchalsky, A., 1973. Network Thermodynamics: dynamic modelling of biochemical systems. *Quarterly Rev. Biophysics*, 6:1-134.

Parker, J.J., Hamdy, M.Y., Curry, R.B. & Roller, W.L., 1981. Simulation of buried warm water pipes beneath a greenhouse. *Trans. Amer. Soc. Agric. Eng.*, 24:1022-1025,1029.

Peavy, B.A., 1978. *Determination and verification of thermal response factors for thermal conduction applications*. U.S. Dept. of Commerce, National Bureau of Standards, Final Report, NSBIR 77-1405.

Penning de Vries, F.W.T., 1972. A model for simulating transpiration of leaves with special attention to stomatal functioning. *J. Appl. Ecol.*, 9:57-77.

Penning de Vries, F.W.T., 1975. Use of assimilates in higher plants. In: Cooper, J.P. (Ed). *Photosynthesis and productivity in different environments*. Cambridge University Press, Cambridge.

Penning de Vries, F.W.T. & van Laar, H.H., 1982. Simulation of growth processes and the model BACROS. In: Penning de Vries, F.W.T. & van Laar, H.H. (Eds.) *Simulation of plant growth and crop production*. Simulation Monographs, PUDOC, Wageningen.

Penning de Vries, F.W.T., Jansen, D.M., ten Berge, H.F.M. & Bakema, A., 1989. *Simulation of ecophysical processes of growth in several annual crops*. Simulation Monographs, PUDOC, Wageningen.

Phillips, P., 1984. Commercial Grower attitudes to energy in greenhouses. Paper *'Researchers' and Practioners' Workshop on Energy in Greenhouses'*, Auckland.

Plinius, S.G., 77 AD. Naturalis Historia. Liber XIX:19,4 and 23,5.

Price, D.R. & Peart, R.M., 1973. Simulation model to study the utilisation of waste heat using a combination multiple reservoir and greenhouse complex. *J. Environ. Qual.*, 2:216-224.

Pritsker, A.A.B., 1974. *The GASP IV simulation language*. John Wiley and Sons, Inc.

Rohsenow, W.M. & Hartnett, J.P., 1973. *Handbook of Heat Transfer*. McGraw-Hill Book Company, New York.

Robbins, N.S. & Pharr, D.M., 1987. Leaf area prediction models for cucumber from linear measurements. *HortScience*, 22:1264-1266.

Rosenberg, R.C., 1974. A Users Guide to ENPORT - 4. Wiley, New York.

Ross, J., 1975. Radiative transfer in plant communities. In: Monteith, J.L. (Ed). *Vegetation and the atmosphere. Volume I.* Principles. Academic Press, London.

Ross, J., 1981. *The radiation regime and architecture of plant stands*. W. Junk, The Hague.

Rotz, C.A., Aldrich, R.A. & White, J.W., 1979. Computer predicted energy savings through fuel conservation systems in greenhouses. *Trans. Amer. Soc. Agric. Eng.*, 22:362-366,369.

Russell, G., Marshall, B. & Jarvis, P.G., 1989. *Plant canopies: their growth, form and function*. Cambridge University Press, Cambridge.

Sakaratani, T., 1981. A heat balance method for measuring water flux in the stem of intact plants. *J. Ag. Met. (Japan)*, 37:9-17.

Santamouris, M. & Lefas, C.C., 1986. Thermal analysis and computer control of hybrid greenhouses with sub-surface heat storage. *Energy in Ag.*, 5:161-173.

Sase, S., Kozai, T., Nara, M. & Negishi, H., 1980. Ventilation of greenhouses. I. Wind tunnel measurements of pressure and discharge coefficients for a single-span greenhouse. *J. Ag. Met. (Japan)*, 36:3-12. [In Japanese].

Schapendonk, A.H.C.M., 1984. Effect of maintenance respiration on growth and development of a closed canopy. *Acta Hort.*, 156:155-163.

Schapendonk, A.H.C.M. & Challa, H., 1980. Assimilate requirements for growth and maintenance of the cucumber fruit. *Acta Hort.*, 118:73-82.

Schapendonk, A.H.C.M. & Gaastra, P., 1984a. Physiological aspects of optimal CO_2 control in protected cultivation. *Acta Hort.*, 148:477-484.

Schapendonk, A.H.C.M. & Gaastra, P., 1984b. A simulation study on CO_2 concentration in protected cultivation. *Scientia Hort.*, 23:217-229.

Schapendonk, A.H.C.M. & Brouwer, P., 1984. Fruit growth of cucumber in relation to assimilate supply and sink activity. *Scientia Hort.*, 23:21-33.

Schapendonk, A.H.C.M., Challa, H., Broekharst. P.W. & Udink ten Cate, A.J., 1984. Dynamic climate control: An optimization study for earliness of cucumber production. *Scientia Hort.*, 23:137-150.

Schockert, K. & von Zabeltitz, C., 1980. Energy consumption of greenhouses. *Acta Hort.*, 106:21-26.

Schulze, L, 1955. *Light penetration in glasshouses*. Institut für Technik in Gartenbau und Laudwirtshaft der Technischer-Hochschule, Hannover.

Seemann, J., 1952. Strahlungsverhältnisse in Gewächshäusern. *Archiv für Meteorologie, Geophysik und Bioklimatologie, Series B*, IV(2):193-206.

Seginer, I., 1980. Optimizing greenhouse operation for best aerial environment. *Acta Hort.*, 106:169-178.

Seginer, I. & Levav, N., 1971. Models as tools in greenhouse climate design. Publ. 115. *Technion-Israeli Institute of Technology*, Haifa, Israel.

Seginer, I., Angel, A., Gal, S. & Kantz, D., 1986. Optimal CO_2 enrichment strategy for greenhouses. A simulation study. *J.A.E.R.*, 34:285-304.

Selcuk, M.K., 1971. Analysis, design and performance evaluation of controlled-environment greenhouses. *A.S.H.R.A.E. Trans.*, 77:72-78.

Selcuk, M.K. & Tran, V.V., 1975. Solar stills for agricultural purposes. *Solar Energy,* 17:103-109.

Seneca, L.A., 63 AD. Epistulae morales ad Lucilium. Liber XIX-XX: Ep. 13(122).

Shaffer, M.J., Swan, J.B. & Johnson, M.R., 1984. Coordinated farm and research management (COFARM) data system for soils and crops. *J. Soil Water Conserv.,* 39:320-.

Shell, B. & Staley, L.M., 1985. Economic analysis of greenhouse energy management techniques: A microcomputer spreadsheet model. *Energy in Ag.,* 4:331-345.

Shina, G. & Seginer, I., 1989. Optimal growth control of greenhouse tomato: methodology and some tests. In: Jones, J.W., Dayan, E., Jones, P., Seginer, I., Allen, L.H. & Zipori, I. (Eds.). *On-line computer control system for greenhouses under high radiation and temperature zones.* Final Research Report, BARD Project US-871-84.

Short, T.H., 1984. (Ed.). *Third International Symposium on Energy in Protected Cultivation.* Published as *Acta Horticulturae,* 148.

Short, T.H. & Breuer, J.J.G., 1985. Greenhouse energy demand comparisons for The Netherlands and Ohio, USA. *Acta Hort.,* 174:145-153.

Skov, O., 1989. Light transmission in greenhouses. *Acta Hort.,* 245:86-93.

Slack, G. & Hand, D.W., 1983. The effect of day and night temperature on the growth, development and yield of greenhouse cucumbers. *J. Hort. Sci.,* 58:567-573.

Smith, C.V. & Kingham, H.G., 1970. A contribution to glasshouse design. *Agric. Meteorol.,* 8:447-468.

Sorbie, F.I. & Curry, R.B., 1973. Simulation of lettuce growth in an air-supported plastic greenhouse. *J.A.E.R.,* 18:133-140.

Spencer, J.W., 1972. Computer estimation of direct solar radiation on clear days. *Solar Energy,* 13:437-438.

Spitters, C.J.T., Toussaint, H.A.J.M. & Goudriaan, J., 1986. Separating the diffuse and direct component of global radiation and its implication for modelling canopy photosynthesis. I. Components of incoming radiation. *Agric. For. Met.,* 38:217-229.

Spitters, C.J.T., 1986. Separating the diffuse and direct component of global radiation and its implication for modelling canopy photosynthesis. II. Calculation of canopy photosynthesis. *Agric. For. Met.*, 38:231-242.

Spitters,. C.J.T., van Keulen, H. & van Kraalingen, D.W.G., 1988. A simple and universal crop growth simulator: SUCROS'87. In: Rabbinge, R., Ward, S.A, & van Laar, H.H., (Eds.). *Simulation and systems management in crop protection*. PUDOC, Wageningen.

Stanghellini, C., 1987. Transpiration of greenhouse crops: An aid to climate management. PhD Dissertation, *Agricultural University*, Wageningen.

Stapper, M. & Arkin, G.F., 1980. CORNF: A dynamic growth and development model for maize (*Zea maize* L.). *Texas Agric. Exp. Stn.* Program and Model Doc. No 80-2, Blackland Research Center, Temple, TX.

Stewart, F.C. & Bidwell, R.G.S., 1983. (Eds.). *Plant physiology: a treatise*. Academic Press, New York.

Stigter, C.J. & Musabilha, V.M.M., 1982. The conservative ratio of photosynthetically active to total radiation in the tropics. *J. Appl. Ecol.*, 11:617-636.

Stoffers, J.A., 1967. Radiation absorption of canopy rows. *Acta Hort.*, 46:91-95.

Stoffers, J.A., 1971. Lichtdurchlässigkeit von Gewächshäusern in Blockbauweise. [Light transmission of multi-span greenhouses]. ITT Publ. 39, *IMAG*, Wageningen. [In German].

Streeter, V.L. & Wiley, E.B., 1979. *Fluid mechanics*. 7th Ed. McGraw-Hill Book Co., New York.

Strom, J.S. & Amsen, M.G., 1981. Heat consumption model for greenhouse nurseries. *Acta Hort.*, 115:503-510.

Studman, C.J., 1984. Energy research in Horticulture and Agriculture in Scandinavia and The Netherlands. Report to NZERDC, Contract No. 3318. *Agricultural Engineering Dept.*, Massey University.

Sweeney, D.G., Hand, D.W. & Slack, G., Thornley, J.H.M., 1981. Modelling the growth of winter lettuce. In: Rose, D.A. & Charles-Edwards, D.A., Eds. *Mathematics and Plant Physiology*. Academic Press, Orlando, FL.

Szeicz, G., 1974. Solar radiation for plant growth. *J. Appl. Ecol.*, 11:617-636.

Takakura, T., 1978. (Ed.). *Symposium on Potential Productivity in Protected Cultivation*. Published as *Acta Horticulturae*, 87.

Takakura, T., 1989. Technical models of the greenhouse environment. *Acta Hort.*, 248:49-54.

Takakura, T., Jordan, K.A. & Boyd, L.L., 1971 Dynamic simulation of plant growth and environment in the greenhouse. *Trans. Amer. Soc. Agric. Eng.*, 14:964-971.

Takakura, T., Goudriaan, J. & Louwerse, W., 1975. A behavioural model to simulate stomatal resistance. *Agric. Meteorol.*, 15:393-404.

Takakura, T., Shono, H. & Honjo, T., 1984. Crop management by intelligent computer systems. *Acta Hort.*, 148:317-318.

Takakura, T., Kurata, K. & Honjo, T., 1985. Physical models and the greenhouse climate. *Acta Hort.*, 174:97-104.

Takami, S. & Uchijima, Z., 1977a. A model for the greenhouse environment as affected by the mass and energy exchange of a crop. *J. Ag. Met. (Japan)*, 33:117-127.

Takami, S. & Uchijima, Z., 1977b. A model of the greenhouse with a storage-type heat exchanger and its verification. *J. Ag. Met. (Japan)*, 33:155-166.

Tantau, H-J., 1987. Estimation of the relative opening of leaf stomata using energy balances. *Gartenbauwissenschaft*, 52:94-96.

Temps, R.C. & Coulson, K.L., 1977. Solar radiation incident upon slopes of different orientations. *Solar Energy*, 19:179-184.

Ten Berge, H.F.M., 1986. Heat and water transfer at the bare soil surface. PhD Thesis, *Agricultural University*, Wageningen.

Tetens, O., 1930. Uber einige meteorologische Begriffe. *Zeitschrift Geophysik*, 6:297-309. [In German].

Thekaekara, M.P., 1976. Solar radiation measurement: techniques and instrumentation. *Solar Energy*, 18:309-325.

Thomas, R.B., 1978. The use of specularly-reflecting back walls in greenhouses. *J.A.E.R.*, 23:85-97.

Thornley, J.H.M., 1976. *Mathematical models in plant physiology*. Academic Press, New York.

Thornley, J.H.M., 1977. Growth, maintenance and respiration: a reinterpretation. *Ann. Bot.*, 41:1191-1203.

Tongoni, F. & Serra, G., 1988. (Eds.). *Biological Aspects of Energy Saving in Protected Cultivation*. Published as *Acta Horticulturae*, 229.

Tross, M.J., Degani, D., Ziv, A. & Kopel, R., 1984. An optical liquid filter greenhouse: numerical solution and verification of a thermodynamic model. *Acta Hort.*, 148:401-409.

Udink ten Cate, A.J., 1980. General remarks on greenhouse climate control. *Acta Hort.*, 106:43-47.

Udink ten Cate, A.J., 1983. Modelling and (adaptive) control of greenhouse climates. PhD Dissertation, *Agricultural University*, Wageningen.

Undink ten Cate, A.J. & Challa, H., 1984. On optimal control of the crop growth system. *Acta Hort.*, 148:267-276.

Udink ten Cate, A.J. & van de Vooren, 1978. Adaptive control of the glasshouse heating system. *Acta Hort.*, 76:121-125.

van Bavel, C.H.M., 1978. Projecting crop growth in a fluid-roof solar greenhouse. *Acta Hort.*, 87:301-310.

van Bavel, C.H.M., Damagnez, J. & Sadler, E.J., 1981. The fluid-roof solar greenhouse: Energy budget analysis by simulation. *Agric. Meteorol.*, 23:61-76.

van Bavel, C.H.M., Takakura, T. & Bot, G.P.A., 1985. Global comparison of three greenhouse climate models. *Acta Hort.*, 174:21-33.

van de Braak, N.J., Breuer, J.J.G. & Heyna, B.J., 1984. Cumulative frequency distribution curves of greenhouse heat requirements. *Acta Hort.*, 148:337-344.

van den Brink, G.J., 1982. Climatology of solar irradiance on inclined surfaces. IV. Part II: Validation of calculation models. Report 803.229 IV-2, *Institute of Applied Physics*, Delft, The Netherlands.

van den Muijzenberg, E.W.B., 1980. A history of greenhouses. *Institute of Agricultural Engineering (IMAG)*, Wageningen, 435 pp.

van der Borg, H.H., 1979. (Ed.). *Symposium on Computers in Greenhouse Control*. Published as *Acta Horticulturae*, 106.

van Dixhoorn, J.J., 1977. Simulation of bond graphs on minicomputers. *J. Dyn. Syst. Meas. Control, Trans. A.S.M.E., Series G*, 99:9-14.

van Dixhoorn, J.J. & Evans, F.J., 1974. *Physical structures in systems theory*. Academic Press, London.

van Gulik, 1910. Iets over het gebruik van glas in broeikassen. *Meded. v.d. R.H.L.T.B.*, III:108-118. [In Dutch].

van Ittersum, A., 1972. A calculation of potential rice yields. *Neth. J. Ag. Sci.*, 20:10-.

van Keulen, H., Penning de Vries, F.W.T. & Drews, E.M., 1982. A summary model for crop growth. In: Penning de Vries, F.W.T. & van Laar, H.H. (Eds). *Simulation of plant growth and crop production*. Simulation Monographs, PUDOC, Wageningen.

van Meurs, W.Th.M., 1980. The climate control computer system at the IMAG, Wageningen. *Acta Hort.*, 106:77-83.

Van Wylen, G.J. & Sonntag, R.E., 1976. *Fundamentals of Classical Thermodynamics*. (2nd Ed.). John Wiley & Sons, Inc.

Vanderlip, R.L. & Arkin, G.F., 1977. Simulating accumulation and distribution of dry matter in grain sorghum. *Agron. J.*, 69:917-.

Vogel, G., 1989. (Ed.). *Symposium Growth and Control in Vegetable Production*. Published as *Acta Horticulturae*, 260.

von Caemmerer, S. & Farquhar, G.D., 1981. Some relationships between the biochemistry of photosynthesis and the gas exchange of leaves. *Planta*, 153:376-387.

von Elsner, B., 1980. Significant parameters for characterization of the ventilation and cooling of greenhouses. *Acta Hort.*, 107:91-97.

Walker, J.N., 1965. Predicting temperatures in ventilated greenhouses. *Trans. Amer. Soc. Agric. Eng.*, 8:445-448.

Walker, J.N., Aldrich, R.A. & Short, T.H., 1983. Quantity of airflow for greenhouse structures. In: Hellickson, M.A. & Walker, J.N. (Eds.), *Ventilation of agricultural structures*. A.S.A.E. Monograph No. 6. St. Joseph, Michigan.

Walsh, J.W.T., 1961. *The science of daylight*. McDonald, London.

Warren-Wilson, J., 1967. Stand structure and light penetration. III. *J. Appl. Ecol.*, 4:159-165.

Wass, S.N. & Barrie, I.A., 1984. Application of a model for calculating glasshouse energy requirements. *Energy in Ag.*, 3:99-108.

Weiss, A. & Norman, J.M., 1985. Partitioning solar radiation into direct and diffuse, visible and near-infrared components. *Ag. For. Met.*, 34:205-213.

Wells, C.M., 1982. Evaluation of solar energy simulation programs. Unpublished dissertation, *Lincoln College*, Canterbury.

Wells, C.M. & Studman C.J., 1984. Environmental control of greenhouses. Paper presented at *Control Engineering Applications Seminar*, Massey University.

Wells, C.M., Austin, P.A., Hesketh, T. & Studman, C.J., 1985. Modelling and control for New Zealand greenhouses. *Acta Hort.*, 174:549-554.

White, R.A.J., 1982. Greenhouse energy conservation. *Southern Horticulture*, 4:19-22.

White, R.A.J., 1984. Estimating greenhouse fuel, water and CO_2 consumption with simulation models. Paper *'Researchers' and Practitioners' Workshop on Energy in Greenhouses'*, Auckland.

Wilkerson, G.G., Jones, J.W., Boote, K.J., Ingram, K.T. & Mishoe, J.W., 1983. Modelling soybean growth for crop management. *Trans. Amer. Soc. Agric. Eng.*, 26:63-73.

Willits, D.H., Chandra, P. & Peet, M.M., 1985. Modelling solar energy storage systems for greenhouses. *J.A.E.R.*, 32:73-93.

Wilson, G.L., 1966. Studies on the expansion of the leaf surface. V. Cell division and expansion in a developing leaf as influenced by light and upper leaves. *J. Exp. Bot.*, 17:440-451.

Wisiol, K. & Hesketh, J.D., 1987. (Eds). *Plant growth modelling for resource management. Vol I. Current models and methods. Vol. II. Quantifying plant processes*. CRC Press, Boca Raton, Florida.

Wood, R.W., 1909. Note on the theory of the greenhouse. *Phil. Mag.*, (1909):319.

Wright, A.D. & Keener, M.E., 1982. A test of a maize growth and development model, CORNF. *Agric. Sys.*, 9:181-.

Xi, C. & Down, M.J., 1984. Natural ventilation by convection: a comparison of theory and experiment. Proceedings of the *Conference on Agricultural Engineering,* Bundaberg, Queensland. Institute of Engineers, Australia. pp 44-47.

Yang, X., Short, T.H., Fox, R.D. & Bauerle, W.L., 1989. The microclimate and transpiration of a greenhouse cucumber crop. *Trans. Amer. Soc. Agric. Eng.*, 32:2143-2150.

Zhao, J., Jenkins, B., Shaw, R.H. & Seginer, I., 1985. Heat and water vapour balance of greenhouse plant leaves under convective and infrared heating. *Paper A.S.A.E.*, 85-4052.

Ziv, A., 1983. THERMO - A computer program for dynamic simulation of climate inside a greenhouse. Report. *IBM Israel Scientific Centre*.

A1 NATURAL VENTILATION OF THE TEST GREENHOUSE

In this appendix models to predict natural ventilation of greenhouses are reviewed and an empirical model of the ventilation characteristics of the test greenhouse is described.

A1.1 REVIEW OF EXISTING MODELS

Existing models of natural ventilation of greenhouses can be divided into two categories: analytical and empirical.

Analytical models are based on concepts derived from fluid mechanics, Bernoulli's theorem, and the theory of continuity (Streeter & Wiley, 1979). Bruce (1973, 1977, 1978, 1982) developed a generalized model for the natural ventilation of animal shelters based on the thermal buoyancy effect (the so called stack effect). This has been validated (Bruce, 1977, Xi & Down, 1984) for air movement in a column, but as pointed out by Foster & Down (1987) this may not be widely applicable to real building shapes.

Brocket & Albright (1987) added the effect of wind pressure, to the analysis of Bruce, in a study aimed at designing suitable control systems for natural ventilation.

Horn (1985, 1989) has also derived the equations for the combined affect of wind pressure and thermal buoyancy on ventilation of a standard type of East German greenhouse. This analysis concluded that the relative air exchange rate (volumes per unit time) would decrease for larger greenhouses with similar ratios of window area to surface area.

Kozai & Sase (1978) developed a simulation model of the natural ventilation of a multi-span greenhouse using an iterative technique to find the position of the neutral plane. An improved version of this model (Kozai et al, 1980) was latter developed for a single span greenhouse using wind pressure and discharge coefficients determined from wind tunnel experiments on scale models for differing wind approach angle and varying ventilator window openings (Sase et al, 1980). A major impediment to the adoption of a model such as this, into the greenhouse simulation model, is the extra computational time required to solve the ventilation sub-model at each time step.

Bot (1983) reviewed the literature pertinent to natural ventilation of greenhouses, and developed a theory for the exchange of air through ventilator windows of varying geometry. Particular emphasis was placed on the effect of window opening angle on the flow characteristics. Experiments on scaled and full scale windows were used to test the theory, which gave

satisfactory results. Having established the form of the model experiments were carried out on a greenhouse, using an equilibrium tracer gas method, to fit parameters to a model of ventilation rate, for a Dutch Venlo greenhouse with roof vents. The ventilation rate was found to be linearly related to outside wind speed. Wind direction was only of minor importance in determining ventilation. With lee-ward vents open the ventilation rate varied exponentially with opening aperture. With wind-ward vents open the exponential relationship was observed for small opening, but large openings above the horizontal resulted in increased ventilation rates due to the wind capture effect of the window. The effect of temperature difference between the inside and outside of the greenhouse was only significant at very low wind speeds, or large temperature differences, of the order of 5°C at 1 $m.s^{-1}$ wind speed, 15°C at 2 $m.s^{-1}$, and 35°C at 3 $m.s^{-1}$.

Baytorun & Von Zabeltitz (1987) performed experiments on a single span greenhouse, with both ridge and side vents, and correlated ventilation rate to wind speed, temperature difference, and ventilator opening. They used a dynamic tracer gas method, as did Nederhoff et al (1985).

A1.2 AN EMPIRICAL MODEL FOR THE TEST GREENHOUSE

Due to the simplicity of using the dynamic tracer gas method to determine an empirical model of ventilation exchange of the test greenhouse, it was decided to use this approach rather than work with a general analytical model, which would have added considerably to the computational time required to solve the greenhouse model equations. This decision obviously detracted from the overall generality of the final model.

The tests carried out to determine the ventilation characteristics of the test greenhouse were described in Chapter 3. In line with the findings of Bot (1983) and Baytorun & Von Zabeltitz (1987) it was decided to fit a non-linear models of the general form:

$$N_v = [\alpha_1 \bar{u}_o + \alpha_2 \sqrt{\Delta T}]\left[1 + \alpha_3 A_{top} e^{\alpha_4 A_{top}} + \alpha_5 A_{bot} e^{\alpha_6 A_{bot}}\right] \qquad (A1.1)$$

where N_v is the air exchange rate per hour, $\bar{u}_o$ is the outside wind speed, measured at a reference height of 10 m ($m.s^{-1}$), and ΔT is the temperature difference between inside and outside (°C). (It should be noted that 1 air change per hour is equal to the volume of air in the greenhouse changing once every hour). The combined opening of the ventilator windows, in square meters, are represented by A_{top}, and A_{bot}, for the top (ridge) vents, and the bottom (side) vents respectively. The doors were included with bottom vents.

The constant parameters, α_1 to α_6, were fitted using the Nelder-Meade simplex algorithm (Dennis & Woods, 1987) in MATLAB (MathWorks, 1989). Two separate fits were finally used. The first for modelling infiltration (combined opening area less than 0.05 m²), and the second for ventilation. The fits were respectively:

$$N_v = 0.77\bar{u}_0 + 0.14\sqrt{\Delta T} \qquad (A1.2)$$

and

$$N_v = [0.77\bar{u}_0 + 0.67\sqrt{\Delta T}]\left[1 + 1.5A_{top}e^{-0.15A_{top}} + 1.2A_{bot}e^{-0.04A_{bot}}\right] \qquad (A1.3)$$

The results of the fitting exercise, are shown in Figures A1.1 and A1.2. The infiltration rates and ventilation rate are expressed in air-changes per hour. The correlation coefficient between the measured and predicted ventilation rates was 0.89, and between the measured and predicted infiltration rates 0.97.

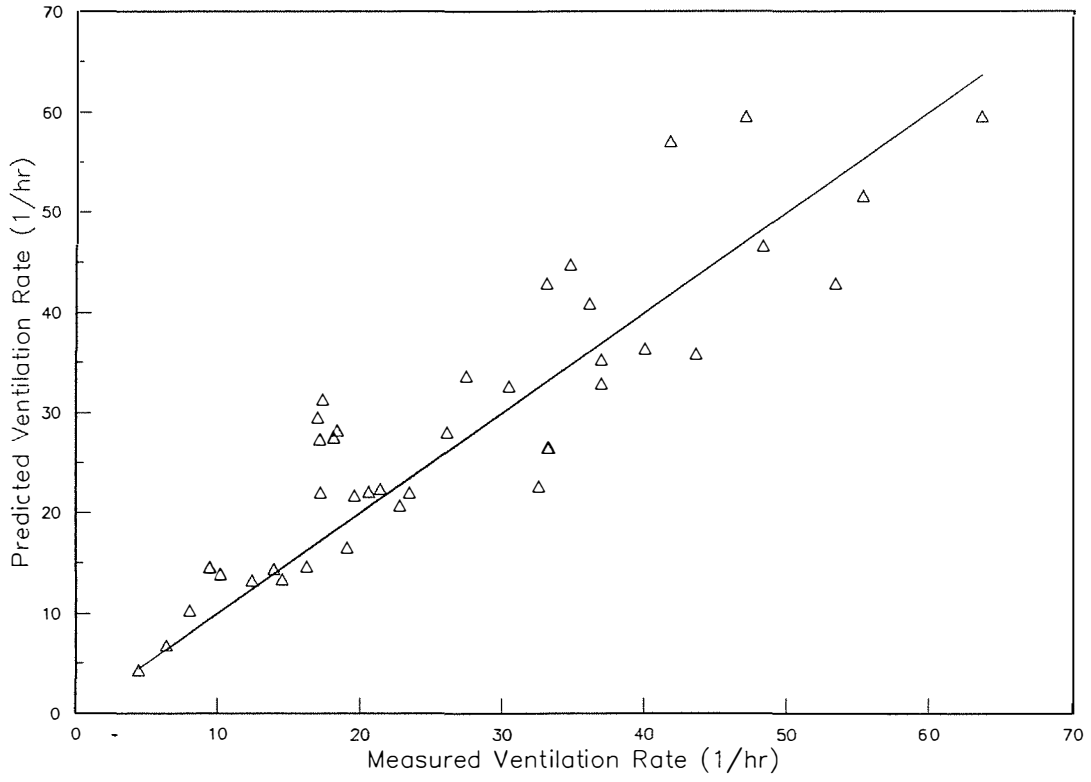

Figure A1.1. Predicted versus Measured Ventilation Rate of Test Greenhouse.

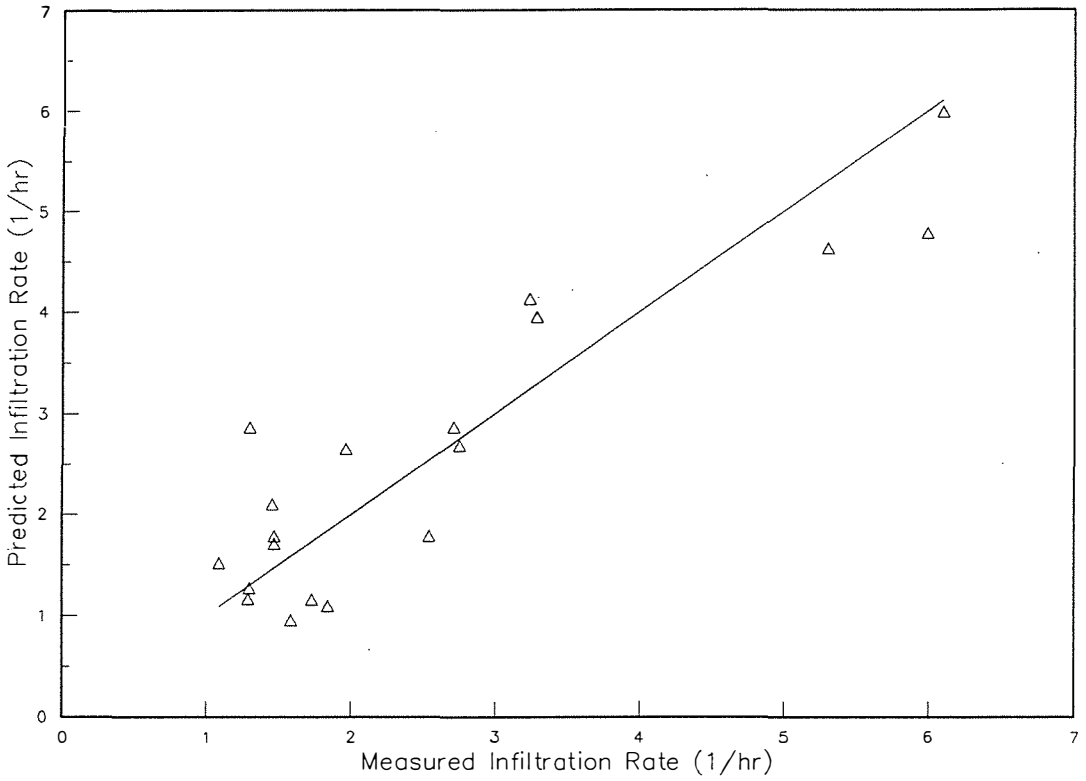

Figure A1.2. Predicted versus Measured Infiltration Rate of Test Greenhouse.

Although there was some disappointment with the lack of good fit between the measurements and the model, it was decided to continue with the modelling using the equations A1.2 and A1.3 to predict ventilation rates. The question of quantifying natural ventilation processes in greenhouse is an area which requires more study. This was discussed in Chapter 7.

A2 INTERNAL RESISTANCE OF CUCUMBER LEAVES

In this appendix the technique used to derive an empirical model of the variation of the internal resistance of cucumber leaves is described, based on the work of Stanghellini (1987), and Yang et al (1989).

A2.1 INTRODUCTION

The internal leaf resistance plays a role in determining both photosynthesis transpiration and of crops. The internal resistance has an affect on determining the photosynthesis via the carbon dioxide limited rate of photosynthesis. This was given in equation 6.72 which is reproduced here:

$$P_{co_2} = 1.83\left\{\frac{C_{co_2} - \Gamma}{r_m + 1.6r_{vci} + 1.36r_{vca}}\right\} \qquad (A2.1)$$

where C_{co_2} is the external carbon dioxide concentration (μl.l-1), Γ is the compensation point carbon dioxide concentration ($\mu l.l^{-1}$), r_m is the mesophyll resistance (s.m^{-1}), r_{vca} is the boundary layer resistance to vapour transfer (s.m^{-1}), and r_{vci} is the internal resistance to vapour transfer (s.m^{-1}). The factor 1.83 converts from ppm to mgCO2.m^{-3}. The factor 1.6 relates carbon dioxide diffusion rate to that of water vapour in a purely diffusive environment, and the factor 1.36 relates the diffusion rate of carbon dioxide to water vapour for a convective process.

In chapter 5 it was shown that the rate of transpiration was given by equation 5.94, which is repeated here:

$$f_{ca} = \frac{2LAI}{(r_{vca} + r_{vci})}(\chi_c' - \chi_a) \qquad (A2.2)$$

where f_{ca} is the transpiration rate (g.m-2floor.s-1), LAI is the leaf area index (m^{2}leaf.m^{-2}floor), χ_c' is the saturation vapour concentration of the crop (g.m^{-3}), and χ_a is the vapour concentration of the air (g.m^{-3}).

From this is can be seen that:

$$r_{vci} = \frac{2LAI}{f_{ca}}(\chi_c' - \chi_a) - r_{vca} \qquad (A2.3)$$

Thus if all the right hand variables are determined by measurement the internal leaf resistance can be estimated.

A2.2 RESULTS

Equation A2.3 was used to determine leaf internal resistance from a series of measurements in the greenhouse. The period from 90 to 94 days after sowing was chosen as the leaf area was reasonably constant at this time (see Figure 6.4). The leaf area index was determined from the non-destructive measurements of leaf dimensions. The transpiration rate was determined from sequential lysimeter readings, and the vapour concentrations from measurements of leaf temperatures, and wet and dry bulb temperatures of the inside air. The boundary layer resistance was estimated using the correlations described in section 5.4.7, the leaf temperature, inside air temperature, and inside air speed. When drainage occurred from the lysimeter it was not possible to determine an accurate transpiration rate and all such data points were excluded.

The results were initially plotted against those variables which were expected to influence the internal resistance. Figure A2.1 shows the internal resistance plotted against the vapour pressure deficit between the leaf and the inside air. The highly correlated points to the left of the graph were predominantly for night conditions and showed that the internal resistance increased as the vapour pressure deficit increased. This was consistent with previous findings (Avissar et al, 1985, Stanghellini, 1987). During the day the relationship was less obvious and pointed to the influence of other factors.

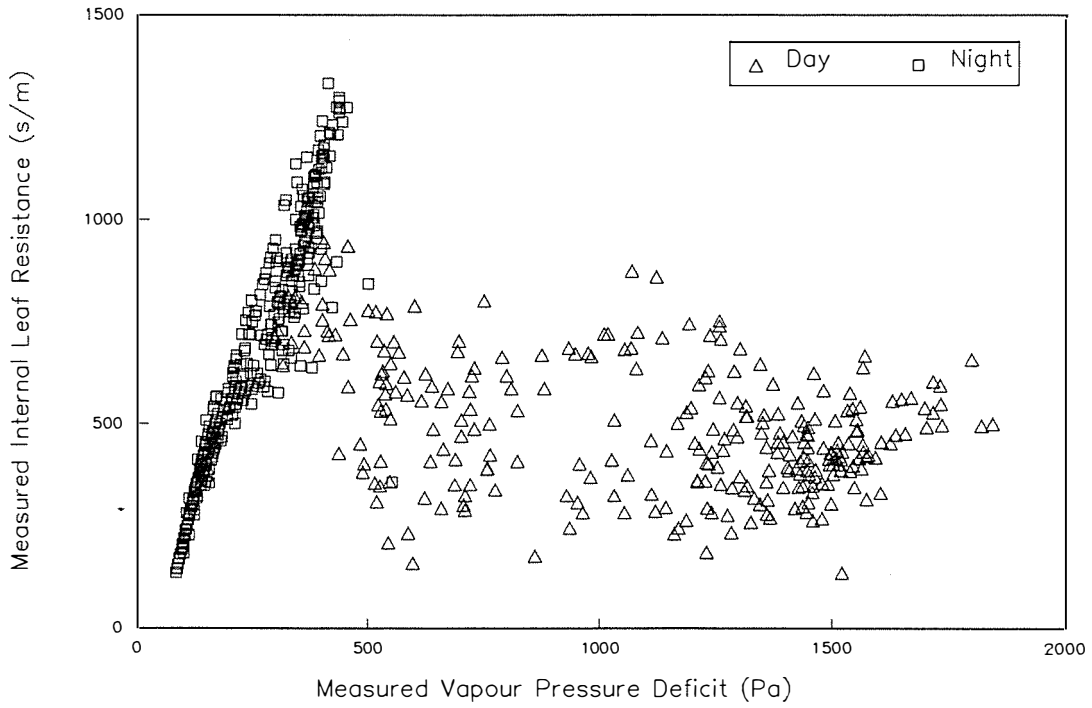

Figure A2.1 Measured Internal Leaf Resistance versus Leaf to Air Vapour Pressure Deficit

Figure A2.2 shows the variation of internal resistance with solar radiation absorbed within the leaf canopy for day time measurements only. Despite considerable variance, due to other factors, there was a discernible trend of decreasing resistance with increasing solar radiation levels. Again this was consistent with previous findings (Behboudian, 1977, Avissar et al, 1985, Stanghellini, 1987, Yang et al, 1989). Bell (1982) proposed a model of stomatal functioning which presupposed that the internal leaf resistance would adjust to maintain the internal carbon dioxide concentration of the leaf at a constant ratio of the carbon dioxide concentration external to the leaf. He then showed, as a consequence of this, that at constant external carbon dioxide concentration the internal resistance would decrease as photosynthesis increased due to increasing light levels.

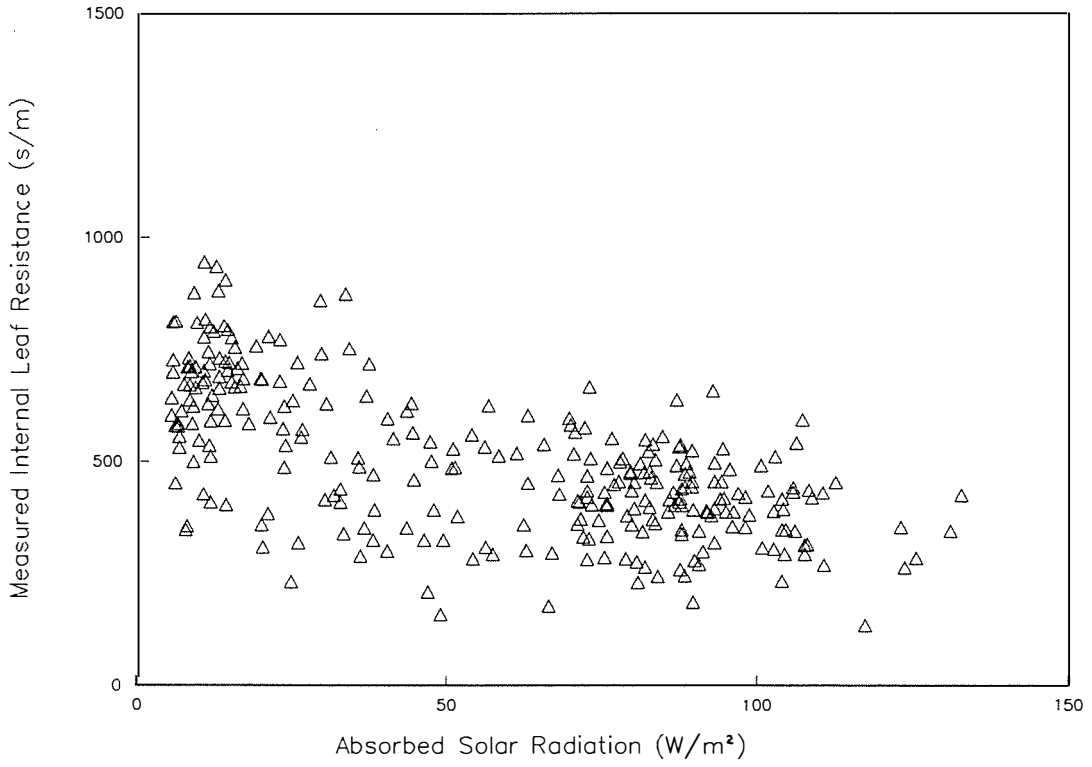

Figure A2.2 Measured Internal Leaf Resistance versus Solar Radiation absorbed in the Leaf Canopy.

In Figure A2.3 internal leaf resistance is plotted against leaf temperature. The points on the left hand side of the graph, at lower temperature, were predominantly night time measurements. While the data was very scattered it appeared that some temperature effect was present, with a minimum at around 30°C. Several authors (Takakura et al, 1975, Avissar et al, 1985, Stanghellini, 1987) have arrived at similar conclusions. It could be postulated that this was another consequence of the leaf trying to maintain a constant ratio of internal to external carbon dioxide

concentration. As temperature departs from about 30°C the mesophyll conductance decreases (see Figure 6.7), causing a decrease in photosynthesis, and consequently an increase in internal resistance.

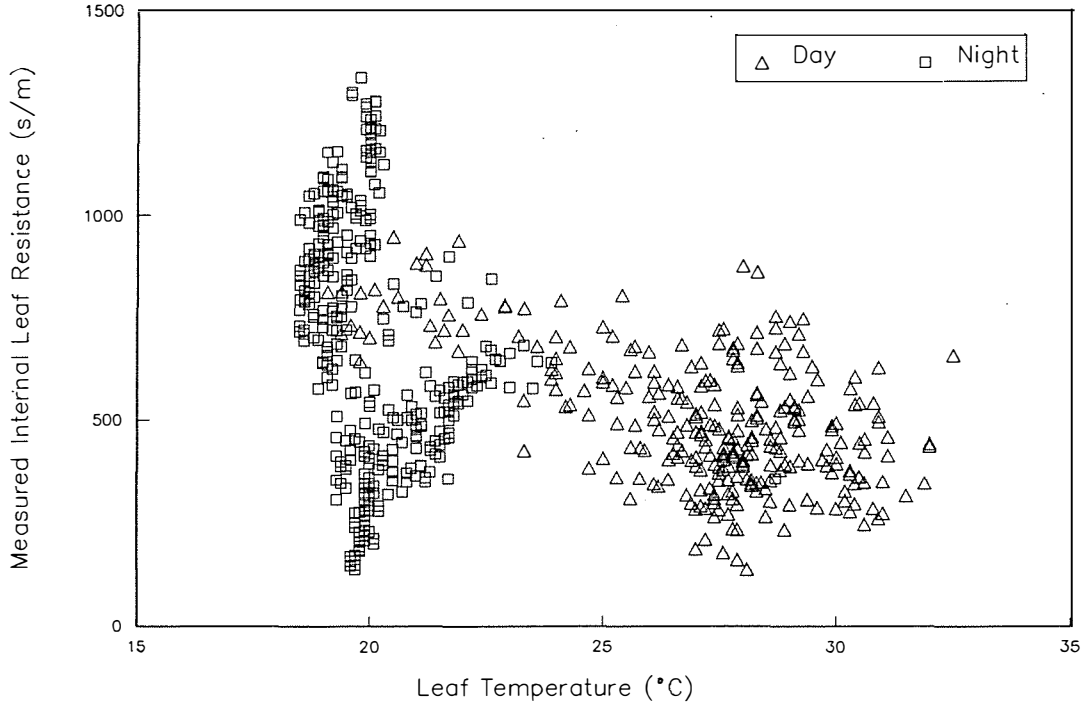

Figure A2.3. Measured Internal Leaf Resistance versus Leaf Temperature.

Several authors have suggested that internal resistance is a strong function of carbon dioxide concentration (Penning de Vries, 1972, Takakura et al, 1975, Bell, 1982). All these authors have suggested that internal resistance will increase with external carbon dioxide concentration in order to maintain the ratio of internal to external carbon dioxide concentration. Other authors have suggested that for well watered greenhouse crops the response to carbon dioxide concentration may be minimal (Stanghellini, 1987, Marcelis, 1989). Figure A2.4 shows the measured internal resistance plotted against carbon dioxide concentration of the inside air during the test period. Note that the points on the right hand, at higher carbon dioxide concentrations, were predominantly night time measurements. Neither during the day nor the night was there an apparent relationship between internal resistance and carbon dioxide concentration. The night time variations were most likely due to variations in other factors, particularly vapour pressure deficit.

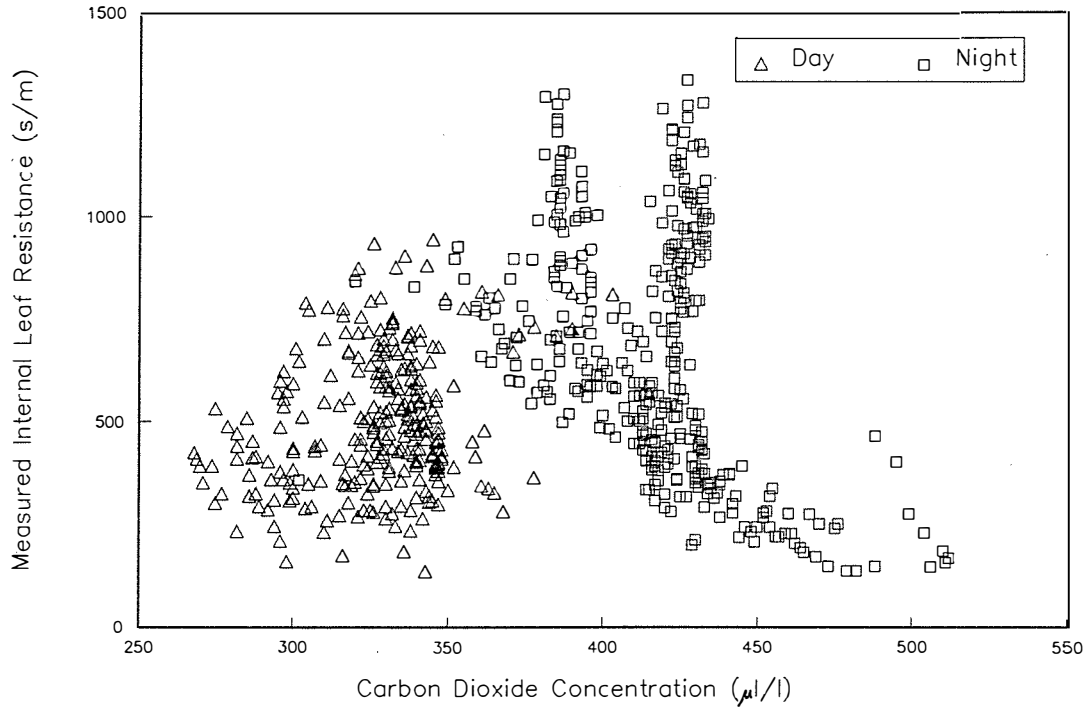

Figure A2.4. Measured Internal Leaf Resistance versus Carbon Dioxide Concentration of the Greenhouse Air.

After detailed consideration of the work of Stanghellini (1987) and Yang et al (1989) and some experimentation it was decided to fit a multiplicative model to the data of the form:

$$r_{Vci} = r_{min}\left\{1.0 + A_1(p_c' - p_a)e^{-A_2 B_{cave}}\right\}\{1.0 + A_3(T_c - T_{opt})^2\} \qquad (A2.4)$$

where r_{min} is the minimum internal resistance ($s.m_{-1}$), p_c' is the saturation vapour pressure (Pa) at the leaf temperature T_c ($^\circ$C), p_a is the vapour pressure of the air inside the greenhouse (Pa), $\overline{B}_c$ is the mean solar radiation absorbed in the leaf canopy averaged over the entire leaf surface area ($W.m^{-2}$), T_{opt} is the temperature for minimum internal resistance ($^\circ$C), and A_1, A_2, and A_3 are the parameters to be determined.

The concept of using mean absorbed solar radiation rather than solar radiation incident at the top of the leaf canopy is justified by Stanghellini (1987) on the basis that as the leaf area index of the leaf canopy increases the actual radiant intensity eliciting stomatal response decreases. The mean absorbed solar radiation is given by:

$$\overline{B}_c = \frac{B_c}{2LAI} \qquad (A2.5)$$

where B_c is the solar radiation absorbed within the leaf canopy ($W.m^{-2}$), and is given by equation 5.57.

Using the Nelder-Meades simplex non-linear fitting technique (Dennis & Woods, 1987) the following best fit parameters were determined.

$$r_{Vci} = 45\left\{1.0 + 0.02(p'_c - p_a)e^{-0.015B_{cave}}\right\}\{1.0 + 0.015(T_c - 30.0)^2\} \qquad (A2.6)$$

Figure A2.5 shows the measured internal leaf resistance versus the simulated internal leaf resistance. The correlation coefficient R^2 was equal to 0.84, which indicated that the fit of the model was sufficiently good to be used within the greenhouse energy and mass balance simulation.

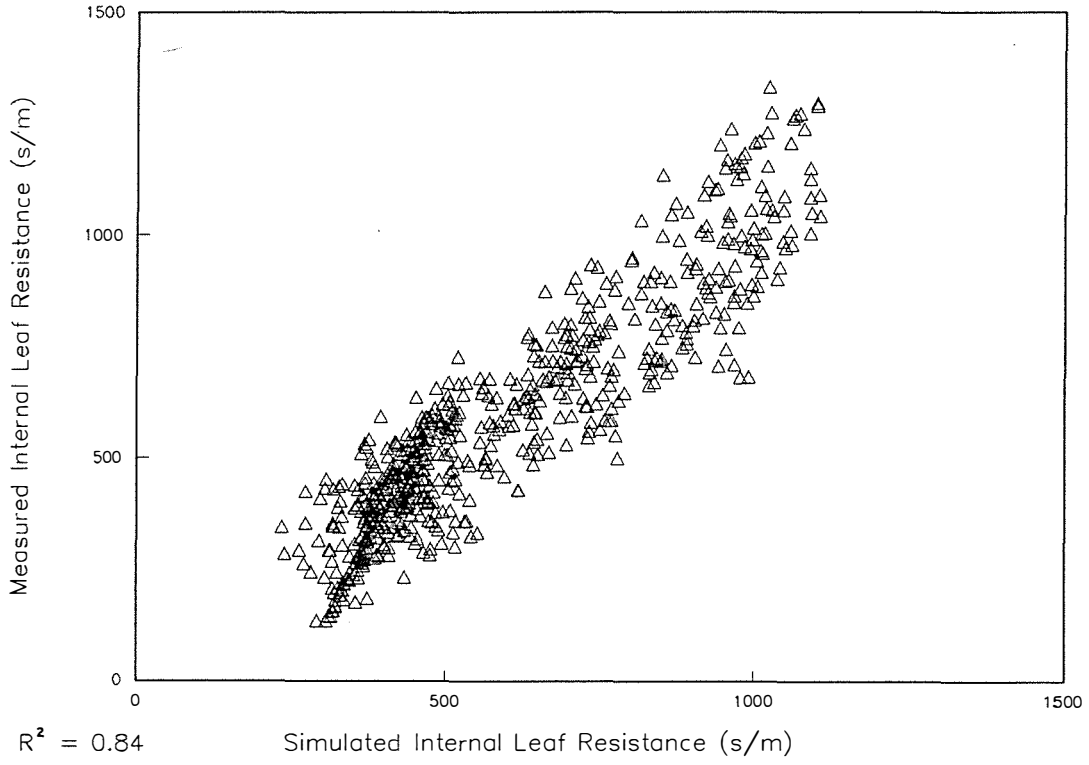

Figure A2.5. Measured Internal Leaf Resistance versus Simulated Internal Leaf Resistance.

A3 PROGRAM LISTINGS AND DATA FILES

A3.1 GREENHOUSE SIMULATION MODEL

The greenhouse simulation model, written in ESL (Hay et al, 1988) in lisited in the following sections. The input data file SIMPUT is listed in section A3.1.13 and the initial plant data INPUT14.CEL in section A3.1.14. The direct and diffuse transmission and absorption data for the greenhouse SKY.DAT and DIFF.DAT are listed in sections A3.2.4 and A3.2.6 respectively.

A3.1.1 Main Simulation Model

```
--
-- File CUCUMBER.ESL
--
-------------------------------------------------------------------------
-- ESL Simulation program CUCUMBER
-- Simulates greenhouse environment and cucumber growth
-------------------------------------------------------------------------
-- Begin the simulation
--
STUDY
--
-- Include models, subroutines, and functions from other files
--
INCLUDE "GLOBAL";
INCLUDE "GEN2";
INCLUDE "SOIL";
INCLUDE "CONVHT";
INCLUDE "INDATA";
INCLUDE "VARIDATA";
INCLUDE "SOLAR";
INCLUDE "DEVELOP";
INCLUDE "PHOTOSYN";
INCLUDE "GROWTH";
INCLUDE "GEMB";
--
--EXPERIMENT
--
USE GLOBAL;
--
-- Simulation variables for the greenhouse model
--
  REAL : Tgi/18.3/,Xgi/0.0/;
  REAL : Tsi/19.0/;
```

```
  REAL : Tai/21.1/,Xai/45.0/;
  REAL : Tci/20.0/,Xci;
  REAL : Tmi/22.7/,Xmi;
  REAL : Tfi/24.0/,Tli/24.0/,T2i/24.0/,T3i/24.0/,T4i/24.0/,T5i/22.0/;
  REAL : XCO2ai;
--
  REAL : Tg,Xg;
  REAL : Ts;
  REAL : Ta,Xa;
  REAL : Tc,Xc;
  REAL : Tm,Xm;
  REAL : Tf,Tl,T2,T3,T4,T5;
  REAL : XCO2a;
--
-- Input and output file specifiers
--
  CHARACTER : Filename(17);
  INTEGER : Err,IJ,Numl,Num2;
--
  FILE : Infile,Outl,Out2,Out3,Out4;
--
-- Read and calculate input parameters
--
  INDATA;
  VARIDATA;
--
-- Initialize crop and root medium moisture content
-- Initialize carbon dioxide content
--
  Xmi := 0.9*Xmmax;
  Xci := 0.9*Xcmax;
  XCO2ai := da*XiCO2a;
--
-- MAIN LOOP FOR READING BOUNDARY CONDITION FILES
--
FOR IJ := 14..26 LOOP
--
-- Open output files and input files
--
  Numl := INT(IJ/10)+48;
  Num2 := IJ - (Numl-48)*10 + 48;
--
-- Main 5 minute output file
--
  Filename(1..14) := "c:\output\outp";
  Filename(15) := ACHAR(Numl);
```

```
  Filename(16) := ACHAR(Num2);
  Filename(17) := ".";
  REWRITE Out1,Filename;
--
-- 5 minute output of heat and mass flow rates
--
  Filename(11..14) := "flow";
  REWRITE Out2,Filename;
--
-- 5 minute output of variable parameters
--
  Filename(11..14) := "para";
  REWRITE Out3,Filename;
--
-- Main daily output file of plant data
--
  Filename(11..14) := "leaf";
  REWRITE Out4,Filename;
--
-- 5 minute boundary value inputs. 1 week in each file
--
  Filename(1..14) := "c:\input\bound";
  OPEN Infile,Filename;
--
-- Beginning of loop to read boundary value file
--
  LOOP
--
-- Set simulation finish time TFIN and communication interval CINT
-- to 300 seconds (= 5 minutes). Force maximum simulation step to be
-- 30 seconds (NSTEP = 10)
--
    TFIN := 300;
    CINT := 300;
    NSTEP := 10.0;
--
-- Read Boundary values from Infile
-- Year, Day, Hour, Minute, Outside Dry Bulb Temp, Outside Wet Bulb Temp
-- Deep Ground Temp, Outside Wind Speed, Global Solar Radiation,
-- Solar Altitude, Solar Azimuth, Opening of Top Ventilators,
-- Opening of Bottom Ventilators, Heater Input,
-- Heater Temperature Diff, Irrigation Amount
--
    READ InFile,Y,Day,Hr,Min,To,Tow,Td,Uo,Sg,SAlt,SAzi,
              Top,Bot,Ht,delT,Irr,IOSTAT=Err;
--
```

```
-- On end of file terminate this loop
--
    TERMINATE Err /= 0;
--
-- Scale input values
--
    To := To/10.0;
    Tow := Tow/10.0;
    Td := Td/10.0;
    Uo := Uo/100.0;
    Top := Top/100.0;
    Bot := Bot/100.0;
    delT := delT/10.0;
    firr := Irr*Nplant/(TFIN*Af);
--
-- Work out if it is the right time to pick fruit (10 o'clock)
--
    IF (Hr = 10.0) AND (Min = 0.0) THEN
      PickTime := TRUE;
    ELSE
      PickTime := FALSE;
    END_IF;
--
-- Calculate solar radiation transmission and absorption and
-- gross photosynthesis
--
    IF (Sg = 0.0) OR (SAlt <= 0.0) THEN
      Bg := 0.0; Bs :=0.0; Bc := 0.0; Bm := 0.0; Bf := 0.0;
      Bcave := 0.0; Bpar := 0.0; FGross := 0.0; Assim := 0.0;
    ELSE
      SOLAR;
      PHOTOSYN(:=Tci);
    END_IF;
--
-- Calculate growth of plant and respiration;
--
    GROWTH(:=Tci);
--
-- Select appropriate simulation algoritmn
-- Night : 2nd order Runge-Kutta with fixed step length
-- Day : 4th/5th order Runge-Kutta with variable step length
--
    IF (Sg = 0.0) THEN ALGO := 3; ELSE ALGO := 1; END_IF;
--
-- Call the Greenhouse Energy and Mass Balance Model
--
```

```
    GEMB(Tg,Ts,Ta,Tc,Tm,Tf,T1,T2,T3,T4,T5,Xg,Xa,Xc,Xm,XCO2a :=
         Tgi,Tsi,Tai,Tci,Tmi,Tfi,T1i,T2i,T3i,T4i,T5i,
         Xgi,Xai,Xci,Xmi,XCO2ai);
--
-- Calculate RH, wet bulb temperature and carbon dioxide concentration
-- at end of 5 minute period
--
    esat := 611.0*exp(17.27*Ta/(Ta+237.3));
    RH := 100.0*ea/esat;
    Taw := Ta - ((esat - ea)/((esat*Lamd*Mw)/
                (R*(Ta+273.15)**2.0)+Gamma));
    CO2a := XCO2a*1e3*R*(Ta+273.15)/(da*1.52*Ma*(Po-ea));
--
-- Output
-- Main 5 minute output
--
    PRINT Out1,Day:6.1,Hr:6.1,Min:6.1,Tg:6.1,Ts:6.1,
     Ta:6.1,Taw:6.1,Tc:6.1,Tm:6.1,
     Tf:6.1,T3:6.1,T5:6.1,
     RH:6.1,fca:10.6,fma:10.6,fup:10.6,
     fvent:10.6,fGross:10.6,fResp:10.6,fGrowth:10.6,CO2a:5.0,
     Wleaf:8.1,Wstem:8.1,Wroot:8.1,WfruitM:8.1,WfruitL:8.1,
     Reserve:8.2,SLA:8.3;
--
-- Heat and mass exchange rates
--
    PRINT Out2,Bg:8.1,Bs:8.1,Bc:8.1,Bf:8.1,
          Cgo:8.1,Cga:8.1,Csa:8.1,Cca:8.1,
          Cma:8.1,Cfa:8.1,Cao:8.1,Cha:8.1,
          Rgsky:8.1,Rsg:8.1,Rcg:8.1,Rcs:8.1,
          Rmg:8.1,Rms:8.1,Rmc:8.1,Rfg:8.1,Rfs:8.1,Rfc:8.1,Rfm:8.1,
          Gsg:8.1,Gfm:8.1,
          Gf1:8.1,G12:8.1,G23:8.1,G34:8.1,G45:8.1,G5d:8.1,
          LEga:8.1,LEca:8.1,LEma:8.1,Eao:8.1,
          fga:10.6,fao:10.6;
--
-- Variable parameters
--
    PRINT Out3,hCgo:8.2,hCga:8.2,hCsa:8.2,hCca:8.2,hCma:8.2,hCfa:8.2,
          hao:8.2,
          hRgsky:8.2,hRsg:8.2,hRcg:8.2,hRcs:8.2,
          hRmg:8.2,hRms:8.2,hRmc:8.2,
          hRfg:8.2,hRfs:8.2,hRfc:8.2,hRfm:8.2,Agdr:8.3,Agdf:8.3,
          Asdr:8.3,Asdf:8.3,Acpdr:8.3,Acpdf:8.3,Acndr:8.3,Acndf:8.3,
          Taugdr:8.3,Taugdf:8.3;
--
```

```
-- Output to screen on hour
--
    IF (Min = 55.0) THEN
      TABULATE Day,Hr,Tg,Ts,Ta,Tc,Tm,Tf,RH,Xg,Xc,Xm,CO2a;
    END_IF;
--
-- Update initial conditions for next simulation period
--
    Tgi := Tg;  Tsi := Ts;  Tai := Ta;  Tci := Tc;  Tmi := Tm;
    Tfi := Tf;  Tli := Tl;  T2i := T2;  T3i := T3;  T4i := T4;
    T5i := T5;
    Xgi := Xg;  Xai := Xa;  Xci := Xc;  Xmi := Xm; XCO2ai := XCO2a;
--
-- Sum for Average Leaf Temp and incident PAR at top of crop
--
     TSum := TSum + Tci;
     LSum := LSum + Bpar;
     Count := Count + 1.0;
--
-- At end of day updata LAI by growing the leaves
--
    IF (Hr = 23) AND (Min = 55.0) THEN
--
--    DEVELOP;
--
-- Update parameters which change on a daily basis
--
      VARIDATA;
--
-- Output plant data to screen
--
      TABULATE PMain,UMain,PLat,ULat,NolM,NolL,AreaM,AreaL,AREA;
--
-- Output plant data to file
--
      PRINT Out4,Day,Light:6.1,Temp:6.1,
            AreaM:9.1,AreaL:9.1,AREA:9.1,NoLM:5,NoLL:5,NOL:5,
            NoFruitA:6,NofruitH:6,WfruitH:10.1,
            Wleaf:8.1,Wstem:8.1,Wroot:8.1,Wfruit:8.1;
--
-- End of daily update section
--
    END_IF;
--
-- end of loop to read 5 minutes of boundary condition data
--
```

```
  END_LOOP;
--
-- Close the output files for week
--
  CLOSE Infile;
  CLOSE Outl;
  CLOSE Out2;
  CLOSE Out3;
  CLOSE Out4;
--
-- end of loop for week of boundary condition data
--
END_LOOP;
--
-- When all input weeks processed end of simulation
--
  PRINT "STUDY COMPLETED";
--
END_STUDY
--
```

A3.1.2 Global Variables

```
--
-- File GLOBAL.ESL
--
-- Global variables used in the simulation model CUCUMBER.ESL
--
-------------------------------------------------------------------------
PACKAGE GLOBAL;
-------------------------------------------------------------------------
-- ESL Package GLOBAL
-------------------------------------------------------------------------
-- Universal constants
--
  CONSTANT REAL : Gamma/66.0/,R/8.31/,Mw/18.0/,Ma/29.0/,Sigma/5.67e-8/;
--
-- Densities
--
  CONSTANT REAL : rhow/1.0e6/,rhoq/2.66e6/,rhocl/2.65e6/,rhoom/1.3e6/;
--
-- Specific heat capacities
--
  CONSTANT REAL : Cpq/0.8/,Cpcl/0.9/,Cpom/1.92/,Cpw/4.18/,Cpv/1.88/;
  CONSTANT REAL : Cpa/1.01/,Cpo/1.01/;
--
```

```
-- Latent heat of vapourization of water
--
  CONSTANT REAL : Lamd/2501.0/;
--
-- Solar Constant
--
  CONSTANT REAL : Ssc/1360.0/;
--
  CONSTANT REAL : Pi/3.14159/;
--
-- Barametric pressure and outside CO2 concentration
--
  CONSTANT REAL : Po/101325.0/,CO2o/350.0/;
--
-- Greenhouse dimensions
--
  REAL : Length,Width,Gutter,Ridge,Offset,BagD,BagH;
--
-- Volumes (m3)
--
  REAL : Va,Vgb,Vs;
--
-- Areas (m2)
--
  REAL : Aroof,Awall,Aend,Agable,Ag,Agb,As,Ah,Amtop,Amside,Am,Af;
--
-- Component thicknesses (m)
--
  REAL : dgl,da,df,dl,d2,d3,d4,d5;
--
-- Densities (g/m3)
--
  REAL : rhogl,rhogb,rhos,rhoa,rhof,rhol,rho2,rho3,rho4,rho5;
--
-- Heat capacity area densities (J/m2 floor.K)
--
  REAL : Phig,Phis,Phia,Phic,Phim,Phif,Phil,Phi2,Phi3,Phi4,Phi5;
--
-- Volumetric fractions in media,floor and soil
-- (quartz, clay, organic, water)
--
  REAL : xqm,xqf,xql,xq2,xq3,xq4,xq5;
  REAL : xclm/0.0/,xclf,xcl1,xcl2,xcl3,xcl4,xcl5;
  REAL : xomm,xomf,xoml,xom2,xom3,xom4,xom5;
  REAL : xwm,xwf,xwl,xw2,xw3,xw4,xw5;
--
```

```
-- Moisture density of floor and soil layers (g H2O/m2 floor)
--
  REAL : Xf,X1,X2,X3,X4,X5;
--
-- Maximum moisture density of crop and media (g H2O/m2 floor)
--
  REAL : Xcmax,Xmmax;
  REAL : FBark/0.5/,Field;
  CONSTANT REAL : WHCc/19.0/;
  REAL : WHCm;
  REAL : Nplant;
  REAL : DMc;
--
-- Absolute Humidity (g H2O/m3)
--
  REAL : Chio,Chig,Chiamax,Chia,Chic,Chim;
--
-- Carbon dioxide concetration (mg CO2/m3)
--
  REAL : XiCO2a/720.0/,XiCO2o;
--
-- Specific heat capacities (J/g.K)
--
  REAL : Cpgl,Cpgb,Cps;
--
-- Surface emissivities
--
  REAL : eg,es,eh,ec,em,ef;
--
-- Media, floor and soil thermal conductivities (W/m °C)
--
  REAL : km,kf,kl,k2,k3,k4,k5;
--
-- Date, time and boundary conditions
--
  REAL : Y,Day,Hr,Min;
  REAL : To,Tow,Td,Uo,Sg;
  REAL : SAlt,SAzi;
  REAL : Top,Bot,Ht,delT,Irr;
--
  REAL : Tave,Todw,Tsky,Th,esky,eo,Taw,ea,esat,RH,VPD,Bcave,Bpar,CO2a;
  REAL : TSum/0.0/,LSum/0.0/;
--
-- Area Indices (m2/m2 floor)
--
  REAL : GAI,SAI,HAI,FAI,MAI,LAI;
```

```
--
  REAL : Lg,Lf,Lc/0.1/;
  REAL : Ua/0.20/;
--
-- View Factors
--
  REAL : Fmm,Fss,Fhh,Taucb,Fcc,Fgsky,Fmf,Fmc,Fmh,Fms,Fmg;
  REAL : Ffm,Ffc,Ffh,Ffs,Ffg;
  REAL : Fcf,Fcm,Fch,Fcs,Fcg,Fsf,Fsm,Fsc,Fsh,Fsg,Fhg,Fhs,Fhc,Fhm,Fhf;
  REAL : SFgsky,SFsg,SFhg,SFhs,SFcg,SFcs,SFch,SFmg,SFms,SFmh,SFmc;
  REAL : SFfg,SFfs,SFfh,SFfc,SFfm;
  REAL : SBlock,HBlock;
--
-- Hydraulic capacities and conductivity
--
  CONSTANT REAL : Capc/0.014/,Capm/0.4/,Kmc/0.004/;
--
-- Variables for light transmission
--
  REAL : Tau(0..9,0..36),Alpha(0..9,0..36);
  REAL : Cloud/0.65/;
  REAL : Az,Div;
  REAL : Sx,So,Sdf,Sdr,Sp,Sn,Sc;
  REAL : Xcirc,SinB,CosB,Cos90B,Kbeta,Kcrit,Kt,Kd;
  REAL : Spdr,Spdf,Sndr,Sndf;
  REAL : Agdr,Agdf,Taugdr,Taugdf;
  REAL : Asdr,Asdf;
  REAL : X,Y,Sigp,Sign;
  REAL : Rhophor,Rhonhor,Rhopdf,Rhondf,Rhopdr,Rhondr;
  REAL : Rhocpdf,Rhocndf,Rhocpdr,Rhocndr;
  REAL : Acpdf,Acndf,Acpdr,Acndr;
  REAL : Taucpdf,Taucndf,Taucpdr,Taucndr;
  REAL : Kbdf,Kbdr,Kpdf,Kpdr,Kndf,Kndr;
  REAL : TauRF,StrucAF;
  REAL : Afp,Afn;
--
-- Heat and Mass Transfer Coefficients
--
  REAL : hCgo,hCga,hCsa,hCcat,hCcab,hCca,hCma,hCfa,hao;
  REAL : hRgsky,hRsg,hRhg,hRhs,hRcg,hRcs,hRch,hRmg,hRms,hRmh,hRmc;
  REAL : hRfg,hRfs,hRfh,hRfc,hRfm;
  REAL : hGsg/0.6/,hGfm,hGfl,hG12,hG23,hG34,hG45,hG5d;
  REAL : rao,rVga,rVca,rVci,rVma;
  REAL : Nv;
--
-- Energy & Mass Flows
```

```
--
  REAL : Bg,Bs,Bc,Bm,Bf;
  REAL : Cgo,Cga,Csa,Cca,Cma,Cfa,Cao,Cha;
  REAL : Gsg,Gfm,Gfl,Gl2,G23,G34,G45,G5d;
  REAL : Rgsky,Rsg,Rhg,Rhs,Rcg,Rcs,Rch,Rmg,Rms,Rmh,Rmc;
  REAL : Rfg,Rfs,Rfh,Rfc,Rfm;
  REAL : LEga,LEca,LEma;
  REAL : Eao,Edrip,Eirr,Eup,Edrn;
  REAL : fga,fdrip,fca,fma,firr,fup,fdrn,fao,ffruit;
  REAL : Fvent,FGross,FResp,FGrowth;
  REAL : f,fprod;
--
-- Water Potentials
--
  REAL : Psic,Psim;
--
-- Variables for plant development model
--
-- Function table for dependence of N on Leaf number (Main Stem)
--
  INTEGER: TabNM/7/;
  CONSTANT REAL: NTabM(2,7)/
  1.0,0.70, 5.0,1.0, 10.0,1.25, 15.0,1.50,
  20.0,1.45, 25.0,1.40, 30.0,1.00/;
--
-- Function table for dependence of N on Leaf number (Laterals)
--
  INTEGER: TabNL/7/;
  CONSTANT REAL: NTabL(2,7)/
  1.0,0.55, 5.0,0.90, 10.0,0.65, 15.0,0.50,
  20.0,0.50, 25.0,0.50, 30.0,0.50/;
--
-- Constants for plant development model
--
  CONSTANT REAL: NecroM/40.0/,NecroL/20.0/;
  CONSTANT REAL: DFactM/3.0/,DFactL/4.0/;
  CONSTANT REAL: Prune/334.0/;
  CONSTANT REAL: Pinch/304.0/;
  CONSTANT REAL: TopNode/27.0/;
  CONSTANT REAL: Laterals/3.0/;
  CONSTANT REAL: FactorM/44000.0/;
  CONSTANT REAL: FactorL/32000.0/;
  REAL         : Init/49.0/;
--
  REAL: PMain/1.0/,PLat/1.0/;
  REAL: PMaini,PLati,KMain,KLat,A,B,UMain,ULat;
```

```
  REAL: dAdP,dBdP,dUdP;
  REAL: AreaM,AreaL,AREA,AREAi;
  REAL: LN,Light,Temp,LFact,Age,N,FDC,RGR;
  REAL: FruitM,FruitL,FruFactM,FruFactL;
  REAL: AEM,AEL,NCMi,NCLi;
  REAL: NM(30),NL(30);
  REAL: NCM(30),LM(30),ARM(30),ARMi(30);
  REAL: NCL(20),LL(20),ARL(20),ARLi(30);
--
  INTEGER: Startday/241/;
  INTEGER: NoLM,NoLL,NOL;
--
-- Variables for growth and respiration models
--
  REAL : dAREA,dAl,SLA;
  REAL : PGRleaf,PGRstem,PGRroot,PGRfruit;
  REAL : Preqleaf,Preqstem,Preqroot,Preqfruit;
  REAL : PGRfruM(10..30),PGRfruL(20);
  REAL : Assim,RespMain,PRequired,Reserve/10.0/,Ratio,ResL;
  REAL : Wleaf,Wstem,Wroot,Wfruit,WfruitM,WfruitL,WfruitH/0.0/;
  REAL : WfruM(10..30),WfruL(20);
  REAL : TFruM(10..30),TFruL(20);
  REAL : AgeFruM(10..30),AgeFruL(20);
  REAL : CO2pleaf,CO2pstem,CO2proot,CO2pfruit,CO2prod,LostFresh;
  INTEGER : NofruitH/0/,NofruitA/0/;
--
-- Parameters for fruit abortion and removal
--
  LOGICAL : PickTime/FALSE/;
  LOGICAL : AbortM(10..30),AbortL(20),HarvM(10..30),HarvL(20);
--
-- CO2 production rates during growth
--
  CONSTANT REAL : CO2leaf/0.243/;
  CONSTANT REAL : CO2stem/0.386/;
  CONSTANT REAL : CO2root/0.425/;
  CONSTANT REAL : CO2fruit/0.458/;
--
-- Assimilate requirement ratios
--
  CONSTANT REAL : ARleaf/0.795/;
  CONSTANT REAL : ARstem/1.150/;
  CONSTANT REAL : ARroot/1.217/;
  CONSTANT REAL : ARfruit/1.515/;
  CONSTANT REAL : MaxGRleaf/1.0/;
  CONSTANT REAL : PGRFmax/0.06/;
```

```
--
-- Maintenance respiration parameters
--
  CONSTANT REAL : Q10/2.0/;
  CONSTANT REAL : TempRef/25.0/;
  CONSTANT REAL : MainRoot/3.33E-7/;
  CONSTANT REAL : MainStem/3.06E-7/;
  CONSTANT REAL : MainLeaf/3.33E-7/;
  CONSTANT REAL : MainFru/1.39E-7/;
--
  CONSTANT REAL : PickW/14400.0/;
--
  CONSTANT REAL : AbortAge/12.0/,RemAge/20.0/,RemW/10000.0/;
--
-- Global Counters
--
  INTEGER : I,J;
  REAL    : Count;
--
END;
--
```

A3.1.3 Function Interpolator

```
--
-- File GEN2.ESL
--
-----------------------------------------------------------------------
PROCEDURE GEN2(INTEGER: N;REAL: TABLE(2,*),x)RETURN REAL;
-----------------------------------------------------------------------
-- Modified from original ESL submodel AFGEN2
-----------------------------------------------------------------------
-- Searches a table of x-y coordinate values and finds
-- which values span the input of x and performs a second
-- order interpolation to obtain a value for y.
-- Over any segment, a number of simple polynomial fits
-- is found and the interpolated function, y, is a
-- weighted average over two of these; the weighting
-- being a function of the independent variable.
-----------------------------------------------------------------------
  REAL: Qn,Qna,Qnb,Qnc;
  REAL: Qln,Qlna,Qlnb,Qlnc,Ycalc;
  REAL: su/0.0/,sl/0.0/,s/0.0/,w/0.0/;
  INTEGER: i;
--
  IF x < TABLE(1,1) THEN
```

```
    Ycalc:= TABLE(2,1);
  ELSE_IF x >= TABLE(1,N) THEN
    Ycalc:= TABLE(2,N);
  ELSE
    i := N;
    WHILE x < TABLE(1,i) LOOP
      i:= i-1;
    END_LOOP;
    WHILE x >= TABLE(1,i+1) LOOP
      i:= i+1;
    END_LOOP;
    s:= (x-TABLE(1,i))/(TABLE(1,i+1)-TABLE(1,i));
    IF s < 1.0e-12 THEN
      w:= 1.0;
    ELSE
      w:= 1.0-s*s*(3.0-2.0*s);
    END_IF;
    IF i = 1 THEN
--
-- take Qn as line Qn=TABLE(2,1)
--
      Qna:= TABLE(2,1);Qnb:= 0.0;Qnc:= 0.0;
    ELSE
      sl:= -(TABLE(1,i)-TABLE(1,i-1))/(TABLE(1,i+1)-TABLE(1,i));
        Qna:= TABLE(2,i);
        Qnc:= ((sl*TABLE(2,i+1)-TABLE(2,i-1))/(1.0-sl)+Qna)/sl;
        Qnb:= TABLE(2,i+1)-Qna-Qnc;
      END_IF;
      IF i = N-1 THEN
--
-- take Qln as line Qln = TABLE(2,N)
--
      Qlna:= TABLE(2,N);Qlnb:= 0.0;Qlnc:= 0.0;
    ELSE
      su:= (TABLE(1,i+2)-TABLE(1,i))/(TABLE(1,i+1)-TABLE(1,i));
      Qlna:= TABLE(2,i);
      Qlnc:= ((su*TABLE(2,i+1)-TABLE(2,i+2))/(1.0-su)+Qlna)/su;
      Qlnb:= TABLE(2,i+1)-Qlna-Qlnc;
    END_IF;
    Qn:= Qna+s*(Qnb+s*Qnc);
    Qln:= Qlna+s*(Qlnb+s*Qlnc);
    Ycalc:= Qn*w+Qln*(1.0-w);
  END_IF;
--
  RETURN Ycalc;
```

```
--
END GEN2;
--
```

A3.1.4 Soil Thermal Properties Routine

```
--
-- File SOIL.ESL
--
-------------------------------------------------------------------------
PROCEDURE SOIL (REAL : xq,xc,xo,xw,fc) RETURN REAL;
-------------------------------------------------------------------------
-- ESL Subroutine SOIL
-- Finds soil thermal conductivity using method
-- of ten Berge (1986) based on De Vries (1963)
-- Inputs xq = volume fraction of quartz minerals
--        xc = volume fraction of clay minerals
--        xo = volume fraction of organic material
--        xw = volume fraction of water
--        fc = volume fraction of water at field capacity
-------------------------------------------------------------------------
-- Thermal conductivies of soil components
--
  CONSTANT REAL : kq/8.8/,kc/0.9/,ko/1.92/,kw/0.57/,ka/0.025/;
--
  REAL : xa,e,ga,k02,k05,kfcsa,kfsa,kfcsw,kfsw,k;
  REAL : faw,fqw,fcw,fow,fww,faa,fqa,fca,foa,fwa;
--
-- Air content (xa) and porosity (e)
--
  xa := 1 - xq - xc - xo - xw;
  e := xa + xw;
--
-- Depolarization factor for ellispsoid
--
  IF xw > fc THEN
    ga := 0.333 - (xa/e)*0.298;
  ELSE
    ga := 0.013 + (xw/fc)*0.085;
  END_IF;
--
  faw := 0.333*(2.0/(1.0+((ka/kw)-1.0)*ga) +
                    1.0/(1.0+((ka/kw)-1.0)*(1.0-2.0*ga)));
  fqw := 0.333*(2.0/(1.0+((kq/kw)-1.0)*ga) +
                    1.0/(1.0+((kq/kw)-1.0)*(1.0-2.0*ga)));
  fcw := 0.333*(2.0/(1.0+((kc/kw)-1.0)*ga) +
```

```
                    1.0/(1.0+((kc/kw)-1.0)*(1.0-2.0*ga)));
  fow := 0.333*(2.0/(1.0+((ko/kw)-1.0)*ga) +
                    1.0/(1.0+((ko/kw)-1.0)*(1.0-2.0*ga)));
  fww := 1.0;
  faa := 1.0;
  fqa := 0.333*(2.0/(1.0+((kq/ka)-1.0)*ga) +
                    1.0/(1.0+((kq/ka)-1.0)*(1.0-2.0*ga)));
  fca := 0.333*(2.0/(1.0+((kc/ka)-1.0)*ga) +
                    1.0/(1.0+((kc/ka)-1.0)*(1.0-2.0*ga)));
  foa := 0.333*(2.0/(1.0+((ko/ka)-1.0)*ga) +
                    1.0/(1.0+((ko/ka)-1.0)*(1.0-2.0*ga)));
  fwa := 0.333*(2.0/(1.0+((kw/ka)-1.0)*ga) +
                    1.0/(1.0+((kw/ka)-1.0)*(1.0-2.0*ga)));
  k02 := 1.25*(fwa*0.02*kw+fqa*xq*kq+fca*xc*kc+foa*xo*ko+faa*(e-0.02)*ka)/
         (fwa*0.02+fqa*xq+fca*xc+foa*xo+faa*(e-0.02));
  k05 := (fww*0.05*kw+fqw*xq*kq+fcw*xc*kc+fow*xo*ko+faw*(e-0.02)*ka)/
         (fww*0.05+fqw*xq+fcw*xc+fow*xo+faw*(e-0.02));
  kfcsa := fqa*xq*kq+fca*xc*kc+foa*xo*ko;
  kfsa := fqa*xq+fca*xc+foa*xo;
  kfcsw := fqw*xq*kq+fcw*xc*kc+fow*xo*ko;
  kfsw := fqw*xq+fcw*xc+fow*xo;
--
  IF xw < 0.02 THEN
-- Air is continuous medium
    k := 1.25*(fwa*xw*kw+kfcsa+faa*xa*ka)/(fwa*xw+kfsa+faa*xa);
  ELSE_IF xw > 0.05 THEN
-- Water is continuous medium
    k := (fww*xw*kw+kfcsw+faw*xa*ka)/(fww*xw+kfsw+faw*xa);
  ELSE
-- Interpolate between xw = 0.02 and xw = 0.05
    k := k02 + (xw-0.02)*(k05-k02)/0.03;
  END_IF;
  RETURN k;
--
END SOIL;
--
```

A3.1.5 Convective Heat Transfer Coefficient Routine

```
--
-- File CONVHT.ESL
--
-----------------------------------------------------------------------
PROCEDURE CONVHT(REAL: U,D,Ts,Ta,Side) RETURN REAL;
-----------------------------------------------------------------------
-- ESL Function CONVHT
```

```
-- Calculates the Nusselt number based on correlations from
-- Monteith and Unsworth (1989) and returns the
-- convective heat transfer coefficient (W/m2.K)
-- Inputs U = wind speed (m/s)
--        D = characteristic dimension (m)
--       Ts = Surface temperature (°C)
--       Ta = Air temperature (°C)
--     Side = code for side of surface in question
--          > 0 top side
--          < 0 bottom side
--          = 0 vertical surface
-------------------------------------------------------------------------
  CONSTANT REAL : g/9.81/;
  CONSTANT REAL : v0/13.3E-6/;
  CONSTANT REAL : K0/18.1E-6/;
  REAL: Tm,Corr,K,v,Re,Gr,Bound,A,B,m,n,Nufor,Nufre,Nu,h;
  LOGICAL : Stable,Forced, Free;
--
  Free   := FALSE;
  Forced := FALSE;
  Stable := FALSE;
--
-- Check for stable conditions
--
  IF ((Side < 0) AND (Ts > Ta)) OR ((Side > 0) AND (Ts < Ta)) THEN
    Stable := TRUE;
  END_IF;
--
-- Calculate RE and GR
--
  Tm := (Ts+Ta)/2.0;
  Corr := 1.0 + 0.007*Tm;
  K := 1200.0*K0*Corr;
  v := v0*Corr;
  Re := U*D/v;
  Gr := g*D*D*D*ABS(Ts - Ta)/((Tm+273.15)*v*v);
  Bound := Gr/(Re*Re);
--
-- Test for transition region
--
  IF Bound < 10.0 THEN
    Forced:= TRUE;
  END_IF;
--
  IF Bound > 0.33 THEN
    Free := TRUE;
```

```
  END_IF;
--
-- Forced convection parameters
--
  IF Forced THEN
    IF Re > 2E4 THEN
      A := 0.032;
      n := 0.8;
    ELSE
      A := 0.60;
      n := 0.5;
    END_IF;
  ELSE
     A := 0.00;
     n := 1.0;
  END_IF;
--
-- Free convection parameters
--
  IF Free THEN
    IF Side = 0 THEN
      IF Gr > 1E9 THEN
        B := 0.11;
        m := 0.33;
      ELSE
        B := 0.58;
        m := 0.25;
      END_IF;
    ELSE
      IF Stable THEN
        B := 0.23;
        m := 0.25;
      ELSE_IF Gr > 1E5 THEN
        B := 0.13;
        m := 0.33;
      ELSE
        B := 0.50;
        m := 0.25;
      END_IF;
    END_IF;
  ELSE
        B := 0.00;
        m := 1.0;
  END_IF;
--
-- Calculate Nussult numbers
```

```
--
  Nufor := A*Re**n;
  Nufre := B*Gr**m;
  Nu := (Nufor**3.0 + Nufre**3.0)**(1.0/3.0);
--
-- Convective heat transfer coefficient
--
  h := Nu*K/D;
  RETURN h;
--
END CONVHT;
--
```

A3.1.6 Data Input and Initialization Routine

```
--
-- File INDATA.ESL
--
------------------------------------------------------------------------
PROCEDURE INDATA;
------------------------------------------------------------------------
-- ESL Subroutine INDATA
-- Reads input data from:
--       DIFF5 = diffuse radiation transmission and absorption
--        SKY5 = direct radiation transmission and absorption
-- INPUT14.CEL = initial cell counts for all leaves
--      SIMPUT = simulation parameters
-- Initializes simulation parameters
------------------------------------------------------------------------
USE GLOBAL;
--
  REAL : Dummy;
--
  FILE : Tranfile,Datafile,Leafile;
--
-- Read light transmission table (diffuse and direct light)
--
  OPEN Tranfile, "c:\input\diff5.";
  READ Tranfile;
  READ Tranfile,Tau(0,0),Alpha(0,0);
  CLOSE Tranfile;
--
  OPEN Tranfile,"c:\input\sky5.";
  READ Tranfile;
  FOR I := 1..9 LOOP
    FOR J := 1..I*4 LOOP
```

```
      READ Tranfile,Tau(I,J),Alpha(I,J);
    END_LOOP;
  END_LOOP;
  CLOSE Tranfile;
--
-- Read initial leaf cell numbers
--
  OPEN Leafile, "c:\input\inputl4.cel";
  READ Leafile,Dummy,PMain,PLat,AREA,AREAi;
  FOR I := 1..30 LOOP
    READ Leafile,NCM(I);
  END_LOOP;
  FOR I := 1..20 LOOP
    READ Leafile,NCL(I);
  END_LOOP;
  CLOSE Leafile;
--
-- Read greenhouse parameters
--
  OPEN Datafile, "c:\input\simput.";
  READ Datafile;
  READ Datafile;
  READ Datafile,Length,Width,Gutter,Ridge;
  READ Datafile;
  READ Datafile,Offset;
  READ Datafile;
  READ Datafile,rhogl,rhogb,rhos;
  READ Datafile;
  READ Datafile,Cpgl,Cpgb,Cps;
  READ Datafile;
  READ Datafile,xqf,xql,xq2,xq3,xq4,xq5;
  READ Datafile;
  READ Datafile,xclf,xcll,xcl2,xcl3,xcl4,xcl5;
  READ Datafile;
  READ Datafile,xomf,xoml,xom2,xom3,xom4,xom5;
  READ Datafile;
  READ Datafile,xwf,xwl,xw2,xw3,xw4,xw5;
  READ Datafile;
  READ Datafile,eg,es,eh,ec,em,ef;
  READ Datafile;
  READ Datafile,dgl,df,dl,d2,d3,d4,d5;
  READ Datafile;
  READ Datafile,Vgb,Vs;
  READ Datafile;
  READ Datafile,As,Fss,SBlock;
  READ Datafile;
```

```
  READ Datafile,Ah,Fhh,HBlock;
  READ Datafile;
  READ Datafile,TauRF,StrucAF;
  READ Datafile;
  READ Datafile,Afp,Afn;
  READ Datafile;
  READ Datafile,Nplant,BagD,BagH,Fmm;
  READ Datafile;
  READ Datafile,X,Sigp,Sign;
  CLOSE Datafile;
--
-- Calculate Surface Areas
--
  Af := Length*Width;
  Aroof := Length*(Sqrt(Width**2.0 + (Ridge - Gutter)**2.0));
  Awall := 2.0*Length*Gutter;
  Aend := 2.0*Width*Gutter;
  Agable := Width*(Ridge - Gutter);
  Ag := Aroof + Awall + Aend + Agable;
  Amtop := Nplant*Pi*BagD*BagD/4.0;
  Amside := Nplant*Pi*BagD*BagH;
  Am := Amtop + Amside;
--
-- Area Indices (m2/m2 floor)
--
  GAI := Ag/Af;
  SAI := As/Af;
  HAI := Ah/Af;
  MAI := Am/Af;
  FAI := (Af - Amtop)/Af;
--
-- Greenhouse Volume and Average Greenhouse height (m)
--
  Va := Af*(Ridge + Gutter)/2.0;
--
-- Characteristic dimensions
--
  Lf := (Length+Width)/2.0;
  Lg := Gutter + Aroof/(2.0*Length);
--
-- Moisture content of floor and soil layers (g H20/m2 floor)
--
  Xf := df*xwf*rhow;
  Xl := dl*xwl*rhow;
  X2 := d2*xw2*rhow;
  X3 := d3*xw3*rhow;
```

```
  X4 := d4*xw4*rhow;
  X5 := d5*xw5*rhow;
--
-- Fraction of quartz minerals and organic matter in the root medium
--
  xqm := 0.3*(1.0-FBark);
  xomm := 0.3*FBark;
--
-- water holding capacity, field capacity, and maximum water concentration
-- of root medium
--
  WHCm := (0.55-0.60*FBark+2.6*FBark*FBark);
  Field := WHCm*(xqm*rhoq + xomm*rhoom)/rhow;
  Xmmax := WHCm*Amtop*BagH*(xomm*rhoom + xqm*rhoq)/Af;
--
-- Heat Capacities (solid portions) (J/m2 floor.K)
--
  Phig := GAI*dgl*rhogl*Cpgl + Vgb*rhogb*Cpgb/Af;
  Phis := Vs*rhos*Cps/Af;
  Phim := Amtop*BagH*(xomm*rhoom*Cpom + xqm*rhoq*Cpq)/Af;
  Phif := df*(xqf*rhoq*Cpq + xclf*rhocl*Cpcl + xomf*rhoom*Cpom);
  Phil := dl*(xql*rhoq*Cpq + xcll*rhocl*Cpcl + xoml*rhoom*Cpom);
  Phi2 := d2*(xq2*rhoq*Cpq + xcl2*rhocl*Cpcl + xom2*rhoom*Cpom);
  Phi3 := d3*(xq3*rhoq*Cpq + xcl3*rhocl*Cpcl + xom3*rhoom*Cpom);
  Phi4 := d4*(xq4*rhoq*Cpq + xcl4*rhocl*Cpcl + xom4*rhoom*Cpom);
  Phi5 := d5*(xq5*rhoq*Cpq + xcl5*rhocl*Cpcl + xom5*rhoom*Cpom);
--
-- Initialize fruit variables
--
  FOR I := 10..30 LOOP
    AbortM(I) := FALSE;
    HarvM(I) := FALSE;
    WfruM(I) := 0.0;
    TFruM(I) := 0.0;
  END_LOOP;
  FOR I := 1..20 LOOP
    AbortL(I) := FALSE;
    HarvL(I) := FALSE;
    WfruL(I) := 0.0;
    TFruL(I) := 0.0;
  END_LOOP;
--
-- Generate N tables.
--
  FOR I:=1..30 LOOP
    LN:=I;
```

```
    NM(I) := GEN2(TabNM,NTabM(1..2,1..TabNM),LN);
  END_LOOP;
--
  FOR I:=1..20 LOOP
    LN:=I;
    NL(I) := GEN2(TabNL,NTabL(1..2,1..TabNL),LN);
  END_LOOP;
--
-- Thermal conductivities of floor and soil layers
--
  kf := SOIL(xqf,xclf,xomf,xwf,0.09);
  k1 := SOIL(xq1,xcl1,xom1,xw1,0.09);
  k2 := SOIL(xq2,xcl2,xom2,xw2,0.09);
  k3 := SOIL(xq3,xcl3,xom3,xw3,0.09);
  k4 := SOIL(xq4,xcl4,xom4,xw4,0.09);
  k5 := SOIL(xq5,xcl5,xom5,xw5,0.09);
--
-- Initialize LAI and plant organ dry weights
--
  LAI := AREA*Nplant/(Af*10000.0);
  Wleaf := LAI*Af*20000.0/Nplant;
  Wstem := (10.0/77.0)*Wleaf;
  Wroot := (13.0/77.0)*Wleaf;
  WFruit := 0.0;
--
-- Initialize total dry matter of crop, heat capacity,
-- and maximum water holding capacity (concentration)
--
  DMc := (Wleaf+Wstem+Wroot+WFruit)/1000.0;
  Phic := DMc*Nplant*Cpom/Af;
  Xcmax := WHCc*DMc*Nplant/Af;
--
-- Initialize potential growth rates and potential assimilate
-- requirements of plant organs
--
  dAREA := (AREA - AREAi)/86400.0;
  PGRleaf := MaxGRleaf*dAREA;
  PGRstem := (10.0/77.0)*PGRleaf;
  PGRroot := (13.0/77.0)*PGRleaf;
  Preqleaf := PGRleaf*ARLeaf;
  Preqstem := PGRstem*ARstem;
  Preqroot := PGRroot*ARroot;
  PGRfruit := 0.0;
  Preqfruit := 0.0;
```

```
--
END INDATA;
--
```

A3.1.7 Daily Variable Parameter Routine

```
--
-- File VARIDATA.ESL
--
-------------------------------------------------------------------------
PROCEDURE VARIDATA;
-------------------------------------------------------------------------
-- ESL Subroutine VARIDATA
-- Updates simulation parameters which vary on a daily basis
-------------------------------------------------------------------------
USE GLOBAL;
--
-- Average depth of air accounting for growth of crop
--
  da := Va/Af - (Amtop*BagH)/Af - LAI*0.002 - Vgb/Af - Vs/Af;
--
-- Diffuse Radiation extinction coefficients, reflectivities,
-- transmissivities and apsorptivities
--
  Y := X + 1.774*(X + 1.182)**(-0.733);
  Kbdf := 0.83 + 0.115*LOG(X) - 0.077*LOG(LAI) + 0.053*LOG(X)*LOG(LAI);
  Kpdf := Kbdf*SQRT(1.0 - Sigp);
  Kndf := Kbdf*SQRT(1.0 - Sign);
  Rhophor := (1.0-SQRT(1.0 - Sigp))/(1.0+SQRT(1.0 - Sigp));
  Rhonhor := (1.0-SQRT(1.0 - Sign))/(1.0+SQRT(1.0 - Sign));
  Rhopdf := (0.90 + 0.075*LOG(X))*Rhophor;
  Rhondf := (0.90 + 0.075*LOG(X))*Rhonhor;
  Rhocpdf := Rhopdf - (Rhopdf + Afp - 1.0)*EXP(-2.0*Kpdf*LAI);
  Rhocndf := Rhondf - (Rhondf + Afn - 1.0)*EXP(-2.0*Kndf*LAI);
  Taucpdf := (1.0 - Rhocpdf)*EXP(-Kpdf*LAI);
  Taucndf := (1.0 - Rhocndf)*EXP(-Kndf*LAI);
  Acpdf := 1.0 - Rhocpdf - Taucpdf;
  Acndf := 1.0 - Rhocndf - Taucndf;
--
-- View Factors
--
  Taucb := exp(-Kbdf*LAI);
  Fcc := 1.0 - (1.0 - Taucb)/LAI;
  Fgsky := 0.60;
  Fmf := (1.0 - (Fmm*Am/Amside))/2.0;
  Fmc := (1.0 - Fmm - Fmf)*(1.0 - Taucb);
```

```
  Fms := (1.0 - Fmm - Fmf)*Taucb*SBlock;
  Fmh := (1.0 - Fmm - Fmf)*Taucb*HBlock;
  Fmg := (1.0 - Fmm - Fmf)*Taucb*(1.0 - SBlock - HBlock);
  Ffm := Fmf*MAI/FAI;
  Ffc := (1.0 - Ffm)*(1.0 - Taucb);
  Ffs := (1.0 - Ffm)*Taucb*SBlock;
  Ffh := (1.0 - Ffm)*Taucb*HBlock;
  Ffg := (1.0 - Ffm)*Taucb*(1.0 - SBlock - HBlock);
  Fcf := Ffc*FAI/(2.0*LAI);
  Fcm := Fmc*MAI/(2.0*LAI);
  Fch := (1.0 - Fcc - Fcm - Fcf)*HBlock;
  Fcs := (1.0 - Fcc - Fcm - Fcf)*SBlock;
  Fcg := (1.0 - Fcc - Fcm - Fcf)*(1.0 - SBlock - HBlock);
  Fhf := Ffh*FAI/HAI;
  Fhm := Fmh*MAI/HAI;
  Fhc := Fch*2.0*LAI/HAI;
  Fhs := (1.0 - Fhh - Fhc - Fhm - Fhf)*(SBlock);
  Fhg := (1.0 - Fhh - Fhc - Fhm - Fhf)*(1.0 - SBlock);
  Fsf := Ffs*FAI/SAI;
  Fsm := Fms*MAI/SAI;
  Fsc := Fcs*2.0*LAI/SAI;
  Fsh := Fhs*HAI/SAI;
  Fsg := 1.0 - Fss - Fsh - Fsc - Fsm - Fsf;
--
-- Script F factors for radiative transfers
--
  SFgsky := eg*Fgsky;
  SFsg := 1.0/((1.0 - es)/es + 1.0/Fsg + SAI*(1.0 - eg)/(GAI*eg));
  SFhg := 1.0/((1.0 - eh)/eh + 1.0/Fhg + HAI*(1.0 - eg)/(GAI*eg));
  SFhs := 1.0/((1.0 - eh)/eh + 1.0/Fhs + HAI*(1.0 - es)/(SAI*es));
  SFcg := 1.0/((1.0 - ec)/ec + 1.0/Fcg + 2.0*LAI*(1.0 - eg)/(GAI*eg));
  SFcs := 1.0/((1.0 - ec)/ec + 1.0/Fcs + 2.0*LAI*(1.0 - es)/(SAI*es));
  SFch := 1.0/((1.0 - ec)/ec + 1.0/Fch + 2.0*LAI*(1.0 - eh)/(HAI*eh));
  SFmg := 1.0/((1.0 - em)/em + 1.0/Fmg + MAI*(1.0 - eg)/(GAI*eg));
  SFms := 1.0/((1.0 - em)/em + 1.0/Fms + MAI*(1.0 - es)/(SAI*es));
  SFmh := 1.0/((1.0 - em)/em + 1.0/Fmh + MAI*(1.0 - eh)/(HAI*eh));
  SFmc := 1.0/((1.0 - em)/em + 1.0/Fmc + MAI*(1.0 - ec)/(2.0*LAI*ec));
  SFfg := 1.0/((1.0 - ef)/ef + 1.0/Ffg + FAI*(1.0 - eg)/(GAI*eg));
  SFfs := 1.0/((1.0 - ef)/ef + 1.0/Ffs + FAI*(1.0 - es)/(SAI*es));
  SFfh := 1.0/((1.0 - ef)/ef + 1.0/Ffh + FAI*(1.0 - eh)/(HAI*eh));
  SFfc := 1.0/((1.0 - ef)/ef + 1.0/Ffc + FAI*(1.0 - ec)/(2.0*LAI*ec));
  SFfm := 1.0/((1.0 - ef)/ef + 1.0/Ffm + FAI*(1.0 - em)/(MAI*em));
--
END VARIDATA;
--
```

A3.1.8 Solar Radiation Partitioning Routine

```
--
-- File SOLAR.ESL
--
-------------------------------------------------------------------------
PROCEDURE SOLAR;
-------------------------------------------------------------------------
-- ESL Subroutine SOLAR
-- Separates solar radiation into direct, diffuse, PAR and NIR
-- components and calculates the solar absorption at the glazing,
-- structure, crop, root medium and floor
-------------------------------------------------------------------------
USE GLOBAL;
--
-- Determin solar radiation components
--
    SinB := SIN(SAlt*Pi/180.0);
    CosB := COS(SAlt*Pi/180.0);
    Cos90B := COS((90-SAlt)*Pi/180.0);
    Sx := Ssc*(1.0 + 0.033*COS(2.0*Pi*Day/365.0));
    Kbeta := 0.847 - 1.61*SinB + 1.04*SinB**2.0;
    Kcrit := (1.47 - Kbeta)/1.66;
    So := Sx*SinB;
    Kt := Sg/So;
    IF Kt <= 0.22 THEN
      Kd := 1;
    ELSE_IF Kt <= 0.35 THEN
      Kd := 1.0 - 6.4*(Kt - 0.22)**2.0;
    ELSE_IF Kt <= Kcrit THEN
      Kd := 1.47 - 1.66*Kt;
    ELSE
      Kd := Kbeta;
    END_IF;
    Sdf := Sg*Kd;
    Sdr := Sg - Sdf;
    Xcirc := (1.0 - Kd**2.0)*Cos90B**2.0*CosB**3.0;
    Sc := Sdf*(Xcirc/(1.0 + Xcirc));
    Sdr := Sdr + Sc;
    Sdf := Sdf - Sc;
    Sp := Sg*(0.6 - 0.1*(1.0 - Kd**2.0));
    Sn := Sg - Sp;
    Spdf := Sp*(1.0 + 0.3*(1.0 - Kd**2.0)*(Sdf/Sg));
    IF Spdf > Sp THEN Spdf := Sp; END_IF;
    IF Spdf > Sdf THEN Spdf := Sdf; END_IF;
    Spdr := Sp - Spdf;
```

```
    Sndf := Sdf - Spdf;
    Sndr := Sn - Sndf;
--
-- Transmission of greenhouse. Absorption of glazing and structure
--
    I := 9 - INT(SAlt/10.0 - 0.01);
    Div := 90.0/I;
    Az := SAzi - Offset;
    IF Az < 0.0 THEN Az := 360.0 + Az; END_IF;
    J := INT(Az/Div) + 1;
    Taugdr := Tau(I,J)*TauRF;
    Taugdf := Tau(0,0)*TauRF;
    Agdr := Alpha(I,J)*(1.0 - StrucAF) + Tau(I,J)*(1.0 - TauRF);
    Agdf := Alpha(0,0)*(1.0 - StrucAF) + Tau(0,0)*(1.0 - TauRF);
    Asdr := Alpha(I,J)*StrucAF;
    Asdf := Alpha(0,0)*StrucAF;
--
-- Crop extinction coefficients, reflectivities, and absorptivities
-- for direct radiation
--
    Kbdr := SQRT(X*X + (CosB/SinB)**2.0)/Y;
    Kpdr := Kbdr*SQRT(1.0 - Sigp);
    Kndr := Kbdr*SQRT(1.0 - Sign);
    Rhopdr := Rhophor*2.0*Kpdr/(1.0+Kpdr);
    Rhondr := Rhonhor*2.0*Kndr/(1.0+Kndr);
    Rhocpdr := Rhopdr -  (Rhopdr + Afp - 1.0)*EXP(-2.0*Kpdr*LAI);
    Rhocndr := Rhondr -  (Rhondr + Afn - 1.0)*EXP(-2.0*Kndr*LAI);
    Taucpdr := (1.0 - Rhocpdr)*EXP(-Kpdr*LAI);
    Taucndr := (1.0 - Rhocndr)*EXP(-Kndr*LAI);
    Acpdr := 1.0 - Rhocpdr - Taucpdr;
    Acndr := 1.0 - Rhocndr - Taucndr;
--
-- Solar radiation absorption by glazing, structure, crop, root medium
-- and floor
--
    Bg := Agdr*Sdr + Agdf*Sdf;
    Bs := Asdr*Sdr + Asdf*Sdf;
    Bc := Acpdr*Taugdr*Spdr + Acpdf*Taugdf*Spdf +
          Acndr*Taugdr*Sndr + Acndf*Taugdf*Sndf;
    Bm := (Afp*Taucpdr*Taugdr*Spdr + Afp*Taucpdf*Taugdf*Spdf +
          Afn*Taucndr*Taugdr*Sndr + Afn*Taucndf*Taugdf*Sndf)*(1.0-FAI);
    Bf := (Afp*Taucpdr*Taugdr*Spdr + Afp*Taucpdf*Taugdf*Spdf +
          Afn*Taucndr*Taugdr*Sndr + Afn*Taucndf*Taugdf*Sndf)*FAI;
--
-- Average absorbed solar radiation in the crop per unit leaf area
--
```

```
    Bcave := Bc/(2.0*LAI);
--
-- Photosynthetically active radiation at top of crop
--
    Bpar := Taugdr*Spdr + Taugdf*Spdf;
--
END SOLAR;
--
```

A3.1.9 Crop Development Model

```
--
-- File DEVELOP.ESL
--
-- Contains the subroutines for leaf and plant development
--
------------------------------------------------------------------------
PROCEDURE RGRt(REAL:P,Q,A,B,U,dAdP,dBdP,dUdP,LN) RETURN REAL;
------------------------------------------------------------------------
-- ESL Subroutine RGRt
-- Finds the relative growth rate of a leaf
-- Inputs P = plastochron age
--        Q = relative growth rate (plastochrons per plastochron)
--        A = parameter A from Horie's model
--        B = parameter B from Horie's model
--        U = number of unfolding leaf
--     dAdP = rate of change of A on plastochron basis
--     dBdP = rate of change of B on plastochron basis
--     dUdP = rate of change of U on plastochron basis
--       LN = leaf number
------------------------------------------------------------------------
  REAL: RGR;
--
  IF LN >= P THEN RGR := 0.0;
  ELSE_IF LN >= U THEN RGR := A+dAdP*(P-LN);
  ELSE RGR := A+dAdP*(P-U)+dBdP*(U-LN)+dUdP*(B-A);
  END_IF;
  RETURN Q*RGR;
--
END RGRt;
--
------------------------------------------------------------------------
PROCEDURE dFdT(REAL:U,N,LN) RETURN REAL;
------------------------------------------------------------------------
-- ESL Subroutine dFdT
-- Calculates the rate of change of fraction of
```

```
-- dividing cells in a leaf
-- Inputs U = number of unfolding leaf
--         N = parameter determining rate of maturation of a leaf
--        LN = leaf number
-----------------------------------------------------------------------
  REAL: F;
--
  IF U - LN < 0.0 THEN F := 1.0;
  ELSE_IF U - LN < N THEN F := (1.0 - (U - LN)/N);
  ELSE  F := 0.0;
  END_IF;
  RETURN F;
--
END dFdT;
--
-----------------------------------------------------------------------
PROCEDURE LEAF(REAL: NC,L,INC,RGR,FDC);
-----------------------------------------------------------------------
-- ESL Subroutine LEAF
-- Analytical integration of the D.E. describing the relative
-- number of cells along the mib-rib of a leaf
-- Also return leaf length (cm)
-- Inputs INC = initial relative number of cells
--         RGR = relative growth rate of leaf
--         FDC = fraction of dividing cells in the leaf
-- Ouputs  NC = final realtive number of cells
--           L = length of leaf
-----------------------------------------------------------------------
--
  NC := INC*EXP(RGR*FDC);
  L := 0.1*NC*(4.0 - 3.0*FDC);
--
END LEAF;
--
-----------------------------------------------------------------------
PROCEDURE STEM(REAL: P,Q,A,B,U,dAdP,dBdP,dUdP,
                     IP,Age,Light,Temp,Init,Factor);
-----------------------------------------------------------------------
-- ESL Subroutine STEM
-- Calculates the plastochron age of a stem by analytical
-- integrationas of the D.E. for node initiation rate
-- Also relative growth rate of the stem on a plastochron basis
-- Values of model parameters A & B and number of unfolding leaf U
-- Rates of change of A, B and U
-- Inputs IP = initial plastochron age
--        Age = plastochron age of main stem (used for laterals)
```

```
--     Light = average daily light intensity
--      Temp = average daily temperature
--      Init = age to initiate stem
--    Factor = reduction factor accounting for presence of fruit
-- Outputs P = final plastochron age
--         Q = rate relative growth rate of stem
--         A = a parameter used in the model
--         B = a parameter used in the model
--         U = the number of the leaf which is unfolding
--      dAdP = rate of change of A on plastochron basis
--      dBdP = rate of change of B on plastochron basis
--      dUdP = rate of change of U on plastochron basis
-----------------------------------------------------------------------
-- Constant Parameters for Node development sub-model
-- from Horie et al, 1976.
--
  CONSTANT REAL: As/0.22/,Ad/1.17/,La/5.7/;
  CONSTANT REAL: Bs/0.34/,Bd/2.07/,Lb/8.0/;
  CONSTANT REAL: Cs/3.30/,Cd/3.30/,Lc/10.0/;
  CONSTANT REAL: Lp/3.0/;
--
-- Function table for temperature dependence of node formation rate
--
  INTEGER: TabT/5/;
  CONSTANT REAL: TempTab(2,5)/
    0.0,0.0, 12.0,0.0, 18.0,0.8, 24.0,1.0, 40.0,1.0/;
--
-- Function table for light dependence of node formation rate
--
  INTEGER: TabL/5/;
  CONSTANT REAL: LightTab(2,5)/
    0.0,0.584, 1.0,0.8, 2.0,0.95, 4.0,1.0, 10.0,1.0/;
--
  REAL: QsTemp,QsLight,Qs,N,LFact,C,dCdP;
--
-- Find Stationary rate of node formation
--
  QsTemp := GEN2(TabT,TempTab,Temp);
  QsLight := GEN2(TabL,LightTab,Light);
  Qs := QsTemp*QsLight*Factor;
--
-- Actual rate of node formation
--
  Q := Qs*(1.0-EXP(-P/Lp));
--
-- Solve the differential equation for P.
```

```
--
  IF Age > Init THEN
    P := Lp*LOG(EXP(Qs/Lp)*(EXP(IP/Lp)-1.0)+1.0);
  ELSE
    P := IP;
  END_IF;
--
-- Calculate rates of change of parameters on Plastachron basis
--
  A := As + Ad*exp(-P/La);
  B := Bs + Bd*exp(-P/Lb);
  C := Cs - Cd*exp(-P/Lc);
  U := P - C/A;
  dAdP := (As - A)/La;
  dBdP := (Bs - B)/Lb;
  dCdP := (Cs - C)/Lc;
  dUdP := 1.0 - (A*dCdP-C*dAdP)/(A*A);
--
END STEM;
--
-----------------------------------------------------------------------
PROCEDURE DEVELOP;
-----------------------------------------------------------------------
-- ESL Subroutine DEVELOP
-- Determines the development of the stem and laterals
-- and the individual leaf expansions
-- Based on leaf expansion determines potential growth rates of
-- dry matter in leaves, stem, and root and potential assimilate
-- requirements
-----------------------------------------------------------------------
USE GLOBAL;
--
  REAL : Zero/0.0/;
--
  AREAi := AREA;
--
-- Average Light and Temp
-- Reset Integrators
--
  Light := LSum*0.0864/Count;
  Temp := TSum/Count;
  TSum := 0.0;
  LSum := 0.0;
  Count := 0.0;
--
  LFact := 2.9 + 0.49*Light;
```

```
  FruFactM := 1.0 - (WfruitM/FactorM)**2.0;
  IF FruFactM < 0.0 THEN FruFactM := 0.0; END_IF;
  FruFactL := 1.0 - (WFruitL/(Laterals*FactorL))**2.0;
  IF FruFactL < 0.0 THEN FruFactL := 0.0; END_IF;
--
-- Invoke Stem Model for development of main stem
--
  PMaini := PMain;
  Age := PMain;
  STEM(PMain,KMain,A,B,UMain,dAdP,dBdP,dUdP,
       PMaini,Age,Light,Temp,Zero,FruFactM);
--
-- Calculate growth of individual leaves on main stem and total leaf area
--
  AreaM := 0.0;
  NoLM := 0;
--
  FOR I := 1..30 LOOP
    LN := I;
    N:=NM(I)*LFact;
    RGR := RGRt(PMain,KMain,A,B,UMain,dAdP,dBdP,dUdP,LN);
    FDC := dFdT(UMain,N,LN);
    NCMi := NCM(I);
    LEAF(NCM(I),LM(I),NCMi,RGR,FDC);
    PREPARE "MAIN",Day,I,RGR,FDC,NCMi;
    IF (PMain - LN*DfactM > NecroM) OR
       ((Day >= Pinch) AND (LN > TopNode)) OR
       (Day >= Prune) OR
       (LN >= PMain) THEN
      LM(I) := 0.0;
      ARM(I) := 0.0;
    ELSE
      IF LN <= UMain THEN NoLM := NoLM + 1; END_IF;
      AEM := LM(I)*LM(I);
      IF AEM <= 100 THEN ARM(I):= 0.524*AEM;
      ELSE ARM(I):=0.688*AEM-16.4;
      END_IF;
    END_IF;
    AreaM:=AreaM+ARM(I);
  END_LOOP;
--
-- Invoke Stem Model for developement of laterals
--
  PLati := PLat;
  STEM(PLat,KLat,A,B,ULat,dAdP,dBdP,dUdP,
       PLati,Age,Light,Temp,Init,FruFactL);
```

```
--
  AreaL := 0.0;
  NoLL := 0;
--
  FOR I := 1..20 LOOP
    LN := I;
    N:=NL(I)*LFact;
    RGR := RGRt(PLat,KLat,A,B,ULat,dAdP,dBdP,dUdP,LN);
    FDC := dFdT(ULat,N,LN);
    NCLi := NCL(I);
    LEAF(NCL(I),LL(I),NCLi,RGR,FDC);
    IF (PLat - LN*DfactL > NecroL) OR
       ((Day >= Prune) AND (I <= 3)) OR
       (LN >= PLat) THEN
      LL(I) := 0.0;
      ARL(I) := 0.0;
    ELSE
      IF LN <= ULat THEN NoLL := NoLL + INT(Laterals); END_IF;
      AEL := LL(I)*LL(I);
      IF AEL <= 100 THEN ARL(I):= 0.524*AEL;
      ELSE ARL(I):=0.688*AEL-16.4;
      END_IF;
    END_IF;
    AreaL := AreaL + ARL(I)*Laterals;
  END_LOOP;
--
  AREA := AreaM + AreaL;
  LAI := AREA*Nplant/(Af*10000.0);
  NOL := NoLM + NoLL;
--
  Lc := SQRT((AREA/NOL)/0.68)/100.0;
--
-- Calculate potential growth rates for leaves, stem, and roots
--
  PGRleaf := 0.0;
  FOR I := 1..30 LOOP
    dAl := ARM(I) - ARMi(I);
    IF dAl > 0.0 THEN
      PGRleaf := PGRleaf + MaxGRleaf*dAl/86400.0;
    ELSE
      Wleaf := Wleaf + dAl/SLA;
    END_IF;
    ARMi(I) := ARM(I);
  END_LOOP;
  FOR I := 1..20 LOOP
    dAl := ARL(I) - ARLi(I);
```

```
    IF dAl > 0.0 THEN
      PGRleaf := PGRleaf + MaxGRleaf*dAl/86400.0;
    ELSE
      Wleaf := Wleaf + dAl/SLA;
    END_IF;
    ARLi(I) := ARL(I);
  END_LOOP;
--
  PGRstem := (10.0/77.0)*PGRleaf;
  PGRroot := (13.0/77.0)*PGRleaf;
  Preqleaf := PGRleaf*ARLeaf;
  Preqstem := PGRstem*ARstem;
  Preqroot := PGRroot*ARroot;
--
END DEVELOP;
--
```

A3.1.10 Photosynthesis Routine

```
--
-- File PHOTOSYN.ESL
--
------------------------------------------------------------------------
PROCEDURE PHOTOSYN(REAL : Tci);
------------------------------------------------------------------------
-- ESL Subroutine PHOTOSYN
-- Calculates the gross photosynthesis using the model of Gijzen &
-- ten Cate (1988) by using Gaussian integration across leaf angle
-- classes and height within the crop canopy
------------------------------------------------------------------------
USE GLOBAL;
--
-- Table of variation of endogenous photosynthetic capacity
--
  CONSTANT REAL : EPCTab(2,5)/
     0.0,0.0, 5.0,0.0, 30.0,2.0, 40.0,0.0, 100.0,0.0/;
--
-- Table of variation of mesophyll conductance with temperature
--
  CONSTANT REAL : MesTab(2,5)/
     0.0,0.0, 5.0,0.0, 25.0,0.004, 40.0,0.0, 100.0,0.0/;
--
-- Constants for photosynthesis model
--
  CONSTANT REAL : Q10Comp/1.7/,Q10Resp/2.0/,Eff0/0.017/;
  CONSTANT REAL : Rd20/0.05/,Comp25/40.0/;
```

```
--
-- Parameters for Gaussian Integration
--
  CONSTANT REAL : XGauss(3)/0.1127, 0.5000, 0.8873/;
  CONSTANT REAL : WGauss(3)/0.2778, 0.4444, 0.2778/;
--
-- Variables for photosynthesis model
--
  REAL : MesCond,rm,Compoint,Eff,Rd;
  REAL : Pend,PCO2,PNmax,PGmax,PGShd,PGSun,PGs,Pt,PGross;
  REAL : Idf,Itot,Idr,Ishd,Ibeam,Isun;
  REAL : LAIC,FracSun;
  INTEGER : I1,I2;
--
-- Calculate photosynthetic capacity parameters
-- Dark Respiration
--
  Rd := Rd20*Q10Resp**(0.1*(Tci-20.0));
--
-- Mesophyll resistance
--
  MesCond := GEN2(5,MesTab(1..2,1..5),Tci);
  IF (MesCond < 0.000001) THEN rm := 3.0E30;
  ELSE rm := 1.0/MesCond;
  END_IF;
--
-- Endogenous photosynthetic capacity
--
  Pend := GEN2(5,EPCTab(1..2,1..5),Tci);
--
-- CO2 compensation point
--
  Compoint := Comp25*Q10Comp**(0.1*(Tci-25.0));
--
-- Initial light use efficiency and max photosynthesis for CO2 limitation
--
  IF (CO2a > Compoint) THEN
    Eff := Eff0*(CO2a - Compoint)/(CO2a+2.0*Compoint);
    PNCO2 := 1.83*(CO2a - Compoint)/(rm + 1.36*rVca + 1.6*rVci);
  ELSE Eff := 0.0; PNCO2 := 0.0;
  END_IF;
--
-- Maximum net photosysnthesis
--
  IF (Pen < 0.000001) THEN FNmax := 0.0;
  ELSE PNmax := Pen*(1.0-EXP(-PNCO2/Pen));
```

```
  END_IF;
--
-- Maximum Gross photosynthesis
--
  PGmax := PNmax + Rd;
--
-- Reduction of PGmax by high reserve levels
--
  ResL := Reserve/(Wleaf+Wstem+Wroot);
  IF (ResL < 0.40) THEN
    PGmax := PGmax;
  ELSE_IF (ResL < 0.45) THEN
    PGmax := PGmax*(10.0-ResL*20.0);
  ELSE
    PGmax := 0.000001;
  END_IF;
--
-- Gaussian Integration in crop canopy profile to
-- calculate the gross photosynthetic rate
--
  PGross := 0.0;
--
-- Loop for 3 heights in canopy
--
  FOR Il := 1..3 LOOP
    LAIC := LAI*XGauss(Il);
--
-- Components of visible (PAR) radiation
--
    Idf := (1.0 - Rhocpdf)*Taugdf*Spdf*Kpdf*EXP(-Kpdf*LAIC);
    Itot := (1.0 - Rhocpdr)*Taugdr*Spdr*Kpdr*EXP(-Kpdr*LAIC);
    Idr := (1.0 - Sigp)*Taugdr*Spdr*Kbdr*EXP(-Kbdr*LAIC);
    Ishd := Idf+Itot-Idr;
    Ibeam := (1.0 - Sigp)*Taugdr*Spdr/SinB;
--
-- Photosynthesis of shaded leaves
--
    PGShd := PGmax*(1.0-EXP(-Ishd*Eff/PGmax));
--
-- Loop over leaf angle distribution for photosynthesis of sunlit leaves
--
    PGSun := 0.0;
    FOR I2 := 1..3 LOOP
      Isun := Ishd+Ibeam*XGauss(I2);
      PGs := PGmax*(1.0 - EXP(-Isun*Eff/PGmax));
      PGSun := PGSun + PGs*WGauss(I2);
```

```
    END_LOOP;
--
-- Fraction of sunlit leaves at each height in canopy
--
    FracSun := EXP(-Kbdr*LAIC);
--
-- Total photosynthesis in leaf layer
--
    Pt := FracSun*PGSun + (1.0 - FracSun)*PGShd;
--
-- Gaussian integration
--
    PGross := PGross + Pt*WGauss(Il);
--
  END_LOOP;
--
-- Gross photosynthesis per unit floor area
--
  FGross := PGross*LAI;
--
-- Gross photosynthesis (assimilation) per plant
--
  Assim := FGross*Af/Nplant;
--
END PHOTOSYN;
--
```

A3.1.11 Crop Growth and Respiration Routine

```
--
-- File GROWTH.ESL
--
-------------------------------------------------------------------------
PROCEDURE GROWTH(REAL : Tci);
-------------------------------------------------------------------------
-- ESL Subroutine GROWTH
-- Calculate the maintenance and growth respiration, reserve level,
-- and partitioning
-- Input Tci = crop temperature
-------------------------------------------------------------------------
USE GLOBAL;
--
  REAL : Factor;
  INTEGER : LastFM;
--
-- Calculate Maintenance Respiration
```

```
--
  RespMain := (Wroot*MainRoot + Wstem*MainStem + Wleaf*MainLeaf +
              Wfruit*MainFru)*Q10**(0.1*(Tci-TempRef));
  FResp := RespMain*Nplant/Af;
--
-- Calculate Reserve levels of carbohydrate
--
  Reserve := Reserve + (Assim - RespMain)*300.0*30.0/44.0;
  IF Reserve < 0.0 THEN
    Wleaf := Wleaf + Reserve*0.77/1.8;
    Wstem := Wstem + Reserve*0.10/1.8;
    Wroot := Wroot + Reserve*0.13/1.8;
    Reserve := 0.0;
  END_IF;
--
-- Calculate growth of fruit
--
  LostFresh := 0.0;
  PGRfruit := 0.0;
  IF DAY >= Pinch THEN
    LastFM := INT(TopNode);
  ELSE
    LastFM := 30;
  END_IF;
--
-- Loop for main stem
--
  FOR I := 10..LastFM LOOP
    IF (NOT AbortM(I)) AND (NOT HarvM(I)) AND (I <= UMain) THEN
      TFruM(I) := TFruM(I) + 1.0;
      AgeFruM(I) := TFruM(I)/288.0;
      Factor := EXP(-0.6*(AgeFruM(I)-15.0));
      PGRFruM(I) := PGRFmax*4.0*Factor/((1.0+Factor)**2.0);
      PGRfruit := PGRfruit + PGRFruM(I);
    ELSE
      PGRFruM(I) := 0.0;
    END_IF;
  END_LOOP;
--
-- Loop for laterals
--
  FOR I := 1.. 20 LOOP
    IF (NOT AbortL(I)) AND (NOT HarvL(I)) AND (I <= ULat) THEN
      TFruL(I) := TFruL(I) + 1.0;
      AgeFruL(I) := TFruL(I)/288.0;
      Factor := EXP(-0.6*(AgeFruL(I)-15.0));
```

```
      PGRFruL(I) := PGRFmax*4.0*Factor/((1.0+Factor)**2.0);
      PGRfruit := PGRfruit + PGRFruL(I)*Laterals;
    ELSE
      PGRFruL(I) := 0.0;
    END_IF;
  END_LOOP;
--
-- Potential assimilate requirement for fruit growth
--
  Preqfruit := PGRfruit*ARfruit;
--
-- Assimilate requirements for potential growth per second
--
  PRequired := Preqleaf + Preqstem + Preqroot + Preqfruit;
--
-- Convert to 5 minute requirement
--
  PRequired := PRequired*300.0;
--
-- Ratio of reserve to requirements
--
  IF Reserve < PRequired THEN
    Ratio := Reserve/PRequired;
    Reserve := 0.0;
  ELSE
    Ratio := 1.0;
    Reserve := Reserve - Prequired;
  END_IF;
--
-- Growth of organs and CO2 production (growth respiration)
--
  Wleaf := Wleaf + Ratio*PGRleaf*300.0;
  Wstem := Wstem + Ratio*PGRstem*300.0;
  Wroot := Wroot + Ratio*PGRroot*300.0;
--
  CO2pLeaf := Ratio*PGRleaf*CO2leaf;
  CO2pStem := Ratio*PGRstem*CO2stem;
  CO2pRoot := Ratio*PGRroot*CO2root;
  CO2pfruit := Ratio*PGRfruit*CO2fruit;
--
-- Growth of individual fruit, abortion and picking
--
-- Loop for main stem
--
  WfruitM := 0.0;
--
```

```
  FOR I := 10..LastFM LOOP
    IF (NOT AbortM(I)) AND (NOT HarvM(I)) THEN
      WfruM(I) := WfruM(I) + Ratio*PGRfruM(I)*300.0;
      WfruitM := WfruitM + WfruM(I);
      IF (PickTime) THEN
        IF (WFruM(I) >=PickW)
       OR ((AgeFruM(I) >= RemAge) AND (WFruM(I) >=RemW)) THEN
       HarvM(I) := TRUE;
          WfruitH := WfruitH + WfruM(I);
          NoFruitH := NoFruitH + 1;
       LostFresh := LostFresh + WfruM(I)*0.96/(1000.0*0.04);
        ELSE_IF (AgeFruM(I) >=RemAge) AND (WFruM(I) < RemW) THEN
          AbortM(I) := TRUE;
          NofruitA := NoFruitA + 1;
       LostFresh := LostFresh + WfruM(I)*0.96/(1000.0*0.04);
     END_IF;
      END_IF;
      IF (AgeFruM(I) >= AbortAge) AND (WfruM(I) < 0.2*PickW) THEN
        AbortM(I) := TRUE;
        NofruitA := NoFruitA + 1;
      END_IF;
    ELSE
      WfruM(I) := 0.0;
    END_IF;
  END_LOOP;
--
-- Loop for laterals
--
  WFruitL := 0.0;
--
  FOR I := 1..20 LOOP
    IF (NOT AbortL(I)) AND (NOT HarvL(I)) THEN
      WfruL(I) := WfruL(I) + Ratio*PGRfruL(I)*300.0;
      WfruitL := WfruitL + WfruL(I)*Laterals;
      IF (PickTime) THEN
        IF (WFruL(I) >=PickW)
       OR ((AgeFruL(I) >= RemAge) AND (WFruL(I) >= RemW)) THEN
       HarvL(I) := TRUE;
          WfruitH := WfruitH + WfruL(I)*Laterals;
          NoFruitH := NoFruitH + INT(Laterals);
       LostFresh := LostFresh + Laterals*WfruL(I)*0.96/(1000.0*0.04);
        ELSE_IF (AgeFruL(I) >=RemAge) AND (WFruL(I) < RemW) THEN
          AbortL(I) := TRUE;
          NofruitA := NoFruitA + INT(Laterals);
      LostFresh := LostFresh + Laterals*WfruL(I)*0.96/(1000.0*0.04);
    END_IF;
```

```
      END_IF;
      IF (AgeFruL(I) >= AbortAge) AND (WfruL(I) < 0.2*PickW) THEN
        AbortL(I) := TRUE;
        NofruitA := NoFruitA + INT(Laterals);
      END_IF;
    ELSE
      WfruL(I) := 0.0;
    END_IF;
  END_LOOP;
--
-- Add total fruit weight
--
  WFruit := WfruitM + WfruitL;
--
-- Total CO2 production and lost of fresh weight per second
--
  CO2prod := CO2pLeaf + CO2pStem + CO2pRoot + CO2pFruit;
  FGrowth := CO2prod*Nplant/Af;
  ffruit := LostFresh/300.0;
--
-- Specific leaf area
--
  SLA := AREA/Wleaf;
--
-- Total crop dry matter, dry matter heat capacity,
-- and maximum water holding capacity
--
  DMc := (Wleaf+Wstem+Wroot+WFruit)/1000.0;
  Phic := DMc*Nplant*Cpom/Af;
  Xcmax := WHCc*DMc*Nplant/Af;
--
END GROWTH;
--
```

A3.1.12 Greenhouse Energy and Mass Balance Model

```
--
-- File GEMB.ESL
--
-----------------------------------------------------------------------
MODEL GEMB(REAL : Tg,Ts,Ta,Tc,Tm,Tf,Tl,T2,T3,T4,T5,Xg,Xa,Xc,Xm,XCO2a :=
           REAL : Tgi,Tsi,Tai,Tci,Tmi,Tfi,Tli,T2i,T3i,T4i,T5i,
                  Xgi,Xai,Xci,Xmi,XCO2ai);
-----------------------------------------------------------------------
-- ESL Model GEMB (Greenhouse Energy & Mass Balances)
--
```

```
-- Dynamic simulation of the greenhouse environmental state variables.
-- Enthalpy of glazing, structure, crop, root media, soil layers,
-- and air.
-- Water content of glazing, crop, root media and air.
-- Inputs Tgi = initial temperature of glazing
--        Tsi = initial temperature of structure
--        Tai = initial temperature of inside air
--        Tci = initial temperature of crop
--        Tmi = initial temperature of root medium
--        Tfi = initial temperature of floor
--        Tli = initial temperature of soil layer 1
--        T2i = initial temperature of soil layer 2
--        T3i = initial temperature of soil layer 3
--        T4i = initial temperature of soil layer 4
--        T5i = initial temperature of soil layer 5
--        Xgi = initial moisture concentration on glazing
--        Xai = initial moisture content of inside air
--        Xmi = initial moisture content of root medium
--        Xci = initial moisture content of crop
--     XCO2ai = initial CO2 concentration of inside air
-- Outputs Tg = final temperature of glazing
--         Ts = final temperature of structure
--         Ta = final temperature of inside air
--         Tc = final temperature of crop
--         Tm = final temperature of root medium
--         Tf = final temperature of floor
--         Tl = final temperature of soil layer 1
--         T2 = final temperature of soil layer 2
--         T3 = final temperature of soil layer 3
--         T4 = final temperature of soil layer 4
--         T5 = final temperature of soil layer 5
--         Xg = final moisture concentration on glazing
--         Xa = final moisture content of inside air
--         Xm = final moisture content of root medium
--         Xc = final moisture content of crop
--      XCO2a = final CO2 concentration of inside air
-------------------------------------------------------------------------
USE GLOBAL;
--
-- Enthalpies
--
  REAL : Hg,Hs,Ha,Hc,Hm,Hf;
  REAL : H1,H2,H3,H4,H5;
--
NOSORT;
INITIAL
```

```
--
-- Initialize dynamic variables
--
  Tg := Tgi;  Ts := Tsi;  Ta := Tai;  Tc := Tci;  Tm := Tmi;
  Tf := Tfi;  Tl := Tli;  T2 := T2i;  T3 := T3i;  T4 := T4i;  T5 := T5i;
  Xg := Xgi; Xa := Xai; Xc := Xci; Xm := Xmi;
  XCO2a := XCO2ai;
--
-- Determine the sky temperature
--
  eo := 611.0*exp(17.27*Tow/(Tow+237.3)) - Gamma*(To-Tow);
  IF eo < 0.0 THEN eo := 0.0; END_IF;
  Todw := (237.3*ALOG(eo/611.0))/(17.27-ALOG(eo/611.0));
  IF Sg = 0.0 THEN esky := 0.741 + 0.0062*Todw;
  ELSE esky := 0.727 + 0.006*Todw;
  END_IF;
  IF SAlt > 10.0 THEN
    IF Kt <= 0.22 THEN Cloud := 1.0;
    ELSE_IF Kt <= Kcrit THEN Cloud := (Kcrit - Kt)/(Kcrit - 0.22);
    ELSE Cloud := 0.0;
    END_IF;
  END_IF;
  esky := esky + Cloud*(1.0 - esky - 8.0/(To + 273.15));
  Tsky := (To+273.15)*esky**0.25-273.15;
--
-- Outside CO2 concentration
--
  Chio := Mw*eo/(R*(To+273.15));
  XiCO2o := (CO2o/1e3)*1.52*Ma*(Po-eo)/(R*(To+273.15));
--
-- Inside CO2 concentration
--
  XiCO2a := XCO2a/da;
--
-- inside air parameters
--
  ea := (Xa*R*(Ta+273.15))/(Mw*da);
  rhoa := Ma*(Po - ea)/(R*(Ta+273.15));
  Phia := rhoa*da*Cpa;
--
-- Initial enthalpy contents
--
  Hg := Tg*(Phig + Xg*Cpw);
  Hs := Ts*(Phis);
  Ha := Ta*(Phia + Xa*Cpv) + 2501*Xa;
  Hc := Tc*(Phic + Xc*Cpw);
```

```
  Hm := Tm*(Phim + Xm*Cpw);
  Hf := Tf*(Phif + Xf*Cpw);
  Hl := Tl*(Phil + Xl*Cpw);
  H2 := T2*(Phi2 + X2*Cpw);
  H3 := T3*(Phi3 + X3*Cpw);
  H4 := T4*(Phi4 + X4*Cpw);
  H5 := T5*(Phi5 + X5*Cpw);
--
-- Initial water potentials
--
  Psic := -(1.0 - Xc/Xcmax)/Capc;
  Psim := -(1.0 - Xm/Xmmax)/Capm;
--
-- Heat input
--
  IF delT <= 0.0 THEN
    Cha := 0.0;
    Th := Ts;
  ELSE
    Th := Ta + (delT/ALOG((76.0 - Ta)/(76.0 - Ta - delT)));
    IF Ht > 3500.0 THEN Cha := 1.5*(Th-Ta);
    ELSE Cha := 0.5*(Th-Ta);
    END_IF;
  END_IF;
--
-- Convective heat transfer coefficients
--
  hCgo := CONVHT(Uo,Lf,Tg,To,1.0);
  hCga := CONVHT(Ua,Lg,Tg,Ta,0.0);
  hCsa := (CONVHT(Ua,2.0,Ts,Ta,0.0)+CONVHT(Ua,0.1,Ts,Ta,1.0))/2.0;
  hCca := (CONVHT(Ua,Lc,Tc,Ta,1.0)+CONVHT(Ua,Lc,Tc,Ta,-1.0))/2.0;
  hCfa := CONVHT(Ua,Lf,Tf,Ta,1.0);
  hCma := hCfa;
--
-- Conductance between floor and soil layers (W/m2.K)
--
  xwm := Xm*Af/(Amtop*BagH*rhow);
  km := SOIL(xqm,xclm,xomm,xwm,Field);
  hGfm := 2.0/(BagH/km + df/kf);
  hGfl := 2.0/(df/kf + dl/kl);
  hG12 := 2.0/(dl/kl + d2/k2);
  hG23 := 2.0/(d2/k2 + d3/k3);
  hG34 := 2.0/(d3/k3 + d4/k4);
  hG45 := 2.0/(d4/k4 + d5/k5);
  hG5d := 2.0*k5/d5;
--
```

```
-- Equivalent radiative heat transfer coefficients (W.m2.K)
--
  Tave := (Tg + Tsky)/2.0;
  hRgsky := 4.0*SFgsky*Sigma*(Tave+273.15)**3.0;
  Tave := (Ts + Tg)/2.0;
  hRsg := 4.0*SFsg*Sigma*(Tave+273.15)**3.0;
  Tave := (Th + Tg)/2.0;
  hRhg := 4.0*SFhg*Sigma*(Tave+273.15)**3.0;
  Tave := (Th + Ts)/2.0;
  hRhs := 4.0*SFhs*Sigma*(Tave+273.15)**3.0;
  Tave := (Tc + Tg)/2.0;
  hRcg := 4.0*SFcg*Sigma*(Tave+273.15)**3.0;
  Tave := (Tc + Ts)/2.0;
  hRcs := 4.0*SFcs*Sigma*(Tave+273.15)**3.0;
  Tave := (Tc + Th)/2.0;
  hRch := 4.0*SFch*Sigma*(Tave+273.15)**3.0;
  Tave := (Tm + Tg)/2.0;
  hRmg := 4.0*SFmg*Sigma*(Tave+273.15)**3.0;
  Tave := (Tm + Ts)/2.0;
  hRms := 4.0*SFms*Sigma*(Tave+273.15)**3.0;
  Tave := (Tm + Th)/2.0;
  hRmh := 4.0*SFmh*Sigma*(Tave+273.15)**3.0;
  Tave := (Tm + Tc)/2.0;
  hRmc := 4.0*SFmc*Sigma*(Tave+273.15)**3.0;
  Tave := (Tf + Tg)/2.0;
  hRfg := 4.0*SFfg*Sigma*(Tave+273.15)**3.0;
  Tave := (Tf + Ts)/2.0;
  hRfs := 4.0*SFfs*Sigma*(Tave+273.15)**3.0;
  Tave := (Tf + Th)/2.0;
  hRfh := 4.0*SFfh*Sigma*(Tave+273.15)**3.0;
  Tave := (Tf + Tc)/2.0;
  hRfc := 4.0*SFfc*Sigma*(Tave+273.15)**3.0;
  Tave := (Tf + Tm)/2.0;
  hRfm := 4.0*SFfm*Sigma*(Tave+273.15)**3.0;
--
-- Ventilation rate (airchange rate per hour)
--
  IF (Top+Bot < 0.05) THEN
    Nv := 0.77*Uo + 0.14*SQRT(ABS(Ta - To));
  ELSE
    Nv := (0.77*Uo + 0.67*SQRT(ABS(Ta - To)))*
          (1.0 + 1.5*Top*EXP(-0.15*Top) + 1.2*Bot*EXP(-0.04*Bot));
  END_IF;
--
-- Advective heat transfer coefficient (W/m2 floor.K)
--
```

```
  hao := Phia*Nv/3600.0;
  rao := rhoa*Cpa/hao;
--
-- Leaf internal resistance
--
  VPD := 611.0*exp(17.27*Tc/(Tc+237.3)) - ea;
  rVci := 15.0*(1.0 + 0.162*VPD*exp(-0.055*Bcave))*
                  (1.0 + 0.0012*(Tc - 30.0)**2.0);
--
-- Evaporative heat transfer coefficinets (W/m2.K) (0.93 from Lewis number)
--
  rVga := 0.93*rhoa*Cpa/hCga;
  rVca := 0.93*rhoa*Cpa/HCca;
  rVma := 0.93*rhoa*Cpa/hCma;
--
DYNAMIC
--
-- Convective heat transfer rates
--
  Cgo := hCgo*GAI*(Tg-To);
  Cga := hCga*GAI*(Tg-Ta);
  Csa := hCsa*SAI*(Ts-Ta);
  Cca := hCca*2.0*LAI*(Tc-Ta);
  Cma := hCma*MAI*(Tm-Ta);
  Cfa := hCfa*FAI*(Tf-Ta);
  Cao := hao*(Ta-To);
--
-- Conductive heat transfer rates
--
  Gsg := hGsg*SAI*(Ts-Tg);
  Gfm := hGfm*(1.0-FAI)*(Tf-Tm);
  Gf1 := hGf1*(Tf-T1);
  G12 := hG12*(T1-T2);
  G23 := hG23*(T2-T3);
  G34 := hG34*(T3-T4);
  G45 := hG45*(T4-T5);
  G5d := hG5d*(T5-Td);
--
-- Radiative heat transfer rates
--
  Rgsky := hRgsky*GAI*(Tg - Tsky);
  Rsg := hRsg*SAI*(Ts - Tg);
  Rhg := hRhg*HAI*(Th - Tg);
  Rhs := hRhs*HAI*(Th - Ts);
  Rcg := hRcg*2.0*LAI*(Tc - Tg);
  Rcs := hRcs*2.0*LAI*(Tc - Ts);
```

```
  Rch := hRch*2.0*LAI*(Tc - Th);
  Rmg := hRmg*MAI*(Tm - Tg);
  Rms := hRms*MAI*(Tm - Ts);
  Rmh := hRmh*MAI*(Tm - Th);
  Rmc := hRmc*MAI*(Tm - Tc);
  Rfg := hRfg*FAI*(Tf - Tg);
  Rfs := hRfs*FAI*(Tf - Ts);
  Rfh := hRfh*FAI*(Tf - Th);
  Rfc := hRfc*FAI*(Tf - Tc);
  Rfm := hRfm*FAI*(Tf - Tm);
--
-- Evaporative mass transfer rates
--
  Chig := (Mw*611.0*exp(17.27*Tg/(Tg+237.3)))/(R*(Tg+273.15));
  Chic := (Mw*611.0*exp(17.27*Tc/(Tc+237.3)))/(R*(Tc+273.15));
  Chim := (Mw*611.0*exp(17.27*Tm/(Tm+237.3)))/(R*(Tm+273.15));
  Chiamax := (Mw*611.0*exp(17.27*Ta/(Ta+237.3)))/(R*(Ta+273.15));
  Chia := Xa/da;
  f := (GAI/rVga)*(Chig - Chia);
  fga := IF (Xg <= 0.0) AND (f > 0.0) THEN 0.0 ELSE f;
  f := (2.0*LAI/(rVci+rVca))*(Chic - Chia);
  fca := IF (Xc <= 0.0) AND (f > 0.0) THEN 0.0 ELSE f;
  f := ((1.0-FAI)/rVma)*(Chim - Chia);
  fma := IF (Xm <= 0.0) AND (f > 0.0) THEN 0.0 ELSE f;
  fprod := fga + fca + fma;
--
-- Advective mass transfer rates
--
  f := (Chia - Chio)/rao;
  fao := IF (Chia >= Chiamax) AND (f < fprod) THEN fprod*1.05
           ELSE_IF (Chia <= Chio) AND (f > fprod) THEN fprod*0.95
           ELSE f;
  fdrip := IF (Xg > 0.0002*GAI*rhow) AND (fga < 0.0) THEN -fga ELSE 0.0;
  fdrn := IF Xm > Xmmax THEN firr ELSE 0.0;
  fup := IF (Psim > Psic) THEN Kmc*(Psim - Psic) ELSE 0.0;
--
-- Latent Heat Transfer Rates
--
  LEga := fga*Lamd;
  LEca := fca*Lamd;
  LEma := fma*Lamd;
  Eao := fao*Lamd;
--
  Edrip := fdrip*Cpw*Tg;
  Eirr := firr*Cpw*Td;
  Eup := fup*Cpw*Tm;
```

```
  Edrn := fdrn*Cpw*Tm;
--
-- CO2 exchange
--
  Fvent := (XiCO2a - XiCO2o)/rao;
--
-- Dynamic equations
--
  Hg' := Bg - Cgo - Cga + Gsg - Rgsky + Rsg + Rhg + Rcg + Rmg + Rfg
           - LEga - Edrip;
  Hs' := Bs - Csa - Gsg - Rsg + Rhs + Rcs + Rms + Rfs;
  Ha' := Cga + Csa + Cca + Cma + Cfa + Cha - Cao + LEga + LEca + LEma
           - Eao;
  Hc' := Bc - Cca - Rcg - Rcs - Rch + Rmc + Rfc - LEca + Eup;
  Hm' := Bm - Cma + Gfm - Rmg - Rms -Rmh - Rmc + Rfm
           - LEma + Eirr - Eup - Edrn;
  Hf' := Bf - Cfa - Gfm - Gf1 - Rfg - Rfs - Rfh - Rfc - Rfm;
  H1' := Gf1 - G12;
  H2' := G12 - G23;
  H3' := G23 - G34;
  H4' := G34 - G45;
  H5' := G45 - G5d;
--
  Xg' := - fga - fdrip;
  Xa' := fga + fca + fma - fao;
  Xc' := fup - fca - ffruit;
  Xm' := firr - fma - fup - fdrn;
--
  XCO2a' := FResp + CO2prod - FGross - Fvent;
--
STEP
--
-- Calculate temperatures
--
  Tg := Hg/(Phig + Xg*Cpw);
  Ts := Hs/(Phis);
  Ta := (Ha - Xa*2501)/(Phia + Xa*Cpv);
  Tc := Hc/(Phic + Xc*Cpw);
  Tm := Hm/(Phim + Xm*Cpw);
  Tf := Hf/(Phif + Xf*Cpw);
  T1 := H1/(Phi1 + X1*Cpw);
  T2 := H2/(Phi2 + X2*Cpw);
  T3 := H3/(Phi3 + X3*Cpw);
  T4 := H4/(Phi4 + X4*Cpw);
  T5 := H5/(Phi5 + X5*Cpw);
--
```

```
-- Calculate water potentials
--
  Psic := -(1.0 - Xc/Xcmax)/Capc;
  Psim := -(1.0 - Xm/Xmmax)/Capm;
--
-- Update inside air parameters
--
  IF Xa < 0.0 THEN ea := 0.0;
  ELSE ea := (Xa*R*(Ta+273.15))/(Mw*da);
  END_IF;
  rhoa := Ma*(Po - ea)/(R*(Ta+273.15));
  Phia := rhoa*da*Cpa;
--
-- CO2 concentration
--
  XiCO2a := XCO2a/da;
--
END GEMB;
--
```

A3.1.13 Simulation Input File

The simulation input file SIMPUT is listed below.

```
Input data for greenhouse energy mass balance model
Greenhouse Cardinal Dimensions (Length, Width, Gutter Height, Ridge Height)
15.5 6.6 2.1 4.0
Offset of Greenhouse minor axis from North South
-30.0
Densities (g.m-3) (glazing, glazing bars, structure)
2.7e6 2.7e6 7.8e6
Heat Capacities (J.g-1.K-1) (Glazing, glazing bars, structure)
0.84 0.89 0.44
Volume fractions of quartz in floor and soil layers
0.20 0.20 0.20 0.20 0.20 0.30
Volume fractions of clay minerals floor and in soil layers
0.15 0.15 0.15 0.15 0.15 0.30
Volume fraction of organic matter in floor and soil layers
0.30 0.30 0.30 0.30 0.30 0.05
Volume fraction of water in floor and soil layers
0.35 0.35 0.35 0.35 0.35 0.35
Emissivities (Glazing, structure, heater, crop, media, floor)
0.94 0.92 0.85 0.95 0.95 0.67
Thickness of glazing, floor and soil layers (m)
0.003 0.01 0.02 0.04 0.08 0.16 0.32
Total Volume of glazing bars, structural elements (m3)
```

0.074 0.165
Surface area of structure(m2), view factor (Fss), Radiation Blockage(SBlock)
112.8 0.3 0.15
Surface area of heater (m2), view factor (Fhh), Radiation Blockage(HBlock)
10.0 0.15 0.02
Transmission reduction factor (TauRF), structure absorption factor (StrucAF)
0.84 0.44
Absorptivity of the floor for PAR and NIR radiation
0.80 0.80
Number of plants, diameter and height of media bags and sel view factor (Fmm)
140.0 0.2 0.2 0.24
Leaf inclination parameter and Scattering coefficient in PAR and NIR
1.0 0.2 0.8

A3.1.14 Initial Plant Data

The initial plant input file INPUT14.CEL is listed below. The first row is respectively plastochron index of main stem, plastochron index of lateral (1.0 implies not initiated), total leaf area (cm^2), total leaf area one day previously. The remaining column data is the relative cell count along the mid-rib of 30 leaves on the main stem, and 20 leaves on a lateral. A value of 1.0 implies that the leaf has not yet initiated.

17.2 1.0 389.7 310.1
31.6
27.9
35.2
44.7
41.4
29.7
19.0
12.7
9.7
7.4
5.7
4.3
3.2
2.4
1.8
1.4
1.0
1.0
1.0

1.0
1.0
1.0
1.0
1.0
1.0
1.0
1.0
1.0
1.0
1.0
1.0
1.0
1.0
1.0
1.0
1.0
1.0
1.0
1.0
1.0
1.0
1.0
1.0
1.0
1.0
1.0
1.0
1.0
1.0
1.0

A3.2 LIGHT TRANSMISSION MODEL

In this section listings of the light transmission program GST2, written for a FORTRAN compiler, are given. Only those parts of the original program which were modified in some way have been included. The modified lines are high-lighted. An explaination of the changes can be found in Chapter 4. Further information regarding the complete program can be found in Bellamy, 1991.

A3.2.1 Main Light Transmission Program GST2.F

```
      PROGRAM GST2
      LOGICAL*1 BUF(8)
      DIMENSION C(50,6,3),DIM(50,14),PNOR(50,3),DIST(50,6),
     *  WAZI(50),SLOPE(50),ABSORB(50),TAU(9,36),ALPH(9,36),
     *  HORIZ(50,0:1000,3),VERT(50,0:5000,3),DIFT(50),
     *  DFTR(100,40),DITR(100,40),TTR(100,40),VF(50)
      CHARACTER*80 CODE
C
C     PROGRAM MODIFIED BY CMWELLS JAN 89 TO CREATE
      TRANSMISSION TABLES
C
      PARAMETER(PI=3.14159265)
      COMMON C,DIM,PNOR,DIST,WAZI,SLOPE,GW,GBW,ANG,NP,HORIZ,VERT,
     *       DIFT,DFTR,DITR,VF,NG1,NG2,WX,WY,W,ABSORB,DIRT
      OPEN(UNIT=2,FILE='SHAPE.DAT',STATUS='OLD')
      OPEN(UNIT=5,FILE='GST.OUT')
      OPEN(UNIT=4,FILE='GHOUSE.DAT')
C
      CALL TIME(BUF)
      WRITE(5,789)BUF
  789 FORMAT(10X,8A1,//)
C
C      READ CODE FROM HEAD OF DATA FILE 'SHAPE.DAT'
      READ(2,250) CODE
C      READ RUN TIME INFORMATION. LONGITUDE, LATITUDE, DAY OF
C      YEAR, HOUR, ANGLE OF HOUSES MINOR DIMENSION FROM NORTH,
C      NO. OF PLANES, GRID WIDTH, GLAZING BAR WIDTH,GLASS WIDTH.
      READ(2,1) RLAT,RLONG,IY,MO,ID,IH,ANG,NP,W,GBW,GW,MODE,DIRT
    1   FORMAT(2F6.1,4I3,F6.1,I3,F5.2,2F6.1,I2,F5.2)
C
      NG1=-1
      NG2=-1
C
C      VALUES OF CO-ORDINATES READ INTO ARRAY C
      DO 70 I=1,NP
```

```
      DO 4 J=1,4
      READ(2,2)(C(I,J,K),K=1,3)
    2   FORMAT(3F6.1)
    4   CONTINUE
C
C       CALCULATE THE PLANES NORMAL VECTOR AND AZIMUTH
      IF((C(I,1,2).EQ.C(I,2,2)).AND.(C(I,2,1).GT.C(I,1,1)))THEN
       WAZI(I)=0.0
      ELSEIF((C(I,1,1).EQ.C(I,2,1)).AND.(C(I,1,2).GT.C(I,2,2)))
        THEN
       WAZI(I)=PI/2.0
      ELSEIF((C(I,1,1).EQ.C(I,2,1)).AND.(C(I,1,2).LT.C(I,2,2)))
        THEN
       WAZI(I)=3.0*PI/2.0
      ELSE
       WAZI(I)=PI
      ENDIF
C
      IF((WAZI(I).EQ.0.0).OR.(WAZI(I).EQ.PI))THEN
       C(I,6,1)=C(I,3,1)
       C(I,6,2)=C(I,1,2)
       C(I,6,3)=C(I,1,3)
       C(I,5,1)=C(I,4,1)
       C(I,5,2)=C(I,1,2)
       C(I,5,3)=C(I,1,3)
      ELSE
       C(I,6,1)=C(I,1,1)
       C(I,6,2)=C(I,3,2)
       C(I,6,3)=C(I,1,3)
       C(I,5,1)=C(I,1,1)
       C(I,5,2)=C(I,4,2)
       C(I,5,3)=C(I,1,3)
      ENDIF
C
C       CALCULATE THE NORMAL
       DIST(I,1)=((C(I,1,1)-C(I,2,1))**2+(C(I,1,2)-C(I,2,2))**2)
     *  **0.5
       DIST(I,3)=((C(I,3,1)-C(I,6,1))**2+(C(I,3,2)-C(I,6,2))**2
     *  +(C(I,3,3)-C(I,6,3))**2)**0.5
       DIST(I,4)=((C(I,4,1)-C(I,5,1))**2+(C(I,4,2)-C(I,5,2))**2
     *  +(C(I,4,3)-C(I,5,3))**2)**0.5
       DIST(I,5)=((C(I,5,1)-C(I,2,1))**2+(C(I,5,2)-C(I,2,2))**2
     *  +(C(I,5,3)-C(I,2,3))**2)**0.5
       DIST(I,6)=((C(I,6,1)-C(I,2,1))**2+(C(I,6,2)-C(I,2,2))**2
     *  +(C(I,6,3)-C(I,2,3))**2)**0.5
       IF(DIST(I,3).GT.DIST(I,4))THEN
```

```
 79          DIST(I,2)=DIST(I,3)
 80         ELSE
 81          DIST(I,2)=DIST(I,4)
 82         ENDIF
 83    C
 84         SLOPE(I)=ACOS(((C(I,6,1)-C(I,3,1))**2+(C(I,6,2)-C(I,3,2))**2
 85        *  )**0.5/DIST(I,3))
 86    C
 87         PNOR(I,1)=SIN(SLOPE(I))*SIN(WAZI(I))
 88         PNOR(I,2)=SIN(SLOPE(I))*COS(WAZI(I))
 89         PNOR(I,3)=COS(SLOPE(I))
 90    C
 91    C      EACH SLOPE IS NOW SPECIFIED BY 6 CO-ORDINATES AND A NORMAL
 92    C       VECTOR. THE CO-ORDINATES ARE W.R.T. THE GREENHOUSE AXES.
 93    C      FULLY SPECIFY THE PLANE BY READING VALUES FOR:
 94    C        1. WIDTH AND DEPTH OF MEMBERS UP(2) AND ALONG(1) THE
                   PLANE -CM
 95    C        2. DISTANCE BETWEEN THE MEMBERS -CM
 96    C        3. THICKNESS OF CLADDING(S)     -CM
 97    C        4. EXTINCTION CO-EFFICIENT OF CLADDING(S) -1/CM
 98    C        5. REFRACTIVE INDEX OF CLADDING(S)
 99    C        6. REFLECTANCE OF SURFACE
100    C
101         READ(2,207)(DIM(I,J), J=1,14)
102    C
103    C      FIND INTERSECTION POINTS OF EACH PLANE WITH THE GRID.
104    C      EXPRESS CORNERS OF PLANE IN U,V CO-ORDINATES.
105         P2U=0.0
106         P2V=0.0
107         P3U=DIST(I,6)
108         P3V=DIST(I,3)
109         P4U=DIST(I,5)
110         P4V=DIST(I,4)
111         P1U=DIST(I,1)
112         P1V=0.0
113    C
114    C      FIND INTERSECTION POINTS OF PLANE WITH GRID.
115         NV=DIST(I,2)/W+1.0
116         DO 50 K=0,NV
117         HORIZ(I,K,1)=P2U+(K*W-P2V)*(P3U-P2U)/(P3V-P2V)
118         IF(P4V.EQ.P3V)THEN
119          HORIZ(I,K,2)=1000.0
120         ELSE
121          HORIZ(I,K,2)=P3U+((K*W- P3V)*(P4U-P3U))/(P4V-P3V)
122         ENDIF
123         IF(P4V.EQ.P1V)THEN
```

```
124           HORIZ(I,K,3)=0.0
125          ELSE
126           HORIZ(I,K,3)=P4U+((K*W-P4V)*(P1U-P4U))/(P1V-P4V)
127          ENDIF
128       50 CONTINUE
129       C
130          RNU=DIST(I,1)/W
131          RN=AINT(RNU)
132          IF(RNU.EQ.RN)THEN
133           NU=RNU
134          ELSE
135           NU=RN+1.0
136          ENDIF
137          DO 60 K=0,NU
138          IF(P3U.EQ.P2U)THEN
139           VERT(I,K,1)=0.0
140          ELSE
141           VERT(I,K,1)=P2V+((P3V-P2V)*(K*W-P2U))/(P3U-P2U)
142          ENDIF
143          VERT(I,K,2)=P3V+((P4V-P3V)*(K*W-P3U))/(P4U-P3U)
144          IF(P1U.EQ.P4U)THEN
145           VERT(I,K,3)=0.0
146          ELSE
147           VERT(I,K,3)=P4V+((P1V-P4V)*(K*W-P4U))/(P1U-P4U)
148          ENDIF
149       60   CONTINUE
150       C
151       C      FIND WHICH PLANES ARE THE FLOOR AND BACKWALL
152          IF((ANINT(PNOR(I,3)).EQ.1).AND.(ANINT(DIM(I,14)).EQ.-1))THEN
153           IF(NG1.EQ.-1)THEN
154            NG1=I
155            D1X=C(I,2,1)-C(I,1,1)
156            D1Y=C(I,1,2)-C(I,4,2)
157            NGX=D1X
158            NGY=D1Y
159            WX=D1X/NGX
160            WY=D1Y/NGY
161           ELSE
162            NG2=I
163           ENDIF
164          ELSEIF((C(I,2,2).EQ.0.0).AND.(C(I,1,2).EQ.0.0))THEN
165           LEND=I
166          ENDIF
167       70   CONTINUE
168          WRITE(5,250) CODE
169          WRITE(5,210) D1X,D1Y,W
```

```
      WRITE(4,250) CODE
C
C      IF NG2 IS NOT EQUAL TO -1 THEN THIS IS A SPLIT LEVEL HOUSE.
C      FIND THE SIZE OF THE FLOOR GRID.
      IF(NG2.EQ.-1)THEN
       MX=NGX
       MY=NGY
      ELSE
       MX=2*NGX
       MY=2*NGY
      ENDIF
C
      DSAL=PI/18.0
      DO 305 IDJ=1,9
      DSAZ=PI/FLOAT(IDJ)/2.0
      DO 300 JDJ=1,IDJ
C      TYPE 3456,IDJ,JDJ
 3456 FORMAT('ALT LOOP ',I6,'  AZI LOOP ',I6)
      DO 30 I=1,NP
   30 ABSORB(I)=0.0
      SALT=(PI+DSAL)/2 - DSAL*FLOAT(IDJ)
      SAZI=DSAZ*(FLOAT(JDJ)-0.5)
      SA=DSAZ*(SIN(SALT+0.5*DSAL)-SIN(SALT-0.5*DSAL))
      ANG=0.0
C
      SALTDE=SALT*180.0/PI
      SAZIDE=SAZI*180.0/PI
C
C     START WITH DIRECT RAY NORMAL INTENSITY OF 100
      DRN=100.0
      DRH=DRN*SIN(SALT)
      SRAYX=COS(SALT)*SIN(SAZI-ANG)
      SRAYY=COS(SALT)*COS(SAZI-ANG)
      SRAYZ=SIN(SALT)
C
C      INITIALIZE ARRAYS DITR AND TTR
      DO 35 IK=1,MX
      DO 35 IJ=1,MY
      TTR(IK,IJ)=0.0
      DITR(IK,IJ)=0.0
   35   CONTINUE
C
C      TRACE RAYS THROUGH THE COA OF EACH GRID ELEMENT OF THOSE
C      PLANES EXPOSED TO THE SUN
      DO 190 I=1,NP
      WSAZI=SAZI-(ANG+WAZI(I))
```

```
216          DOT=SIN(SLOPE(I))*COS(SALT)*COS(WSAZI)
                  + SIN(SALT)*COS(SLOPE(I))
217    C
218    C      IF DOT IS NEGATIVE THE SUN IS BEHIND THE PLANE.
219          IF(DOT.LE.0.0) GOTO 190
220          RAIN=ACOS(DOT)
221    C      IF THIS PLANE IS THE GROUND THEN LOOP TO NEXT PLANE.
222          IF((I.EQ.NG1).OR.(I.EQ.NG2)) GOTO 190
223    C
224    C      IF THIS PLANE IS BLACK AND OPAQUE LOOP TO THE NEXT PLANE.
225          IF(DIM(I,11).EQ.0.0.AND.DIM(I,14).EQ.0.0)GOTO 190
226          RNU=DIST(I,1)/W
227          RN=AINT(RNU)
228          IF(RNU.EQ.RN)THEN
229           NU=RNU
230          ELSE
231           NU=RN+1.0
232          ENDIF
233          NV=DIST(I,2)/W+1.0
234          DO 185 K=1,NV
235          DO 180 J=1,NU
236          CALL COA(I,J,K,COAX,COAY,COAZ,AREA,NOP)
237    C
238    C      IF NOP EQUALS 0 THEN THIS GRID ELEMENT IS NOT PART OF
239    C      THE PLANE.
240          IF(NOP.EQ.0)GOTO 180
241          CALL RAY(I,SRAYX,SRAYY,SRAYZ,DRN,DOT,COAX,COAY,COAZ,AREA)
242      180      CONTINUE
243      185      CONTINUE
244      190   CONTINUE
245    C
246    C      HAVE NOW RUN THROUGH EACH PLANE FOR THIS HOUR.CALCULATE THE
247    C      SPACE AVERAGE TRANSMISSIVITY AND GRID TRANSMISSIVITY.
248          DRAO=DRH*WX*WY
249    C
250    C      AVERAGE DIRECT TRANSMISSIVITY(AVDTR)
251          TDRAD=0.0
252          DO 200 LK=1,MY
253          DO 200 LJ=1,MX
254          TDRAD=TDRAD+DITR(LJ,LK)
255          DITR(LJ,LK)=100.0*DITR(LJ,LK)/DRAO
256      200   CONTINUE
257    C
258          AVDTR=TDRAD/(DRAO*MY*MX)
259    C
260    C     ABSORPTION
```

```
C
      SORP=0.0
      DO 202 I=1,NP
      ABSORB(I)=ABSORB(I)/(DRAO*MY*MX)
  202 SORP=SORP+ABSORB(I)
      ABSORB(NG1)=AVDTR
      WRITE(5,240) SALTDE,SAZIDE,SA,AVDTR,SORP
      WRITE(5,290) (ABSORB(I),I=1,NP)
      DO 205 I=1,MX
  205      WRITE(5,280)(DITR(I,J),J=1,MY)
C
      WRITE(4,260) AVDTR,SORP,IDJ,JDJ
  207   FORMAT(6F6.1,2F7.4,4F6.3,2F5.2)
  210   FORMAT(30X,'TRANSMISSIVITY OF GREENHOUSE'/29X,30('*'),
     *  //1X,'SPECIFICATIONS:LENGTH=',F4.1,' METRES'/16X,
     *  'WIDTH =',F4.1,' METRES'/16X,'GRID WIDTH=',F5.2,' METRES')
C
  240   FORMAT(//'DIRECT TRANSMISSIVITY'/1X,20('*')//1X,
     *  'SOLAR ALTITUDE=',F4.1,' DEGREES'/1X,
     *  'SOLAR AZIMUTH=',F6.2,' DEGREES'/1X,
     *  'SOLID ANGLE OF SKY=',F7.5,'  STERDIAN'/1X,
     *  'AVERAGE DIRECT TRANSMISSIVITY =',F5.3/1X,
     *  'AVERAGE COVERING ABSORPTIVITY =',F5.3)
C
  250   FORMAT(A80)
  260   FORMAT(2(F8.3),2(I6))
  280   FORMAT(1X,40(F5.1,1X))
  290   FORMAT(1X,'ABSORPTIVITY OF SURFACES '/
     *    10(F8.3)//)
C
  300   CONTINUE
  305   CONTINUE
      CALL TIME(BUF)
      WRITE(5,789)BUF
      CLOSE(2)
      CLOSE(5)
      CLOSE(4)
      OPEN(5,FILE='GHOUSE.DAT',STATUS='OLD')
      OPEN(4,FILE='SKY.DAT')
      READ(5,250) CODE
      DO 400 J=1,9
      DO 400 K=1,J
  400 READ(5,260) TAU(J,K),ALPH(J,K)
      DO 410 J=1,9
      DO 420 K=1,J
      KK=J*2+1-K
```

```
307          TAU(J,KK)=TAU(J,K)
308          ALPH(J,KK)=ALPH(J,K)
309     420  CONTINUE
310          DO 430 K=1,J
311          KK=J*2+K
312          TAU(J,KK)=TAU(J,K)
313          ALPH(J,KK)=ALPH(J,K)
314     430  CONTINUE
315          DO 440 K=1,J
316          KK=J*4+1-K
317          TAU(J,KK)=TAU(J,K)
318          ALPH(J,KK)=ALPH(J,K)
319     440  CONTINUE
320     410  CONTINUE
321          WRITE(4,250) CODE
322          DO 500 J=1,9
323          DO 500 K=1,J*4
324     500  WRITE(4,260) TAU(J,K),ALPH(J,K),J,K
325          CLOSE(5)
326          CLOSE(4)
327          END
```

A3.2.2 Ray Tracing Subroutine RAY.F

```
1            SUBROUTINE RAY(I,SRAYX,SRAYY,SRAYZ,DRN,DOT,
                            COAX,COAY,COAZ,AREA)
2       C
3            DIMENSION C(50,6,3),DIM(50,14),PNOR(50,3),DIST(50,6),
4           *  WAZI(50),SLOPE(50),HORIZ(50,0:1000,3),VERT(50,0:5000,3),
5           *  DIFT(50),DFTR(100,40),DITR(100,40),VF(50),ABSORB(50)
6            COMMON C,DIM,PNOR,DIST,WAZI,SLOPE,GW,GBW,ANG,NP,HORIZ,VERT,
7           *       DIFT,DFTR,DITR,VF,NG1,NG2,WX,WY,W,ABSORB,DIRT
8
9       C
10      C      TEST TO SEE IF THIS POINT IS SHADED.
11           M=1
12           MM=1
13           XO=SRAYX
14           YO=SRAYY
15           ZO=SRAYZ
16           CALL TRACE(XO,YO,ZO,I,COAX,COAY,COAZ,XRI,YRI,ZRI,LPR,
17          *             XTI,YTI,ZTI,LPT,T,R,XR,YR,ZR,INTE)
18           IF(INTE.EQ.0) GOTO 180
19           BEAM=DRN*AREA*DOT
20           RSO=T*BEAM
21           ABSORB(I)=ABSORB(I)+(BEAM*(1.0-T-R))
```

```
      X1=XTI
      Y1=YTI
      Z1=ZTI
      N1=LPT
  125   IF(N1.EQ.0) GOTO 155
      IF(RS0.EQ.0.0) GOTO 155
      IF((N1.EQ.NG1).OR.(N1.EQ.NG2))THEN
       CALL RADSUM(RS0,X1,Y1)
      ELSE
       CALL TRACE(X0,Y0,Z0,N1,X1,Y1,Z1,XRI,YRI,ZRI,LPR,
     *             XTI,YTI,ZTI,LPT,T,R,XR,YR,ZR,INTE)
       ABSORB(N1)=ABSORB(N1)+(RS0*(1.0-T-R))
       X2=XTI
       Y2=YTI
       Z2=ZTI
       N2=LPT
       RS1=RS0*T
  130    IF(N2.EQ.0) GOTO 135
      IF(RS1.EQ.0.0)GOTO 135
      IF((N2.EQ.NG1).OR.(N2.EQ.NG2))THEN
       CALL RADSUM(RS1,X2,Y2)
      ELSE
       CALL TRACE(X0,Y0,Z0,N2,X2,Y2,Z2,XRI,YRI,ZRI,LPR,
     *             XTI,YTI,ZTI,LPT,T,R,XR,YR,ZR,INTE)
       ABSORB(N2)=ABSORB(N2)+(RS1*(1.0-T-R))
       IF((LPT.EQ.NG1).OR.(LPT.EQ.NG2))THEN
        RS2=RS1*T
        CALL RADSUM(RS2,XTI,YTI)
       ENDIF
       IF((LPR.EQ.NG1).OR.(LPR.EQ.NG2))THEN
        RS3=RS1*R
        CALL RADSUM(RS3,XRI,YRI)
       ENDIF
      ENDIF
  135   IF(MM.EQ.2) GOTO 150
      CALL TRACE(X0,Y0,Z0,N1,X1,Y1,Z1,XRI,YRI,ZRI,LPR,
     *            XTI,YTI,ZTI,LPT,T,R,XR,YR,ZR,INTE)
       X2=XRI
       Y2=YRI
       Z2=ZRI
       N2=LPR
       RS1=RS0*R
       X0=XR
       Y0=YR
       Z0=ZR
       MM=MM+1
```

```
68           GOTO 130
69      150      ENDIF
70      155   IF(M.EQ.2) GOTO 180
71           CALL TRACE(SRAYX,SRAYY,SRAYZ,I,COAX,COAY,COAZ,XRI,YRI,ZRI,
72          *             LPR,XTI,YTI,ZTI,LPT,T,R,XR,YR,ZR,INTE)
73           RSO=R*DRN*AREA*DOT
74           XO=XR
75           YO=YR
76           ZO=ZR
77           X1=XRI
78           Y1=YRI
79           Z1=ZRI
80           N1=LPR
81           M=M+1
82           GOTO 125
83      180   CONTINUE
84      185   CONTINUE
85      190   RETURN
86           END
```

A3.2.3 Transmission Subroutine TRANS.F

The following subroutine is called to calculate the light transmission and absortion at each light ray intersection with a plane in the greenhouse. Line 23 was modified to include the effect of dirt accumulation on the primary cover.

```
 1           SUBROUTINE TRANS(RAI,N,DPR,TC,R)
 2    C
 3           DIMENSION C(50,6,3),DIM(50,14),PNOR(50,3),DIST(50,6),
 4          *  WAZI(50),SLOPE(50),HORIZ(50,0:1000,3),VERT(50,0:5000,3),
 5          *  DIFT(50),DFTR(100,40),DITR(100,40),VF(50)
 6           COMMON C,DIM,PNOR,DIST,WAZI,SLOPE,GW,GBW,ANG,NP,HORIZ,VERT,
 7          *          DIFT,DFTR,DITR,VF,NG1,NG2,WX,WY,W,ABSORB,DIRT
 8           IF(RAI.GE.1.56) RAI=1.56
 9           IF(RAI.LE.0.001) RAI=0.001
10           AR=ASIN(SIN(RAI)/DIM(N,11))
11           IF(AR.GE.1.56)THEN
12            AR=1.56
13           ELSEIF(AR.LE.0.0001)THEN
14            AR=0.0001
15           ENDIF
16           S1=(SIN(RAI-AR))**2
17           S2=(SIN(RAI+AR))**2
18           S3=(TAN(RAI-AR))**2
19           S4=(TAN(RAI+AR))**2
```

```
      RPER=S1/S2
      RPLL=S3/S4
      SL=DIM(N,7)/COS(AR)
      TA=EXP(-DIM(N,9)*SL)*(1.0-DIRT)
      TPLL1=(TA*(1.0-RPLL)**2)/(1.0-(RPLL*TA)**2)
      TPER1=(TA*(1.0-RPER)**2)/(1.0-(RPER*TA)**2)
      RPLL1=RPLL*(1.0+TA*TPLL1)
      RPER1=RPER*(1.0+TA*TPER1)
C
      IF(DIM(N,12).EQ.0.0)THEN
       R=(RPLL1+RPER1)/2.0
       TC=(TPLL1+TPER1)/2.0
      ELSE
       AR=ASIN(SIN(RAI)/DIM(N,12))
       IF(AR.GE.1.56)THEN
        AR=1.56
       ELSEIF(AR.LE.0.0001)THEN
        AR=0.0001
       ENDIF
       S1=(SIN(RAI-AR))**2
       S2=(SIN(RAI+AR))**2
       S3=(TAN(RAI-AR))**2
       S4=(TAN(RAI+AR))**2
       RPER=S1/S2
       RPLL=S3/S4
       SL=DIM(N,8)/COS(AR)
       TA=EXP(-DIM(N,10)*SL)
       TPLL2=(TA*(1.0-RPLL)**2)/(1.0-(RPLL*TA)**2)
       TPER2=(TA*(1.0-RPER)**2)/(1.0-(RPER*TA)**2)
       RPLL2=RPLL*(1.0+TA*TPLL2)
       RPER2=RPER*(1.0+TA*TPER2)
       TC=0.5*((TPLL1*TPLL2)/(1.0-RPLL1*RPLL2)+(TPER1*TPER2)/
     *   (1.0-RPER1*RPER2))
       IF(DPR.GT.0.0)THEN
       R=0.5*(RPLL1+(TC*RPLL2*TPLL1)/TPLL2+RPER1+(TC*RPER2*TPER1)/
     *    TPER2)
       ELSE
       R=0.5*(RPLL2+(TC*RPLL1*TPLL2)/TPLL1+RPER2+(TC*RPER1*TPER2)/
     *    TPER1)
       ENDIF
      ENDIF
      RETURN
      END
```

A3.2.4 Direct Light Transmission And Absorption Data

The direct light transmission and absorption input file SKY.DAT is listed below. The column are respectively transmissivity, absorptivity, solar elevation sector, and solar azimuth sector.

```
 DATA FOR MASSEY GREENHOUSE NO 23 RUN 5
   0.767   0.153     1     1
   0.767   0.153     1     2
   0.767   0.153     1     3
   0.767   0.153     1     4
   0.760   0.179     2     1
   0.760   0.170     2     2
   0.760   0.170     2     3
   0.760   0.179     2     4
   0.760   0.179     2     5
   0.760   0.170     2     6
   0.760   0.170     2     7
   0.760   0.179     2     8
   0.757   0.212     3     1
   0.749   0.210     3     2
   0.752   0.190     3     3
   0.752   0.190     3     4
   0.749   0.210     3     5
   0.757   0.212     3     6
   0.757   0.212     3     7
   0.749   0.210     3     8
   0.752   0.190     3     9
   0.752   0.190     3    10
   0.749   0.210     3    11
   0.757   0.212     3    12
   0.737   0.251     4     1
   0.731   0.261     4     2
   0.727   0.253     4     3
   0.725   0.227     4     4
   0.725   0.227     4     5
   0.727   0.253     4     6
   0.731   0.261     4     7
   0.737   0.251     4     8
   0.737   0.251     4     9
   0.731   0.261     4    10
   0.727   0.253     4    11
   0.725   0.227     4    12
   0.725   0.227     4    13
   0.727   0.253     4    14
   0.731   0.261     4    15
```

0.737	0.251	4	16
0.737	0.290	5	1
0.726	0.305	5	2
0.712	0.307	5	3
0.699	0.296	5	4
0.695	0.265	5	5
0.695	0.265	5	6
0.699	0.296	5	7
0.712	0.307	5	8
0.726	0.305	5	9
0.737	0.290	5	10
0.737	0.290	5	11
0.726	0.305	5	12
0.712	0.307	5	13
0.699	0.296	5	14
0.695	0.265	5	15
0.695	0.265	5	16
0.699	0.296	5	17
0.712	0.307	5	18
0.726	0.305	5	19
0.737	0.290	5	20
0.737	0.341	6	1
0.729	0.355	6	2
0.720	0.356	6	3
0.707	0.348	6	4
0.681	0.327	6	5
0.666	0.293	6	6
0.666	0.293	6	7
0.681	0.327	6	8
0.707	0.348	6	9
0.720	0.356	6	10
0.729	0.355	6	11
0.737	0.341	6	12
0.737	0.341	6	13
0.729	0.355	6	14
0.720	0.356	6	15
0.707	0.348	6	16
0.681	0.327	6	17
0.666	0.293	6	18
0.666	0.293	6	19
0.681	0.327	6	20
0.707	0.348	6	21
0.720	0.356	6	22
0.729	0.355	6	23
0.737	0.341	6	24
0.758	0.482	7	1

0.749	0.492	7	2
0.734	0.475	7	3
0.719	0.446	7	4
0.700	0.407	7	5
0.665	0.365	7	6
0.634	0.321	7	7
0.634	0.321	7	8
0.665	0.365	7	9
0.700	0.407	7	10
0.719	0.446	7	11
0.734	0.475	7	12
0.749	0.492	7	13
0.758	0.482	7	14
0.758	0.482	7	15
0.749	0.492	7	16
0.734	0.475	7	17
0.719	0.446	7	18
0.700	0.407	7	19
0.665	0.365	7	20
0.634	0.321	7	21
0.634	0.321	7	22
0.665	0.365	7	23
0.700	0.407	7	24
0.719	0.446	7	25
0.734	0.475	7	26
0.749	0.492	7	27
0.758	0.482	7	28
0.811	0.812	8	1
0.797	0.833	8	2
0.790	0.823	8	3
0.781	0.773	8	4
0.752	0.688	8	5
0.708	0.571	8	6
0.674	0.459	8	7
0.651	0.364	8	8
0.651	0.364	8	9
0.674	0.459	8	10
0.708	0.571	8	11
0.752	0.688	8	12
0.781	0.773	8	13
0.790	0.823	8	14
0.797	0.833	8	15
0.811	0.812	8	16
0.811	0.812	8	17
0.797	0.833	8	18
0.790	0.823	8	19

0.781	0.773	8	20
0.752	0.688	8	21
0.708	0.571	8	22
0.674	0.459	8	23
0.651	0.364	8	24
0.651	0.364	8	25
0.674	0.459	8	26
0.708	0.571	8	27
0.752	0.688	8	28
0.781	0.773	8	29
0.790	0.823	8	30
0.797	0.833	8	31
0.811	0.812	8	32
0.957	2.420	9	1
0.925	2.483	9	2
0.923	2.479	9	3
0.895	2.384	9	4
0.870	2.191	9	5
0.846	1.903	9	6
0.825	1.539	9	7
0.777	1.121	9	8
0.776	0.750	9	9
0.776	0.750	9	10
0.777	1.121	9	11
0.825	1.539	9	12
0.846	1.903	9	13
0.870	2.191	9	14
0.895	2.384	9	15
0.923	2.479	9	16
0.925	2.483	9	17
0.957	2.420	9	18
0.957	2.420	9	19
0.925	2.483	9	20
0.923	2.479	9	21
0.895	2.384	9	22
0.870	2.191	9	23
0.846	1.903	9	24
0.825	1.539	9	25
0.777	1.121	9	26
0.776	0.750	9	27
0.776	0.750	9	28
0.777	1.121	9	29
0.825	1.539	9	30
0.846	1.903	9	31
0.870	2.191	9	32
0.895	2.384	9	33

```
0.923   2.479     9    34
0.925   2.483     9    35
0.957   2.420     9    36
```

A3.2.5 Diffuse Light Transmission Program DIFF2.F

The following new program was written for a FORTRAN compiler to calculate the diffuse light transmision from uniform overcast, standard overcast, and clear skies using the direct light transmission tables produced by GST2. An example of the output is given in section A3.2.6

```
 1          PROGRAM DIFF2
 2    C     CALCULATES THE DIFFUSE TRANSMISSIVITY OF A STRUCTURE BASED
 3    C     ON DIRECT TRANSMISSIVITY DATA IN FILE GHOUSE.DAT FOR
 4    C     UNIFORM OVERCAST, STANDARD OVERCAST, AND CLEAR SKIES
 5    C
 6          DIMENSION ABSORB(2),SOCSUM(2),UOCSUM(2),B(9,9),
 7         *   CLEAR(9,9),CLEARSUM(2,9,9)
 8          CHARACTER*80 CODE
 9          PARAMETER (PI=3.14159265)
10          OPEN(5,FILE='SKY.DAT',STATUS='OLD')
11          OPEN(4,FILE='DIFF.OUT')
12          READ(5,1000) CODE
13     1000 FORMAT(A80)
14          UOCB=0.0
15          SOCB=0.0
16          DO 10 I=1,2
17          UOCSUM(I)=0.0
18          SOCSUM(I)=0.0
19          DO 10 J=1,9
20          DO 10 K=1,9
21          CLEAR(J,K)=0.0
22          B(J,K)=0.0
23       10 CLEARSUM(I,J,K)=0.0
24          DSAL=PI/18.0
25    C      DIFF=1.0
26    C      UOCRAD=DIFF/PI
27    C      SOCRADZ=DIFF*9.0/(7.0*PI)
28          DO 305 IDJ=1,9
29          DSAZ=PI/FLOAT(IDJ)/2.0
30          SALT=(PI+DSAL)/2 - DSAL*FLOAT(IDJ)
31          DO 300 JDJ=1,IDJ*4
32          SAZI=DSAZ*(FLOAT(JDJ)-0.5)
33          SA=DSAZ*(SIN(SALT+0.5*DSAL)-SIN(SALT-0.5*DSAL))
34          READ(5,260) (ABSORB(I),I=1,2)
35       260 FORMAT(2(F8.3))
```

```
C       UOCD=UOCRAD*SIN(SALT)*SA
C       SOCD=SOCRADZ*(1.0+2.0*SIN(SALT))*SIN(SALT)*SA/3.0
        UOCD=SIN(SALT)*SA
        SOCD=(1.0+2.0*SIN(SALT))*SIN(SALT)*SA/3.0
        UOCB=UOCB+UOCD
        SOCB=SOCB+SOCD
        DO 30 J=1,9
        SUNALT=(PI+DSAL)/2 -DSAL*FLOAT(J)
        DSUNAZ=PI/FLOAT(J)/2.0
        DO 30 K=1,J
        SUNAZI=DSUNAZ*(FLOAT(K)-0.5)
        IF(J.EQ.IDJ.AND.K.EQ.JDJ) GOTO 30
        COSA=SIN(SUNALT)*SIN(SALT)
                        + COS(SUNALT)*COS(SALT)*COS(SUNAZI-SAZI)
        X=1.0-EXP(-0.32/SIN(SALT))
        Y=1.0+COSA*COSA
        Z=1.0-COSA
        CLEAR(J,K)=X*Y*SIN(SUNALT)*SA/Z
        B(J,K)=B(J,K)+CLEAR(J,K)
   30   CONTINUE
        DO 20 I=1,2
        UOCSUM(I)=UOCSUM(I)+UOCD*ABSORB(I)
        SOCSUM(I)=SOCSUM(I)+SOCD*ABSORB(I)
        DO 40 J=1,9
        DO 40 K=1,J
   40   CLEARSUM(I,J,K)=CLEARSUM(I,J,K)+CLEAR(J,K)*ABSORB(I)
   20   CONTINUE
  300   CONTINUE
  305   CONTINUE
        WRITE(4,270) (UOCSUM(I)/UOCB,I=1,2)
  270   FORMAT(' DIFFUSE TRANSMISSIVITY FOR UNIFORM OVERCAST SKY'/
       * 2(F7.3))
        WRITE(4,280) (SOCSUM(I)/SOCB,I=1,2)
  280   FORMAT(' DIFFUSE TRANSMISSIVITY FOR STANDARD OVERCAST SKY'/
       * 2(F7.3))
        DO 50 J=1,9
        ALT=95.0-10.0*FLOAT(J)
        DO 50 K=1,J
        AZI=90.0*(FLOAT(K)-0.5)/FLOAT(J)
        DO 60 I=1,2
   60   CLEARSUM(I,J,K)=CLEARSUM(I,J,K)/B(J,K)
        WRITE(4,290) ALT,AZI,(CLEARSUM(I,J,K),I=1,2)
  290   FORMAT(' SOLAR ALT ',F5.2,' AZI ',F5.2)
   50   CONTINUE
```

```
79          CLOSE(5)
80          CLOSE(4)
81          END
```

A3.2.6 Diffuse Light Transmission And Absorption Data

The diffuse light transmission and absorption input file DIFF.DAT is listed below. The columns are respectively transmissivity and absorptivity.

```
 DIFFUSE TRANSMISSIVITY FOR UNIFORM OVERCAST SKY
  0.733  0.366
 DIFFUSE TRANSMISSIVITY FOR STANDARD OVERCAST SKY
  0.733  0.318
 SOLAR ALT 85.00 AZI 45.00
  0.754  0.342
 SOLAR ALT 75.00 AZI 22.50
  0.769  0.391
 SOLAR ALT 75.00 AZI 67.50
  0.790  0.389
 SOLAR ALT 65.00 AZI 15.00
  0.769  0.434
 SOLAR ALT 65.00 AZI 45.00
  0.783  0.431
 SOLAR ALT 65.00 AZI 75.00
  0.778  0.415
 SOLAR ALT 55.00 AZI 11.25
  0.771  0.492
 SOLAR ALT 55.00 AZI 33.75
  0.781  0.490
 SOLAR ALT 55.00 AZI 56.25
  0.772  0.469
 SOLAR ALT 55.00 AZI 78.75
  0.766  0.447
 SOLAR ALT 45.00 AZI  9.00
  0.775  0.572
 SOLAR ALT 45.00 AZI 27.00
  0.787  0.572
 SOLAR ALT 45.00 AZI 45.00
  0.776  0.549
 SOLAR ALT 45.00 AZI 63.00
  0.764  0.514
 SOLAR ALT 45.00 AZI 81.00
  0.754  0.485
 SOLAR ALT 35.00 AZI  7.50
  0.788  0.695
 SOLAR ALT 35.00 AZI 22.50
```

```
 0.803  0.697
SOLAR ALT 35.00 AZI 37.50
 0.791  0.670
SOLAR ALT 35.00 AZI 52.50
 0.776  0.624
SOLAR ALT 35.00 AZI 67.50
 0.759  0.570
SOLAR ALT 35.00 AZI 82.50
 0.746  0.531
SOLAR ALT 25.00 AZI  6.43
 0.814  0.902
SOLAR ALT 25.00 AZI 19.29
 0.834  0.913
SOLAR ALT 25.00 AZI 32.14
 0.823  0.884
SOLAR ALT 25.00 AZI 45.00
 0.807  0.825
SOLAR ALT 25.00 AZI 57.86
 0.786  0.742
SOLAR ALT 25.00 AZI 70.71
 0.764  0.655
SOLAR ALT 25.00 AZI 83.57
 0.750  0.593
SOLAR ALT 15.00 AZI  5.62
 0.859  1.315
SOLAR ALT 15.00 AZI 16.88
 0.893  1.355
SOLAR ALT 15.00 AZI 28.13
 0.881  1.325
SOLAR ALT 15.00 AZI 39.38
 0.865  1.252
SOLAR ALT 15.00 AZI 50.63
 0.844  1.134
SOLAR ALT 15.00 AZI 61.88
 0.820  0.985
SOLAR ALT 15.00 AZI 73.13
 0.796  0.829
SOLAR ALT 15.00 AZI 84.38
 0.783  0.71
SOLAR ALT  5.00 AZI  5.00
 0.900  1.609
SOLAR ALT  5.00 AZI 15.00
 0.986  1.845
SOLAR ALT  5.00 AZI 25.00
 0.973  1.821
SOLAR ALT  5.00 AZI 35.00
```

```
 0.958  1.749
SOLAR ALT  5.00 AZI 45.00
 0.937  1.622
SOLAR ALT  5.00 AZI 55.00
 0.915  1.446
SOLAR ALT  5.00 AZI 65.00
 0.890  1.237
SOLAR ALT  5.00 AZI 75.00
 0.870  1.032
SOLAR ALT  5.00 AZI 85.00
 0.857  0.899
```